

POLITECNICO DI MILANO
DIPARTIMENTO DI MATEMATICA

MATHEMATICAL MODELS AND METHODS IN ENGINEERING
XXXI CYCLE

**On the determination
of discontinuous coefficients
in semilinear elliptic and parabolic
boundary value problems
arising in cardiac electrophysiology**

Author:
Luca RATTI

Supervisor:
Prof. Elena BERETTA

Co-Supervisor:
Prof. Marco VERANI

The Chair of the Doctoral Programme:
Prof. Irene SABADINI



“Penso che la matematica sia una delle manifestazioni più significative dell’amore per la sapienza, e ha forse una capacità unica tra tutte le scienze di passare dalla osservazione delle cose visibili all’immaginazione delle cose invisibili. Questo forse è il segreto della forza della matematica.”

Ennio De Giorgi

Abstract

The objective of this thesis is the investigation of inverse problems related to semilinear boundary value problems involved with the mathematical description of the cardiac electrical activity. The long-term purpose which motivates the research in this field is to discuss the possibility of identifying ischemic areas within the cardiac tissue only by means of non-invasive measurements. We tackle this issue within the mathematical framework of the theory of Inverse Problems, pursuing an approach which focuses both on analytical and on numerical aspects.

Mathematical models allowing for a satisfactory description of the cardiac electrophysiology have been developed since the late 70s, and consist in coupled systems of nonlinear parabolic partial differential equations and ordinary differential equations. When considering the presence of ischemic areas within the tissue, discontinuous alterations of the coefficients are entailed: we consider the inverse problem of determining such inhomogeneities from the knowledge of the electrical potential on the boundary of the domain. Despite some contributions have been recently given in this field, a complete theoretical investigation of this inverse problem has not yet been carried out. The main guidelines of our study are both the extension of the existing theoretical results and the development of effective and rigorous numerical reconstruction algorithms. We proceed by formulating simplified versions of the problem of interest, and then extending the results on subsequent refinements of the model. We also rely on the introduction of *regularization hypotheses*, namely, *a priori* assumptions regarding the inhomogeneity to be identified, which help in restoring the well-posedness of the inverse problem: particular attention is given to the task of localizing ischemic areas of small size.

Regarding the identification of small inclusions (both in a semilinear elliptic and parabolic problem), we rely on the formulation of an asymptotic expansion of the boundary voltage with respect to the size of the inclusion in order to analyze the well-posedness of the inverse problem and also to introduce a reconstruction algorithm, based on a Topological Optimization approach.

When removing any *a priori* assumption and tackling the detection of arbitrarily large inclusions, no theoretical result regarding the well-posedness of the inverse problem is known; we instead focus on the rigorous deduction of a reconstruction algorithm for the approximation of its solution. The devised technique, which relies both on the regularization theory for inverse problems and on a relaxation strategy, allows for satisfactory reconstructions.

We finally move towards the application of the introduced techniques on the full complexity of the application model. We hence investigate the well-posedness of the direct problem, extending the existing results in the literature. An additional aspect which is taken into account, from a numerical perspective, is the *a posteriori* error analysis of the discrete solver of the direct problem, which is preliminary for an efficient application of the developed reconstruction algorithms.

Sommario

Lo scopo del presente lavoro di tesi è l'analisi di un problema inverso relativo ad un problema al contorno semilineare per la descrizione matematica dell'attività elettrica del cuore. L'obiettivo di lungo termine che motiva la ricerca in questo campo è la possibilità di identificare la presenza di regioni ischemiche nel tessuto cardiaco attraverso misurazioni non invasive. La tematica è affrontata nel contesto della teoria dei Problemi Inversi, focalizzandosi sia su aspetti analitici che numerici.

Modelli matematici per la descrizione dell'elettrofisiologia cardiaca sono stati sviluppati dagli anni 70, e si articolano in sistemi che presentano equazioni paraboliche alle derivate parziali accoppiate con equazioni differenziali ordinarie. La presenza di aree ischemiche nel tessuto implica di considerare un'alterazione discontinua dei parametri: ci occupiamo pertanto del problema inverso di determinare tali inomogeneità dalla conoscenza del potenziale elettrico sulla superficie del dominio. Nonostante si siano registrati diversi contributi in questo campo negli ultimi anni, non è ancora stata condotta una completa analisi teorica del problema inverso. Le linee guida di questo studio sono perciò sia l'estensione di risultati teorici esistenti sia lo sviluppo di algoritmi di ricostruzione numerici che siano efficaci e rigorosi. Procediamo formulando versioni semplificate del problema di interesse, per estendere poi i risultati a raffinamenti successivi del modello. Ci basiamo inoltre sull'introduzione di *ipotesi di regolarizzazione*, ossia assunzioni *a priori* circa le inomogeneità da identificarsi, le quali aiutano a ripristinare la buona posizione del problema inverso: un'attenzione particolare è fornita al problema di localizzare aree ischemiche di piccole dimensioni.

Per quanto riguarda l'identificazione di piccole inclusioni (sia in problemi ellittici che parabolici), il risultato cruciale è la formulazione di uno sviluppo asintotico per la perturbazione del potenziale elettrico di bordo rispetto alle dimensioni dell'inclusione, che permette di analizzare la buona posizione del problema inverso e anche di dedurre un algoritmo di ricostruzione basato su un approccio di Ottimizzazione Topologica.

Se si rimuove invece ogni ipotesi *a priori* e si affronta la ricerca di inclusioni arbitrariamente grandi, non esiste alcun risultato circa la buona posizione del problema inverso; ci concentriamo invece sulla deduzione rigorosa di un algoritmo di ricostruzione per l'approssimazione della soluzione. La tecnica approntata, che si basa sia sulla teoria della regolarizzazione per problemi inversi sia sul rilassamento del problema di ottimizzazione associato, permette di ottenere risultati soddisfacenti.

Infine, ci accingiamo ad applicare le tecniche introdotte sul modello applicativo nella sua complessità. A questo scopo, è prima necessario studiare la buona posizione del problema diretto, estendendo i risultati presenti in letteratura. Un ulteriore aspetto che viene considerato, da un punto di vista numerico, è l'analisi *a posteriori* dell'errore commesso nell'approssimazione numerica del problema diretto, studio preliminare per incrementare l'efficienza degli algoritmi di ricostruzione.

Contents

Abstract	v
1 Introduction	1
1.1 Motivation	1
1.1.1 The bidomain and the monodomain models	2
1.1.2 Constitutive laws for the ionic current	4
1.1.3 Modeling the presence of an ischemic region	5
1.1.4 Measuring the electrical activity of the heart	6
1.2 Identification of ischemias from boundary measurements	7
1.2.1 Model simplification	8
1.2.2 Regularization hypotheses	8
1.3 A brief bibliographical review	9
1.4 Main contributions of the thesis	11
2 Identification of small inclusions in a semilinear elliptic boundary value problem	15
2.1 Analysis of the direct problem	16
2.2 Analysis of the inverse problem	18
2.3 A topological gradient-based reconstruction algorithm	25
2.3.1 Identification in presence of a single measurement	29
2.3.2 Identification in presence of multiple measurements	32
2.3.3 Partial measurements	33
2.4 Numerical results	34
2.4.1 Circular-shaped inclusion detection	35
2.4.2 Inclusion of unknown shape	36
2.4.3 Partial measurements	38
2.4.4 Identification of multiple inclusions	38
2.4.5 Identification of inclusions in presence of anisotropy	39
2.4.6 Effect of experimental noise	41
3 Detection of small inclusions in a semilinear parabolic boundary value problem	45
3.1 The monodomain model of cardiac electrophysiology	46
3.2 Well posedness of the direct problem	48
3.2.1 Well posedness of the background problem	48

3.2.2	Well posedness of the perturbed problem	49
3.3	Energy estimates	55
3.4	The asymptotic formula	60
3.5	A topological gradient-based reconstruction algorithm	65
3.6	Numerical results	70
3.6.1	Finite Element approximation	70
3.6.2	Reconstruction of small inclusions	72
3.6.3	Reconstruction in presence of experimental noise	73
3.6.4	Reconstruction from partial discrete data	74
3.6.5	Reconstruction of larger inclusions	75
4	A Shape Optimization approach for the reconstruction of large inclusions in a semilinear elliptic problem	77
4.1	Small perturbations of a large inclusion	78
4.1.1	The direct problem in presence of an inclusion: a review	78
4.1.2	Energy estimates	79
4.1.3	Asymptotic expansion	83
4.2	A shape-derivative based reconstruction algorithm	87
4.2.1	Representation formula for the shape gradient	87
4.2.2	Algorithm formulation and implementation	88
4.2.3	Numerical results	89
5	A phase-field approach for the identification of arbitrary inclusions in a semilinear elliptic boundary value problem	93
5.1	Direct problem analysis	95
5.2	Optimization problem and its regularization	100
5.3	Relaxation: a phase-field approach	103
5.3.1	Optimality conditions	106
5.4	Discrete framework and reconstruction algorithm	107
5.4.1	Convergence analysis as $h \rightarrow 0$	108
5.4.2	Reconstruction algorithm: a Parabolic Obstacle Problem approach	109
5.5	Numerical results	113
5.5.1	Reconstruction of inclusions of arbitrary shape and topology	113
5.5.2	Initial guess	115
5.5.3	Mesh size and adaptation	116
5.5.4	Robustness with respect to measurements	116
5.6	Comparison with the Shape Derivative approach	117
5.6.1	Sharp interface limit of the Optimality Conditions	118
5.6.2	Comparison with the shape derivative algorithm	123
5.7	Alternative: a saddle-point problem	124
5.7.1	Reconstruction algorithm: Uzawa Total Variation flow	125
5.7.2	Numerical results and comparison with the phase-field relaxation	126

6	Well-posedness results for the monodomain problem	129
6.1	Assumptions and statement of the main results	130
6.2	Proof of Theorem 6.1	132
6.3	Proof of Theorem 6.2	139
6.4	Proof of Theorem 6.3	151
7	<i>A posteriori</i> error analysis for the monodomain model	155
7.1	A Newton-Galerkin scheme for the approximation of the monodomain model	156
7.2	Residual operators	159
7.3	<i>A posteriori</i> estimators	163
7.3.1	Efficiency of the estimators	166
7.4	Numerical experiments	170
7.4.1	Spatial and temporal analysis	170
7.4.2	Linearization analysis	172
	Conclusions	175

Chapter 1

Introduction

1.1 Motivation: mathematical models of the electrical activity of the heart

Mathematical models of the electrical activity of the heart represent a research field of growing interest. During the last decades, thanks to the development of non-invasive techniques allowing to observe and measure inner properties of the organ, even at a cellular scale, it has been possible to develop and validate several accurate and comprehensive models. Moreover, the implementation of effective numerical techniques associated with such models has increased the interest in their regards from a clinical and predictive standpoint. The heart functioning is a multi-physics and multi-scale phenomenon: only to recall its main features, the description of a single heartbeat requires to deal with models for the propagation of an electrical stimulus throughout the tissue, for the nonlinear elastic deformation of the muscle and for the fluid dynamics of blood in the cavities (see [119]). All such phenomena are strictly coupled, and each of them is characterized by a strong correlation between the behavior of the tissue at a cellular scale and at an organ scale.

In this introductory section, we provide an overview on the mathematical description of the cardiac electrophysiology, namely, we focus on the process according to which it is possible to propagate an electrical stimulus within the heart. The main instrument which has enabled to perform experimental observations regarding the cardiac electrical activity is the electrocardiogram, ECG, introduced by A. D. Waller [139] in 1887. As it was experimentally deduced, the propagation of an electrical signal in the cells of the heart, and in particular the active response of the myocardium cells to an electrical stimulus, is the trigger for the contraction and deformation of the tissue. The most relevant physical quantity involved in the phenomenon is the *transmembrane potential*, namely the difference between the internal and the external electrical potential across the cell membrane, caused by the ability of such membrane to keep ionic species within the cell. The resting value of the transmembrane potential is denoted with u_{rest} , and typically ranges between $-100mV$ and $-70mV$. When an electrical stimulation occurs, the transmembrane potential increases: if the growth stops below a threshold u_{thresh} , the cell quickly returns to the resting potential, whereas if the threshold is exceeded the membrane changes its behavior, allowing for the motion of positive ions. This process is known as *depolarization* (phase 0), after which the transmembrane potential reaches its maximum

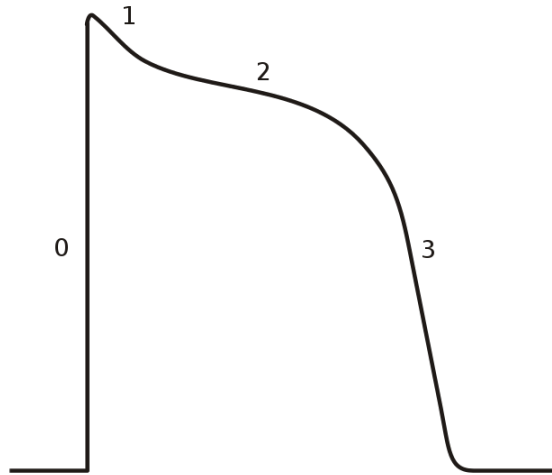


Figure 1.1: Action potential in a ventricular myocardial cell

value u_{max} of about $40mV$. After the depolarization, the potential returns to its negative resting state through a slower process of *repolarization*. A first quick decrease (phase 1) is followed by a slow plateau phase (2), sustained by a balance between the inward movement of positive ions and outward movement of negative ones. After the closure of the channels responsible for the income of positive ions, the cell undergoes a final step of complete repolarization (phase 4), going back to the initial resting state. The complete process of depolarization and repolarization is called *action potential* of the cardiac cells, and is depicted in Figure 1.1. A mathematical model describing the cardiac electrophysiology must be able to reproduce such a nonlinear behavior at a cellular scale. Moreover, the interaction between neighboring cells must be taken into account, entailing a diffusive effect at a macroscopic scale. Several factors affect this phenomenon, such as the complex geometry of the organ and the presence of preferred directions for the propagation of the electrical signal (fibers). Finally, also the generation of the electrical stimulus should be addressed, together with its fast propagation through the net of Purkinje fibers: this last topic is outside the present discussion.

1.1.1 The bidomain and the monodomain models

We depict here one of the most widely-used model in cardiac electrophysiology, the *bidomain model*, proposed by Tung in 1978 [135]: for an exhaustive discussion, we refer to [132]. The model is based on a continuum approach: namely, when describing the physical quantities involved in the model, we neglect the fine structure of the tissue (namely, the complexity induced by the presence of cells at a microscopic scale), and do not distinguish between a point in the domain and another one. This is possible according to a homogenization process and can be intended as a suitable averaging strategy on a mesoscale, allowing to preserve the main local features of the physical quantities and to disregard the fine scale inhomogeneities. The bidomain model, in particular, envisages the presence of two *domains*, an intracellular and an extracellular one: as an outcome of the homogenization, both of them are present in each point of the tissue.

According to the second Maxwell's law, applied in the quasi-stationary case, the electrical field \vec{E} satisfies

$$\operatorname{rot}\vec{E} = 0; \quad (1.1)$$

this implies the existence of an electrical potential u , s.t. $\vec{E} = -\nabla u$. In order to distinguish between the internal and external domain, we address to the *intracellular* electrical potential as u_i , whereas u_e is the *extracellular* potential. Let \vec{J} be the electrical current density: the following conservation law holds:

$$-\operatorname{div}\vec{J} = s, \quad (1.2)$$

where the term s denotes the (possible) presence of current sources within the tissue. Distinguishing between internal and external currents, we introduce the linear constitutive laws for the ones appearing in the left-hand side: $\vec{J}_i(x) = K_i(x)\nabla u_i(x)$, $\vec{J}_e(x) = K_e(x)\nabla u_e(x)$. Disregarding external applied currents, the source terms can be determined by taking into account the accumulation of charges on both sides of the membrane (namely, in both the domains), and a possible interchange represented by a transmembrane ionic current, I_{ion} :

$$\begin{aligned} s_i &= \frac{\partial q_i}{\partial t} + \sigma I_{ion}, \\ s_e &= \frac{\partial q_e}{\partial t} - \sigma I_{ion}, \end{aligned} \quad (1.3)$$

being σ the area of the cell membrane per unit volume. By total charge conservation,

$$\frac{\partial q_i(x)}{\partial t} + \frac{\partial q_e(x)}{\partial t} = 0 \quad \forall x \in \Omega.$$

The last constitutive law we need to invoke is the following one:

$$u(x) := u_i(x) - u_e(x) = \frac{q_i(x) + q_e(x)}{2\sigma C_m}, \quad (1.4)$$

being C_m the electrical capacity of the membrane. Collecting all the terms, we finally get the expression of the bidomain model:

$$\begin{cases} \operatorname{div}(K_i\nabla u_i) + \operatorname{div}(K_e\nabla u_e) = 0 & \text{in } \Omega \times (0, T), \\ \operatorname{div}(K_i\nabla u_i) = \sigma C_m \frac{\partial(u_i - u_e)}{\partial t} + \sigma I_{ion} & \text{in } \Omega \times (0, T). \end{cases} \quad (1.5)$$

A set of initial data for the system can be introduced, e.g. by specifying the values of u_i and u_e at time 0. As a result of a faster propagation of an activation stimulus throughout a parallel network of fibers, we can impose that at an initial time some regions of the tissue have a higher value of transmembrane potential $u_i - u_e$. As a boundary condition, we can impose a homogeneous Neumann condition for the potential, prescribing null current flows outside the organ:

$$\begin{aligned} J_i &= -\nabla u_i \cdot \nu = 0 \quad \text{on } \partial\Omega \times (0, T), \\ J_e &= -\nabla u_e \cdot \nu = 0 \quad \text{on } \partial\Omega \times (0, T). \end{aligned} \quad (1.6)$$

This condition can be related also to a natural conormal derivative for the differential operators appearing in (1.5), by considering the structure of the conductivity tensors K_i and K_e . In particular,

the heart tissue is usually modeled as an anisotropic conductor, characterized by the presence of fibers and sheets or laminae. As a result, both K_i and K_e possess in each point three orthogonal eigenvectors: one parallel to the fibers, one lying on the lamina (and orthogonal to the fiber) and the third one, denoted as transmural, which coincides with the normal direction when restricted to the boundaries; hence, on the boundary of the domain the normal and the conormal derivative coincide. The choice of a constitutive law for the ionic current I_{ion} is the object of study in the next subsection. In any case, I_{ion} nonlinearly depends on the transmembrane potential u . The bidomain model reported in (1.5) thus consists in a system of two coupled evolutive equations with nonlinear reaction terms.

A well-established simplification of the bidomain system consists in the so-called *monodomain* model, based on the assumption (not supported by any experimental evidence) that the conductivity properties of the interior and exterior domains are proportional, i.e.

$$K_e = \lambda K_i.$$

Under this assumption, defining $K = \frac{\lambda}{1+\lambda} K_i$ we can reformulate (1.5) in terms of the single variable u , obtaining:

$$\begin{cases} \operatorname{div}(K \nabla u) = \sigma C_m \frac{\partial u}{\partial t} + \sigma I_{ion}(u) & \text{in } \Omega, \\ K \nabla u \cdot \nu = 0 & \text{on } \partial\Omega, \\ u(x, 0) = u_0(x) & \text{in } \Omega. \end{cases} \quad (1.7)$$

Another typical assumption allowing for the introduction of the monodomain model consists in approximating both K_i and K_e by a suitable average tensor $\tilde{K} = (K_e K_i)^{-1} (K_e + K_i)$, yielding the same expression as in 1.7.

1.1.2 Constitutive laws for the ionic current

As anticipated in the previous subsection, the choice of a suitable constitutive law for the ionic current represents a crucial aspect of the formulation both of the monodomain and of the bidomain model. In order to correctly describe the current induced by the motion of ions through the membrane, the expression of I_{ion} must in principle take into account several variables: first of all the transmembrane potential u , secondly the concentration of each ionic species involved in the process (which are in the order of tens), and finally a number of *gating variables*, describing the properties of the ion gates present on the membrane and allowing for the transition of charges. Models based on similar laws for I_{ion} are referred to as *physiological* models: according to experimental evidence and conjectures, several scientists proposed many of them in the last decades. We recall here the Hodgkin-Huxley model, the Beeler-Reuter and the Luo-Rudy one. For a more detailed overview, we refer to [132].

Another important class of models is represented by the *phenomenological* ones, whose aim is to provide a mathematical formula for I_{ion} allowing for a satisfactory description of the evolution of u , with the introduction of the lowest number of additional variables. A preliminary model, entailing only the dependence of I_{ion} on u , is represented by the following cubic function: $I_{ion} = f(u)$,

$$f(u) = A(u - u_{rest})(u - u_{thresh})(u - u_{max}); \quad (1.8)$$

according to this choice, nevertheless, the monodomain system is only able to capture the fast depolarization phase of the active potential (see phase 0 of Figure 1.1). More refined phenomenological models require the introduction of a second variable w , denoted as *recovery* variable, which does not possess a specific physical meaning. Such models are hence characterized by a formula such as $I_{ion} = f(u, w)$; the evolution of the recovery variable w needs also to be described, and is typically modeled by means of a nonlinear ordinary differential equation

$$\frac{\partial w}{\partial t}(x, t) + g(u(x, t), w(x, t)) = 0,$$

together with an initial datum $w_0(x)$. When prescribing the expression of f and g , one may obtain several different models. We report here some of them, under the assumption that the transmembrane potential is rescaled so that $u_{rest} = 0$, $u_{max} = 1$, $u_{thresh} = a \in (0, 1)$:

- Fitzhugh-Nagumo (see [77] and [110])

$$f(u, w) = Au(u - a)(u - 1) + w \quad g(u, w) = \epsilon(v - \gamma w);$$

- Rogers-MacCulloch (see [123])

$$f(u, w) = Au(u - a)(u - 1) + uw \quad g(u, w) = \epsilon(v - \gamma w);$$

- Aliev-Panfilov, first version (as it was initially proposed in [7])

$$f(u, w) = Au(u - a)(u - 1) + uw \quad g(u, w) = \left(\epsilon_0 + \frac{\mu_1 w}{u + u_2} \right) (Au(u - 1 - a) + w);$$

- Aliev-Panfilov (the version usually employed in literature; see, e.g., [41])

$$f(u, w) = Au(u - a)(u - 1) + uw \quad g(u, w) = \epsilon(Au(u - 1 - a) + w);$$

- Mitchel-Schaeffer (see [108], and [39] for a regularized version)

$$f(u, w) = \frac{1}{\tau_{in}} u^2 (u - 1) w - \frac{1}{\tau_{out}} \quad g(u, w) = \begin{cases} \frac{1}{\tau_{open}} (w - 1) & \text{if } w \leq w_{gate}, \\ \frac{1}{\tau_{close}} w & \text{if } w > w_{gate}. \end{cases}$$

In Figure 1.2, we report the numerical simulation of the active potential in a cell by means of two phenomenological models, in order to allow for a comparison with the expected shape reported in Figure 1.1.

1.1.3 Modeling the presence of an ischemic region

The introduced models allow also to describe some pathological behaviors of the heart, by taking into account modifications of the main parameters. In particular, we focus our attention on the case of myocardial ischemia, characterized by severely reduced blood perfusion in a specific region of the tissue. According to biological observations, the conductivity properties of the cells in an ischemic region are altered, and in particular, the cells are no longer excitable. As a consequence, when supposing that a region $\omega \subset \Omega$ is ischemic, we consider two main modifications of the equation in (1.7):

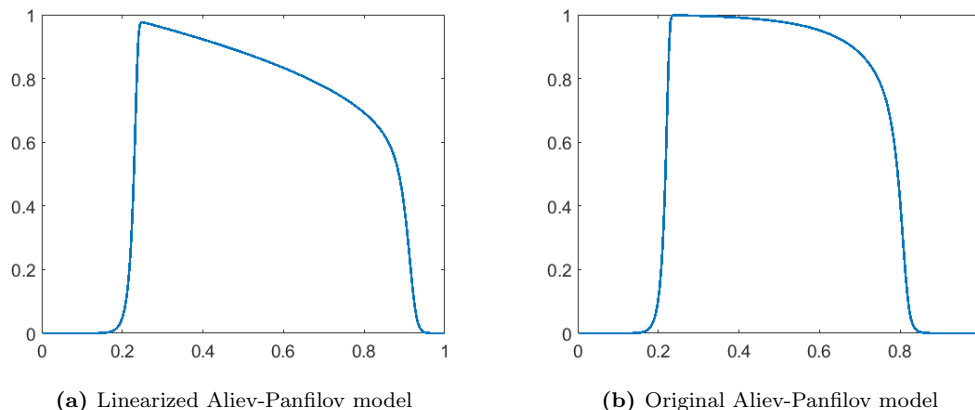


Figure 1.2: Simulated action potential in a single cell

- the conductivity tensor is supposed to have a discontinuous transition between the healthy reference value K_0 and the ischemic value K_1 : K is replaced by K_ω given by

$$K_\omega = K_0 + (K_1 - K_0)\chi_\omega,$$

being χ_ω the indicator function of ω . This is in accordance with the discussion in [112];

- the ionic current is switched off inside the ischemic region. Namely, I_{ion} is replaced with $(1 - \chi_\omega)I_{ion}$. This is in accordance with the model proposed in [129].

Alternative approaches are possible, among which we cite the modification of the parameters of the ionic gates comparing in the expression of the Mitchell-Schaeffer method proposed in [8].

1.1.4 Measuring the electrical activity of the heart

The main application purpose of the present work of thesis is the identification of an ischemic region within the myocardium by means of data acquired through non-invasive measurements. The routine non-invasive physical exam associated with the cardiac electrophysiology is the electrocardiogram (ECG), which is performed by placing electrodes on the patient skin, mainly on the torso. Such electrodes allow registering the propagation of the small electric waves continuously generated by the heart functioning. In particular, from the evolution of the acquired voltage in the electrodes, one may distinguish a P-wave, associated to the fast depolarization of the atria, a QRS-complex, generated by ventricular depolarization, and a T-wave, due to the process of polarization of the ventricles. Deviations from the standard pattern can help clinicians diagnosing an arrhythmia, previous heart attacks, as well as pathologies related to the electrical conduction. Unfortunately, the information deriving from ECG measurements is affected by noise and errors due to both the instrumentation and the complexity of the phenomenon under investigation, which involves electrical conduction in a non-homogeneous and non-stationary medium. As a consequence, ECG measurements are not sufficient for reliable diagnosis, and it is often necessary to couple them with other exams and tests.

More detailed data can be obtained through invasive techniques, such as intracardiac catheter recording along the endocardium, the inner wall of the heart. In this physical exam, a catheter enables to carry small electrodes on the surface of the heart cavities, in order to locally monitor the cardiac electric potential behavior.

Throughout the analysis presented in this thesis, we aim to recover information on ischemic portions of the tissue by means of the knowledge of the value of the electrical potential on the surface of the heart, or on a portion of the surface. According to what previously outlined, this information can in principle be acquired through invasive techniques such as an intracardiac catheter. In perspective, moreover, this consists in a first step towards the identification problem by means of ECG data, which would require an additional coupling with a model for the propagation of electric signals within the torso.

1.2 Identification of ischemic regions from boundary measurements: an inverse problem

We are finally able to formulate the main goal of the thesis in terms of an inverse problem. We now formulate the following initial and boundary value problem, associated with the phenomenological model presented in Subsection 1.1:

$$\left\{ \begin{array}{ll} \frac{\partial u}{\partial t} - \operatorname{div}(K_\omega \nabla u) + (1 - \chi_\omega)f(u, w) = 0 & \text{in } \Omega, \\ \frac{\partial w}{\partial t} + g(u, w) = 0 & \text{in } \Omega, \\ K_\omega \nabla u \cdot \nu = 0 & \text{on } \partial\Omega, \\ u(x, 0) = u_0(x) \quad w(x, 0) = w_0(x) & \text{in } \Omega. \end{array} \right. \quad (1.9)$$

We introduce the following couple of problems:

Definition 1.1 (Direct problem). Knowing the ischemic region ω , determine the electrical potential u associated to ω through (1.9);

Definition 1.2 (Inverse problem). Knowing the electrical potential, and in particular only the boundary measurement $u_{meas} = u|_{\partial\Omega \times (0, T)}$, determine the inclusion ω associated to u_{meas} through (1.9).

The notation of direct and inverse problem is in accordance with classical definitions and can be compared to many examples arising from various application contexts, see e.g. [90], [95]. As it will be outlined in the sequel, the main difficulties which characterize the presented inverse problem from a mathematical standpoint are twofold:

- i) on the one side, the initial and boundary value problem (1.9) consists of a coupled system involving the presence of nonlinear terms;
- ii) on the other side, the boundary potential u_{meas} (which represents the datum according to which we aim at identifying ω) is associated to a single measurement of the standard electrical activity of the heart. Conversely, analogous inverse problems tackle the reconstruction of coefficients

of a boundary value problem by virtue of a large set of data, associated, e.g., to boundary measurements acquired in several experiments with different settings.

Coherently with the above-outlined difficulties, during the thesis we follow a stepwise approach, introducing simpler problems which can be analyzed in details, and extending the obtained results on progressively more complicated problems. We also rely on additional *a priori* knowledge on the ischemic regions to be identified.

1.2.1 Model simplification

The monodomain model, as depicted in Section 1.1, allows to describe the evolution of the cardiac transmembrane potential u throughout the heartbeat via a semilinear parabolic equation coupled with a nonlinear ordinary differential equation taking into account the evolution of a suitable recovery variable w .

A possible simplification of the model consists in considering a less refined constitutive law for the ionic current. In (1.8) we outlined that, describing I_{ion} as a cubic function of u alone we may be able to track the evolution of u at least in the first phase of the action potential cycle. This allows dealing only with a parabolic (semilinear) equation, disregarding any coupling effect.

Nevertheless, our first approach to the inverse problem relies instead on a more radical simplification. In particular, we consider the stationary case of the monodomain model and replace the initial stimulus given by u_0, w_0 by an external current f applied in each point of the domain. Moreover, we disregard the anisotropic behavior of the tissue. Such a simplified model can be considered as a blueprint, useful to tackle the main mathematical challenges of the original problem and to set the starting point for the successive analysis: indeed, we still keep track of the nonlinear feature of the original model. In particular, we will deal with the following problem:

$$\begin{cases} -\operatorname{div}(k_\omega \nabla u) + (1 - \chi_\omega)u^3 = f & \text{in } \Omega, \\ k_\omega \nabla u \cdot \nu = 0 & \text{on } \partial\Omega, \end{cases} \quad (1.10)$$

where $k_\omega = k_0 + (k_1 - k_0)\chi_\omega$ and k_0, k_1 are two positive scalars (for the sake of simplicity, one may rescale it to 1 and $k < 1$ respectively). In case we consider a simplified version of the monodomain model, we do not refer to ω as an ischemic region, but simply as an inhomogeneity in the coefficient or, more frequently, an *inclusion*.

1.2.2 Regularization hypotheses

When dealing with an inverse problem characterized by few data at disposal, the most important mathematical issues are represented by the analysis of the uniqueness and of the stability of the solution. Namely, we want to ensure that, for a fixed boundary measurement, there exists a unique ischemia associated to it, and moreover, if we consider small perturbations of the boundary datum, small perturbations of the associated solution are entailed. This requirement is typically not satisfied by inverse problems as the ones stated above, unless some *regularization hypotheses* are introduced. Such hypotheses can be intended as further *a priori* knowledge of the solution: namely, if we know in advance that the solution we want to identify (in our case, the ischemic region) satisfies some particular assumptions, we may introduce them in the problem by restricting the space in which

we look for the solution. When doing so, uniqueness and stability of the inverse problem might be restored.

In the thesis, the main regularization hypothesis we rely on, at a preliminary stage, is the small-size assumption: namely, we suppose that the ischemia we want to detect is small with respect to the size of the heart. The modeling assumption on the small size of the inclusion, instrumental to the derivation of several theoretical results, is verified in practice in the case of residual ischemias after myocardial infarction (see [19]).

Nevertheless, a fundamental task of the foreseen application of our analysis is the detection from ECG data of ischemias without any constraint: ischemic regions might be of any size and shape, and can even consist of a finite number of disjoint connected components. For this reason, in the thesis we also consider the case of the detection of larger inclusions, aiming at removing any possible *a priori* knowledge on ω .

1.3 A brief bibliographical review

The problem of identifying the coefficient a conductivity coefficient from boundary data is strictly related to one of the most relevant and studied inverse problems of the last decades, the *inverse conductivity problem*, also referred as the *Calderón problem*. In [46], Calderón posed the following issue: given the boundary value problem

$$\begin{cases} -\operatorname{div}(\gamma \nabla u) = 0 & \text{in } \Omega, \\ \gamma \nabla u \cdot \nu = f & \text{on } \partial\Omega, \end{cases} \quad (1.11)$$

decide whether the coefficient γ can be uniquely determined by the knowledge of the Neumann-to-Dirichlet map Λ_γ , being $\Lambda_\gamma : H^{-\frac{1}{2}}(\partial\Omega) \rightarrow H^{\frac{1}{2}}(\partial\Omega)$ such that, for each $f \in H^{-\frac{1}{2}}(\partial\Omega)$, then $\Lambda_\gamma(f) = u|_{\partial\Omega}$, where u the solution of 1.11 with Neumann datum f . Additional requirements involve investigating the stability of γ with respect to perturbation of the data Λ_γ , as well as the development of a reconstruction procedure for identifying γ . Throughout the years, several mathematicians have tackled the proposed problem, developing numerous strategies yielding a great class of results.

We now provide a short overview of some of the most relevant breakthroughs. The task of uniqueness was initially tackled by assuming that the coefficient γ satisfies (piecewise) analytic regularity: a global uniqueness result was obtained in [96]. In the case of dimension $n \geq 3$, extending the strategy developed in [133], a global uniqueness result is valid under the assumption $\gamma \in W^{2,\infty}$. Recently, in [48] global uniqueness has been proved in dimension $n \geq 3$ only under the assumption that the coefficient to be reconstructed is a Lipschitz function. Regarding the two-dimensional case, we cite the global uniqueness property obtained in [109] in case $\gamma \in W^{2,p}$, together with the breakthrough result from [20], concluding for global uniqueness only under the assumption that $\gamma \in L^\infty$. In respect of the stability issue, we report the results from [3] in dimension $n \geq 3$ as well as [25] in $n = 2$, both yielding global logarithmic stability, i.e., the continuity modulus in the stability estimate is of logarithmic type. In [106] it has been proved that, despite regularity *a priori* assumption, the logarithmic stability estimate cannot be improved, and it is hence optimal

In order to move towards a problem which is closer to our application, we should consider a family of results obtained by the analysis of the Calderón problem under the assumption that the

coefficient to be identified is discontinuous, and in particular piecewise constant (which is shared with our purpose). Regarding a result of uniqueness in such a context, we refer to [71], whereas Lipschitz stability results are contained in [6] in case the coefficient to be determined belongs to a finite-dimensional space, and in [4] (logarithmic) stability results are derived for the reconstruction of an inclusion along which the coefficient γ is discontinuous.

We moreover briefly investigate the possibility of reconstructing a coefficient according to the knowledge of a finite number of measurements (i.e., couples of Neumann and Dirichlet data), instead of the full map Λ_γ . In the context of identification of piecewise constant coefficient, such a task is possible only under the knowledge of further information regarding the inclusion to be identified, namely by introducing suitable *a priori* assumptions: finitely many measurements are sufficient to determine uniquely and in a stable (Lipschitz) way the inclusion, e.g., when it belongs to a specific class of domains with prescribed shape, or when the volume of the inclusion is small compared to the volume of the domain (see [13] for an extended review). In particular, in [93] the identification of cylinders or discs is tackled with a single measurements, whereas in [87] a strategy for a class of star-shaped domains is developed, and [24] covers the reconstruction of polyhedra and polygons: all this works, unfortunately, deeply rely on the linear structure of the direct problem, and such strategies prove to be difficultly extendable to the electrophysiological problem. Moreover, the last two presented works also rely on a suitable choice of the (unique) measurement at disposal: this is in contrast with our case, in which it is not possible to select convenient boundary data, since they are associated with the standard electrical activity of the heart and not on a prescribed stimulus. Conversely, the techniques allowing for a unique reconstruction of inclusions of small size (see [78], [51]), are more feasible to be adapted on the nonlinear problem of interest: for this reason, they will be preliminarily included in the present dissertation.

Regarding the purpose of outlining a strategy capable of identifying the solution γ associated with the measured data, several reconstruction algorithms have been proposed. We remark an important distinction between *direct* and *variational* methods. The algorithms belonging to the first class typically provide an explicit formula for the computation of the solution, whereas the variational methods rely on an optimization problem associated to the inverse problem, namely by minimizing a misfit functional with suitable regularization terms.

Among the direct methods allowing for the reconstruction of arbitrary inclusions, we report the D-bar method (see [130]), the factorization method (see [42]), the enclosure method (see [89]) and the monotonicity method (see [134]). All these techniques deeply rely on the linear expression of the direct problem, entailing the availability of closed formulas for some particular solutions or potentials, and moreover on the possibility to arbitrarily choose the boundary currents associated to the reconstruction data. These features discourage us from the extensions of such methods on the nonlinear problem of interest: as a consequence, our strategy focuses on the development of variational reconstruction algorithms. Among the existing ones, we cite the NOSER method [56], which tackle the minimization of the misfit functional through Newton iterations. Furthermore, the shape-optimization approach, with suitable regularization, prescribes a strategy allowing to deform an initial guess of the inclusion according to the shape sensitivity of the functional: see [97] [87], [2] and [10]; in [88] this approach is coupled with topology optimization. The level set technique, based on an alternative representation of the shape of the inclusion, also allows for topological

perturbations: see [128] and [44], as well as [53]. A related strategy is represented by the augmented Lagrangian approach developed in [55]. In [22], Levenberg-Marquardt and Landweber algorithms are proposed, which are able to deal also with nonlinear direct problems. Moreover, a relaxation strategy for the optimization problem has been explored by means of Modica-Mortola and Mumford-Shah functionals in [124] and recently in [66]. Finally, we recall also the approach related to Bayesian statistical inversion, see [94].

Concerning the reconstruction algorithms in the case of small inclusions, both direct and variational methods usually rely on an asymptotic formula for the perturbation of the boundary potential to identify the location and additional features of the shape of the inclusions. For an extended review, we refer to [13, Chapter 5]). We only recall, among the direct approaches, the constant current projection algorithm in [14], together with the linear sampling method ([63]) and the MUSIC algorithm ([68]), developed for an inverse scattering problem, which inspired several techniques also for the inverse conductivity problem, see [43]. Although these algorithms have proved to be effective, they strictly depend on the linearity of the direct problem, especially concerning explicit formulas for single and double layer potentials, and the analytic expression of some particular solutions. Variational techniques involved in the reconstruction of small inclusions, usually involving tools from topological optimization, have been developed for linear problems in several contexts (see for instance [18] and [70] for crack detection, [15] and [50] for the detection of sound obstacles, [100] and [32] for image processing, [21] for image segmentation), and have been successfully applied for the inverse (linear) conductivity problem ([52], [17]) to identify the position of the center of small conductivity inclusions. For the nonlinear problem at hand, a preliminary result in this direction has been achieved in [30] and motivates our study.

As a final remark, we report that the inverse problem of identifying ischemias from measurements of surface potentials has been tackled in an optimization framework for numerical purposes in a significant number of recent papers, see in particular [8, 40, 54, 85, 105, 112, 126]. Nevertheless, a detailed mathematical analysis of the inverse problem has never been performed, mainly due to outlined difficulties involving the small number of measurement at disposal and the nonlinearity both of the inverse and of the direct problem.

1.4 Main contributions of the thesis

The goal of the thesis is to pave the way for a rigorous analysis of the inverse problem defined in 1.2 both from a theoretical and a reconstruction standpoint. In a stepwise fashion, we focus on the following main objectives:

- **Identification of small inclusions in an elliptic semilinear boundary value problem**

We first tackle the inverse problem associated with problem (1.10) under the assumption that the inclusions to be detected are of small size. In this context, exploiting theoretical results recently achieved in [30], we are able to prove a (local) Lipschitz stability results for the inverse problem, which consists in the first theoretical result achieved in this field. Moreover, we develop a reconstruction algorithm for the identification of the solution by means of few measurements (or even a single one), based on the computation of the topological gradient of a suitable cost functional. Several numerical experiments associated to various test cases

assess the accuracy of the proposed technique, as well as its robustness with respect to noisy and partial measurements. This analysis, which is the object of Chapter 2, has been published in [33], except for the stability estimate.

- **Identification of small inclusions in a parabolic semilinear initial and boundary value problem**

The successive step is to consider the identification of small inclusions in a more complicated boundary value problem, namely when the evolutive monodomain model is considered with the simplest phenomenological law for the ionic current, reported in (1.8). We first focus on the development of a novel theoretical result involving this inverse problem, i.e. an asymptotic formula for electrical potential perturbations caused by internal conductivity inhomogeneities of low volume fraction. Exploiting this result, we implement a reconstruction procedure based on the computation of the topological gradient of a suitable cost functional, involving the solution of an adjoint problem. Numerical results obtained on a three-dimensional idealized left ventricle geometry for different measurement settings assess the feasibility and robustness of the proposed algorithm. This discussion is the object of Chapter 3 and has been published in [28].

- **Reconstruction of large inclusions in an elliptic semilinear problem: a shape derivative approach**

We afterward consider the identification of inclusions again in the stationary case, but removing the assumption of small size. As a first approach, we develop a shape derivative reconstruction algorithm. Such a method only requires *a priori* knowledge of the topology of the inclusion to be reconstructed, and aims at detecting it by updating an initial guess, according to the shape gradient of a suitable misfit functional. In order to derive a rigorous expression for the shape gradient, we need to theoretically investigate the asymptotic perturbation of the boundary voltage (and associated quantities) under small perturbations of a large inclusion. After proving such results, we formulate the algorithm in details and provide a satisfactory numerical validation. This is object of Chapter 4.

- **Reconstruction of large inclusions in an elliptic semilinear problem: a phase-field approach**

Focusing on the same problem, we develop a novel approach for the presented inverse problem, which allows removing any *a priori* assumption on the inclusion. We formulate a constraint minimization problem involving a quadratic mismatch functional enhanced with a regularization term which penalizes the perimeter of the inclusion to be identified. We introduce a phase-field relaxation of the problem, employing a Modica-Mortola functional and assessing the Γ -convergence of the relaxed functional to the original one. After computing the optimality conditions of the phase-field optimization problem and introducing a discrete Finite Element formulation, we propose an iterative algorithm and prove convergence properties. Several numerical results are reported, assessing the effectiveness and the robustness of the algorithm in identifying arbitrarily-shaped inclusions. Finally, we compare our approach to a couple of alternative methods, in particular focusing on shape-derivative based technique, comparing it to the sharp interface limit of the proposed relaxed problem. This discussion, which is the

object of Chapter 5, has been published in [35]

- **Towards the identification of ischemias in the monodomain model: analysis of the direct problem**

The last part of the thesis is dedicated to preliminary results which are required in order to extend the presented discussion to the case of the monodomain model for the full heartbeat description. When dealing with the initial and boundary value problem (1.9), before tackling the goal of detecting small ischemic areas (by means of topology optimization tools) or arbitrarily large ones, it is necessary to extend the results available in the present literature involving the well-posedness of the direct problem itself. In Chapter 6, we state and prove an existence, uniqueness and comparison result of classical solutions of the monodomain model without ischemias, as well as a result of existence and uniqueness of weak solutions in the perturbed case. We can eventually prove additional regularity for the perturbed potential, in view of a useful comparison result. This discussion is also the object of a paper in preparation, [29]

- **Towards the identification of ischemias in the monodomain model: *a posteriori* numerical error analysis**

The final step of our study is devoted to the numerical analysis of a Newton-Galerkin solver for the monodomain problem. In fact, when aiming at extending to the monodomain case the developed reconstruction algorithms (and in particular the ones for large inclusions, which requires the solution of the direct problem several times), it is necessary to tackle the task of reducing the computational cost. One strategy is represented by the introduction of an adaptive algorithm, allowing for a speedup in the computation of the approximated solution of the direct problem. Such an approach requires to perform a numerical *a posteriori* error analysis of the problem, in particular deriving computable error estimators. This is the object of Chapter 7, and also of a work under review, [120].

Chapter 2

Identification of small inclusions in a semilinear elliptic boundary value problem

In this chapter, we focus on the detection of small inclusions in the semilinear elliptic problem introduced in Chapter 1 as a simplified version of the monodomain problem. We start by briefly outlining the formulation of the problem and the related assumptions. According to the expression provided in Section 1.2.1, we consider the following boundary value problem:

$$\begin{cases} -\Delta U + U^3 = f & \text{in } \Omega \\ \partial_\nu U = 0 & \text{on } \partial\Omega, \end{cases} \quad (2.1)$$

which is related to the case in which no inhomogeneity in the coefficients is present. We assume that the background value of the scalar conductivity coefficient is 1, that f is a known forcing term, and that Ω is an open connected subset of \mathbb{R}^n , $n = 2, 3$. Problem (2.1) is addressed as the *background* problem, and its solution U is defined the *unperturbed* potential. We now consider an alteration of the coefficients of the problem induced by the presence of an inclusion $\omega \subset \Omega$. Throughout this chapter, we deal with inclusions ω_ε of small size which are well separated from the boundary, i.e. such that:

$$|\omega_\varepsilon| \rightarrow 0 \text{ as } \varepsilon \rightarrow 0 \quad (2.2)$$

$$\exists \tilde{K}_0 \subset \Omega \text{ compact s.t. } \omega_\varepsilon \subset \subset \tilde{K}_0, \quad \text{dist}(\partial\Omega, \tilde{K}_0) \geq d_0 > 0. \quad (2.3)$$

In addition, the majority of the results formulated in the chapter assume that ω_ε satisfy more specific conditions, namely that

$$\omega_\varepsilon = (z + \varepsilon D) = \{x \in \Omega \text{ s.t. } \exists d \in D : x = z + \varepsilon d\}, \text{ s.t. } \text{dist}(z, \partial\Omega) \geq d_0 > 0 \quad (2.4)$$

being D an open, bounded and regular domain containing the origin. The inclusion ω_ε therefore consists of a single connected set, with center z , prescribed shape D and small size. When an inhomogeneity ω_ε is introduced in Ω , the coefficients of the semilinear elliptic problem are altered

as described in Section 1.1.3. As a result, the *perturbed* potential u_ε is the solution of the following problem:

$$\begin{cases} -\operatorname{div}(k_\varepsilon \nabla u_\varepsilon) + (1 - \chi_{\omega_\varepsilon})u_\varepsilon^3 = f & \text{in } \Omega \\ \partial_\nu u_\varepsilon = 0 & \text{on } \partial\Omega, \end{cases} \quad (2.5)$$

where $\chi_{\omega_\varepsilon}$ is the indicator function of the set ω_ε and $k_\varepsilon = 1 - (1 - k)\chi_{\omega_\varepsilon}$, $k < 1$. According to the introduced boundary value problems, we define:

Definition 2.1 (Direct problem). Knowing the inclusion ω_ε , determine the perturbed potential u_ε associated to ω_ε through (2.5);

and conversely

Definition 2.2 (Inverse problem). Knowing the perturbed potential, and in particular only the boundary measurement $u_{meas} = u_\varepsilon|_{\partial\Omega}$, determine the inclusion ω_ε associated to u_{meas} through (2.5)

As deeply analyzed in Section 1.3, the well-posedness of the stated inverse problem is an open issue, i.e. according to the present literature, it is impossible to assess that for a fixed datum u_{meas} the solution ω_ε exists, is unique, and continuously depends on the datum. In this chapter, although, we assume that the inhomogeneity to be identified satisfies also (2.2), and in particular (2.4). These assumptions are referred to as *regularization* hypotheses: indeed, if we *a priori* restrict the search for the solution within the class of inclusions satisfying them, we are able to recover some results of well-posedness. We remark that this restricts the class of problems which are the object of discussion: in particular, if (2.4) is considered, we suppose to know in advance the shape D of the inclusion, and the inverse problem 2.2 reduces to the individuation of its center z .

The main results of this chapter, except for Section 2.2, are published in [33]. In particular, in Section 2.1 we report the most relevant results regarding the well-posedness of the direct problem and further properties of its solution, which are already available in the literature, see [30]. In Section 2.2, we instead focus on the analysis of the inverse problem. In particular, we exploit the asymptotic expansion of the perturbation of boundary potential derived in [30] in order to prove a local Lipschitz stability result for the solution of the inverse problem under the assumption (2.4). In Section 2.3, we introduce a Topological Optimization framework for the inverse problem, by formulating a minimization problem on a suitable functional, for which we introduce the concept of topological gradient. We then exploit the introduced asymptotic expansion in order to provide a representation formula for the gradient, and we use it to formulate a rigorous reconstruction algorithm. In Section 2.4, we show through several numerical experiments the effectiveness and feasibility of the introduced algorithm.

2.1 Analysis of the direct problem

We start by recalling the well-posedness results available for the direct problem. The weak formulation of the Neumann homogeneous problem (2.5) reads as follows: find $u \in V = H^1(\Omega)$ s.t.

$$\langle T(u) - F, v \rangle_* = 0 \quad \forall v \in V, \quad (2.6)$$

where $\langle \cdot, \cdot \rangle_*$ is the duality pairing between V and its dual space V^* and $F, T(u) \in V^*$ are defined by:

$$\begin{aligned} \langle T(u), v \rangle_{V^*, V} &= \int_{\Omega} k(x) \nabla u \cdot \nabla v + \int_{\Omega} (1 - \chi_{\omega}) u^3 v, \\ \langle F, v \rangle_{V^*, V} &= \int_{\Omega} f v, \quad f \in L^p(\Omega), \quad p \geq 2. \end{aligned} \quad (2.7)$$

We refer to those inclusions ω_{ε} of small dimensions which are well separated from the boundary, i.e. satisfying (2.2) and (2.3).

Proposition 2.1. *For every forcing term $f \in L^p(\Omega)$, $p \geq 2$, and every admissible inclusion ω_{ε} , problem (2.6) admits a unique solution $u_{\varepsilon} \in V$.*

The proof of Proposition 2.1 can be found in [30] and relies on the properties of the operator T previously defined, and in particular on the fact that it is strictly monotonic. The argument also relies on the following Poincarè inequality, which is derived from [102, Theorem 8.11]: $\forall v \in H^1(\Omega)$,

$$\|v\|_{H^1(\Omega)} \leq C \left(\|\nabla v\|_{L^2(\Omega)} + \|v\|_{L^2(\Omega \setminus \omega_{\varepsilon})} \right), \quad (2.8)$$

where the constant C can be chosen s.t. it is independent of ε .

In order to derive further results which will be useful for the analysis of the inverse problem, we make use of the unperturbed potential U introduced in (2.1). The existence and uniqueness of U is assessed by [30, Proposition 4.2], where it is also proved that U and ∇U are Hölder continuous functions and the norm of U in the space $W^{1,\infty}(\Omega)$ is bounded by a suitable norm of f , namely:

$$\|U\|_{L^{\infty}(\Omega)}, \|\nabla U\|_{L^{\infty}(\Omega)} \leq C(\|f\|_{L^p(\Omega)} + \|f\|_{L^p(\Omega)}^3),$$

Moreover, further regularity can be proved also for the perturbed potential, exploiting the interior estimates from [82] and extending them up to the boundary, concluding that u_{ε} is Hölder continuous on $\overline{\Omega}$ (see [30, equation (4.14)]). Furthermore, the following *energy estimates* hold for the difference between unperturbed and perturbed solutions:

$$\begin{aligned} \|u_{\varepsilon} - U\|_{H^1(\Omega)} &\leq |\omega_{\varepsilon}|^{\frac{1}{2}} \\ \|u_{\varepsilon} - U\|_{L^2(\Omega)} &\leq |\omega_{\varepsilon}|^{\frac{1}{2} + \eta}, \quad 0 < \eta < \frac{1}{5} \end{aligned} \quad (2.9)$$

The proof of these estimates is carried out under an additional assumption on the forcing term f , namely that

$$\exists m > 0 \text{ s.t. } f(x) \geq m \quad \forall x \in \Omega. \quad (2.10)$$

This restriction can be avoided, as it is possible to weaken (2.10) by only assuming that f does not identically vanish, i.e.

$$\|f\|_{L^p(\Omega)} \neq 0 \quad (2.11)$$

Indeed, in the proofs delivered in [30], hypothesis (2.10) is only required in order to prove that the following estimate from below holds:

$$\exists C = C(|\Omega \setminus \omega_{\varepsilon}|, m) > 0 \text{ s.t. } \int_{\Omega \setminus \omega_{\varepsilon}} q_{\varepsilon} > C, \quad \text{where } q_{\varepsilon} = U^2 + U u_{\varepsilon} + u_{\varepsilon}^2.$$

Hence, we can substitute it as follows: if $f \in L^p(\Omega)$ satisfies (2.11), then $\exists C = C(|\Omega \setminus \omega_\varepsilon|, f) > 0$ s.t. $\int_{\Omega \setminus \omega_\varepsilon} q_\varepsilon > C$. Indeed, if f satisfies (2.11), then also U cannot identically vanish, otherwise it could not solve (2.1). Hence, denoting $M = \|U\|_\infty$, we can ensure that $M > 0$. Consider

$$\Omega_0 = \{x \in \Omega : |U(x)| \leq M/2\} \text{ and } \Omega_1 = \{x \in \Omega : |U(x)| > M/2\} :$$

as U is continuous in Ω (see Proposition 4.2 in [30], independent of hypothesis (2.10)), we conclude that $|\Omega_1| > 0$. We introduce \tilde{U} defined as follows:

$$\tilde{U}(x) = \begin{cases} M/2 & x \in \Omega_1 \\ 0 & x \in \Omega_0. \end{cases}$$

By definition, $U^2(x) \geq \tilde{U}^2(x) \quad \forall x \in \Omega$; hence, we obtain:

$$\int_{\Omega \setminus \omega_\varepsilon} q_\varepsilon \geq \int_{\Omega \setminus \omega_\varepsilon} \frac{3}{4} U^2 \geq \int_{\Omega \setminus \omega_\varepsilon} \frac{3}{4} \tilde{U}^2 \geq \tilde{C} M^2 |\Omega_1| = C > 0.$$

We remark that hypothesis (2.10) allows to write an estimate for the quantity q_ε (and therefore for $\|u_\varepsilon - U\|_{H^1(\Omega)}$) which is independent of U and ultimately from the choice of the forcing term f , whereas the weakened one, (2.11), entails an estimate which depends on M and Ω_1 and hence on f . Nevertheless, this allows to use (2.9) and its consequences in the proposed weaker hypothesis, and does not compromise the effectiveness of such estimate in the case of our application.

2.2 Analysis of the inverse problem

The crucial result contained in [30] is the asymptotic expansion of the perturbation induced in the boundary potential by the introduction of an inclusion of small size. We report here the result in the general case: the proof can be found in [30].

Theorem 2.1. *Let ω_ε be a family of subdomains satisfying (2.2) and (2.3), $f \in L^p(\Omega)$, $p > n$, and let f satisfy (2.10) (or (2.11)). Then, there exist a subsequence $\{u_{\varepsilon_n}\}$, a Radon measure μ and a symmetric matrix-valued function $\mathcal{M} \in L^2(\Omega; \mu)$ s.t. $w_\varepsilon = u_\varepsilon - U$ satisfies, for any $y \in \partial\Omega$:*

$$w_\varepsilon(y) = |\omega_\varepsilon| \int_{\Omega} [(1-k)\mathcal{M}\nabla U \cdot \nabla_x N_U(\cdot, y) + U^3(z)N_U(\cdot, y)] d\mu + o(|\omega_\varepsilon|). \quad (2.12)$$

The function N_U appearing in the first order term of the expansion is the Neumann function related to the operator $-\Delta + 3U^2$, i.e. the solution, for each $y \in \Omega$, of

$$\begin{cases} -\Delta_x N_U(x, y) + 3U^2(x)N_U(x, y) = \delta(x - y) & \text{in } \Omega \\ \partial_{\nu_x} N_U(x, y) = 0 & \text{on } \partial\Omega. \end{cases} \quad (2.13)$$

We now restrict ourselves to a more specific class of inclusions, namely those of the form (2.4). In this case, the expansion in Theorem 2.1 can be written as

$$w_\varepsilon(y) = \varepsilon^n [(1-k)\nabla U(z)^T \mathcal{M} \nabla_x N_U(z, y) + U^3(z)N_U(z, y)] + o(\varepsilon^n). \quad (2.14)$$

The matrix $M \in \mathbb{R}^{n \times n}$ is called *polarization tensor* and depends only on the coefficient k and on the shape D of the inclusion. Moreover, it can be explicitly computed for some specific shapes (see, e.g., [13] for a detailed derivation): for instance, if $n = 2$ and the inclusion has circular shape, the following expression holds:

$$M = \frac{2}{1+k} |D| \mathbf{I}_{2 \times 2}. \quad (2.15)$$

If the inclusion has elliptical shape with major axis aligned in the direction b and ratio r between the axes,

$$M = M(k, b, r) = R^T \widetilde{M} R, \quad (2.16)$$

being

$$\widetilde{M} = (k-1) |D| \begin{pmatrix} \frac{1+r}{1+kr} & 0 \\ 0 & \frac{1+r}{r+k} \end{pmatrix}, \quad R = \begin{pmatrix} b_x & -b_y \\ b_y & b_x \end{pmatrix}.$$

Remark 2.1. Exploiting the enhanced energy estimate $\|U - u_\varepsilon\|_{L^2(\Omega)} \leq C|\omega_\varepsilon|^{\frac{1}{2}+\eta}$, $\eta \in (0, \frac{1}{5}]$ (see [30, Theorem 4.3]) together with the estimate $\left\|v_\varepsilon^{(j)} - v^{(j)}\right\|_{L^2(\Omega)} \leq C|\omega_\varepsilon|^{\frac{1}{2}+\eta}$, $\eta \in (0, \frac{1}{\max\{d, 2\}})$ (see [47, Lemma 1]), we can conclude that the remainder term appearing in (2.12) satisfies:

$$o(|\omega_\varepsilon|) \leq C|\omega_\varepsilon|^{1+\beta}, \quad \beta \in \left(0, \frac{1}{5}\right].$$

In this section, we aim at exploiting the asymptotic expansion in (2.14) in order to derive the unique well-posedness result available for the inverse problem under consideration: a (local) stability estimate of the solution z (the center of the inclusion to be detected) with respect to a suitable norm of the datum, $u_{meas} = u_\varepsilon|_{\partial\Omega}$. The analysis performed in this section is valid under more restrictive assumptions on the source term and the unperturbed potential, namely:

Assumption 1. Consider $f \in C^\alpha(\overline{\Omega})$ and require $\nabla U(z) \neq 0 \forall z \in \Omega$.

The requirements on f in particular imply, by elliptic regularity results, that $U \in C^{2+\alpha}(\Omega)$. The main result we aim to prove is the following one:

Theorem 2.2. *There exist some constants ε_0 , δ_0 , C_1 and C_2 such that, $\forall \varepsilon < \varepsilon_0$ and $\forall z, z'$ s.t. $\varepsilon^{-n} \|u_\varepsilon - u'_\varepsilon\|_{L^\infty(\partial\Omega)} \leq \delta_0$ where u_ε and u'_ε are the solutions of (2.5) in presence of an inclusion of the form $\{z + \varepsilon D\}$ and $\{z' + \varepsilon D\}$ respectively, it holds:*

$$|z - z'| \leq C_1 \varepsilon^{-n} \|u_\varepsilon - u'_\varepsilon\|_{L^\infty(\partial\Omega)} + C_2 \varepsilon^{\beta n},$$

for all $\beta \in (0, 1/5)$.

In order to prove Theorem 2.2, we first need to derive preliminary results regarding the Neumann function N_U . First of all, it is possible to decompose $N_U(x, y) = N(x, y) + Z(x, y)$, where N is the Neumann function associated to the Laplace operator and Z a regular reminder, i.e., they solve the following problems:

$$\begin{cases} -\Delta_x N(x, y) = \delta_y(x) & \text{in } \Omega \\ \partial_{\nu_x} N(x, y) = \frac{1}{|\partial\Omega|} & \text{on } \partial\Omega. \end{cases} \quad (2.17)$$

$$\begin{cases} -\Delta_x Z(x, y) + 3U^2(x)Z(x, y) = -3U^2(x)N(x, y) & \text{in } \Omega \\ \partial_{\nu_x} Z(x, y) = -\frac{1}{|\partial\Omega|} & \text{on } \partial\Omega. \end{cases} \quad (2.18)$$

Moreover, the Neumann function N can be decomposed as $N(x, y) = \Phi(x - y) + R(x, y)$, where

$$\Phi(x - y) = \begin{cases} -\frac{1}{2\pi} \ln|x - y| & n = 2 \\ \frac{1}{n(n-2)\alpha_n} |x - y|^{2-n} & n \geq 3 \end{cases} \quad (2.19)$$

is the fundamental solution of the Laplace operator (being α_n the volume of the unit ball in \mathbb{R}^n), and the residual R satisfies

$$\begin{cases} -\Delta_x R(x, y) = 0 & \text{in } \Omega \\ \partial_{\nu_x} R(x, y) = \frac{1}{|\partial\Omega|} - \partial_{\nu_x} \Phi(x - y) & \text{on } \partial\Omega. \end{cases} \quad (2.20)$$

According to the results in [78], the following properties hold:

- $N(x, y) = N(y, x)$ (symmetry of the Neumann function)
- $N(\cdot, y), N(x, \cdot) \in W^{1,p}(\Omega) \forall p \in \left[1, \frac{n}{n-1}\right)$
- $\nabla_x N(x, \cdot) \cdot \alpha \in L^p(\Omega) \forall \alpha \in \mathbb{R}^n, \forall p \in \left[1, \frac{n}{n-1}\right)$
- $D_x^2 N(x, \cdot) \alpha \cdot \beta \notin L^1(\Omega) \forall \alpha, \beta \in \mathbb{R}^n, \alpha, \beta \neq 0$.

We now show that the same results hold on N_U :

Proposition 2.2. *Consider N_U defined as in (2.13), $N_U(x, y) = \Phi(x - y) + R(x, y) + Z(x, y)$. Then,*

- $N_U(x, y) = N_U(y, x)$ (symmetry of the Neumann function)
- $N_U(\cdot, y), N_U(x, \cdot) \in W^{1,p}(\Omega) \forall p \in \left[1, \frac{n}{n-1}\right)$
- $\nabla_x N_U(x, \cdot) \cdot \alpha \in L^p(\Omega) \forall \alpha \in \mathbb{R}^n, \forall p \in \left[1, \frac{n}{n-1}\right)$
- $D_x^2 N_U(x, \cdot) \alpha \cdot \beta \notin L^1(\Omega) \forall \alpha, \beta \in \mathbb{R}^n, \alpha, \beta \neq 0$.

Proof. We first of all remark that according to (2.18), $Z(\cdot, y)$ is the solution of an elliptic problem with continuous coefficients and source term in $L^p(\Omega)$: via elliptic regularity results (see e.g. [84, Lemma 2.4.1.4]), $Z(\cdot, y) \in W^{2,p}(\Omega)$ and moreover, according to local Hölder estimates for the gradient (see e.g. [82, Theorem 4.15]), we can ensure that $\nabla Z(\cdot, y)$ is Hölder continuous away from y .

In order to prove that N_U is symmetric, we can adapt the proof of [74, Theorem 13, Chapter 2]. Take $x, y \in \Omega$ and denote $v(z) = N_U(z, x)$ and $w(z) = N_U(z, y)$: we remark that, away from x ,

$\nabla v + 3U(z)^2 v = 0$ and away from y $\nabla w + 3U(z)^2 w = 0$. Moreover $\frac{\partial v}{\partial \nu} = \frac{\partial w}{\partial \nu} = 0$ for $z \in \partial\Omega$. Define $V = \Omega \setminus B(x, \varepsilon) \setminus B(y, \varepsilon)$, for $0 < \varepsilon < \min\{\frac{1}{2} \text{dist}(x, y), \text{dist}(x, \partial\Omega), \text{dist}(y, \partial\Omega)\}$. It holds that

$$\begin{aligned} & \int_{\partial B(x, \varepsilon)} \frac{\partial v}{\partial \nu} w + \int_{\partial B(y, \varepsilon)} \frac{\partial v}{\partial \nu} w \\ &= \int_{\partial V} \frac{\partial v}{\partial \nu} w - \int_{\partial\Omega} \frac{\partial v}{\partial \nu} w = \int_V \text{div}(\nabla v w) = \int_V \nabla v \cdot \nabla w + \int_V \Delta v w \\ &= \int_V \nabla v \cdot \nabla w - \int_V 3U^2 v w = \int_V \nabla v \cdot \nabla w + \int_V \Delta w v = \int_V \text{div}(\nabla w v) = \int_{\partial V} \frac{\partial w}{\partial \nu} v \\ &= \int_{\partial B(x, \varepsilon)} \frac{\partial w}{\partial \nu} v + \int_{\partial B(y, \varepsilon)} \frac{\partial w}{\partial \nu} v \end{aligned}$$

We now aim at considering $\varepsilon \rightarrow 0$. On $\partial B(x, \varepsilon)$ since w is a smooth function on away from y and $\frac{\partial v}{\partial \nu} = \frac{\partial N_U(\cdot, x)}{\partial \nu} = \frac{\partial \Phi(x-z)}{\partial \nu} + \frac{\partial R}{\partial \nu} + \frac{\partial Z}{\partial \nu}$, where both R and Z are smooth functions: hence, for a suitable continuous function c ,

$$\begin{aligned} & \int_{\partial B(x, \varepsilon)} \frac{\partial v}{\partial \nu} w = \int_{\partial B(x, \varepsilon)} \frac{\partial \Phi(x-z)}{\partial \nu} w(z) + \int_{\partial B(x, \varepsilon)} c(z) \\ &= \int_{\partial B(x, \varepsilon)} \frac{1}{n\alpha_n \varepsilon^{n-1}} w(z) + \int_{\partial B(x, \varepsilon)} c(z) = \int_{\partial B(x, \varepsilon)} w(z) + \int_{\partial B(x, \varepsilon)} c(z) \rightarrow w(x). \end{aligned}$$

Conversely, since $v(z) = \Phi(z-x) + R(z, x) + Z(z, x)$ and $\Phi(z-x) = o(\varepsilon^{n-1})$ when $z \in \partial B(x, \varepsilon)$, we conclude

$$\int_{\partial B(x, \varepsilon)} \frac{\partial w}{\partial \nu} v \rightarrow 0.$$

With analogous arguments, one can show

$$\int_{\partial B(y, \varepsilon)} \frac{\partial w}{\partial \nu} v \rightarrow v(y) \quad \text{and} \quad \int_{\partial B(y, \varepsilon)} \frac{\partial v}{\partial \nu} w \rightarrow 0.$$

Finally we conclude that, letting $\varepsilon \rightarrow 0$, $w(x) = v(y)$, namely $N(x, y) = N(y, x)$.

From the fact that $Z(\cdot, y) \in W^{2,p}(\Omega)$ and $N(\cdot, y) \in W^{1,p}(\Omega)$, we immediately have $N_U(\cdot, y) \in W^{1,p}(\Omega) \forall p \in \left[1, \frac{n}{n-1}\right)$, $\nabla_x N_U(x, \cdot) \cdot \alpha \in L^p(\Omega) \forall \alpha \in \mathbb{R}^n$, whereas $D_x^2 N_U(x, \cdot) \alpha \cdot \beta \notin L^1(\Omega) \forall \alpha, \beta \in \mathbb{R}^n$, $\alpha, \beta \neq 0$. \square

We now move towards the stability result. Analogously to what performed in [78, Lemma 3.3], it is possible to extend formula (2.14) to all $y \in \bar{\Omega}$ s.t. $\text{dist}(y, z) \geq d_0$. Denote with $F_z(y)$ the first order term in expansion (2.14) for an inclusion centered in z , and $DF_z[dz](y)$ its (Fréchet) differential with respect to z :

$$\begin{aligned} F_z(y) &= (1-k)M\nabla U(z) \cdot \nabla_x N_U(z, y) + U^3(z)N_U(z, y) \\ DF_z[dz](y) &= (1-k)MD^2U(z)dz \cdot \nabla_x N_U(z, y) + (1-k)M\nabla U(z) \cdot D_x^2 N_U(z, y)dz \\ &\quad + 3U^2(z)\nabla U(z) \cdot dz N_U(z, y) + 3U^2(z)\nabla_x N_U(z, y) \cdot dz. \end{aligned}$$

When considering two different inclusions centered in z and z' , we let

$$H(z, z') = \|F_z - F_{z'}\|_{L^\infty(\partial\Omega)}$$

The following two results allow to prove the stability of the center z of the inclusion with respect to perturbations of the boundary data, measured in the L^∞ norm.

Lemma 2.1. *For every pair of sequences $\{z_m\}$, $\{z'_m\}$ such that $\text{dist}(\{z_m\} \cup \{z'_m\}, \partial\Omega) \geq d_0$ and $H(z_m, z'_m) \rightarrow 0$ as $m \rightarrow +\infty$, we have that $|z_m - z'_m| \rightarrow 0$*

Proof. The thesis can be thoroughly rewritten as

$$\begin{aligned} \forall \{z_m\}, \{z'_m\}, \text{ if } \forall \zeta > 0 \quad \exists M_1 > 0 \text{ s.t. } H(z_m, z'_m) \leq \zeta \quad \forall m \geq M_1 \\ \text{then } \forall \eta > 0 \quad \exists M_2 > 0 \text{ s.t. } |z_m - z'_m| \leq \eta \quad \forall m \geq M_2; \end{aligned}$$

by contradiction, suppose

$$\begin{aligned} \exists \{z_m\}, \{z'_m\} \text{ s.t. } \forall \zeta > 0 \quad \exists M_1 > 0 \text{ s.t. } H(z_m, z'_m) \leq \zeta \quad \forall m \geq M_1 \\ \text{and } \exists \eta > 0 \text{ s.t. } |z_m - z'_m| \geq \eta \quad \forall m \end{aligned}$$

In particular, select the subsequences (still referred as $\{z_m\}, \{z'_m\}$) such that, e.g.,

$$H(z_m, z'_m) \leq \frac{1}{m} \quad \text{and} \quad |z_m - z'_m| > \eta.$$

Since $\{z_m\}, \{z'_m\} \subset \Omega$ are bounded, $\exists z, z' \in \Omega$ s.t., possibly up to a subsequence,

$$z_m \rightarrow z, \quad z'_m \rightarrow z', \quad |z - z'| > \eta, \quad (2.21)$$

and as a consequence of the hypothesis, $\text{dist}(z, \partial\Omega), \text{dist}(z', \partial\Omega) \geq d_0$. Fix now $y \in \partial\Omega$ and consider the Neumann function $N_U(\cdot, y)$: by the regularity of N far from y and the regularity of Z everywhere, we can ensure that $N_U(\cdot, y)$ and $\nabla_x N_U(\cdot, y)$ are continuous functions far from the boundary: in particular, the function $F_z(y)$ with $y \in \partial\Omega$ is continuous with respect to z , if z is sufficiently far from the boundary. Since $\text{dist}(z_m, \partial\Omega) \geq d_0$, $\text{dist}(z'_m, \partial\Omega) \geq d_0$ and since $H(z_m, z'_m) \rightarrow 0$,

$$F_z(y) = \lim_m F_{z_m}(y) = \lim_m F_{z'_m}(y) = F_{z'}(y) \quad \forall y \in \partial\Omega.$$

Consider the expression of $G(y) = F_z(y) - F_{z'}(y)$:

$$\begin{aligned} G(y) &= (1-k)M\nabla U(z) \cdot \nabla_x N_U(z, y) + U^3(z)N_U(z, y) \\ &\quad - (1-k)M\nabla U(z') \cdot \nabla_x N_U(z', y) - U^3(z')N_U(z', y) \end{aligned} \quad (2.22)$$

We observe that $G(y)$ is the solution of the following Cauchy problem:

$$\begin{cases} -\Delta_y G(y) + 3U^2(y)G(y) = 0 & \text{in } \Omega \setminus \{z, z'\} \\ \partial_{\nu_y} G(y) = 0 & \text{on } \partial\Omega \\ G(y) = 0 & \text{on } \partial\Omega, \end{cases}$$

Indeed, taking advantage of the symmetry of N_U and since z, z' are well separated from $\partial\Omega$,

$$\begin{aligned} \partial_{\nu_y} N_U(z, y) &= \nabla_y N_U(z, y) \cdot \nu = \nabla_x N_U(y, z) \cdot \nu = \partial_{\nu_x} N_U(y, z) = \partial_{\nu_x} N_U(z, y) = 0 \\ \partial_{\nu_y} \nabla_x N_U(z, y) &= \nabla_x \partial_{\nu_y} N_U(z, y) = \nabla_x \partial_{\nu_y} N_U(y, z) = 0 \end{aligned}$$

and moreover, $\forall z \neq y$,

$$\begin{aligned} (-\Delta_y + 3U^2(y))N_U(z, y) &= (-\Delta_x + 3U^2(z))N_U(y, z) = (-\Delta_x + 3U^2(z))N_U(z, y) = 0 \\ (-\Delta_y + 3U^2(y))\nabla_x N_U(z, y) &= \nabla_y(-\Delta_x + 3U^2(z))N_U(y, z) = \nabla_y(-\Delta_x + 3U^2(z))N_U(z, y) = 0. \end{aligned}$$

According to the unique continuation property for the Cauchy problem for elliptic equations with regular coefficients [5, Theorem 1.9], we conclude that $G = 0$ in $\Omega \setminus \{z, z'\}$. This entails a contradiction: indeed, due to the definition of N and to the regularity of Z , the terms $N_U(z, y)$ and $N_U(z', y)$ show a singularity when approaching z and z' , of the kind $\ln|y - z|$ if $n = 2$ or $|y - z|^{-1}$ if $n = 3$. Those singularity cannot cancel with the terms $\nabla_x N(z, y)$, which grow with a different rate (namely, as $|y - z|^{d-1}$); according to the expression of G in (2.22), the coefficient appearing in front of $N_U(z, y)$ and $N_U(z', y)$ do not vanish because of Assumption 1: the only solution to guarantee $G(y) = 0$ would be to put $z = z'$, which is in contrast with (2.21). \square

Lemma 2.2. *There exist two positive constants δ and C depending on d_0, Ω, D, k , such that*

$$\forall z, z' \text{ s.t. } H(z, z') \leq \delta \Rightarrow |z - z'| < CH(z, z')$$

Proof. The proof is done by contradiction, by supposing that

$$\forall \delta, \forall C \exists z, z' \text{ s.t. } H(z, z') \leq \delta \text{ and } |z - z'| > CH(z, z'),$$

which is equivalent to

$$\forall \delta, \forall C \quad \exists z, z' \text{ s.t. } H(z, z') \leq \delta \text{ and } \frac{H(z, z')}{|z - z'|} < \frac{1}{C}.$$

Consider the sequences $\{z_m\}, \{z'_m\}$ associated with the values, e.g., $\delta_m = \frac{1}{m}$ and $C_m = m$: we immediately remark that

$$H(z_m, z'_m) \rightarrow 0 \quad \text{and} \quad \frac{H(z_m, z'_m)}{|z_m - z'_m|} \rightarrow 0.$$

In view of Lemma 2.2, $z_m \rightarrow z, z'_m \rightarrow z'$ and $z = z'$. Consider now the sequence $\{dz_m\} = \left\{ \frac{z_m - z'_m}{|z_m - z'_m|} \right\}$: since $|dz_m| = 1$, there exists a converging subsequence (still denoted as dz_m):

$$dz_m \rightarrow dz \in \mathbb{R}^n, \quad |dz| = 1. \quad (2.23)$$

By the definition of the Fréchet derivative and by linearity:

$$0 = \lim_m \frac{\|F_{z_m} - F_{z'_m}\|_{L^\infty(\partial\Omega)}}{|z_m - z'_m|} = \lim_m \frac{\|DF_{z_m}[z_m - z'_m]\|_{L^\infty(\partial\Omega)}}{|z_m - z'_m|} = \lim_m \|DF_{z_m}[dz_m]\|_{L^\infty(\partial\Omega)},$$

whence

$$\lim_m DF_{z_m}[dz_m](y) = 0 \quad \forall y \in \partial\Omega.$$

Since $\forall y \in \partial\Omega$

$$DF_{z_m}[dz_m](y) - DF_z[dz](y) = DF_{z_m}[dz_m - dz](y) + (DF_{z_m}[dz](y) - DF_z[dz](y)). \quad (2.24)$$

Notice that, by elliptic regularity results applied to U and N_U , in view of Assumption 1 and since $y \in \partial\Omega$, the function $DF_z[dz](y)$ is continuous with respect to z . Hence the first term in the left-hand side vanishes as $m \rightarrow +\infty$ since $dz_m \rightarrow dz$ and DF_{z_m} is uniformly bounded. Also the second

term in (2.24) vanishes by the continuity of DF_z . In conclusion, $DF_{z_m}[dz_m](y) \rightarrow DF_z[dz](y)$ and $DF_z[dz](y) = 0 \forall y \in \partial\Omega$. Again by the expression of $DF_z[dz]$, and by the symmetry of $N_U(x, y)$, as in the proof of Lemma 2.1, it is easy to verify that

$$\begin{cases} -\Delta_y DF_z[dz](y) + 3U^2(y)DF_z[dz](y) = 0 & \text{in } \Omega \setminus \{z\} \\ \partial_{\nu_y} DF_z[dz](y) = 0 & \text{on } \partial\Omega \\ DF_z[dz](y) = 0 & \text{on } \partial\Omega, \end{cases}$$

which entails (again via [5, Theorem 1.9]) that $DF_z[dz](y) = 0$. Together with the fact that $|dz| = 1$ and that ∇U does not vanish (due to Assumption 1), this is a contradiction with the fact that $D_x^2 N_U(z, y)\alpha \cdot \beta \notin L^1(\Omega)$. \square

It is finally possible to prove Theorem 2.2.

Proof. From the asymptotic expansion (2.12), we can ensure that $\exists \varepsilon_0 : \forall \varepsilon \leq \varepsilon$,

$$\begin{aligned} u_\varepsilon(y) - U(y) &= \varepsilon^n F_z(y) + \eta_1(\varepsilon, y) & \forall y \in \partial\Omega \\ u'_\varepsilon(y) - U(y) &= \varepsilon^n F_{z'}(y) + \eta_2(\varepsilon, y) & \forall y \in \partial\Omega \end{aligned}$$

being $\eta_1(\varepsilon, y), \eta_2(\varepsilon, y) = o(\varepsilon^n)$, and according to Remark 2.1,

$$\|\eta_1(\varepsilon, y)\|_{L^\infty(\partial\Omega)} + \|\eta_2(\varepsilon, y)\|_{L^\infty(\partial\Omega)} \leq C\varepsilon^{(1+\beta)n}.$$

Computing the difference between the expansions and taking the $L^\infty(\partial\Omega)$, we obtain

$$H(z, z') \leq \varepsilon^{-n} \|u_\varepsilon - u'_\varepsilon\|_{L^\infty(\partial\Omega)} + C\varepsilon^{\beta n} \leq \delta_0 + C\varepsilon^{\beta n}.$$

By choosing δ_0 and ε s.t. $\delta_0 + C\varepsilon^{\beta n} \leq \delta$ appearing in Lemma 2.2, we can apply such result and conclude the thesis. \square

By following the same approach as in [78], we can extend the result of Theorem 2.2 to the case of inclusions of the kind:

$$\omega_\varepsilon = \bigcup_{k=1}^K (z_k + \varepsilon \rho_k D), \quad (2.25)$$

consisting of K different connected components of the same shape with relative ratios ρ_k ; z_k and ρ_k satisfying

$$|z_k - z_j| \geq d_0 > 0 \quad \forall k \neq j, \quad \text{dist}(z_k, \partial\Omega) \geq d_0, \quad d_0 \leq \rho_k \leq D_0.$$

In this case, the (local) stability result assumes the form:

Theorem 2.3. *There exist some positive constants $\varepsilon_0, \delta_0, C_1, C_2$ s.t. if $\varepsilon < \varepsilon_0$ and $\varepsilon^{-n} \|u_\varepsilon - u'_\varepsilon\|_{L^\infty(\partial\Omega)} < \delta_0$, being u_ε and u'_ε associated to inclusions $\omega_\varepsilon, \omega'_\varepsilon$ satisfying (2.25), then:*

- (i) $K = K'$ and, after appropriate reordering,
- (ii) $|z_k - z'_k| + |\rho_k - \rho'_k| < C_1 \varepsilon^{-n} \|u_\varepsilon - u'_\varepsilon\|_{L^\infty(\partial\Omega)} + C_2 \varepsilon^{\beta n}$ for $k = 1, \dots, K$.

The proof is analogous to the one of [78, Theorem 1.1], adapting the argument to the semilinear problem in consideration as performed in the proofs of the previous results.

2.3 A topological gradient-based reconstruction algorithm

In this section, we describe a topological optimization framework which we can exploit to tackle the solution of the inverse problem. In particular, let us introduce the following objective functional:

$$J(\Omega_\varepsilon) = \int_{\partial\Omega} (u_\varepsilon - u_{meas})^2 d\sigma, \quad (2.26)$$

where Ω_ε denotes the domain Ω in which a small inclusion ω_ε is inserted, and u_ε the corresponding solution of the direct problem (2.5) in Ω_ε . Hence, we can rephrase the inverse problem in Definition 2.2 as follows: given the boundary datum u_{meas} , find ω_ε satisfying (2.3) and (2.4) such that

$$J(\Omega_\varepsilon) \rightarrow \min. \quad (2.27)$$

In order to solve problem (2.27), we need to describe the variation of the functional J from the unperturbed case (associated to a domain Ω without inclusions and to the corresponding potential U , the solution of (2.1)) to the case where an inclusion is present. This calls into play the topological gradient of the functional J , although with some differences with the original definition in [45] (see [52], [17]): in the case at hand, indeed, we are perturbing the topology of the domain by inserting inclusions instead of holes.

In particular, hypothesis (2.4) prescribes that the introduced inclusion is uniquely described by two variables: the position z of the center and the dimension ε . Hence, we can introduce the following simplified notation: hereon we will refer to $J(\Omega_\varepsilon)$ as $j(\varepsilon; z)$. Moreover, we notice that, when $\varepsilon = 0$, the function j does not depend on z . Hence we define, for the case in consideration, the *topological gradient* of J evaluated in Ω as the function $G : \Omega \rightarrow \mathbb{R}$ yielding the following expansion as $\varepsilon \rightarrow 0$:

$$j(\varepsilon; z) = j(0) + \varepsilon^n G(z) + o(\varepsilon^n), \quad z \in \Omega. \quad (2.28)$$

Therefore, at a first-order approximation, the value of $G(z)$ describes the variation of the functional j when introducing a small inclusion of center z . This entails that the best strategy to reduce j is to introduce the inclusion in the point where G attains its negative minimum value, provided that this latter exists.

In order to exploit for the sake of reconstruction the topological gradient, it is important to compute it in an alternative way with respect to the one described by the definition (2.28); this would indeed require the solution of several direct problems for each position $z \in \Omega$ where we want to estimate the topological gradient $G(z)$. We are able to prove a useful representation formula for the topological gradient G in every $z \in \Omega$ which only requires to solve two differential problems. We first of all need to prove the following ancillary result, which exploits the expansion in (2.14):

Lemma 2.3. *In the same hypotheses of Theorem 2.1, there exists a positive constant $C = C(k, d_0, f, \Omega)$ such that the perturbation on the boundary datum $(u_\varepsilon - U)|_{\partial\Omega}$ fulfills:*

$$\|u_\varepsilon - U\|_{L^2(\partial\Omega)} \leq C\varepsilon^{2n}. \quad (2.29)$$

Proof. The Neumann function N_U of the operator $-\Delta + 3U^2$ can be written as:

$$N_U(x, y) = \Phi(x, y) + \tilde{z}(x, y) \quad \forall x, y \in \Omega, \quad x \neq y, \quad (2.30)$$

where Φ is the fundamental solution of the operator $-\Delta$ (see (2.19)) and $\tilde{z} = Z + R$ defined in (2.18) and (2.20) respectively; moreover, for every $y \neq x$, $\tilde{z}(x, y)$ is the solution of

$$\begin{cases} -\Delta_x \tilde{z}(x, y) + 3U^2 \tilde{z}(x, y) = -3U^2 \Phi(x - y) & \text{in } \Omega \\ \partial_{\nu_x} \tilde{z}(x, y) = -\partial_{\nu} \Phi(x - y) & \text{on } \partial\Omega. \end{cases} \quad (2.31)$$

Consider an inclusion ω_ε satisfying (2.4), hence centered in a point z s.t. $\text{dist}(z, \partial\Omega) \geq d_0$. Then, the function $y \mapsto \Phi(y - z) \in L^2(\Omega)$ and also $y \mapsto \partial_{\nu} \Phi(y - z)|_{\partial\Omega} \in H^{1/2}(\partial\Omega)$. By regularity results on elliptic equations (see e.g. [74], [1]) one may conclude that $\tilde{z}(\cdot, z) \in H^2(\Omega)$ and $\tilde{z}(\cdot, z)|_{\partial\Omega} \in H^{3/2}(\partial\Omega)$. In particular, $\|\tilde{z}(\cdot, z)|_{\partial\Omega}\|_{L^2(\partial\Omega)}$ and $\|\nabla_x \tilde{z}(\cdot, z)|_{\partial\Omega}\|_{L^2(\partial\Omega)}$ are bounded by a constant $\tilde{C}_1 = \tilde{C}_1(d_0, \Omega)$. Moreover, as already reported, according to Proposition 4.2 in [30], it holds:

$$\|U\|_{L^\infty(\Omega)}, \|\nabla U\|_{L^\infty(\Omega)} \leq \tilde{C}(\|f\|_{L^p(\Omega)} + \|f\|_{L^p(\Omega)}^3) \leq \tilde{C}_2 = \tilde{C}_2(\|f\|_{L^p(\Omega)}). \quad (2.32)$$

Hence, from the expansion (2.14),

$$\begin{aligned} \|u_\varepsilon - U\|_{L^2(\partial\Omega)}^2 &= \int_{\partial\Omega} |u_\varepsilon(y) - U(y)|^2 d\sigma \\ &\leq 2(1 - k)^2 \varepsilon^{2n} \int_{\partial\Omega} (M \nabla U(z) \cdot \nabla_x N_U(z, y))^2 d\sigma + 2\varepsilon^{2n} \int_{\partial\Omega} U^6(z) N_U^2(z, y) d\sigma + o(\varepsilon^{2n}) \\ &\leq C \varepsilon^{2n} (\|\nabla N_U\|_{L^2(\partial\Omega)}^2 + \|N_U\|_{L^2(\partial\Omega)}^2) + o(\varepsilon^{2n}) \quad (\text{exploiting (2.32)}) \\ &\leq C \varepsilon^{2n} \left(\int_{\partial\Omega} |\nabla \Phi(z - y)|^2 + \int_{\partial\Omega} |\nabla_x \tilde{z}(z, y)|^2 + \int_{\partial\Omega} |\Phi(z - y)|^2 + \int_{\partial\Omega} |\tilde{z}(z, y)|^2 \right) + o(\varepsilon^{2n}). \end{aligned}$$

Thanks to (2.3), the regularity of Φ guarantees that the first and the third boundary integrals in the previous sum are controlled by a constant, whereas the second and the fourth ones are bounded thanks to elliptic regularity, as stated above. Therefore, we can infer that

$$\|u_\varepsilon - U\|_{L^2(\partial\Omega)}^2 \leq C \varepsilon^{2n} + o(\varepsilon^{2n}), \quad \text{where } C = C(d_0, \Omega, f, k, |\partial\Omega|).$$

□

Before expressing the desired result regarding the topological gradient, we need to prove a general representation formula of the following kind:

Lemma 2.4. *Consider a function w solving the auxiliary problem*

$$\begin{cases} -\Delta w + 3U^2 w = 0 & \text{in } \Omega \\ \partial_{\nu} w = h & \text{on } \partial\Omega, \end{cases} \quad (2.33)$$

being $h \in H^{-1/2}(\partial\Omega)$ a generic function. Then,

$$\int_{\partial\Omega} N_U(z, y) h(y) d\sigma(y) = w(z), \quad (2.34)$$

Proof. We proceed analogously to what done for the proof of Proposition 2.2. Since w is a solution of an elliptic problem with regular coefficients, according to [84, Theorem 2.4.2.6] $w \in H^2(\Omega)$ and

moreover, according to local Hölder estimates [82, Theorem 4.15] w and ∇w are continuous in Ω . Consider a ball $B = B(z, \eta)$, being $\eta < \delta_0$, and define $V = \Omega \setminus B$; taking into account the problems solved by w and N_U and exploiting the symmetry of N_U ,

$$\begin{aligned}
\int_{\partial B} \partial_{\nu_y} N_U(z, y) w(y) d\sigma(y) &= \int_{\partial V} \partial_{\nu_y} N_U(z, y) w(y) d\sigma(y) = \int_V \operatorname{div}_y (\nabla_y N_U(z, y) w(y)) dy \\
&= \int_V \nabla_y N_U(z, y) \cdot \nabla w(y) dy + \int_V \Delta_y N_U(z, y) w(y) dy \\
&= \int_V \nabla_y N_U(z, y) \cdot \nabla w(y) dy + \int_V \Delta_x N_U(y, z) w(y) dy \\
&= \int_V \nabla_y N_U(z, y) \cdot \nabla w(y) dy + \int_V 3U(y)^2 N_U(y, z) w(y) dy \\
&= \int_V \operatorname{div}_y (N_U(z, y) \nabla w(y)) dy - \int_V N_U(z, y) \Delta w(y) dy + \int_V 3U(y)^2 N_U(y, z) w(y) dy \\
&= \int_{\partial V} \partial_\nu w(y) N_U(z, y) d\sigma(y) = \int_{\partial B} \partial_\nu w(y) N_U(z, y) d\sigma(y).
\end{aligned}$$

As done in the proof of Proposition 2.2, when the radius η of B tends to 0, it follows that $\int_{\partial B} \partial_{\nu_y} N_U(z, y) w(y) d\sigma(y) \rightarrow w(z)$, whereas $\int_{\partial B} \partial_\nu w N_U(z, y) \rightarrow 0$. \square

Remark 2.2. As a consequence, it also holds

$$\int_{\partial \Omega} \nabla_x N_U(z; y) h(y) d\sigma(y) = \nabla \left(\int_{\partial \Omega} N_U(z; y) h(y) d\sigma(y) \right) = \nabla w(z). \quad (2.35)$$

It is now possible to obtain a representation formula for the topological gradient G appearing in (2.28).

Theorem 2.4 (Representation formula for the topological gradient). *Under the assumptions of Theorem 2.1, the topological gradient G of the functional J fulfills, for any acceptable $z \in \Omega$:*

$$G(z) = (1 - k) \nabla U(z)^T M(z) \nabla W(z) + U^3(z) W(z), \quad (2.36)$$

where W is the solution of the following adjoint problem:

$$\begin{cases} -\Delta W + 3U^2 W = 0 & \text{in } \Omega \\ \partial_\nu W = U - u_{meas} & \text{on } \partial \Omega. \end{cases} \quad (2.37)$$

Proof. Recall the expression of the reduced cost functional: if w_ε satisfies the assumption (2.4), then

$$J(\Omega_\varepsilon) = j(\varepsilon; z) = \frac{1}{2} \|u_\varepsilon - u_{meas}\|_{L^2(\partial \Omega)}^2.$$

By direct computation,

$$\begin{aligned}
j(\varepsilon; z) - j(0) &= \frac{1}{2} \|u_\varepsilon - u_{meas}\|_{L^2(\partial \Omega)}^2 - \|U - u_{meas}\|_{L^2(\partial \Omega)}^2 \\
&= \frac{1}{2} \|u_\varepsilon\|_{L^2(\partial \Omega)}^2 - \int_{\partial \Omega} u_\varepsilon u_{meas} - \frac{1}{2} \|U\|_{L^2(\partial \Omega)}^2 + \int_{\partial \Omega} U u_{meas} \\
&= \frac{1}{2} \|u_\varepsilon - U\|_{L^2(\partial \Omega)}^2 - \|U\|_{L^2(\partial \Omega)}^2 + \int_{\partial \Omega} u_\varepsilon U - \int_{\partial \Omega} u_\varepsilon u_{meas} + \int_{\partial \Omega} U u_{meas} \\
&= \frac{1}{2} \|u_\varepsilon - U\|_{L^2(\partial \Omega)}^2 + \int_{\partial \Omega} (u_\varepsilon - U)(U - u_{meas}).
\end{aligned}$$

Thanks to Lemma 2.3, the first term of the last expression can be estimated as follows:

$$\|u_\varepsilon - U\|_{\partial\Omega}^2 \leq C\varepsilon^{2n} = o(\varepsilon^n).$$

The second term, exploiting (2.14), can be written as:

$$\begin{aligned} \int_{\partial\Omega} (u_\varepsilon - U)(U - u_{meas}) &= \varepsilon^n \int_{\partial\Omega} (1 - k) \nabla U(z)^T M(z) \nabla N_U(z; y) (U(y) - u_{meas}(y)) d\sigma(y) \\ &\quad + \varepsilon^n \int_{\partial\Omega} U^3(z) N_U(z; y) (U(y) - u_{meas}(y)) d\sigma(y) + o(\varepsilon^n). \end{aligned}$$

Consider $h(y) = U(y) - u_{meas}(y)$ and apply the representation formulae (2.34) and (2.35) using the solution W of the auxiliary problem (2.33) (which in this case is exactly the adjoint problem (2.37)):

$$\begin{aligned} \int_{\partial\Omega} (u_\varepsilon - U)(U - u_{meas}) &= \int_{\partial\Omega} (u_\varepsilon(y) - U(y)) h(y) d\sigma(y) \\ &= \varepsilon^n \int_{\partial\Omega} (1 - k) \nabla U(z)^T M(z) \nabla N_U(z; y) h(y) d\sigma(y) \\ &\quad + \varepsilon^n \int_{\partial\Omega} U^3(z) N_U(z; y) h(y) d\sigma(y) + o(\varepsilon^n) \\ &= \varepsilon^n [(1 - k) \nabla U(z)^T M(z) \nabla W(z) + U^3(z) W(z)] + o(\varepsilon^n), \end{aligned}$$

and thus the formula (2.36). \square

Remark 2.3. An extension of the problem discussed so far which is indeed of interest for the sake of the application we have in mind is the reconstruction of inclusions provided that a set of measured data are available only on a portion of the boundary. This approximates the actual procedure of measuring the electrical potential, recovering information by means of a finite number of electrodes. Let $\Gamma \subset \partial\Omega$, $|\Gamma| \neq 0$ be the portion of boundary on which u_{meas}^Γ is known. The results provided so far for the inverse problem can be also recovered in this case, starting from the definition of the cost functional

$$J^\Gamma(\Omega_\varepsilon) = \int_\Gamma (u_\varepsilon - u_{meas}^\Gamma)^2 d\sigma,$$

which leads to a similar definition of topological gradient G . It is possible to prove that the same representation formula in (2.36) holds in this case, except for the definition of the adjoint state W , which is instead given by the following adjoint problem:

$$\begin{cases} -\Delta W + 3U^2 W = 0 & \text{in } \Omega \\ \partial_\nu W = (U - u_{meas}^\Gamma) & \text{on } \Gamma \\ \partial_\nu W = 0 & \text{on } \partial\Omega. \end{cases} \quad (2.38)$$

Remark 2.4. Another important extension suggested by the biological application consists in considering the effect of anisotropic conductivity coefficients, which may describe in a more accurate way the electrical properties of the heart tissue. Extending the dissertation of Remark 5.2 in [30], we can compute the representation formula for the topological gradient also in the case when the

coefficient $k_\varepsilon(x) = 1 - (1 - k)\chi_{\omega_\varepsilon}(x)$ is replaced with $K_\varepsilon(x) = K_1(x)\chi_{\Omega \setminus \omega_\varepsilon}(x) + K_2(x)\chi_{\omega_\varepsilon}(x)$, being K_1 and K_2 matrix-valued regular coefficients satisfying, $\forall x \in \Omega$: $K_1(x), K_2(x)$ are symmetric and

$$|\xi|^2 \leq \xi^T K_1(x) \xi \leq \beta_1 |\xi|^2 \quad \alpha_2 |\xi|^2 \leq \xi^T K_2(x) \xi \leq \beta_2 |\xi|^2 \quad \forall \xi \in \mathbb{R}^n,$$

with $0 < \alpha_2 \leq \beta_2 < 1$ and $\beta_1 \geq 1$. The expression of the topological gradient of the cost functional J in the anisotropic case reads as follows:

$$G(z) = M_{ij}(K_1(z) - K_2(z))_{ik} \frac{\partial U}{\partial x_k}(z) \frac{\partial W}{\partial x_j}(z) + U^3(z)W(z) \quad (2.39)$$

Taking advantage of the assumptions made so far and of the theoretical results that have been proved, we are now ready to set up a topological gradient-based reconstruction algorithm for the inverse problem. In particular, we remark that, under the hypothesis (2.4), we restrict ourselves to the identification of the position of the center of a small inclusion of prescribed shape. This can be performed by exploiting the formula (2.28) as explained before: if the topological gradient G attains its (negative) minimum in $\bar{z} \in \Omega$,

$$\begin{aligned} G(\bar{z}) < 0 &\Rightarrow j(\varepsilon; \bar{z}) < j(0) \\ G(\bar{z}) \leq G(z) \quad \forall z \in \Omega &\Rightarrow j(\varepsilon; \bar{z}) \leq j(\varepsilon; z) \quad \forall z \in \Omega, \end{aligned}$$

which means that the introduction of a small inhomogeneity at $z = \bar{z}$ yields the maximum negative variation of the functional J . Finally, thanks to the adjoint approach, we have obtained the representation formula (2.36) for the topological gradient, which allows to compute $G(z)$ by solving two boundary value problems.

The boundary datum, when dealing with a practical application, is derived from a measurement. Instead, for the sake of testing the algorithm, we suppose in the sequel to know *a priori* the exact shape and location of the inclusion and we solve the direct problem (2.5) to compute the corresponding potential on the whole domain, from which we extract the boundary datum u_{meas} .

2.3.1 Identification in presence of a single measurement

According to the strategy proposed in [52], a *one-shot* algorithm based on the topological gradient can be implemented (see Algorithm 1). The numerical approximation of problems (2.5), (2.1) and

Require: domain Ω , forcing term f , boundary datum u_{meas}

Ensure: approximated centre of the inclusion, \bar{z}

compute U by solving (2.1);

compute W by solving (2.37);

determine G according to (2.36);

find \bar{z} s.t. $G(\bar{z}) \leq G(z) \quad \forall z \in \Omega$.

Algorithm 1: Reconstruction of a single inclusion of small dimensions

(2.37) is performed through the Galerkin-Finite Element Method. To this purpose, we introduce a discretization \mathcal{T}_h of the domain Ω , e.g. made of triangular elements if $n = 2$, and define the discrete subspace $V_h = X_h^r \cap V$, where

$$X_h^r(\Omega) = \{v \in C(\bar{\Omega}) : v|_K \in \mathbb{P}_r(K) \quad \forall K \in \mathcal{T}_h\},$$

being \mathbb{P}_r the space of polynomials of degree r .

When applying the finite element method on problem (2.5), whose weak formulation is reported in (2.6), we must tackle the solution of a nonlinear system of equations. Indeed, introducing the operator $S : V \rightarrow V^*$, $S(u) = T(u) - F$, the discrete approximation of the direct problem (2.5) reads:

$$\text{find } u_h \in V_h \text{ s.t. } \langle S(u_h), v_h \rangle_* = 0 \quad \forall v_h \in V_h. \quad (2.40)$$

By denoting the basis $\{\varphi_i\}_{i=1}^{N_h}$ of V_h (where $N_h = \dim(V_h)$) by

$$u_h(x) = \sum_{i=1}^{N_h} u_i \varphi_i(x), \quad x \in \Omega,$$

(2.40) can be equivalently rewritten as the following algebraic system:

$$\begin{aligned} \text{find } \underline{u} \in \mathbb{R}^{N_h} \text{ s.t. } \underline{S}(\underline{u}) &= 0, \\ \text{being } S_i(\underline{u}) &= \langle S(u_h), \varphi_i \rangle_* \text{ and } (\underline{u})_i = u_i, \end{aligned} \quad (2.41)$$

which is a nonlinear system (due to nonlinearity of T) of N_h equations in N_h unknowns. One of the most common strategies to tackle the nonlinearity is the Newton method, which generates a sequence $\{\underline{u}^{(k)}\}$ to approximate the solution \underline{u} as follows:

$$\begin{cases} \underline{u}^{(0)} \text{ given} \\ \underline{u}^{(k+1)} = \underline{u}^{(k)} + \underline{\delta u}^{(k)}, \quad k = 0, 1, \dots, \end{cases} \quad (2.42)$$

where $\underline{\delta u}^{(k)}$ is the solution of the linearized system

$$J(\underline{u}^{(k)}) \underline{\delta u}^{(k)} = -\underline{S}(\underline{u}^{(k)}), \quad (2.43)$$

and $J(\underline{u}^{(k)})$ is the Jacobian matrix of the vectorial function \underline{S} , evaluated at $\underline{u}^{(k)}$. The sequence $\{\underline{u}^{(k)}\}$ converges to the solution \underline{u} of (2.41) if $\underline{u}^{(0)}$ is chosen sufficiently close to \underline{u} (according to the Newton-Kantorovich theorem, see e.g. [140]). We remark that problem (2.43) is the algebraic counterpart of the following linear problem: find $\delta u_h^{(k)} \in V_h$ s.t.

$$\langle dS(u_h^{(k)})[\delta u_h^{(k)}], v_h \rangle_* = - \langle S(u_h^{(k)}), v_h \rangle_* \quad \forall v_h \in V_h, \quad (2.44)$$

where $dS(w)[\cdot] : V \rightarrow V^*$ is the Frechét derivative of S evaluated at w . Hence, the possibility to invert the matrix $J(\underline{u}^{(k)}) \in \mathbb{R}^{N_h \times N_h}$ is equivalent to the well-posedness of (2.44), for which we now provide a detailed numerical analysis.

First consider the linearized problem (2.43), which we have to solve at each step, or equivalently (2.44), which explicitly reads: find $u_h \in V_h$ such that

$$\begin{aligned} \int_{\Omega} k_{\varepsilon}(x) \nabla \delta u_h \cdot \nabla v_h + \int_{\Omega \setminus \omega} 3 \left(u_h^{(k)} \right)^2 \delta u_h v_h &= \\ = \int_{\Omega} f v_h - \int_{\Omega} k \nabla u_h^{(k)} \cdot \nabla v - \int_{\Omega \setminus \omega_{\varepsilon}} \left(u_h^{(k)} \right)^3 v_h &\quad \forall v_h \in V_h. \end{aligned} \quad (2.45)$$

Such a problem is indeed well-posed, according to the following result:

Proposition 2.3. *If $u_h^{(0)} \in V_h \cap L^\infty(\Omega)$, problem (2.45) admits an unique solution $u_h^{(k)}$ in $V_h \subset V = H^1(\Omega)$ for every k . Moreover,*

$$\exists C_k > 0 \text{ s.t. } \|u_h^{(k)}\|_{H^1(\Omega)} \leq C_k \left(\|f\|_{H^{-1}(\Omega)} + \|u_h^{(0)}\|_{H^1(\Omega)}^3 \right).$$

Proof. Consider the first iteration: for a fixed initial point $u_h^{(0)}$ in $V_h \cap L^\infty(\Omega)$, the linear operator $-s(u_h^{(0)}, \cdot) = -\langle \mathcal{S}(u_h^{(0)}), \cdot \rangle_*$ and the bilinear form $ds[u_h^{(0)}](\cdot, \cdot) = \langle d_{u_h^{(0)}} \mathcal{S} \cdot, \cdot \rangle_*$ are continuous: for all $u_h, v_h \in V_h$, it holds:

$$\begin{aligned} \left| ds[u_h^{(0)}](u_h, v_h) \right| &\leq \|\nabla u_h\|_{L^2(\Omega)} \|\nabla v_h\|_{L^2(\Omega)} + 3 \|u_h^{(0)}\|_{L^\infty(\Omega)}^2 \|u_h\|_{L^2(\Omega)} \|v_h\|_{L^2(\Omega)} \\ &\leq \max \left\{ 1, 3 \|u_h^{(0)}\|_{L^\infty(\Omega)}^2 \right\} \|u_h\|_{H^1(\Omega)} \|v_h\|_{H^1(\Omega)}; \\ \left| s(u_h^{(0)}, v_h) \right| &\leq \|f\|_{L^2(\Omega)} \|v_h\|_{L^2(\Omega)} + \|\nabla v_h\|_{L^2(\Omega)} \|\nabla u_h^{(0)}\|_{L^2(\Omega)} + \|u_h^{(0)}\|_{L^6(\Omega)}^3 \|v_h\|_{L^2(\Omega)} \\ &\leq \left(\|f\|_{L^2(\Omega)} + \max \left\{ 1, C_{Sob}^2 \|u_h^{(0)}\|_{H^1(\Omega)}^3 \right\} \right) \|v_h\|_{H^1(\Omega)}. \end{aligned}$$

Nevertheless, the bilinear form is not coercive in V_h , indeed:

$$ds[u_h^{(0)}](u_h, u_h) = \int_{\Omega} k_\varepsilon \nabla u_h \cdot \nabla u_h + \int_{\Omega} 3\chi_{\Omega \setminus \omega_\varepsilon} \left(u_h^{(k)} \right)^2 u_h^2$$

and a lower bound of the latter quantity in terms of the H^1 -norm of u_h cannot be obtained because of the presence of the indicator function over $\Omega \setminus \omega_\varepsilon$ in the reaction term. The weak coercivity is instead guaranteed, with constant $k > 0$:

$$\begin{aligned} ds[u_h^{(0)}](u_h, u_h) + k \|u_h\|_{L^2(\Omega)}^2 &= \int_{\Omega} k_\varepsilon \nabla u_h \cdot \nabla u_h + \int_{\Omega} 3\chi_{\Omega \setminus \omega_\varepsilon} \left(u_h^{(0)} \right)^2 u_h^2 + \int_{\Omega} k u_h^2 \\ &\geq \int_{\omega_\varepsilon} k \nabla u_h \cdot \nabla u_h + \int_{\Omega \setminus \omega_\varepsilon} \nabla u_h \cdot \nabla u_h + \int_{\Omega} k u_h^2 \\ &\geq k \|\nabla u_h\|_{L^2(\Omega)}^2 + k \|u_h\|_{L^2(\Omega)}^2 = k \|u_h\|_{H^1(\Omega)}^2. \end{aligned}$$

Hence, it is possible to apply the Nečas theorem (or the Fredholm Alternative), see e.g. [74], Chapter 6, which entails the well-posedness of the problem (2.45) for $k = 0$ only if the *homogeneous problem* has an unique solution, i.e.:

$$ds[u_h^{(0)}](u_h, v_h) = 0 \quad \forall v_h \in V_h \quad \Leftrightarrow \quad u_h = 0. \quad (2.46)$$

To prove it, consider that, if $w \in V_h \subset V = H^1(\Omega)$ solves (2.46), then it also satisfies:

$$\int_{\Omega} k \nabla w \cdot \nabla v_h + \int_{\Omega \setminus \omega_\varepsilon} 3 \left(u_h^{(0)} \right)^2 w v_h = 0 \quad \forall v_h \in V_h.$$

Hence, with $v_h = w$,

$$\nabla w = 0 \text{ in } \Omega, \quad w = 0 \text{ in } \Omega \setminus \omega_\varepsilon. \quad (2.47)$$

According to the Poincarè inequality (2.8), this is sufficient to guarantee that $w = 0$ in Ω , and this entails the uniqueness of the solution of (2.46) and thus the well-posedness of (2.45) for $k = 0$.

The stability estimate is guaranteed by Nečas' theorem, yielding

$$\left\| u_h^{(1)} \right\|_{H^1(\Omega)} \leq \frac{1}{k} \left\| g(u_h^{(0)}, \cdot) \right\|_{H^{-1}} \leq C_k (\|f\|_{L^2(\Omega)} + \left\| u_h^{(0)} \right\|_{H^1(\Omega)}^3).$$

Hence, the solution $\delta u_h^{(0)}$ of (2.45) with $k = 0$ exists and is unique in V_h , and with a procedure similar to the one used on the homogeneous problem, one may prove that $\delta u_h^{(0)} \in C^{0,\alpha} \supset L^\infty(\Omega)$. Moreover, also $u_h^{(1)} \in H^1(\Omega) \cap L^\infty(\Omega)$, and this can be iterated to prove the thesis on each $k > 0$, by induction. \square

We have therefore set the numerical strategy for the approximate solution of problem (2.6): the well-posedness of the algebraic problems (2.43) to be solved at each step is entailed by the latter proposition, whereas the convergence of the sequence $\{u_h\}_{h>0}$ is guaranteed by the Kantorovich theorem (see [140]), which exploits the Lipschitz-continuity of the functional $\mathcal{S}(u) = T(u) - F$.

Through this strategy, it is possible to solve the direct problem (2.5) with the exact inclusion in order to obtain the boundary data, as well as the unperturbed problem (2.1) required by Algorithm 1. Differently, the approximation of the adjoint problem (2.37), which is a linear problem, immediately leads to the solution of a linear algebraic system, for which a well-posedness is guaranteed via the Lax-Milgram lemma. Once U and W have been computed, the expression of the topological gradient $G(z)$ of the function j is given by (2.36), where one has to exploit the *a priori* knowledge on the shape of the inclusion to choose the proper polarization tensor. For example, while looking for circular-shaped inclusions, we obtain (see (2.15)):

$$G(z) = \frac{2(1-k)}{1+k} |D| \nabla U(z) \cdot \nabla W(z) + U^3(z) W(z). \quad (2.48)$$

Thanks to the discretization introduced, the approximation of the value of the topological gradient G is known in each node of the triangulation \mathcal{T}_h . Hence, the search for its minimum point \bar{z} is performed by a simple inspection between the nodal values of G . This, of course, requires the usage of a sufficiently fine mesh \mathcal{T}_h ; otherwise, one may use any finite-dimensional optimization algorithm but entailing the evaluation of G (and possibly its derivative, namely the Hessian of j) in points where the values of U and W have not been computed.

2.3.2 Identification in presence of multiple measurements

The proposed Algorithm 1 allows to reconstruct the position of the exact inclusion with a single measurement of the boundary datum. However, it exploits a first-order expansion of the cost functional, and this can affect the precision of the reconstruction, due to the disregarded higher-order terms. In order to overcome this drawback, similarly to the approach proposed in [52], it is possible to take advantage of *multiple measurements*. Consider $N^f > 1$ different non zero forcing terms $f_i, i = 1, \dots, N^f$, and suppose to know the respective boundary data $u_{meas,i}$, that is, the solutions of the direct problem (2.5) with the same inclusion ω_ε and the corresponding source term f_i . Introduce the cost functional

$$J(\Omega_\varepsilon) = \sum_{i=1}^N \alpha_i J_i(\Omega_\varepsilon), \quad \text{where } J_i(\Omega_\varepsilon) = \int_{\partial\Omega} (u_\varepsilon - u_{meas,i})^2$$

and $\{\alpha_i\}_{i=1}^{N^f}$ is a set of weights such that

$$\alpha_i > 0, \quad \sum_{i=1}^{N^f} \alpha_i = 1.$$

Then, the minimum point \bar{z} of the topological gradient $G(z) = \sum_i \alpha_i G_i(z)$ provides a better approximation of the inclusion's center than the minima \bar{z}_i of each G_i , the topological gradient of J_i , filtering possible errors induced by the asymptotic analysis carried out on each functional J_i . Hence, we perform a slight variation of Algorithm 1, in the case where multiple observations are available:

Require: domain Ω , forcing terms f_i , boundary data $u_{meas,i}$, $i = 1, \dots, N^f$

Ensure: approximated center of the inclusion, \bar{z}

for $i = 1, \dots, N^f$ **do**

 compute U_i by solving (2.1) with forcing term f_i ;

 compute W_i by solving (2.37) with Neumann datum $U_i - u_{meas,i}$;

 determine G_i according to (2.36);

end for

compute $G(z) = \sum_{i=1}^{N^f} \alpha_i G_i(z)$;

find \bar{z} s.t. $G(\bar{z}) \leq G(z) \quad \forall z \in \Omega$.

Algorithm 2: Reconstruction of a single inclusion, many measurements

A possible way to define the weights $\{\alpha_1, \dots, \alpha_{N^f}\}$ is to take

$$\alpha_i = \frac{j_i(0)/|\min_{\Omega} G_i|}{\sum_{i=1}^{N^f} j_i(0)/|\min_{\Omega} G_i|}, \quad i = 1, \dots, N^f, \quad (2.49)$$

which entails that the information provided by the topological gradient G_i associated to a large value of the cost functional $j_i(0)$ is considered to carry more significant information than the one associated to a smaller value G_j , $j \neq i$. We remark that this requires the calculation (for each $i = 1, \dots, N^f$) of $j_i(0) = \int_{\Gamma_i} (u_{meas}^{\Gamma} - U)^2$, which does not yield a significant computational cost, once the unperturbed problem (2.1) has been solved.

2.3.3 Partial measurements

We describe another alternative to Algorithm 1, related to Remark 2.3, which is more interesting for the sake of application. Suppose to have information on the boundary potential on a portion Γ of $\partial\Omega$ of the form:

$$\Gamma = \bigcup_{i=1}^{N^{\Gamma}} \Gamma_i, \quad (2.50)$$

with Γ_i open, connected, $|\Gamma_i| \neq 0$ for all $i = 1, \dots, N^{\Gamma}$. This configuration can model the presence of N^{Γ} different measurement devices on the boundary of the domain, on which we recover information of the potential u_{meas}^{Γ} . Moreover, as in Algorithm 2, we set up the optimization of an averaged cost functional

$$J(\Omega_{\varepsilon}) = \sum_{i=1}^{N^{\Gamma}} \alpha_i J_i(\Omega_{\varepsilon}), \quad \text{where now} \quad J_i(\Omega_{\varepsilon}) = \int_{\Gamma_i} (u_{\varepsilon} - u_{meas})^2$$

is the cost functional related to the single portion Γ_i of the boundary. This yields an alternative reconstruction procedure, involving multiple partial measurements obtained with the same forcing term f , as reported in Algorithm 3.

Require: domain Ω , forcing term f , boundary data u_{meas}^Γ
Ensure: approximated centre of the inclusion, \bar{z}
 compute U by solving (2.1) with forcing term f ;
for $i = 1, \dots, N^\Gamma$ **do**
 compute W_i by solving (2.37) with Neumann datum $(U - u_{meas}^\Gamma)\chi_{\Gamma_i}$;
 determine G_i according to (2.36);
end for
 compute $G(z) = \sum_{i=1}^{N^f} \alpha_i G_i(z)$;
 find \bar{z} s.t. $G(\bar{z}) \leq G(z) \quad \forall z \in \Omega$.
Algorithm 3: Reconstruction of a single inclusion, partial measurements

We remark that, since the formula (2.36) for the topological gradient and the adjoint problem (2.37) are linear with respect to W , using homogeneous weights $\alpha_i = 1/N^\Gamma$ would be equivalent to rely on Algorithm 1 with boundary data acquired on the whole Γ . Instead, the choice of weights proposed in (2.49) allows to assign a better predictive value to the information derived by measurements on the portions Γ_i which correspond to larger values of the cost functionals j_i .

2.4 Numerical results

We now show some numerical results obtained by applying Algorithms 1, 2 and 3 in several 2-dimensional benchmark cases. The goal is manifold:

- i) first of all (in section 2.4.1) we verify the effectiveness of the reconstruction, introducing a small inhomogeneity of circular shape in a two-dimensional domain Ω , simulating the associated boundary potential u_{meas} (or $u_{meas,i}$ for $i = 1, \dots, N^f$, in the case of multiple measurements), and computing the distance between the center of the exact inclusion and the detected one;
- ii) in section 2.4.2 we assess the feasibility of the algorithms when the shape of the inclusion to detect is unknown, and the reconstruction is performed with the polarization tensor of the circle. Indeed, we exploit hypothesis (2.4) to assimilate an inclusion of small dimension to a circle, at a first approximation;
- iii) in section 2.4.3, we test the reconstruction of circular inclusion in the case of measures performed on portions of the boundary, according to Algorithm 3, considering a source term which is significant for the foreseen application;
- iv) in section 2.4.4, we test the reconstruction of multiple circular inclusions, exploiting Algorithm 3 and reporting the presence of multiple local minima in the topological gradient;
- v) in section 2.4.5, we assess the performance of Algorithm 3 in the case where the polarization tensor features anisotropic effects, exploring in different benchmark cases the effect of different rates of anisotropy on the reconstruction results;

- vi) finally, in section 2.4.6, we verify the stability of the procedure proposed in Algorithms 2 and 3 with respect to the presence of a measurement noise on the datum u_{meas} .

In each experiment, the solution of the differential problems is performed via the Galerkin-Finite Element Method, as explained in Section 2.3. In order to properly consider inhomogeneities of small dimensions ($diam(\Omega)/diam(\omega_\varepsilon) \leq 0.05$), a triangulation of Ω made by a large number of elements ($\approx 30,000$) is considered. Indeed, since the position of the inclusion is unknown, it is impossible to perform a local refinement of the mesh (which would increase the quality of the mesh without yielding a large cost due to the greater size of the linear system to solve). However, thanks to the *one-shot* approach, the reconstruction procedure is not expensive at all, and the overall computational time is in general of the order of the minute * (e.g. when applying Algorithm 2 with $N^f = 2$ sources on a mesh of about 30,000 elements, the computational time is about 10'', whereas Algorithm 3 on a mesh of about 100,000 elements with $N^\Gamma = 16$ takes almost 100'').

In the case of multiple observations, we use the source terms proposed in [52] for the linear problem: $f_1(x, y) = x$, $f_2(x, y) = y$, $f_3(x, y) = xy$, $f_4(x, y) = 0.5(x^2 - y^2)$, for all $(x, y) \in \Omega$. This allows to assess the effectiveness of our reconstruction procedure in a benchmark case which is similar to the ones proposed in the literature for the linear problem. Similarly e.g. to the results shown in [52], also in our case it is not necessary to use more than $N^f = 4$ forcing terms: in particular, each simulation is carried out with $N^f = 1, \dots, 4$ and, if the reconstructed position does not undergo a significant change after the introduction of a new measurement, the procedure is stopped. The weights α_i in the averaged functional are chosen as in (2.49). When testing Algorithm 3, instead, the chosen source term is inspired by the foreseen application.

2.4.1 Circular-shaped inclusion detection

We report the numerical results obtained for the detection of the center of small circular inclusions in different positions of the domain $\Omega = B(0, 1)$. In Figure 2.1 we plot the topological gradient $G(z)$, superimposing its negative minimum (white cross) and the boundary of the exact inclusion (white circle of radius 0.04). The minima detected in all the cases are reported in Table 2.1, where we also compute the Euclidean distance between the reconstructed position and the exact inclusion's center. In the column N_f we specify how many measurements were needed for finding the minima.

Real inclusion	Detected inclusion	N_f	Error
(0, 0.1)	(0.014, 0.106)	2	0.016
(0.4, 0.3)	(0.363, 0.296)	3	0.037
(-0.65, 0)	(-0.603, 0.005)	2	0.047
(0.4, -0.5)	(0.431, -0.500)	3	0.031

Table 2.1: Detection of a circular-shaped inclusion: results

We observe that the algorithm detects the position of the inclusion with an average error of 0.04 in Euclidean norm, which is comparable to the size of the inclusion itself. Moreover, significant differences can be observed according to the position of the inclusion. Except for the inclusions

*We performed the simulations with a laptop with CPU frequency of 2.10GHz, RAM 8GB

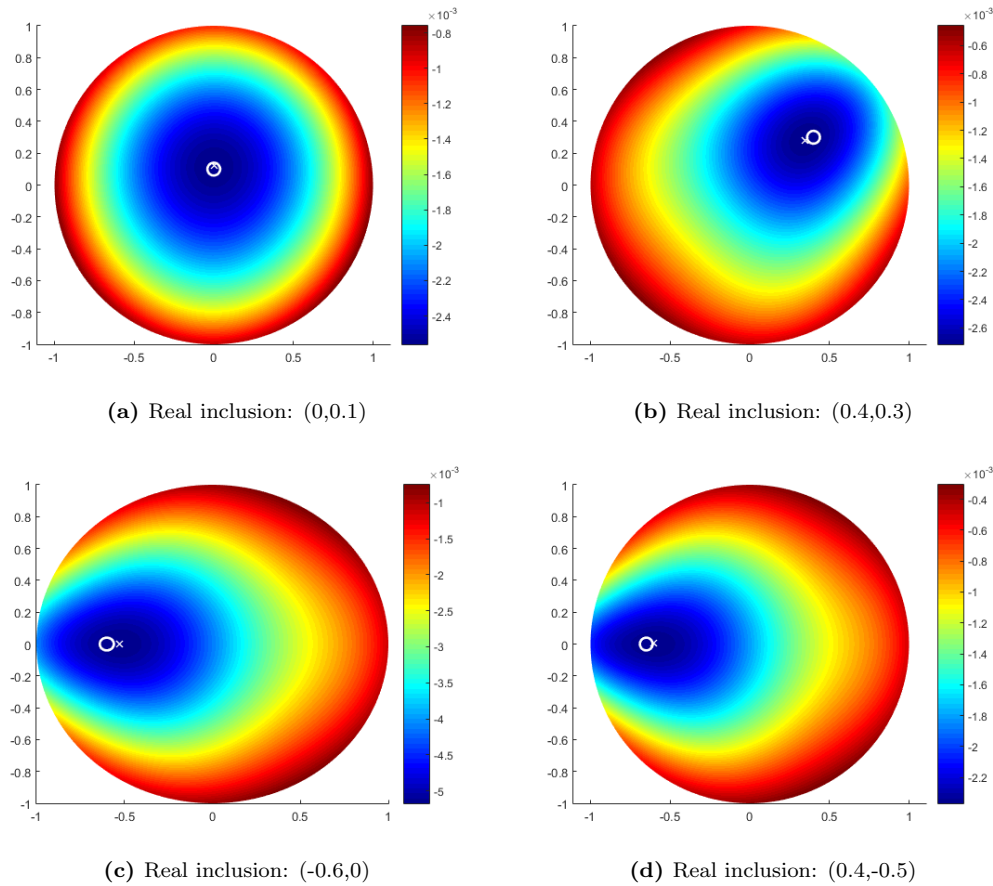


Figure 2.1: Detection of a circular-shaped inclusion

located very close to the center, it holds that the closer the inclusion to the boundary, the more accurate the reconstruction. However, if the inclusion is excessively close to boundary, the minimum is detected along the boundary itself, which is of course in contrast with hypothesis (2.4).

2.4.2 Inclusion of unknown shape

Whether cannot rely on *a priori* knowledge on the shape of the inclusion to be identified, the expression of the polarization tensor is in general not available. Nevertheless, even in this case, we can apply the proposed algorithm for the reconstruction of small circular inclusions to identify the position of inclusions with small size and unknown shape. In this section, we show that formula (2.48), related to circular-shaped inclusions, can be successfully applied to detect (at some extent) inclusions whose shape is unknown. In a first case, we reconstruct the center of an inclusion of elliptic shape both with the exact polarization tensor (2.16) and with the one related to the circular shape, given (2.15): see Figure 2.2 and Table 2.2. Then, we test the identification of inclusions with more involved shapes, for which the polarization tensor is unknown. We report the qualitative results of the detection of an L-shaped inclusion obtained by means of the polarization tensor of the

circle (see Figure 2.3).

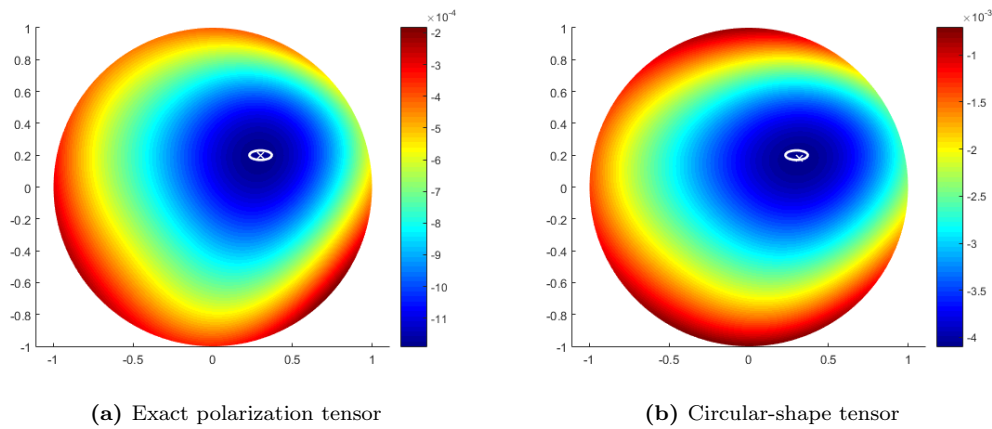


Figure 2.2: Elliptic-shaped inclusion detection with different tensors

M	Real inclusion center	x and y real semi-axis	Detected center	Error
Ellipse	(0.3, 0.2)	(0.07, 0.03)	(0.302, 0.196)	0.005
Circle	(0.3, 0.2)	(0.07, 0.03)	(0.320, 0.181)	0.028
Ellipse	(0.5, 0)	(0.04, 0.02)	(0.487, -0.013)	0.018
Circle	(0.5, 0)	(0.04, 0.02)	(0.549, 0.009)	0.050

Table 2.2: Elliptic-shaped inclusion detection with different tensors: results

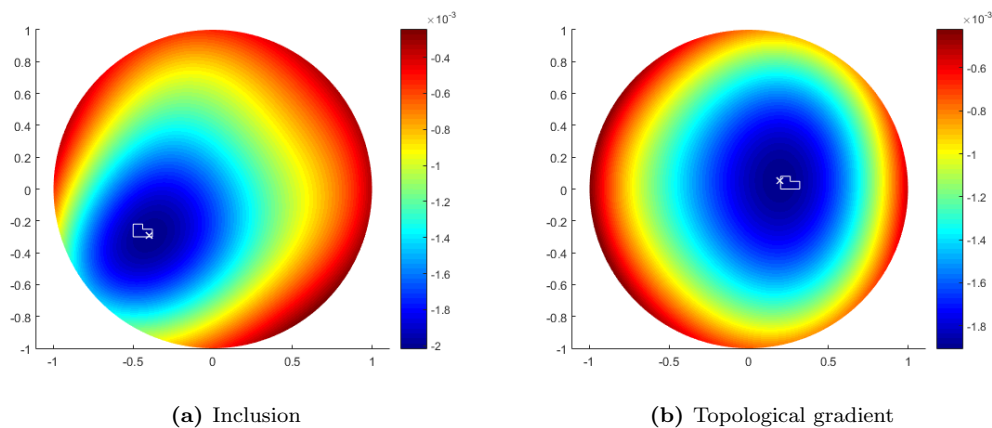


Figure 2.3: L-shaped inclusion detection using the tensor corresponding to the circular shape

In the case of inclusions of elliptic shape, we remark that the reconstruction error using the polarization tensor of the circle is actually higher than, but comparable to, the one with the correct tensor. Hence, the proposed *one-shot* algorithm can be used when dealing with the reconstruction of inclusions of unknown shape and small dimensions, to provide a first approximation of the center

by using the topological gradient associated to the polarization tensor of the circle. This can consist in an initial guess for an iterative scheme, based e.g. on the level-set technique or on the evaluation of the shape gradient of the functional J , if a shape optimization procedure is exploited for the complete reconstruction of the geometry of the inclusion.

2.4.3 Partial measurements

In this section, we test Algorithm 3 for the reconstruction of a small circular inhomogeneity in the domain $\Omega = B(0, 1)$ using measurements of the potential on a portion Γ of the boundary. In particular, we consider a source term $f(x, y) = 1 - \exp(-r_s^2 / ((x - x_s)^2 + (y - y_s)^2))$, which attains its maximum value in $(x_s, y_s) \in \Omega$ and exponentially decays outside a circular neighborhood of radius r_s , approximating the electrical stimulus originated in a specific region. Moreover, the region Γ is of the form prescribed by (2.50), where Γ_i are equivalent arcs of length $2\pi\ell$.

We report some results of the reconstruction algorithm in the case where the exact inclusion has center $(0.5, 0.4)$, the forcing stimulus is centered in $(0, 0)$ with radius $r_s = 0.3$, $\ell = 1/48$ and we consider different numbers of portions N^Γ : see Table 2.3 for the quantitative results and Figure 2.4, where Γ is marked with a thick black line.

N^Γ	Detected inclusion	Error
8	(0.629, 0.530)	0.183
12	(0.482, 0.346)	0.057
16	(0.508, 0.423)	0.025
24	(0.489, -0.398)	0.011

Table 2.3: Reconstruction with partial measurements: results

2.4.4 Identification of multiple inclusions

We now test the effectiveness of the reconstruction algorithm when applied to data related to multiple inclusions. We point out that, as reported in [30], the generalization of the asymptotic expansion (2.14) to the case when $\omega_\varepsilon = \sum_{l=1}^L z_l + \varepsilon D_l$ reads as follows:

$$(u_\varepsilon - U)(y) = \varepsilon^n \sum_{l=1}^L [(1 - k)\nabla U(z_l)^T M(z_l)\nabla_x N_U(z_l, y) + U^3(z_l)N_U(z_l, y)] + o(\varepsilon^n), \quad \text{as } \varepsilon \rightarrow 0, \quad \forall y \in \partial\Omega. \quad (2.51)$$

It is possible to deduce from (2.51) a reconstruction formula for the topological gradient, and to devise a (possibly) iterative reconstruction algorithm to reconstruct L different inclusions of arbitrarily different shapes. In the present work, however, we consider the case in which all the inclusions to be identified are supposed to be of circular shape. Moreover, according to the results reported in subsection 2.4.2, this may be the natural choice in order to avoid the requirement of *a priori* knowledge on the different shapes D_l . In Figure 2.5 we show that the topological gradient computed as in Algorithm 3 identifies different local minima in presence of multiple inclusions. The global minimum, in particular, is found to be very close to one of the inclusions; the subregion where

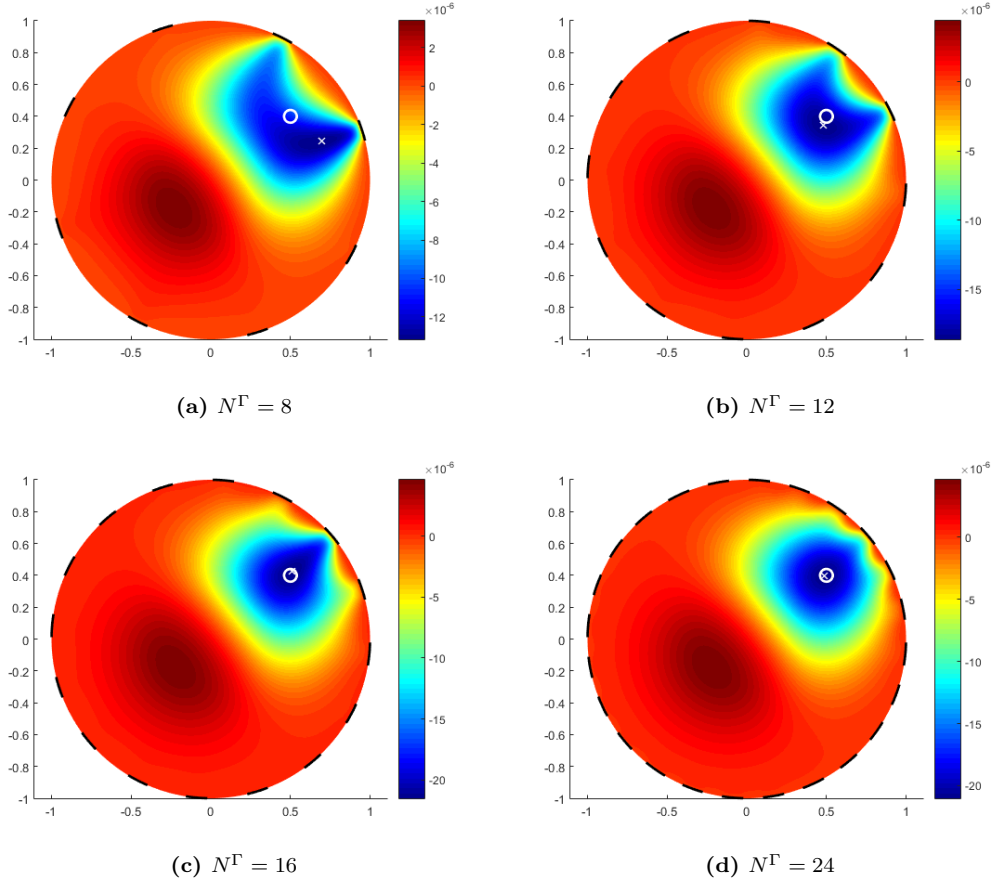


Figure 2.4: Reconstruction with partial measurements: results

the topological gradient is under a given threshold (say, $\tau = (1-\alpha)G(\bar{z})$, being \bar{z} the global minimum point, for a small, chosen $\alpha \in (0, 1/2)$), would contain all the inclusions. Only if the inclusions are too close each other, the algorithm may fail in distinguish them.

2.4.5 Identification of inclusions in presence of anisotropy

In this subsection, we show some results related to the case of an anisotropic medium. We suppose the expressions of the anisotropic conductivity matrices K_1 and K_2 to be known, and exploit them in the application of Algorithm 3, in the formulation of the background and adjoint problem as well as in the computation of the polarization tensor, according to Remark 2.4 and formula (2.39). Given the spectral decomposition of K_1 :

$$K_1(x) = \lambda_1(x)v_1(x) \otimes v_1(x) + \lambda_2(x)v_2(x) \otimes v_2(x),$$

where $\lambda_i(x)$ are the (positive real) eigenvalues of $K_1(x)$ and $v_i(x)$ the respective eigenvectors, we consider two benchmark cases. We suppose the eigenvalues λ_1 , λ_2 to be constant within Ω and the eigenvectors in each point to be either parallel to the Cartesian axes (Test A), or to the radial

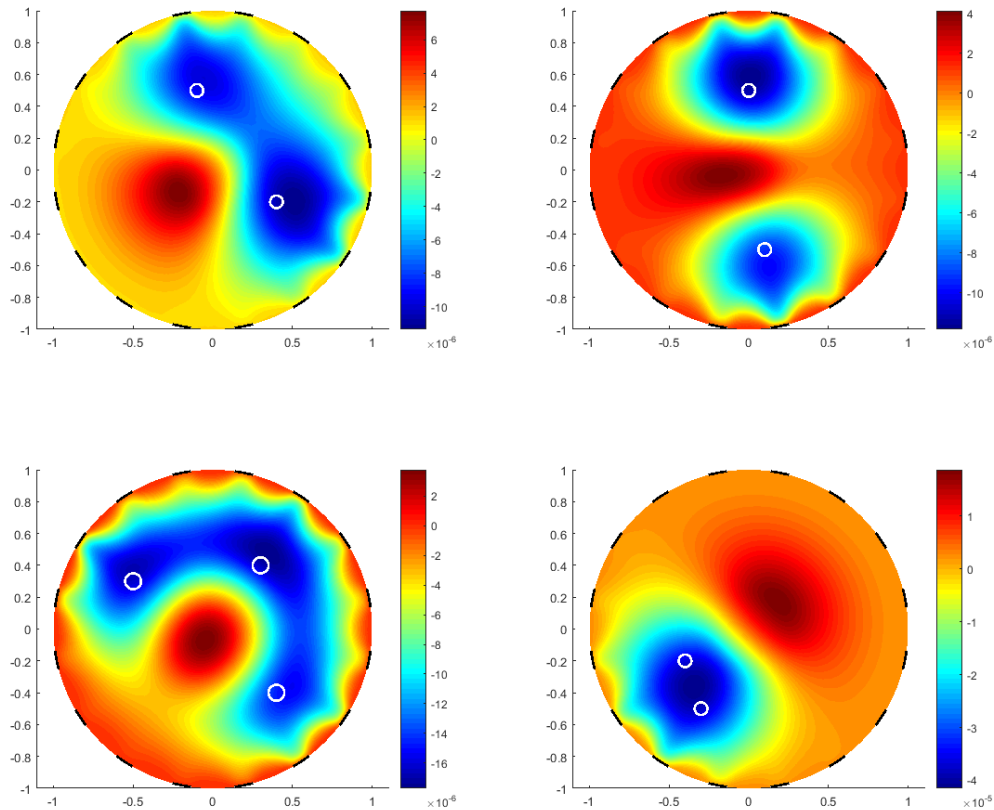


Figure 2.5: Identification of multiple circular inclusions

and the tangential directions with respect to the center of the domain (Test B). We assume that $K_2(x) = \kappa K_1(x)$, with $\kappa \ll 1$: dealing with inclusions of small size, the expression of the conductivity inside ω_ε is not the object of the present investigation. In Figure 2.6 and Table 2.4 we report some qualitative and quantitative results of the reconstruction algorithm, in presence of different parameters λ_x, λ_y (the eigenvalues associated to the principal directions in Test A) or $\lambda_\rho, \lambda_\theta$ (in Test B).

Test	Detected inclusion	Error
Test A: $\lambda_x = 1, \lambda_y = 2$	(0.444, 0.251)	0.064
Test A: $\lambda_x = 1, \lambda_y = 3$	(0.474, 0.230)	0.102
Test A: $\lambda_x = 2, \lambda_y = 1$	(0.438, 0.272)	0.047
Test A: $\lambda_x = 3, \lambda_y = 1$	(0.436, 0.218)	0.090
Test B: $\lambda_\rho = 1, \lambda_\theta = 2$	(0.470, 0.360)	0.092
Test B: $\lambda_\rho = 1, \lambda_\theta = 3$	(0.467, -0.378)	0.103

Table 2.4: Reconstruction in the anisotropic case: results with real inclusion in (0.4,0.3)

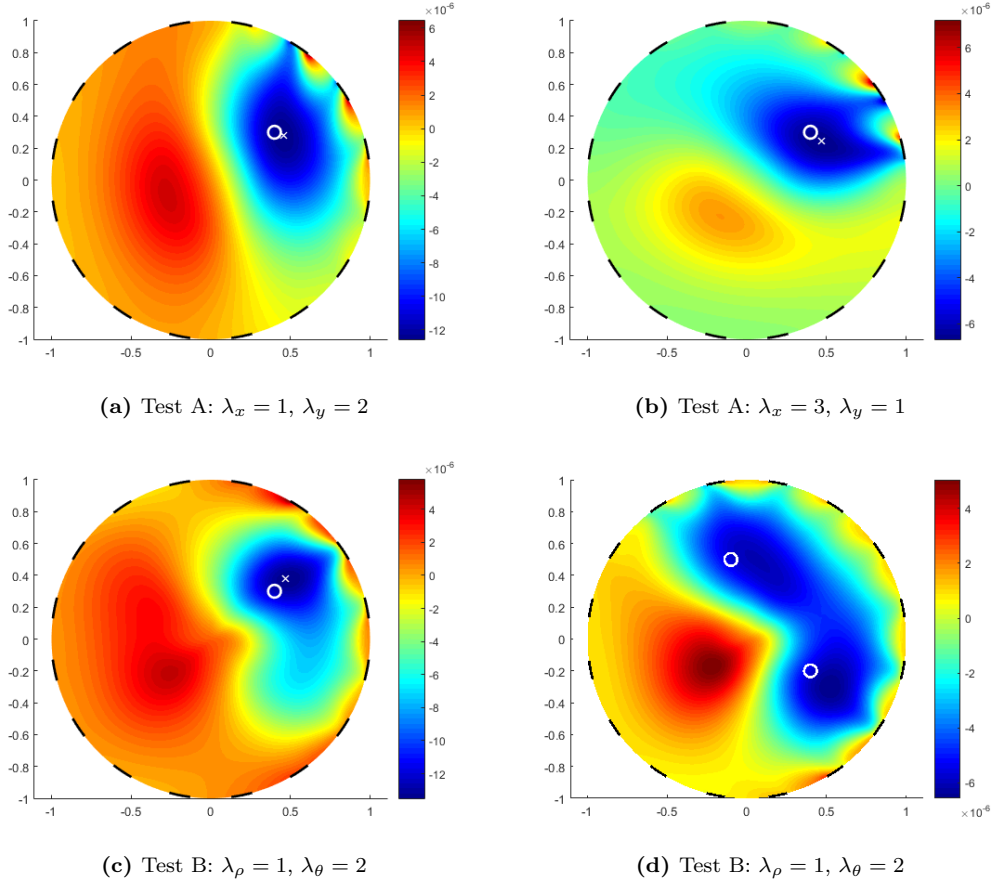


Figure 2.6: Results in the anisotropic case

The position of the exact inclusion is detected in all the proposed configurations, although the accuracy seems to decrease when the ratio between the eigenvalues increases.

2.4.6 Effect of experimental noise

In this last subsection, we show the stability of Algorithms 2 and 3 with respect to possible experimental or measurement noise on the boundary data. We neglect in this case possible anisotropic effects, aiming at identifying a single inclusion. We perturb the value of the exact solution computed on the boundary up to a fixed percentage p ($\tilde{u}_{meas}(x) = u_{meas}(x)(1 - p/2 + rand(x)p)$, where $rand(x)$ is a random number between 0 and 1 for each $x \in \Omega$), assessing the performances of the reconstruction procedures. Some results in the case of the reconstruction of circular-shaped inclusions with multiple measurements are reported in Figure 2.7 and in Table 2.5. We conducted the simulation 100 times with different realizations of the random experimental noise, reporting the average error obtained; the cases where the inclusion was detected on the boundary (and thus the reconstruction fails) are not taken into account, but are reported in Table 2.5 as “failure” cases. In Table 2.6 and in Figure 2.8, instead, we report the results obtained in the case of partial measu-

rements affected by noise, in the case of $N^\Gamma = 12, 16, 24$ portions of the boundary of length $2\pi\ell$, $\ell = 1/48$. Each simulation was conducted 20 times with different random errors; the average results are then reported.

Percentage	Real inclusion's center	Failure	Mean error
1%	(0.2,-0.2)	0%	0.026
2%	(0.2,-0.2)	0%	0.034
5%	(0.2,-0.2)	0%	0.082
10%	(0.2,-0.2)	33%	0.212

Table 2.5: Results under experimental errors: multiple measurements

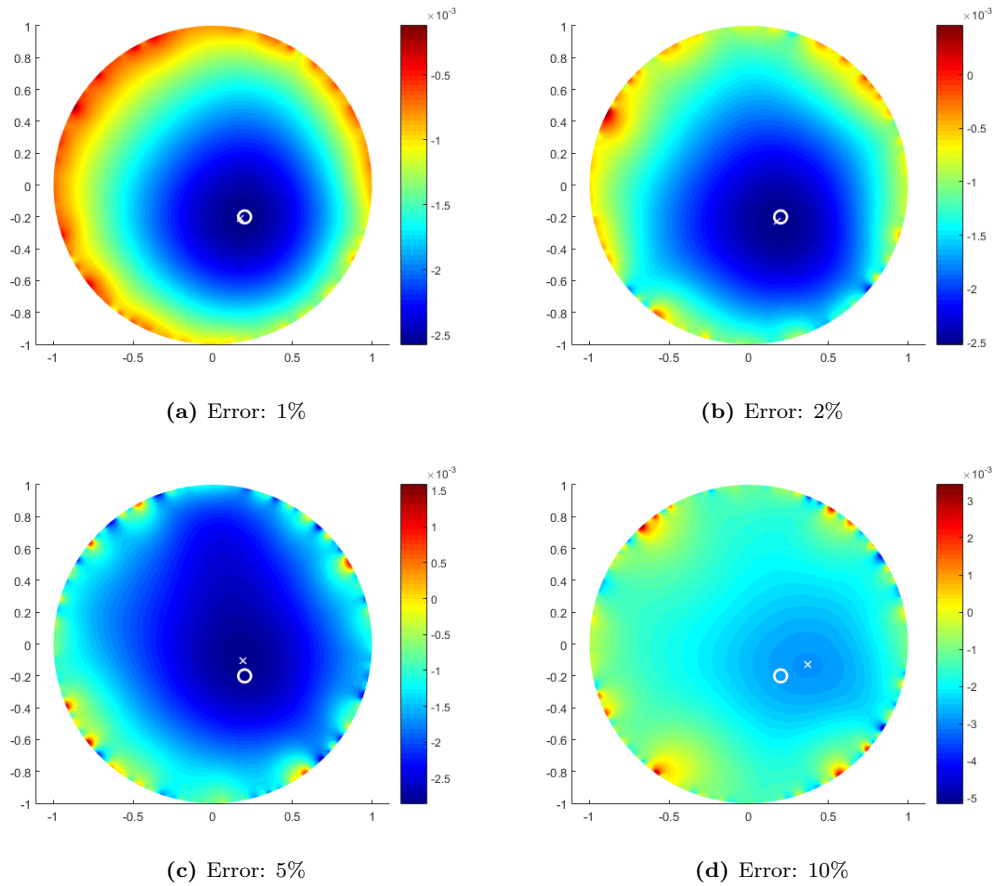
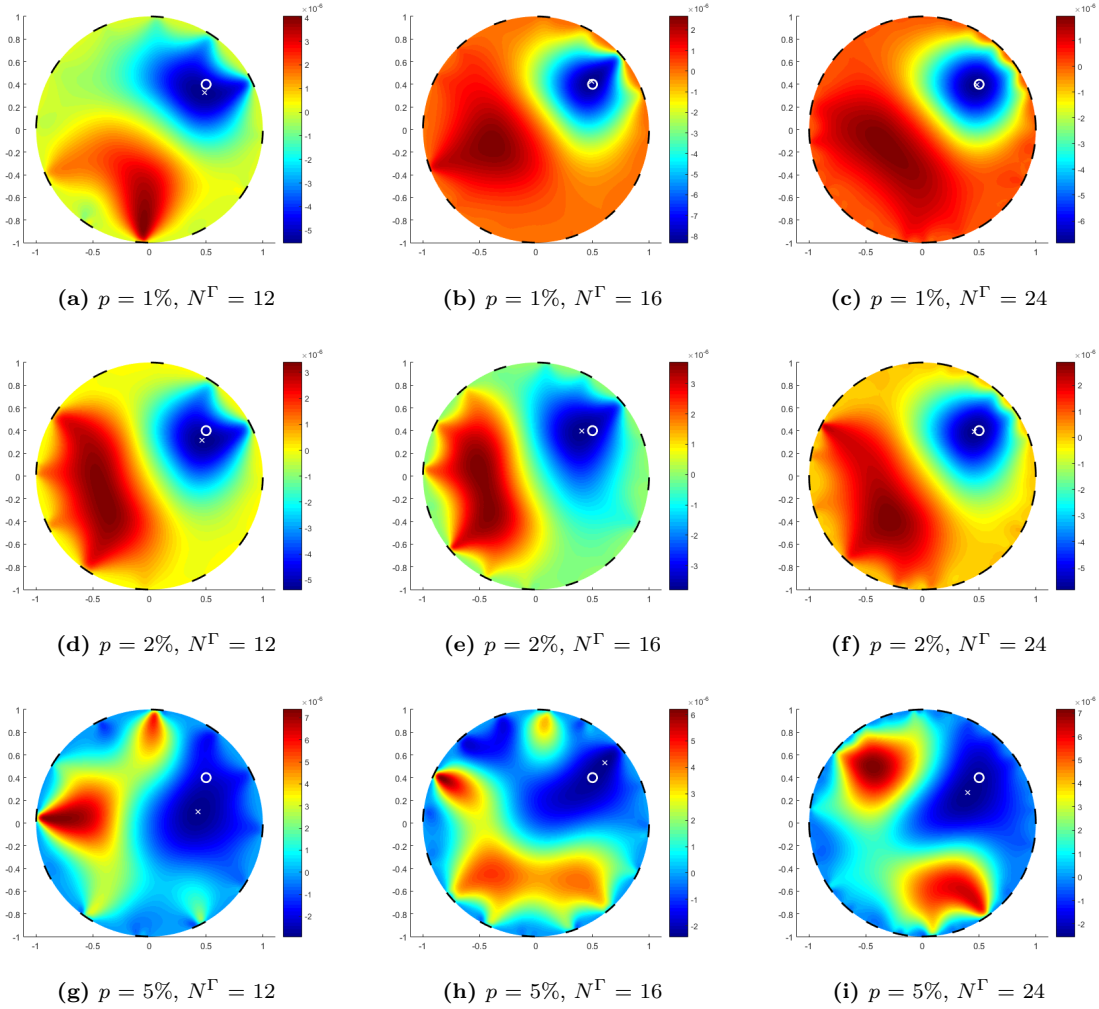


Figure 2.7: Results under experimental errors: multiple measurements

We point in the first case, i.e. the reconstruction with many measurements, that the detected position is stable under small perturbations of the data (namely, the error in reconstruction grows almost linearly with respect to the experimental noise), but there exists a threshold value (e.g., in the first case, below 10%) above which the information provided by the topological gradient is too noisy to be meaningful for the sake of reconstruction. The same happens in the second case, for each

	$N^\Gamma = 12$	$N^\Gamma = 16$	$N^\Gamma = 24$
$p = 1\%$	0.087	0.030	0.021
$p = 2\%$	0.103	0.087	0.040
$p = 5\%$	0.254	0.170	0.138

Table 2.6: Results under experimental errors: partial measurements**Figure 2.8:** Results under experimental errors: partial measurements

number N^Γ of portions Γ_i considered. This consists in a numerical validation of the local stability result proved in Section 2.2 for the inverse problem under discussion.

Chapter 3

Detection of small inclusions in a semilinear parabolic boundary value problem

In this chapter, we develop theoretical analysis and numerical reconstruction techniques for the solution of an inverse boundary value problem dealing with a semilinear parabolic equation, which consists in a significant intermediate problem in order to tackle the full complexity of the evolution of the electric potential in the myocardial tissue.

The determination of diffusion coefficients as well as of reaction terms for parabolic equations and, to a lesser extent, also the identification of unknown inclusions in the spatial domain is an extensively studied class of inverse problems (see, e.g., [91] [36], [90], [111] and references therein). Even when dealing with boundary value problems involving linear partial differential equations, the corresponding inverse problems turn out to be nonlinear, and this entails severe difficulties both for the well-posedness analysis and for the development of reconstruction algorithms. The problem we consider in this chapter is a mathematical challenge itself, never considered before from a rigorous analytical viewpoint. Indeed, here the difficulties include the nonlinearity of both the direct and the inverse problem, as well as the lack of measurements at disposal.

Our approach in tackling this problem is to develop a rigorous theoretical investigation both for the analysis and the numerical approximation of this inverse problem, inspired by the results obtained in a simpler stationary case in [30] and in Chapter 2. In particular, additional assumptions are needed to obtain rigorous theoretical results, namely by considering small-size conductivity inhomogeneities. We thus model ischemic regions as small inclusions ω_ε where the electric conductivity is significantly smaller than the one of healthy tissue and there is no ion transport. We establish a rigorous asymptotic expansion of the boundary potential perturbation due to the presence of the inclusion adapting to the parabolic nonlinear case the approach introduced by Capdeboscq and Vogelius in [47] for the case of the linear conductivity equation. A similar approach has also been used in Thermal Imaging (see, e.g., [12]).

We use these results to set a reconstruction procedure for detecting the inclusion. To this aim,

as in Chapter 2, we propose a reconstruction algorithm based on topological optimization, where a suitable quadratic functional is minimized to detect the position of the inclusion under a small size assumption (see also [52]). This requires the solution of two initial and boundary value problems, the background problem and the adjoint one, which are discretized by means of a Galerkin finite element method. Numerical results obtained on an idealized left ventricle geometry assess the feasibility of the proposed procedure. Several numerical test cases also show the robustness of the reconstruction procedure with respect to measurement noise, unavoidable when dealing with real data.

The chapter is organized as follows. In Section 3.1 we briefly describe the model and the direct and inverse problems which are the object of study. In Section 3.2 we show some suitable well-posedness results concerning the direct problems, in the unperturbed (background) and perturbed cases. In Section 3.3 we prove useful energy estimates of the difference of the solutions of the two previous problems. The asymptotic expansion formula is derived in Section 3.4 and the reconstruction algorithm in Section 3.5. Numerical results are finally provided in Section 3.6.

3.1 The monodomain model of cardiac electrophysiology

Throughout the chapter we consider the following (background) initial and boundary value problem

$$\begin{cases} \nu C_m u_t - \operatorname{div}(k_0 \nabla u) + \nu f(u) = 0, & \text{in } \Omega \times (0, T), \\ \frac{\partial u}{\partial n} = 0, & \text{on } \partial\Omega \times (0, T), \\ u(0) = u_0, & \text{in } \Omega, \end{cases} \quad (3.1)$$

where $\Omega \subset \mathbf{R}^3$ is a bounded set with boundary $\partial\Omega$, and $k_0 \in \mathbb{R}, k_0 > 0$.

As outlined in Chapter 1, this problem consists in a particular version of the *monodomain model* describing the macroscopic electric activity of the heart [132, 61]. This equation yields a macroscopic model of the cardiac tissue, arising from the superposition of intra and extra cellular media, both assumed to occupy the whole heart volume (bidomain model), making the hypothesis that the extracellular and the intracellular conductivities are proportional quantities. Here Ω is the domain occupied by the ventricle, u is the (transmembrane) electric potential, $f(u)$ is a nonlinear term modeling the ionic current flows across the membrane of cardiac cells, k_0 is the conductivity tensor of the healthy tissue, $C_m > 0$ and $\nu > 0$ are two constant coefficients representing the membrane capacitance and the surface area-to-volume ratio, respectively. For the sake of simplicity, in the following sections we fix $C_m = 1$ and $\nu = 1$. We deal with an insulated heart, namely, we do not consider the effect of the surrounding torso, which behaves as a passive conductor, whence the Neumann boundary conditions. The initial datum u_0 represents the initial activation of the tissue, arising from the propagation of the electrical impulse in the cardiac conduction system.

Throughout this chapter we assume (as performed, e.g., in [61, Sect. 4.2] and [132, Sect. 2.2]) that $f(u)$ is a cubic function,

$$f(u) = A^2(u - u_1)(u - u_2)(u - u_3), \quad u_i \in \mathbb{R}, \quad u_1 < u_2 < u_3; \quad (3.2)$$

this yields a *phenomenological* model which is capable of describing only the first part of the evolution of the heart electrical potential during the heartbeat: namely, the fast propagation of the initial stimulus, and not the slow plateau and repolarization phase. Phenomenological models allowing for

an accurate description of the whole heartbeat require the ionic current to be described as a function of u and at least a gating variable w : such models are not the object of study in this chapter.

Consider now a small inhomogeneity located in a measurable bounded domain $\omega_\varepsilon \subset \Omega$, such that there exists a compact set K_0 , with $\omega_\varepsilon \subset K_0 \subset \Omega$, and a constant $d_0 > 0$ satisfying

$$\text{dist}(\omega_\varepsilon, \Omega \setminus K_0) \geq d_0 > 0. \quad (3.3)$$

Moreover, we assume

$$|\omega_\varepsilon| > 0, \quad \lim_{\varepsilon \rightarrow 0} |\omega_\varepsilon| = 0. \quad (3.4)$$

In the inhomogeneity ω_ε the conductivity coefficient and the nonlinearity take different values with respect the ones in $\Omega \setminus \omega_\varepsilon$. Indeed, according to biological observations, cells in an infarcted area are no longer excitable, and the electrical conductivity in this portion of tissue is much smaller than the one of healthy tissue. As a matter of fact, we incorporate the presence of an ischemia into the model (3.5) by diverting (forcing) the ion transport to go around the infarcted areas, and by varying the conductivity in such regions, similarly to what proposed in [105]. The problem we consider is therefore

$$\begin{cases} u_t^\varepsilon - \text{div}(k_\varepsilon \nabla u^\varepsilon) + \chi_{\Omega \setminus \omega_\varepsilon} f(u^\varepsilon) = 0, & \text{in } \Omega \times (0, T), \\ \frac{\partial u^\varepsilon}{\partial n} = 0, & \text{on } \partial\Omega \times (0, T), \\ u^\varepsilon(0) = u_0, & \text{in } \Omega, \end{cases} \quad (3.5)$$

where χ_D stands for the characteristic function of a set $D \subset \mathbb{R}^3$. Here

$$k_\varepsilon = (k_0 - k_1)\chi_{\Omega \setminus \omega_\varepsilon} + k_1 = \begin{cases} k_0 & \text{in } \Omega \setminus \omega_\varepsilon, \\ k_1 & \text{in } \omega_\varepsilon, \end{cases} \quad (3.6)$$

with $k_0, k_1 \in \mathbb{R}$, $k_0 > k_1 > 0$.

The purpose of this chapter is to deal with the following problems:

Definition 3.1 (Direct problem). Knowing the inclusion ω_ε , determine the perturbed potential $u_\varepsilon(x, t)$ associated to for all $x \in \Omega$, $t \in (0, T)$ it through (3.5);

and conversely

Definition 3.2 (Inverse problem). Knowing the perturbed potential, and in particular only the boundary measurement $u_{meas} = u_\varepsilon|_{\partial\Omega}$ on $\partial\Omega \times (0, T)$, determine the inclusion ω_ε associated to it through (3.5)

The assumption made on the inclusion ω_ε (namely, (3.3) and (3.4)) must be considered as *regularization hypotheses*: i.e., we aim at exploiting them in order to derive rigorous analytical results involved both in the analysis of the inverse problem and in the deduction of a reconstruction algorithm. In order to embed information about prior knowledge on the shape of the ischemia, several different strategies can be considered, especially from an algorithmic point of view. For instance, in [105, 126] the parameters of a level set function are used to describe a non-homogeneous conductivity tensor and the related ionic current. A different approach is taken into account in [8, 54], where the presence of an ischemia is instead described in terms of two (non-homogeneous in space) parameters

of the ionic model; see also, e.g., [40] for similar considerations. Our approach is instead to assume (3.3), (3.4) and proceed analogously as in [30], [33]. In the final sections, we in particular focus on the identification of ischemias which can be assimilated to small spheres, whose position is unknown; note that the whole setting can be extended also to non connected ischemias – recent experimental measurements indeed show that ischemic regions are neither monolithic nor simply localized, see, e.g., [19] – described by a finite number of (small) well-separated inhomogeneities.

3.2 Well posedness of the direct problem

Concerning the mathematical analysis of both the monodomain and the bidomain models, several crucial results have been obtained for instance in [27, 39, 41, 61] in a general context. In the case we are considering, it is possible to prove analogous results and even additional properties both in case of healthy and ischemic tissue. Problem (3.1) hereon will be referred to as the *background problem*; we devote Section 3.2.1 to the analysis of its well-posedness. The well-posedness of the perturbed problem modeling the presence of a small inclusion in the domain will be instead analyzed in Section 3.2.2.

3.2.1 Well posedness of the background problem

We make the following assumptions:

$$\begin{aligned} \Omega &\in C^{2+\alpha}, \quad \alpha \in (0, 1), \\ u_0 &\in C^{2+\alpha}(\bar{\Omega}), \quad u_1 < u_0(x) < u_3 \quad \forall x \in \Omega, \quad \frac{\partial u_0(\sigma)}{\partial n} = 0 \quad \forall \sigma \in \partial\Omega. \end{aligned} \quad (3.7)$$

Moreover, since f has the form (3.2), let us set

$$M_1 := \|f\|_{C([u_1, u_3])}, \quad M_2 := \|f'\|_{C([u_1, u_3])}. \quad (3.8)$$

The following well posedness result holds.

Theorem 3.1. *Let us assume (3.2), (3.7). Then problem (3.1) admits a unique solution $u \in C^{2+\alpha, 1+\alpha/2}(\bar{\Omega} \times [0, T])$ such that*

$$u_1 \leq u(x, t) \leq u_3, \quad (x, t) \in \bar{\Omega} \times [0, T], \quad (3.9)$$

$$\|u\|_{C^{2+\alpha, 1+\alpha/2}(\bar{\Omega} \times [0, T])} \leq C, \quad (3.10)$$

where C is a positive constant depending (at most) on $k_0, T, \Omega, M_1, M_2, \|u_0\|_{C^{2+\alpha}(\bar{\Omega})}$.

Proof. The proof of (3.9) can be obtained using the results in [116] and [104]. In particular, [116, Theorem 4.1, Chapter 2] provides an existence-comparison result for a rather general class of semilinear parabolic boundary value problems, to which problem(3.1) belongs, as we demonstrate. First of all, we remark that the constants $\hat{u} = u_1$ and $\tilde{u} = u_3$ can be considered respectively as an upper and a lower solution of (3.1): they both identically satisfy the equation in $\Omega \times (0, T)$, together with the Neumann boundary condition; whereas thanks to assumption (3.7) it holds that $u_1 \leq u_0(x) \leq u_3$ in Ω . Moreover, the function f appearing in (3.1) satisfies

$$-\lambda(u - v) \leq f(u) - f(v) \leq \lambda(u - v) \quad \forall u, v \in [u_1, u_3], \quad (3.11)$$

with c a positive constant depending on A, u_1, u_2, u_3 . Indeed, since f is differentiable, Lebesgue's mean value theorem ensures that, $\forall u, v \in [u_1, u_3]$ there exists $\xi \in [u_1, u_3]$ such that

$$f(u) - f(v) = f'(\xi)(u - v)$$

and being $f'(u) = 3u^2 - 2(u_1 + u_2 + u_3)u + (u_1u_2 + u_2u_3 + u_3u_1)$ a continuous function, we can surely find $\lambda > 0$ s.t. $|f'(u)| \leq \lambda$ by taking, e.g., $\lambda = M_2$. Then, according to [116, Theorem 4.1, Chapter 2] there exists an unique solution u of (3.1), $u \in C^{2+\alpha, 1+\alpha/2}(\Omega \times (0, T))$ and $u_1 \leq u \leq u_3$. Since u is also continuous on $\Omega \times [0, T]$, it is also possible to recover $u \in C^{2+\alpha, 1+\alpha/2}(\bar{\Omega} \times [0, T])$ by a combination of [104, Theorem 5.1.17 (ii), pag. 201] and [104, Theorem 5.1.20, pag. 205], setting $q(x, t) = -f(u(x, t))$ as a right-hand side. We also have

$$\|u\|_{C^{2+\alpha, 1+\alpha/2}(\bar{\Omega} \times [0, T])} \leq C \left(\|u_0\|_{C^{2+\alpha}(\bar{\Omega})} + \|q\|_{C^{\alpha, \alpha/2}(\bar{\Omega} \times [0, T])} \right).$$

Finally, (3.10) follows from the definitions of q and f and from the bound $u_1 \leq u \leq u_3$. \square

3.2.2 Well posedness of the perturbed problem

Hereon, for the sake of brevity, we will omit in all the integrals the dependence on the space variable and/or on the time variable of the integrated functions, unless it is necessary to avoid misunderstandings. Moreover, all inequalities depending on t are valid for $t \in (0, T)$.

The well-posedness of the perturbed problem (3.5) is provided by the following theorem.

Theorem 3.2. *Assume (3.2), (3.6), (3.7). Then problem (3.5) admits a unique weak solution, i.e. a function u^ε with distributional derivative u_t^ε such that*

$$\begin{aligned} u^\varepsilon &\in L^2(0, T; H^1(\Omega)) \cap C([0, T]; L^2(\Omega)) \cap L^4(\Omega^* \times (0, T)), \\ u_t^\varepsilon &\in L^2(0, T; H^*) + L^{4/3}(\Omega \times (0, T)), \end{aligned} \quad (3.12)$$

where $\Omega^* = \Omega \setminus \omega_\varepsilon$ and $H^* = (H^1(\Omega))'$, satisfying

$$\int_{\Omega} u_t^\varepsilon v + \int_{\Omega} k_\varepsilon \nabla u^\varepsilon \cdot \nabla v + \int_{\Omega} \chi_{\Omega \setminus \omega_\varepsilon} f(u^\varepsilon) v = 0 \quad (3.13)$$

for all $v \in H^1(\Omega)$, and distributionally in time. In addition, $u^\varepsilon \in C^{\alpha, \alpha/2}(\bar{\Omega} \times [0, T])$ and $u_1 \leq u^\varepsilon \leq u_3$.

Proof. Recalling the definition of f , there exist $k \geq 0$, $\alpha_1 > 0$, $\alpha_2 > 0$, $\lambda > 0$ such that

$$\alpha_1 u^4 - k \leq f(u)u \leq \alpha_2 u^4 + k, \quad f'(u) \geq -\lambda. \quad (3.14)$$

Consider problem (3.5) in the weak form as in (3.13) Setting $\tilde{f}(u) = f(u) - u$, (3.13) becomes

$$\int_{\Omega} u_t^\varepsilon v dx + \int_{\Omega} k_\varepsilon \nabla u^\varepsilon \cdot \nabla v dx + \int_{\Omega} \chi_{\Omega \setminus \omega_\varepsilon} u^\varepsilon v dx + \int_{\Omega} \chi_{\Omega \setminus \omega_\varepsilon} \tilde{f}(u^\varepsilon) v dx = 0, \quad \forall v \in H^1(\Omega). \quad (3.15)$$

Observe that, thanks to following the Poincaré type inequality in [30, formula (A.4)]

$$\|z\|_{H^1(\Omega)}^2 \leq S(\Omega) \left(\|\nabla z\|_{L^2(\Omega)}^2 + \|z\|_{L^2(\Omega \setminus \omega_\varepsilon)}^2 \right), \quad \forall z \in H^1(\Omega), \quad (3.16)$$

the bilinear form $a_\varepsilon(u^\varepsilon, v) = \left(\int_\Omega k_\varepsilon \nabla u^\varepsilon \cdot \nabla v dx + \int_{\Omega \setminus \omega_\varepsilon} u^\varepsilon v \right)$ is coercive. Indeed

$$a_\varepsilon(u^\varepsilon, u^\varepsilon) = \int_\Omega k_\varepsilon |\nabla u^\varepsilon|^2 dx + \int_{\Omega \setminus \omega_\varepsilon} (u^\varepsilon)^2 dx \geq S \|u^\varepsilon\|_{H^1(\Omega)}^2, \quad (3.17)$$

where S is a positive constant depending on Ω and k_1 . Through the Faedo-Galerkin approximation scheme it is possible to prove that problem (3.5) admits a unique weak solution u^ε satisfying (3.12). We nevertheless report the main steps of the proof.

1. Discrete problems

Since a_ε is a coercive bilinear form, it associated to an operator $A_\varepsilon : H^1(\Omega) \rightarrow H^1(\Omega)$ such that $a_\varepsilon(u, v) = (A_\varepsilon(u), v)_{H^1}$, and A_ε is compact. According to the spectral theory of the compact (self-adjoint) operators, there exists a basis of $H^1(\Omega)$, orthonormal with respect to the $L^2(\Omega)$ norm, composed by eigenfunctions of A , $\{\Psi_i\}_{i \in \mathbb{N}}$ associated to eigenvalues $\{\lambda_i\}_{i \in \mathbb{N}}$ (see [Raviart-Thomas]). Consider the basis $\{\Psi_i\}_{i \in \mathbb{N}}$ of eigenfunctions of \mathcal{B} and fix a positive $m \in \mathbb{N}$. Define $V_m = \text{span}\{\Psi_i, i = 1, \dots, m\} \subset H^1(\Omega)$ and the orthogonal projection operator $P_m : H^1(\Omega) \rightarrow V_m$

$$P_m : v \mapsto v_m, \quad v_m = \sum_{i=1}^m v_i \Psi_i \quad v_i = \int_\Omega v \Psi_i.$$

One can easily prove that $\|P_m v\|_{L^2(\Omega)} \leq \|v\|_{L^2(\Omega)}$, $\|P_m v\|_{H^1(\Omega)} \leq \left(1 + \frac{k_0}{k_1}\right) \|v\|_{H^1(\Omega)}$. Introduce the functions $\tilde{u}_m, w_m \in V_m$ s.t.

$$u_m(x, t) = \sum_{i=1}^m u_{im}(t) \Psi_i(x)$$

where the components $u_{im} : \mathbb{R} \rightarrow \mathbb{R}$ are the solutions in of the system of ordinary differential equations:

$$\begin{cases} \dot{u}_{im}(t) + \lambda_i u_{im}(t) + \int_\Omega (1 - \chi_\omega) \tilde{f}(u_m(t)) \Psi_i = 0 & i = 1, \dots, m \\ u_m(0) = P_m(u_0) \end{cases} \quad (3.18)$$

The integral terms in the system are well posed due to properties (3.14). According to Cauchy-Peano local existence theorem, since f and \tilde{f} are continuous functions with respect to u , the solution of system (3.18) exists unique in $C^1(0, t_m)$, where t_m may depend on m . In order to conclude that $t_m > T \forall m$, we need to show that $u_m(t)$ and $w_m(t)$ are bounded in $L^\infty(0, T; L^2)$ independently of m , which will be done in the next step.

2. *A priori* estimates

We state and prove the following *a priori* uniform estimates regarding u_m ; i.e., if its components are solutions of system (3.18), they satisfy

$$\|u_m\|_{L^\infty(0, T; L^2)} \leq c_1, \quad (3.19)$$

$$\|u_m\|_{L^2(0, T; H^1)}, \|u_m\|_{L^4(Q_T^*)} \leq c_2, \quad (3.20)$$

$$\|\dot{u}_m\|_{L^2(0, T; H^*) + L^{4/3}(Q_T)} \leq c_3, \quad (3.21)$$

where $\dot{u}_m = \sum_{i=1}^m \dot{u}_{im} \psi_i$ and c_1, c_2, c_3 are positive constants depending on $|\Omega|, T, k_1, f, \|u_0\|_{L^2}$. In order to prove them, take the m equations in (3.18), multiply them times u_{im} and sum together. Exploiting the eigenvalue and eigenvector properties, we obtain:

$$\frac{1}{2} \frac{d}{dt} \|u_m(\cdot, t)\|_{L^2(\Omega)}^2 + a_\varepsilon(u_m(\cdot, t), u_m(\cdot, t)) + \int_\Omega (1 - \chi_{\omega_\varepsilon}) \tilde{f}(u_m(\cdot, t)) u_m(\cdot, t) = 0. \quad (3.22)$$

Taking advantage of the coercivity of a_ε and of the estimate from below (3.14), via Young inequality we get

$$\frac{1}{2} \frac{d}{dt} \|u_m(\cdot, t)\|_{L^2(\Omega)}^2 + S \|u_m(\cdot, t)\|_{H^1(\Omega)}^2 + \alpha_1 \int_{\Omega^*} |u_m(\cdot, t)|^4 \leq \frac{k}{2} |\Omega| + \left(1 + \frac{k}{2}\right) \|u_m(\cdot, t)\|_{L^2(\Omega)}^2;$$

integrating from 0 to $t \leq T$ and using the fact that $\|u_m(0)\|_{L^2} = \|P_m(u_0)\|_{L^2} \leq \|u_0\|_{L^2}$, we obtain the following important estimate:

$$\begin{aligned} & \frac{1}{2} \|u_m(\cdot, t)\|_{L^2(\Omega)}^2 + S \int_0^t \|u_m(\cdot, s)\|_{H^1(\Omega)}^2 + \alpha_1 \|u_m\|_{L^4(\Omega^* \times (0, t))}^4 \\ & \leq \frac{k}{2} |\Omega| t + \left(1 + \frac{k}{2}\right) \int_0^t \|u_m(\cdot, s)\|_{L^2(\Omega)}^2 + \frac{1}{2} \|u_0\|_{L^2(\Omega)}^2. \end{aligned} \quad (3.23)$$

As a consequence of (3.23), thanks to Gronwall's inequality

$$\|u_m(\cdot, t)\|_{L^2(\Omega)}^2 \leq \left(k|\Omega|T + \|u_0\|_{L^2(\Omega)}^2\right) e^{(2+k)t} := c_1^2, \quad (3.24)$$

which proves (3.19).

Moreover, taking (3.23) with $t = T$ via (3.24), we have

$$S \|u_m\|_{L^2(0, T; H^1)}^2 + \alpha_1 \|u_m\|_{L^4(\Omega^* \times (0, T))}^4 \leq \frac{k}{2} |\Omega| T + \left(1 + \frac{k}{2}\right) T c_1^2 + \frac{1}{2} \|u_0\|_{L^2(\Omega)}^2 =: \tilde{c}_2,$$

hence (3.20) holds with $c_2 = \max(\sqrt{\frac{\tilde{c}_2}{S}}, \sqrt[4]{\frac{\tilde{c}_2}{\alpha_1}})$.

Instead, in order to prove (3.21), we need to consider $\dot{u}_m(\cdot, t)$ as a sum of two operators: one in the dual of $H^1(\Omega)$ a.e. in $(0, T)$ (and with square integrable H^* -norm), and one in the dual of $L^4(\Omega \times (0, T))$. Let $v \in H^1(\Omega)$:

$$\langle \dot{u}_m(\cdot, t), v \rangle_* = \sum_{i=1}^m \langle \dot{u}_{im}(t) \Psi_{im}, v \rangle_* = \sum_{i=1}^m \int_\Omega \dot{u}_{im} \Psi_i v = \int_\Omega \dot{u}_m(\cdot, t) v_m,$$

where $v_m = P_m v$. Taking the m equations of (3.18), multiplying each of them by v_i and summing up, we obtain

$$\int_\Omega \dot{u}_m(\cdot, t) v_m = -a_\varepsilon(u_m(\cdot, t), v_m) - \int_{\Omega^*} \tilde{f}(u_m(\cdot, t)) v_m;$$

Consider now $\dot{u}_m^{(1)}$ s.t. $\langle \dot{u}_m^{(1)}, v \rangle_* = -a_\varepsilon(u_m(\cdot, t), v_m)$:

$$|\langle \dot{u}_m^{(1)}(\cdot, t), v \rangle_*| = |\mathcal{B}(u_m(\cdot, t), v_m)| \leq k_0 \|u_m(\cdot, t)\|_{H^1(\Omega)} \left(1 + \frac{k_0}{k_1}\right) \|v\|_{H^1(\Omega)}$$

hence $\|\dot{u}_m^{(1)}\|_{L^2(0,T;H^*)}$ is controlled by $\|u\|_{L^2(0,T;H^1)}$ whence by c_2 . Instead, consider $\dot{u}^{(2)}$ s.t. $\langle \dot{u}_m^{(2)}, v \rangle_* = -\int_{\Omega^*} \tilde{f}(u_m(\cdot, t))v_m$: for each $v \in H^1(\Omega)$, $\Phi \in \mathcal{D}(0, T)$,

$$\left| \langle \dot{u}_m^{(2)}(\cdot, t), v \rangle_*, \Phi(t) \right| = \left| \int_0^T \int_{\Omega^*} \tilde{f}(u_m)v_m\Phi \right| \leq \|\tilde{f}(u_m)\|_{L^{4/3}(\Omega^* \times (0, T))} \|v_m\Phi\|_{L^4(\Omega \times (0, T))}.$$

Hence, using also (3.14),

$$\begin{aligned} \|\dot{u}_m^{(2)}\|_{L^{4/3}(\Omega \times (0, T))} &\leq \left(1 + \frac{k_0}{k_1}\right) \|\tilde{f}(u_m)\|_{L^{4/3}(\Omega^* \times (0, T))} = c \left(\int_0^T \|\tilde{f}(u_m(\cdot, t))\|_{L^{4/3}(\Omega^*)}^{4/3} dt \right)^{3/4} \\ &\leq c \left(\int_0^T \int_{\Omega^*} (\alpha_1 |u_m(\cdot, t)|^4 + k + |u_m(\cdot, t)|)^{4/3} dt \right)^{3/4} \\ &\leq a_1 \|u_m\|_{L^4(\Omega^* \times (0, T))}^3 + a_2 |\Omega|^{3/4} T^{3/4} \leq a_1 c_2^3 + a_2 |\Omega|^{3/4} T^{3/4}. \end{aligned}$$

We hence conclude that $\dot{u}_m \in L^2(0, T; H^*) + L^{4/3}(Q_T)$ and that (3.21) is verified with a suitable c_4 .

3. Convergence to a solution

According to estimate (3.19), the solution of the discrete problem (3.18) is well defined globally in $C^1(0, T; \mathbb{R}^m)$ for each m . Thanks to the provided *a priori* estimates, we know that the sequences $\{u_m\}$, $\{\dot{u}_m\}$ are bounded (uniformly in m) in the spaces $L^2(0, T; H^1) \cap L^4(\Omega^* \times (0, T))$ and $L^2(0, T; H^*) + L^{4/3}(\Omega \times (0, T))$ respectively. According to compactness results, we know that $\exists u \in L^2(0, T; H^1) \cap L^4(\Omega^* \times (0, T))$, $u^* \in L^2(0, T; H^*) + L^{4/3}(\Omega \times (0, T))$ s.t.

$$u_m \xrightarrow{L^2(0, T; H^1)} u, \quad \dot{u}_m \xrightarrow{L^2(0, T; H^*) + L^{4/3}} u^*.$$

Moreover, since $L^2(0, T; H^*) + L^{4/3}(\Omega \times (0, T)) \subset L^{4/3}(0, T; H^*)$, $\{u_m\}$ is such that $\|u_m\|_{L^2(0, T; H^1)}$ and $\|\partial_t u_m\|_{L^{4/3}(0, T; H^*)}$ are bounded independently of m , and by [103, Theorem 5.1, Chapter 1] this implies that, up to a subsequence, $u_m \xrightarrow{L^2(\Omega \times (0, T))} \tilde{u}$.

We now study the asymptotic behaviour when $m \rightarrow +\infty$ of the terms of

$$\langle \dot{u}_m, v \rangle_* + a_\varepsilon(u_m, v) + \int_\Omega (1 - \chi_{\omega_\varepsilon}) \tilde{f}(u_m)v = 0, \quad (3.25)$$

which is equivalent to (3.18) if $v, \psi \in V_m$ and in particular for $v = \Psi_i$.

- consider $v \in H^1(\Omega)$, $\Phi \in \mathcal{D}(0, T)$

$$\left\langle \lim_{m \rightarrow \infty} \langle \dot{u}_m, v \rangle_*, \Phi \right\rangle = - \left\langle \lim_{m \rightarrow \infty} \langle u_m, v \rangle_*, \Phi' \right\rangle = - \left\langle \int_\Omega uv, \Phi' \right\rangle = \langle \langle u_t, v \rangle_*, \Phi \rangle,$$

which implies that $\lim_{m \rightarrow \infty} \langle \dot{u}_m, v \rangle_* = \langle u_t, v \rangle_*$ in a distributional sense. Moreover, since $v\Phi \in L^2(0, T; H^1) \cap L^4(\Omega^* \times (0, T))$ we also have

$$\lim_{m \rightarrow \infty} \langle \langle \dot{u}_m, v \rangle_*, \Phi \rangle = \langle \langle u^*, v \rangle_*, \Phi \rangle,$$

hence in addition $u_t = u^* \in L^2(0, T; H^*) \cap L^{4/3}(\Omega \times (0, T))$;

- consider $v \in H^1(\Omega)$ and $\Phi \in \mathcal{D}(0, T)$: by weak convergence,

$$\lim_{m \rightarrow \infty} \langle a_\varepsilon(u_m, v), \Phi \rangle = \int_0^T \lim_{m \rightarrow \infty} a_\varepsilon(u_m, v\Phi) = \int_0^T a_\varepsilon(u, v\Phi) = \langle a_\varepsilon(u, v), \Phi \rangle;$$

- recall the expression $\tilde{f}(u) = f(u) - u$: one easily proves that, by weak convergences

$$\int_0^T \int_\Omega (1 - \chi_{\omega_\varepsilon}) u_m v \Phi \rightarrow \int_0^T \int_\Omega (1 - \chi_{\omega_\varepsilon}) u v \Phi. \quad (3.26)$$

Nevertheless, also

$$\int_0^T \int_\Omega (1 - \chi_{\omega_\varepsilon}) f(u_m) v \Phi \rightarrow \int_0^T \int_\Omega (1 - \chi_{\omega_\varepsilon}) f(u) v \Phi; \quad (3.27)$$

indeed, since $u_m \xrightarrow{L^2} u$, then (up to a subsequence) the convergence is also pointwise almost everywhere, and this, together with the bound

$$\|(1 - \chi_{\omega_\varepsilon}) f(u_m) v \Phi\|_{L^1(\Omega \times (0, T))} \leq \|f(u_m)\|_{L^{4/3}(\Omega^* \times (0, T))} \|v\|_{L^4(\Omega)} \|\Phi\|_\infty \leq c \|v\|_{L^4(\Omega)} \|\Phi\|_\infty$$

(with $c = c(|\Omega|, T, c_2, k, \alpha_1)$) allows to apply the Lebesgue's theorem of dominated convergence.

Combining all the results that are previously listed, according to (3.25) we obtain that u satisfies distributionally in time

$$\langle u_t, v \rangle_* + a_\varepsilon(u, v) + \int_\Omega (1 - \chi_{\omega_\varepsilon}) \tilde{f}(u) v = 0$$

for all $v \in V_m$, $\forall m$, and since $\{\Psi_m\}$ is dense in $H^1(\Omega)$, the equation is satisfied for all $v \in H^1(\Omega)$. This finally allows to conclude that u is a weak solution of problem (3.5). Moreover, $u \in C([0, T]; L^2(\Omega))$: indeed, it holds that $\langle u_t(\cdot, t), u(\cdot, t) \rangle_* = \frac{1}{2} \frac{d}{dt} \|u(\cdot, t)\|_{L^2(\Omega)}^2$ in the sense of distributions, and hence

$$\frac{1}{2} \frac{d}{dt} \|u(\cdot, t)\|_{L^2(\Omega)}^2 = - \int_\Omega a_\varepsilon(u(\cdot, t), u(\cdot, t)) - \int_\Omega (1 - \chi_{\omega_\varepsilon}) f(u(\cdot, t)) u(\cdot, t),$$

where the right-hand side surely belongs to $L^1(0, T)$. By the fundamental theorem of calculus, one obtains that $u \in C([0, T]; L^2(\Omega))$.

4. Uniqueness

Consider two different solutions u, u' of (3.5). By testing the weak form of (3.5) both for u and u' with $w = u - u'$ and subtracting, we get

$$\frac{1}{2} \frac{d}{dt} \|w(\cdot, t)\|_{L^2(\Omega)}^2 + \int_\Omega k_\varepsilon |\nabla w(\cdot, t)|^2 + \int_\Omega (1 - \chi_{\omega_\varepsilon}) (f(u(\cdot, t)) - f(u'(\cdot, t))) w(\cdot, t) = 0.$$

Using (3.16) and (3.11),

$$\frac{1}{2} \frac{d}{dt} \|w(\cdot, t)\|_{L^2(\Omega)}^2 + S \|w(\cdot, t)\|_{H^1(\Omega)}^2 \leq (1 + \lambda) \|w(\cdot, t)\|_{L^2(\Omega)}^2,$$

and integrating from 0 to T (since $u(\cdot, 0) = u'(\cdot, 0) = u_0$)

$$\frac{1}{2} \|w(\cdot, t)\|_{L^2(\Omega)}^2 + S \|w(\cdot, t)\|_{L^2(0,t;H^1)}^2 \leq (1 + \lambda) \int_0^t \|w(\cdot, s)\|_{L^2(\Omega)}^2;$$

this entails (via Gronwall's inequality) that $\|w(\cdot, t)\|_{L^2(\Omega)} = 0$ for all $t \in (0, T)$. Analogously one proves that $\|w(\cdot, t)\|_{L^2(0,T;H^1)} = 0$ and $\|w_t(\cdot, t)\|_{L^2(0,T;H^*)+L^{4/3}(\Omega \times (0,T))} = 0$ and eventually that u and u' are the same solution.

Denote now the unique weak solution of (3.5) as u^ε . In order to obtain further regularity for u^ε , let $\{\phi_n\}$ be a sequence such that

$$\phi_n \in C^1(\bar{\Omega}), \quad 0 \leq \phi_n(x) \leq 1, \quad \forall x \in \bar{\Omega}, \quad \text{and } \phi_n \rightarrow \chi_{\Omega \setminus \omega_\varepsilon} \text{ in } L^2(\Omega), \quad (3.28)$$

and formulate the approximating problems

$$\begin{cases} u_t^n - \operatorname{div}((k_0 - k_1)\phi_n + k_1)\nabla u^n + \phi_n f(u^n) = 0, & \text{in } \Omega \times (0, T), \\ \frac{\partial u^n}{\partial n} = 0, & \text{on } \partial\Omega \times (0, T), \\ u^n(0) = u_0, & \text{in } \Omega. \end{cases} \quad (3.29)$$

Using the same arguments as in the proof of Theorem 3.1, since the coefficients of (3.29) are sufficiently smooth, we can prove that, $\forall n \in \mathbb{N}$, problem (3.29) admits a unique solution u^n such that

$$u^n \in C^{2+\alpha, 1+\alpha/2}(\bar{\Omega} \times [0, T]), \quad u_1 \leq u^n(x, t) \leq u_3, \quad (x, t) \in \bar{\Omega} \times [0, T].$$

Regarding the sequence of regularized solutions $\{u^n\}$ we can derive uniform estimates similar to the ones for u^ε , and even more restrictive, exploiting the uniform bound $u^n \in [u_1, u_3]$:

$$\|u^n\|_{L^\infty(0,T;L^2)} \leq c_1, \quad (3.30)$$

$$\|u^n\|_{L^2(0,T;H^1)} \leq c_2, \quad (3.31)$$

$$\|u_t^n\|_{L^2(0,T;H^*)} \leq c_3, \quad (3.32)$$

with constants c_1, c_2, c_3 independent of n . Indeed, the weak formulation of problem (3.29) is

$$\int_{\Omega} u_t^n v + \int_{\Omega} ((k_0 - k_1)\phi_n + k_1)\nabla u^n \cdot \nabla v + \int_{\Omega} \phi_n f(u^n) v = 0, \quad \forall v \in H^1(\Omega). \quad (3.33)$$

By considering $v = u^n$, exploiting the coercivity of the bilinear form and (3.11),

$$\frac{1}{2} \frac{d}{dt} \|u^n(\cdot, t)\|_{L^2(\Omega)}^2 + k_1 \|u^n(\cdot, t)\|_{H^1(\Omega)}^2 \leq (k_1 + \lambda) \|u^n(\cdot, t)\|_{L^2(\Omega)}^2;$$

integrating in time and applying Gronwall's inequality we conclude (3.30) and (3.31). Instead,

$$\int_{\Omega} u_t^n v = - \int_{\Omega} ((k_0 - k_1)\phi_n + k_1)\nabla u^n \cdot \nabla v - \int_{\Omega} \phi_n f(u^n) v$$

hence $\|u_t^n\|_{L^2(0,T;H^*)} \leq \|u_t^n\|_{L^2(\Omega \times (0,T))} \leq k_0 \|u^n\|_{L^2(0,T;H^1)} + M_1 |\Omega|^{\frac{1}{2}} T^{\frac{1}{2}}$.

From (3.31) and (3.32) we can argue that $\exists \zeta \in L^2(0, T; H^1), \zeta^* \in L^2(0, T; H^*)$ s.t. $u^n \xrightarrow{L^2(0,T;H^1)} \zeta$ and $u_t^n \xrightarrow{L^2(0,T;H^*)} \zeta^*$, and via [122, Theorem 8.1], we conclude also that (up to a subsequence) $u^n \xrightarrow{L^2(\Omega \times (0,T))} \zeta$ and pointwise almost everywhere. Consider now problem (3.33) solved by u^n and take the limit of each term as $\varepsilon \rightarrow 0$:

- for any $v \in H^1(\Omega)$, $\Phi \in \mathcal{D}(0, T)$

$$\langle \lim_{n \rightarrow \infty} \langle u_t^n, v \rangle_*, \Phi \rangle = - \langle \lim_{n \rightarrow \infty} \langle u^n, v \rangle_*, \Phi' \rangle = - \langle \int_{\Omega} \zeta v, \Phi' \rangle = \langle \langle \zeta_t, v \rangle_*, \Phi \rangle,$$

which implies that $\lim_{n \rightarrow \infty} \langle u_t, v \rangle_* = \langle \zeta_t, v \rangle_*$ in a distributional sense. Moreover, since $v\Phi \in L^2(0, T; H^1)$, by weak convergence we also have

$$\lim_{n \rightarrow \infty} \langle \langle u_t^n, v \rangle_*, \Phi \rangle = \langle \langle \zeta^*, v \rangle_*, \Phi \rangle,$$

hence in addition $\zeta_t = \zeta^* \in L^2(0, T; H^*)$.

- We now prove that

$$\int_{\Omega} ((k_0 - k_1)\phi_n + k_1)\nabla u^n \cdot \nabla v \rightarrow \int_{\Omega} k_{\varepsilon}\nabla \zeta \cdot \nabla v, \quad (3.34)$$

by means of the following splitting: assuming the notation $k^n = ((k_0 - k_1)\phi_n + k_1)$,

$$\int_{\Omega} (k^n \nabla u^n - k_{\varepsilon} \nabla \zeta) \cdot \nabla v = \int_{\Omega} k^n \nabla (u^n - \zeta) \cdot \nabla v + \int_{\Omega} (k^n - k_{\varepsilon}) \nabla \zeta \cdot \nabla v.$$

The first term in the right-hand side tends to 0 due to the weak convergence of u^n and the uniform bound $k^n \leq k_0$; whereas the second term converges to 0 due to dominated convergence theorem.

- Finally, the convergence of the last term holds: for all $v \in H^1(\Omega)$ and in a distributional sense in time,

$$\int_{\Omega} \phi_n f(u^n) v \rightarrow \int_{\Omega} (1 - \chi_{\omega_{\varepsilon}}) f(\zeta) v.$$

This can be proved invoking the dominated convergence theorem, since ϕ_n and u^n converge pointwise (a.e.) and the uniform bound $u^n \in [u_1, u_3]$ implies that $|f(u^n)| \leq M_1$ in $\Omega \times (0, T)$.

Collecting all the results, we can assess that ζ is a weak solution of (3.5), and by uniqueness of the weak solution we conclude that $\zeta = u^{\varepsilon}$. Moreover, by (a.e.) pointwise convergence, u_{ε} satisfies

$$u_1 \leq u^{\varepsilon}(x, t) \leq u_3, \quad \text{a.e. in } \bar{\Omega} \times [0, T]. \quad (3.35)$$

Eventually, the additional (Hölder) regularity on u^{ε} can be recovered via [99, Theorem 10.1, Chapter 3]. Indeed, u^{ε} satisfies

$$u^{\varepsilon} - \operatorname{div}(k_{\varepsilon} \nabla u^{\varepsilon}) = -(1 - \chi_{\omega_{\varepsilon}}) f(u^{\varepsilon});$$

the hypothesis of the theorem hold since $k_{\varepsilon} \in L^{\infty}(\Omega)$, $u_{\varepsilon} \in L^{\infty}(\Omega \times (0, T))$ and hence also $f(u^{\varepsilon}) \in L^{\infty}(\Omega \times (0, T))$. We can extend the results up to the boundary due to the assumptions on $\partial\Omega$ and u_0 , and conclude $u_{\varepsilon} \in C^{\alpha, \alpha/2}(\bar{\Omega} \times [0, T])$. \square

3.3 Energy estimates for $u^{\varepsilon} - u$

In this section we prove some energy estimates for the difference between u^{ε} and u , solutions to problem (3.5) and problem (3.1), respectively, that are crucial to establish the asymptotic formula for $u^{\varepsilon} - u$ of Theorem 3.3 in Section 3.4.

Proposition 3.1. *Assume (3.2), (3.6), (3.7). Setting $w := u^\varepsilon - u$, then*

$$\|w\|_{L^\infty(0,T;L^2(\Omega))} \leq C|\omega_\varepsilon|^{1/2}, \quad (3.36)$$

$$\|w\|_{L^2(0,T;H^1(\Omega))} \leq C|\omega_\varepsilon|^{1/2}. \quad (3.37)$$

Moreover, there exists $0 < \beta < 1$ such that

$$\|w\|_{L^2(\Omega \times (0,T))} \leq C|\omega_\varepsilon|^{\frac{1}{2}+\beta}. \quad (3.38)$$

Here C stands for a positive constant depending (at most) on $k_0, k_1, \Omega, T, M_1, M_2, \|u_0\|_{C^{2+\alpha}(\bar{\Omega})}$.

Proof. Throughout the proof C will be as in the statement of the Theorem. According to the hypotheses, Theorems 3.1 and 3.2 hold. Then w solves the problem

$$\begin{cases} w_t - \operatorname{div}(k_\varepsilon \nabla w) + \chi_{\Omega/\omega_\varepsilon} p_\varepsilon w = -\operatorname{div}(\tilde{k} \chi_{\omega_\varepsilon} \nabla u) + \chi_{\omega_\varepsilon} f(u), & \text{in } \Omega \times (0, T), \\ \frac{\partial w}{\partial n} = 0, & \text{on } \partial\Omega \times (0, T), \\ w(0) = 0, & \text{in } \Omega, \end{cases} \quad (3.39)$$

where we have set $\tilde{k} := k_0 - k_1 > 0$ and

$$p_\varepsilon w := f'(z_\varepsilon)w = f(u^\varepsilon) - f(u), \quad (3.40)$$

z_ε satisfying $u^\varepsilon(x, t) \leq z_\varepsilon(x, t) \leq u(x, t)$. By means of (3.9), (3.35) and recalling (3.8), we have

$$u_1 \leq z_\varepsilon \leq u_3, \quad |p_\varepsilon| = |f'(z_\varepsilon)| \leq M_2, \quad \text{in } \bar{\Omega} \times [0, T]. \quad (3.41)$$

Multiplying the first equation in (3.39) by w and integrating by parts over Ω , we get

$$\frac{1}{2} \frac{d}{dt} \int_{\Omega} w^2 dx + \int_{\Omega} k_\varepsilon |\nabla w|^2 dx + \int_{\Omega} \chi_{\Omega/\omega_\varepsilon} p_\varepsilon w^2 dx = \int_{\Omega} \tilde{k} \chi_{\omega_\varepsilon} \nabla u \cdot \nabla w dx + \int_{\Omega} \chi_{\omega_\varepsilon} f(u) w dx.$$

Adding and subtracting $\int_{\Omega} \chi_{\Omega \setminus \omega_\varepsilon}(x) w^2(x) dx$ and applying (3.17) we obtain

$$\frac{1}{2} \frac{d}{dt} \int_{\Omega} w^2 dx + S \|w\|_{H^1(\Omega)}^2 \leq \int_{\omega_\varepsilon} \tilde{k} \nabla u \cdot \nabla w dx + \int_{\omega_\varepsilon} f(u) w dx - \int_{\Omega} \chi_{\Omega/\omega_\varepsilon} (p_\varepsilon - 1) w^2 dx.$$

Recalling (3.8) and (3.41), thanks to Young's inequality we deduce

$$\begin{aligned} & \frac{1}{2} \frac{d}{dt} \int_{\Omega} w^2 dx + S \|w\|_{H^1(\Omega)}^2 \\ & \leq \tilde{k} \left(\frac{\tilde{k}}{2S} \int_{\omega_\varepsilon} |\nabla u|^2 dx + \frac{S}{2\tilde{k}} \int_{\Omega} |\nabla w|^2 dx \right) + \frac{1}{2} \int_{\omega_\varepsilon} (f(u))^2 dx + \int_{\Omega} \left(M_2 + \frac{3}{2} \right) w^2 dx, \end{aligned}$$

so that

$$\frac{1}{2} \frac{d}{dt} \int_{\Omega} w^2 dx + \frac{S}{2} \|w\|_{H^1(\Omega)}^2 \leq \frac{(\tilde{k})^2}{2S} \int_{\omega_\varepsilon} |\nabla u|^2 dx + \frac{1}{2} \int_{\omega_\varepsilon} M_1^2 dx + \left(M_2 + \frac{3}{2} \right) \int_{\Omega} w^2 dx, \quad (3.42)$$

and finally, see (3.10),

$$\frac{d}{dt} \|w(\cdot, t)\|_{L^2(\Omega)}^2 \leq C \left(|\omega_\varepsilon| + \|w(\cdot, t)\|_{L^2(\Omega)}^2 \right).$$

Recalling that $w(\cdot, 0) = 0$, an application of Gronwall's Lemma implies

$$\|w(\cdot, t)\|_{L^2(\Omega)}^2 \leq C|\omega_\varepsilon|, \quad t \in (0, T), \quad (3.43)$$

and (3.36) follows. Integrating now inequality (3.42) on $(0, T)$ we get

$$\int_{\Omega} w^2(\cdot, T) dx + C \int_0^T \|w(\cdot, t)\|_{H^1(\Omega)}^2 dt \leq C \left(|\omega_\varepsilon| + \int_0^T \|w(\cdot, t)\|_{L^2(\Omega)}^2 dt \right),$$

and a combination with (3.43) gives (3.37).

In order to obtain the more refined estimate (3.38), observe that w also solves problem

$$\begin{cases} w_t - \operatorname{div}(k_0 \nabla w) + \chi_{\Omega/\omega_\varepsilon} p_\varepsilon w = -\operatorname{div}(\tilde{k} \chi_{\omega_\varepsilon} \nabla u^\varepsilon) + \chi_{\omega_\varepsilon} f(u), & \text{in } \Omega \times (0, T), \\ \frac{\partial w}{\partial n} = 0, & \text{on } \partial\Omega \times (0, T), \\ w(\cdot, 0) = 0, & \text{in } \Omega. \end{cases} \quad (3.44)$$

Let us now introduce the auxiliary function \bar{w} , solution to the adjoint problem

$$\begin{cases} \bar{w}_t + \operatorname{div}(k_0 \nabla \bar{w}) - \chi_{\Omega/\omega_\varepsilon} p_\varepsilon \bar{w} = -w, & \text{in } \Omega \times (0, T), \\ \frac{\partial \bar{w}}{\partial n} = 0, & \text{on } \partial\Omega \times (0, T), \\ \bar{w}(\cdot, T) = 0, & \text{in } \Omega. \end{cases} \quad (3.45)$$

By the change of variable $t \rightarrow T - t$, problem (3.45) is equivalent to

$$\begin{cases} z_t - \operatorname{div}(k_0 \nabla z) + \chi_{\Omega/\omega_\varepsilon} \hat{p}_\varepsilon z = \hat{w}, & \text{in } \Omega \times (0, T), \\ \frac{\partial z}{\partial n} = 0, & \text{on } \partial\Omega \times (0, T), \\ z(\cdot, 0) = 0, & \text{in } \Omega, \end{cases} \quad (3.46)$$

where we have set $z(x, t) = \bar{w}(x, T - t)$, $\hat{p}_\varepsilon(x, t) = p_\varepsilon(x, T - t)$, $\hat{w}(x, t) = w(x, T - t)$.

Since the coefficient k_0 is regular, $|\chi_{\Omega/\omega_\varepsilon} \hat{p}_\varepsilon|$ is bounded in $\bar{\Omega} \times [0, T]$ and even $w \in C^{\alpha, \alpha/2}(\bar{\Omega} \times [0, T])$, via [99, Theorem 9.1, Chapter 4] we can assess that

$$z \in W_2^{2,1}(\Omega \times (0, T)) := \{z \in L^2(\Omega \times (0, T)) \mid z \in H^1(0, T; L^2(\Omega)) \cap L^2(0, T; H^2(\Omega))\}.$$

Moreover, multiplying the first equation in (3.46) by z and integrating over Ω , we get

$$\frac{1}{2} \frac{d}{dt} \int_{\Omega} z^2 dx + k_0 \int_{\Omega} |\nabla z|^2 dx + k_0 \int_{\Omega} z^2 dx = \int_{\Omega} \hat{w} z dx - \int_{\Omega} \chi_{\Omega/\omega_\varepsilon} \hat{p}_\varepsilon z^2 dx + k_0 \int_{\Omega} z^2 dx.$$

By means of Young's inequality and recalling (3.41), we have

$$\frac{1}{2} \frac{d}{dt} \|z(\cdot, t)\|_{L^2(\Omega)}^2 + \frac{k_0}{2} \|z(\cdot, t)\|_{H^1(\Omega)}^2 \leq \frac{1}{2k_0} \|\hat{w}(\cdot, t)\|_{L^2(\Omega)}^2 + (M_2 + k_0) \|z(\cdot, t)\|_{L^2(\Omega)}^2,$$

and then

$$\frac{d}{dt} \|z(\cdot, t)\|_{L^2(\Omega)}^2 \leq \frac{1}{k_0} \|\hat{w}(\cdot, t)\|_{L^2(\Omega)}^2 + 2(M_2 + k_0) \|z(\cdot, t)\|_{L^2(\Omega)}^2.$$

Recalling that $z(\cdot, 0) = 0$, an application of Gronwall's Lemma gives

$$\|z(\cdot, t)\|_{L^2(\Omega)}^2 \leq C \|\hat{w}(\cdot, t)\|_{L^2(\Omega)}^2. \quad (3.47)$$

Since $z \in W_2^{2,1}$, surely $z_t \in L^2(0, T; H^1(\Omega))$: let us now multiply the first equation in (3.46) by z_t and integrate over Ω . We get

$$\int_{\Omega} z_t^2 dx + \frac{k_0}{2} \frac{d}{dt} \int_{\Omega} |\nabla z|^2 dx = \int_{\Omega} \hat{w} z_t dx - \int_{\Omega} \chi_{\Omega/\omega_\varepsilon} \hat{p}_\varepsilon z z_t dx.$$

An application of Young's inequality gives

$$\frac{1}{2} \int_{\Omega} z_t^2 dx + \frac{k_0}{2} \frac{d}{dt} \int_{\Omega} |\nabla z|^2 dx \leq \int_{\Omega} (\hat{w})^2 dx + \int_{\Omega} \chi_{\Omega/\omega_\varepsilon} (\hat{p}_\varepsilon)^2 z^2 dx,$$

and then

$$\frac{1}{2} \|z_t(\cdot, t)\|_{L^2(\Omega)}^2 + \frac{k_0}{2} \frac{d}{dt} \|\nabla z(\cdot, t)\|_{L^2(\Omega)}^2 \leq \|\hat{w}(\cdot, t)\|_{L^2(\Omega)}^2 + M_2^2 \|z(\cdot, t)\|_{L^2(\Omega)}^2. \quad (3.48)$$

Combining (3.48) and (3.47), integrating in time on $(0, t)$, and using $\nabla z(\cdot, 0) = 0$ we deduce

$$\|\nabla z(\cdot, t)\|_{L^2(\Omega)}^2 \leq C \|\hat{w}\|_{L^2(\Omega \times (0, t))}^2, \quad t \in (0, T),$$

so that

$$\|z\|_{L^\infty(0, T; H^1(\Omega))}^2 \leq C \|\hat{w}\|_{L^2(\Omega \times (0, T))}^2. \quad (3.49)$$

The same computations also give

$$\|z_t\|_{L^2(\Omega \times (0, T))}^2 \leq C \|\hat{w}\|_{L^2(\Omega \times (0, T))}^2.$$

Consider now problem (3.46), and in particular, rewriting the equation as follow:

$$-\operatorname{div}(k_0 \nabla z) + \chi_{\Omega/\omega_\varepsilon} \hat{p}_\varepsilon z = \hat{w} - z_t,$$

we can interpret (a.e. in $(0, T)$) $z(\cdot, t)$ as the solution of an elliptic problem with regular coefficient k_0 and square integrable right-hand side, whose norm in $L^2(\Omega)$ is bounded by $\|\hat{w}(\cdot, t)\|_{L^2(\Omega)}$. Then, an application of standard elliptic regularity results to problem (3.46) (see [84, Theorem 2.4.2.6]) implies

$$\|z(\cdot, t)\|_{H^2(\Omega)} \leq C(\|\hat{w}(\cdot, t)\|_{L^2(\Omega)} + \|z(\cdot, t)\|_{L^2(\Omega)}) \leq C \|\hat{w}(\cdot, t)\|_{L^2(\Omega)}$$

and eventually

$$\|z\|_{L^2(0, T; H^2(\Omega))}^2 \leq C \|\hat{w}\|_{L^2(\Omega \times (0, T))}^2. \quad (3.50)$$

Recalling the definition of z and \hat{w} , by estimates (3.49) and (3.50) we get

$$\|\bar{w}\|_{L^\infty(0, T; H^1(\Omega))}^2 + \|\bar{w}\|_{L^2(0, T; H^2(\Omega))}^2 \leq C \|w\|_{L^2(\Omega \times (0, T))}^2, \quad (3.51)$$

Finally, we want to prove that there exists $p > 2$ such that

$$\|\bar{w}\|_{L^p(\Omega \times (0, T))} + \|\nabla \bar{w}\|_{L^p(\Omega \times (0, T))} \leq C \|w\|_{L^2(\Omega \times (0, T))}. \quad (3.52)$$

To this aim, on account of (3.51) and Sobolev immersion theorems, we deduce

$$\|\bar{w}\|_{L^6(\Omega \times (0, T))}^2 \leq C \|\bar{w}\|_{L^\infty(0, T; H^1(\Omega))}^2 \leq C \|w\|_{L^2(\Omega \times (0, T))}^2.$$

Moreover, again from (3.51) we have

$$\nabla \bar{w} \in L^\infty(0, T; L^2(\Omega)) \cap L^2(0, T; L^6(\Omega)).$$

From well-known interpolation estimates (cf. [113]) we infer

$$\|\nabla \bar{w}\|_{L^{10/3}(\Omega \times (0, T))}^{10/3} \leq C \|\nabla \bar{w}\|_{L^2(0, T; L^6(\Omega))}^2 \|\nabla \bar{w}\|_{L^{4/3}(0, T; L^2(\Omega))}^{4/3}$$

and therefore, using (3.51),

$$\|\nabla \bar{w}\|_{L^{10/3}(\Omega \times (0, T))}^{10/3} \leq C \|w\|_{L^2(\Omega \times (0, T))}^2 \|w\|_{L^2(\Omega \times (0, T))}^{4/3} \leq C \|w\|_{L^2(\Omega \times (0, T))}^{10/3},$$

so that (3.52) holds for any $p \in (2, \frac{10}{3}]$.

Let us now multiply the evolution equation in (3.44) by \bar{w} and the evolution equation in (3.45) by w , respectively. Integrating on Ω we obtain

$$\int_{\Omega} w_t \bar{w} dx + k_0 \int_{\Omega} \nabla w \cdot \nabla \bar{w} dx + \int_{\Omega} \chi_{\Omega/\omega_\varepsilon} p_\varepsilon w \bar{w} dx = \tilde{k} \int_{\omega_\varepsilon} \nabla u^\varepsilon \cdot \nabla \bar{w} dx + \int_{\omega_\varepsilon} f(u) \bar{w} dx, \quad (3.53)$$

$$\int_{\Omega} \bar{w}_t w dx - k_0 \int_{\Omega} \nabla \bar{w} \cdot \nabla w dx - \int_{\Omega} \chi_{\Omega/\omega_\varepsilon} p_\varepsilon \bar{w} w dx = - \int_{\Omega} w^2 dx. \quad (3.54)$$

Summing up (3.53) and (3.54) we get

$$\int_{\Omega} (w_t \bar{w} + \bar{w}_t w) dx = \tilde{k} \int_{\omega_\varepsilon} \nabla u^\varepsilon \cdot \nabla \bar{w} dx + \int_{\omega_\varepsilon} f(u) \bar{w} dx - \int_{\Omega} w^2 dx,$$

subsequently, an integration in time on $(0, T)$ gives

$$\int_0^T \int_{\Omega} w^2 dx dt = - \int_0^T \int_{\Omega} (w_t \bar{w} + \bar{w}_t w) dx dt + \tilde{k} \int_0^T \int_{\omega_\varepsilon} \nabla u^\varepsilon \cdot \nabla \bar{w} dx dt + \int_0^T \int_{\omega_\varepsilon} f(u) \bar{w} dx dt. \quad (3.55)$$

Recalling the conditions at time $t = 0$ for w and at time $t = T$ for \bar{w} , we get

$$\int_{\Omega} dx \int_0^T (w_t \bar{w} + \bar{w}_t w) dt = \int_{\Omega} \left((w \bar{w})(\cdot, T) - (w \bar{w})(\cdot, 0) - \int_0^T (w \bar{w}_t + \bar{w}_t w) dt \right) dx = 0$$

So that (3.55) becomes

$$\int_0^T \int_{\Omega} w^2 dx dt = \tilde{k} \int_0^T \int_{\omega_\varepsilon} \nabla u^\varepsilon \cdot \nabla \bar{w} dx dt + \int_0^T \int_{\omega_\varepsilon} f(u) \bar{w} dx dt. \quad (3.56)$$

Using now Hölder inequality we deduce

$$\|w\|_{L^2(\Omega \times (0, T))}^2 \leq \|\nabla u^\varepsilon\|_{L^q(\omega_\varepsilon \times (0, T))} \|\nabla \bar{w}\|_{L^p(\omega_\varepsilon \times (0, T))} + \|f(u)\|_{L^q(\omega_\varepsilon \times (0, T))} \|\bar{w}\|_{L^p(\omega_\varepsilon \times (0, T))},$$

where p and q are conjugate indexes and therefore $q \in [10/7, 2)$.

By means of (3.52) and (3.8), from the previous inequality we get

$$\|w\|_{L^2(\Omega \times (0, T))}^2 \leq C \|w\|_{L^2(\Omega \times (0, T))} \left(\|\nabla u^\varepsilon\|_{L^q(\omega_\varepsilon \times (0, T))} + |\omega_\varepsilon|^{\frac{1}{q}} \right),$$

and therefore

$$\|w\|_{L^2(\Omega \times (0, T))} \leq C \left(\|\nabla u^\varepsilon\|_{L^q(\omega_\varepsilon \times (0, T))} + |\omega_\varepsilon|^{\frac{1}{q}} \right). \quad (3.57)$$

Thanks to (3.10) we also have

$$\begin{aligned} \|\nabla u^\varepsilon\|_{L^q(\omega_\varepsilon \times (0, T))} &\leq \|\nabla u^\varepsilon - \nabla u\|_{L^q(\omega_\varepsilon \times (0, T))} + \|\nabla u\|_{L^q(\omega_\varepsilon \times (0, T))} \\ &\leq \|\nabla w\|_{L^q(\omega_\varepsilon \times (0, T))} + C|\omega_\varepsilon|^{\frac{1}{q}}. \end{aligned}$$

Finally, using again Hölder inequality and (3.37), we obtain

$$\begin{aligned} \|\nabla w\|_{L^q(\omega_\varepsilon \times (0, T))} &\leq \left(\int_0^T \left(\int_{\omega_\varepsilon} |\nabla w|^{q \frac{2}{q}} dx \right)^{\frac{q}{2}} \left(\int_{\omega_\varepsilon} 1 dx \right)^{\frac{2-q}{2}} dt \right)^{\frac{1}{q}} \\ &\leq |\omega_\varepsilon|^{\frac{1}{q} - \frac{1}{2}} \left(\int_0^T \|\nabla w\|_{L^2(\Omega)}^2 dt \right)^{\frac{1}{q}} \leq |\omega_\varepsilon|^{\frac{1}{q} - \frac{1}{2}} \|\nabla w\|_{L^q(0, T; L^2 \Omega)} \\ &\leq C(\Omega) |\omega_\varepsilon|^{\frac{1}{q} - \frac{1}{2}} \|\nabla w\|_{L^2(\Omega \times (0, T))} \leq C|\omega_\varepsilon|^{\frac{1}{q}}. \end{aligned}$$

Combining the previous estimate with (3.57), since $\frac{1}{q} \in (\frac{1}{2}, \frac{7}{10}]$ we can conclude that (3.38) holds with $\beta \in (0, \frac{1}{5}]$. \square

3.4 The asymptotic formula

In this section we derive and prove an asymptotic representation formula for $w = u_\varepsilon - u$ in analogy with [30] and [47]. Let $\Phi = \Phi(x, t)$ be any solution of

$$\begin{cases} \Phi_t + k_0 \Delta \Phi - f'(u) \Phi = 0, & \text{in } \Omega \times (0, T), \\ \Phi(T) = 0, & \text{in } \Omega. \end{cases} \quad (3.58)$$

Our main result is the following

Theorem 3.3. *Assume (3.2), (3.6), (3.7). Let u^ε and u be the solutions to (3.5) and (3.1) and Φ a solution to (3.58), respectively. Then, there exist a sequence ω_{ε_n} satisfying (3.3) and (3.4) with $|\omega_{\varepsilon_n}| \rightarrow 0$, a regular Borel measure μ and a symmetric matrix \mathcal{M} with elements $\mathcal{M}_{ij} \in L^2(\Omega, d\mu)$ such that, for $\varepsilon \rightarrow 0$,*

$$\int_0^T \int_{\partial \Omega} k_0 \frac{\partial \Phi}{\partial n} (u^\varepsilon - u) d\sigma dt = |\omega_{\varepsilon_n}| \left\{ \int_0^T \int_{\Omega} (\tilde{k} \mathcal{M} \nabla u \cdot \nabla \Phi + f(u) \Phi) d\mu dt + o(1) \right\}. \quad (3.59)$$

To prove Theorem 3.3, we need to state some preliminary results. Let $v_\varepsilon^{(j)}$ and $v^{(j)}$ be the variational solutions (depending only on $x \in \Omega$) to the problems

$$(PV_\varepsilon) \begin{cases} \operatorname{div}(k_\varepsilon \nabla v_\varepsilon^{(j)}) = 0, & \text{in } \Omega, \\ \frac{\partial v_\varepsilon^{(j)}}{\partial n} = n_j, & \text{on } \partial \Omega, \\ \int_{\partial \Omega} v_\varepsilon^{(j)} d\sigma = 0, \end{cases} \quad (PV_0) \begin{cases} \operatorname{div}(k_0 \nabla v^{(j)}) = 0, & \text{in } \Omega, \\ \frac{\partial v^{(j)}}{\partial n} = n_j, & \text{on } \partial \Omega, \\ \int_{\partial \Omega} v^{(j)} d\sigma = 0, \end{cases} \quad (3.60)$$

n_j being the j -th coordinate of the outward normal to $\partial \Omega$. It can be easily verified that

$$v^{(j)} = x_j - \frac{1}{|\partial \Omega|} \int_{\partial \Omega} x_j d\sigma. \quad (3.61)$$

The following results hold

Proposition 3.2. Let $v_\varepsilon^{(j)}$ and $v^{(j)}$ solutions to (3.60), then there exists $C(\Omega) > 0$ such that

$$\|v_\varepsilon^{(j)} - v^{(j)}\|_{H^1(\Omega)} \leq C(\Omega)|\omega_\varepsilon|^{\frac{1}{2}}. \quad (3.62)$$

Moreover, for some $\eta \in (0, \frac{1}{2})$, there exists $C(\Omega, \eta) > 0$ such that

$$\|v_\varepsilon^{(j)} - v^{(j)}\|_{L^2(\Omega)} \leq C(\Omega, \eta)|\omega_\varepsilon|^{\frac{1}{2}+\eta}. \quad (3.63)$$

Proof. See Lemma 1 in [47]. \square

Proposition 3.3. Let u and u^ε be the solutions to problems (3.1) and (3.5), respectively. Consider $v_\varepsilon^{(j)}$ and $v^{(j)}$ as in (3.60). Then, $\forall \Phi \in C^1(\bar{\Omega} \times [0, T])$ s.t. $\Phi(x, T) = 0$, it holds

$$\int_0^T \int_\Omega \frac{1}{|\omega_\varepsilon|} \chi_{\omega_\varepsilon} \nabla u \cdot \nabla v_\varepsilon^{(j)} \Phi dx dt = \int_0^T \int_\Omega \frac{1}{|\omega_\varepsilon|} \chi_{\omega_\varepsilon} \nabla u^\varepsilon \cdot \nabla v^{(j)} \Phi dx dt + o(1), \quad \varepsilon \rightarrow 0. \quad (3.64)$$

Proof. We follow the ideas in [30] and [47]. Since $w = u^\varepsilon - u$, then we obtain the identity

$$\int_\Omega k_0 \nabla w \cdot \nabla (v^{(j)} \Phi) dx = - \int_\Omega k_0 w \nabla v^{(j)} \cdot \nabla \Phi dx + \int_{\partial\Omega} k_0 w n_j \Phi d\sigma + \int_\Omega k_0 \nabla w \cdot \nabla \Phi v^{(j)} dx. \quad (3.65)$$

Moreover, we have

$$\begin{aligned} \int_0^T \int_\Omega k_\varepsilon \nabla w \cdot \nabla (v_\varepsilon^{(j)} \Phi) dx dt &= \int_0^T \int_\Omega k_\varepsilon \left(\nabla w \cdot \nabla v_\varepsilon^{(j)} \Phi + \nabla w \cdot \nabla \Phi v_\varepsilon^{(j)} + \nabla w \cdot \nabla \Phi (v_\varepsilon^{(j)} - v^{(j)}) \right) dx dt \\ &= \int_0^T \left(- \int_\Omega k_\varepsilon w \nabla v_\varepsilon^{(j)} \cdot \nabla \Phi dx + \int_{\partial\Omega} k_0 w n_j \Phi d\sigma + \int_\Omega k_0 \nabla w \cdot \nabla \Phi v^{(j)} dx \right. \\ &\quad \left. + \int_\Omega (k_\varepsilon - k_0) \nabla w \cdot \nabla \Phi v^{(j)} dx + \int_\Omega k_\varepsilon \nabla w \cdot \nabla \Phi (v_\varepsilon^{(j)} - v^{(j)}) dx \right) dt \\ &= \int_0^T \left(- \int_\Omega k_\varepsilon w \nabla v^{(j)} \cdot \nabla \Phi dx + \int_{\partial\Omega} k_0 w n_j \Phi d\sigma + \int_\Omega k_0 \nabla w \cdot \nabla \Phi v^{(j)} dx \right. \\ &\quad \left. + \int_{\omega_\varepsilon} (k_1 - k_0) \nabla w \cdot \nabla \Phi v^{(j)} dx + \int_\Omega k_\varepsilon \nabla w \cdot \nabla \Phi (v_\varepsilon^{(j)} - v^{(j)}) dx - \int_\Omega k_\varepsilon w \nabla (v_\varepsilon^{(j)} - v^{(j)}) \cdot \nabla \Phi dx \right) dt. \end{aligned}$$

A combination with (3.65) gives

$$\begin{aligned} \int_0^T \int_\Omega k_\varepsilon \nabla w \cdot \nabla (v_\varepsilon^{(j)} \Phi) dx dt &= \int_0^T \left(\int_\Omega k_0 \nabla w \cdot \nabla (v^{(j)} \Phi) dx + \int_{\omega_\varepsilon} (k_1 - k_0) \nabla w \cdot \nabla \Phi v^{(j)} dx \right. \\ &\quad \left. + \int_{\omega_\varepsilon} (k_0 - k_1) w \nabla v^{(j)} \cdot \nabla \Phi dx + \int_\Omega k_\varepsilon \nabla w \cdot \nabla \Phi (v_\varepsilon^{(j)} - v^{(j)}) dx - \int_\Omega k_\varepsilon w \nabla (v_\varepsilon^{(j)} - v^{(j)}) \cdot \nabla \Phi dx \right) dt. \end{aligned}$$

Then, on account of (3.36), (3.37), (3.62), (3.63) and Schwarz inequality, we get

$$\int_0^T \int_\Omega k_\varepsilon \nabla w \cdot \nabla (v_\varepsilon^{(j)} \Phi) dx dt = \int_0^T \left(\int_\Omega k_0 \nabla w \cdot \nabla (v^{(j)} \Phi) dx - \int_{\omega_\varepsilon} \tilde{k} \nabla w \cdot \nabla \Phi v^{(j)} dx \right) dt + o(|\omega_\varepsilon|). \quad (3.66)$$

Let us consider now problems (3.39) and (3.44). Multiplying the first equation in (3.39) by $v_\varepsilon^{(j)} \Phi$ and the first equation in (3.44) by $v^{(j)} \Phi$, an integration by parts on $\Omega \times (0, T)$ gives

$$\int_0^T \int_\Omega \left[w_t v_\varepsilon^{(j)} \Phi + k_\varepsilon \nabla w \cdot \nabla (v_\varepsilon^{(j)} \Phi) + \chi_{\Omega/\omega_\varepsilon} p_\varepsilon w v_\varepsilon^{(j)} \Phi \right] dx dt = \int_0^T \int_{\omega_\varepsilon} \left[\tilde{k} \nabla u \cdot \nabla (v_\varepsilon^{(j)} \Phi) + f(u) v_\varepsilon^{(j)} \Phi \right] dx dt,$$

$$\int_0^T \int_{\Omega} \left[w_t v^{(j)} \Phi + k_0 \nabla w \cdot \nabla (v^{(j)} \Phi) + \chi_{\Omega/\omega_\varepsilon} p_\varepsilon w v^{(j)} \Phi \right] dx dt = \int_0^T \int_{\omega_\varepsilon} \left[\tilde{k} \nabla u^\varepsilon \cdot \nabla (v^{(j)} \Phi) + f(u) v^{(j)} \Phi \right] dx dt.$$

By a combination of the previous three identities we obtain, for $\varepsilon \rightarrow 0$,

$$\begin{aligned} & \int_0^T \int_{\omega_\varepsilon} \tilde{k} \nabla u \cdot \nabla (v_\varepsilon^{(j)} \Phi) dx dt + \int_0^T \int_{\omega_\varepsilon} f(u) v_\varepsilon^{(j)} \Phi dx dt - \int_0^T \int_{\Omega} w_t v_\varepsilon^{(j)} \Phi dx dt - \int_0^T \int_{\Omega} \chi_{\Omega/\omega_\varepsilon} p_\varepsilon w v_\varepsilon^{(j)} \Phi dx dt \\ &= \int_0^T \int_{\omega_\varepsilon} \tilde{k} \nabla u^\varepsilon \cdot \nabla (v^{(j)} \Phi) dx dt + \int_0^T \int_{\omega_\varepsilon} f(u) v^{(j)} \Phi dx dt - \int_0^T \int_{\Omega} w_t v^{(j)} \Phi dx dt \\ & \quad - \int_0^T \int_{\Omega} \chi_{\Omega/\omega_\varepsilon} p_\varepsilon w v^{(j)} \Phi dx dt - \int_0^T \int_{\omega_\varepsilon} \tilde{k} \nabla w \cdot \nabla \Phi v^{(j)} dx dt + o(|\omega_\varepsilon|), \end{aligned}$$

from which we deduce

$$\begin{aligned} & \int_0^T \int_{\omega_\varepsilon} \tilde{k} \nabla u \cdot \nabla (v_\varepsilon^{(j)} \Phi) dx dt = \int_0^T \int_{\Omega} w_t (v_\varepsilon^{(j)} - v^{(j)}) \Phi dx dt + \tilde{k} \int_0^T \int_{\omega_\varepsilon} \left(\nabla u^\varepsilon \cdot \nabla (v^{(j)} \Phi) - \nabla u^\varepsilon \cdot \nabla \Phi v^{(j)} \right) dx dt \\ & + \int_0^T \int_{\omega_\varepsilon} \tilde{k} \nabla u \cdot \nabla \Phi v^{(j)} dx dt - \int_0^T \int_{\Omega} \chi_{\Omega/\omega_\varepsilon} p_\varepsilon w (v_\varepsilon^{(j)} - v^{(j)}) \Phi dx dt + \int_0^T \int_{\omega_\varepsilon} f(u) (v^{(j)} - v_\varepsilon^{(j)}) \Phi dx dt + o(|\omega_\varepsilon|). \end{aligned}$$

By means of (3.57), (3.38), (3.62) and (3.63), and recalling also (3.8) and (3.41), an application of the Hölder inequality both in space and time gives, for $\varepsilon \rightarrow 0$,

$$\tilde{k} \int_0^T \int_{\omega_\varepsilon} \nabla u \cdot \nabla (v_\varepsilon^{(j)} \Phi) dx dt = \int_0^T \int_{\Omega} w_t (v_\varepsilon^{(j)} - v^{(j)}) \Phi dx dt + \tilde{k} \int_0^T \int_{\omega_\varepsilon} \left(\nabla u^\varepsilon \cdot \nabla v^{(j)} \Phi + \nabla u \cdot \nabla \Phi v^{(j)} \right) dx dt + o(|\omega_\varepsilon|),$$

and then

$$\begin{aligned} & \tilde{k} \int_0^T \int_{\omega_\varepsilon} \nabla u \cdot \nabla v_\varepsilon^{(j)} \Phi dx dt = \int_0^T \int_{\Omega} w_t (v_\varepsilon^{(j)} - v^{(j)}) \Phi dx dt \\ & + \tilde{k} \int_0^T \int_{\omega_\varepsilon} \nabla u^\varepsilon \cdot \nabla v^{(j)} \Phi dx dt + \tilde{k} \int_0^T \int_{\omega_\varepsilon} \nabla u \cdot \nabla \Phi (v^{(j)} - v_\varepsilon^{(j)}) dx dt + o(|\omega_\varepsilon|) \\ & = \int_0^T \int_{\Omega} w_t (v_\varepsilon^{(j)} - v^{(j)}) \Phi dx dt + \tilde{k} \int_0^T \int_{\omega_\varepsilon} \nabla u^\varepsilon \cdot \nabla v^{(j)} \Phi dx dt + o(|\omega_\varepsilon|). \end{aligned} \quad (3.67)$$

Consider the first term in the last line of (3.67). Integrating by parts in time and recalling that $\Phi(T) = 0$, $w(0) = 0$, $(v^{(j)} - v_\varepsilon^{(j)})_t = 0$, we finally have (cf. also (3.38), (3.63)), for $\varepsilon \rightarrow 0$,

$$\begin{aligned} & \int_0^T \int_{\Omega} w_t (v_\varepsilon^{(j)} - v^{(j)}) \Phi dx dt = \int_{\Omega} [w(v_\varepsilon^{(j)} - v^{(j)}) \Phi](T) dx - \int_{\Omega} [w(v_\varepsilon^{(j)} - v^{(j)}) \Phi](0) dx \quad (3.68) \\ & - \int_0^T \int_{\Omega} \left(w(v_\varepsilon^{(j)} - v^{(j)})_t \Phi + w(v_\varepsilon^{(j)} - v^{(j)}) \Phi_t \right) dx dt = - \int_0^T \int_{\Omega} w(v_\varepsilon^{(j)} - v^{(j)}) \Phi_t dx dt = o(|\omega_\varepsilon|). \end{aligned}$$

Combining (3.67) and (3.68) we get

$$\tilde{k} \int_0^T \int_{\omega_\varepsilon} \nabla u \cdot \nabla v_\varepsilon^{(j)} \Phi dx dt = \tilde{k} \int_0^T \int_{\omega_\varepsilon} \nabla u^\varepsilon \cdot \nabla v^{(j)} \Phi dx dt + o(|\omega_\varepsilon|), \quad \varepsilon \rightarrow 0, \quad (3.69)$$

then formula (3.64) is true. \square

Proof of Theorem 3.3. Following [47, Sec.3], there exist a regular Borel measure μ , a symmetric matrix \mathcal{M} with elements $\mathcal{M}_{ij} \in L^2(\Omega, d\mu)$, a sequence ω_{ε_n} with $|\omega_{\varepsilon_n}| \rightarrow 0$ such that

$$|\omega_{\varepsilon_n}|^{-1} \chi_{\omega_{\varepsilon_n}} dx \rightarrow d\mu, \quad |\omega_{\varepsilon_n}|^{-1} \chi_{\omega_{\varepsilon_n}} \frac{\partial v_{\varepsilon_n}^{(j)}}{\partial x_i} dx \rightarrow \mathcal{M}_{ij} d\mu, \quad (3.70)$$

in the weak* topology of $C^0(\overline{\Omega})$. On account of (3.10), we deduce also

$$|\omega_{\varepsilon_n}|^{-1} \chi_{\omega_{\varepsilon_n}} \frac{\partial u}{\partial x_i} \frac{\partial v_{\varepsilon_n}^{(j)}}{\partial x_i} dx \rightarrow \mathcal{M}_{ij} \frac{\partial u}{\partial x_i} d\mu, \quad \forall t \in (0, T), \quad (3.71)$$

in the weak* topology of $C^0(\overline{\Omega})$. Moreover, recalling (3.10), (3.38) and (3.61), we get

$$\left| \int_0^T dt \int_{\Omega} \frac{\chi_{\omega_{\varepsilon_n}}}{|\omega_{\varepsilon_n}|} \frac{\partial u^{\varepsilon_n}}{\partial x_i} \frac{\partial v^{(j)}}{\partial x_i} dx \right| \leq C, \quad (3.72)$$

where C is independent of ε_n . Hence

$$|\omega_{\varepsilon_n}|^{-1} \chi_{\omega_{\varepsilon_n}} \frac{\partial u^{\varepsilon_n}}{\partial x_i} \frac{\partial v^{(j)}}{\partial x_i} dx dt \rightarrow d\nu_j \quad (3.73)$$

in the weak* topology of $C^0(\overline{\Omega} \times [0, T])$. Combining (3.71), (3.73) and Proposition 3.3, we obtain

$$d\nu_j = \mathcal{M}_{ij} \frac{\partial u}{\partial x_i} d\mu, \quad \forall t \in (0, T). \quad (3.74)$$

Now, let us multiply the first equation in (3.58) by w and the first equation in (3.44) by Φ . Integrating on $\Omega \times (0, T)$ and then by parts, we get

$$\int_0^T \int_{\Omega} \Phi_t w dx dt + \int_0^T \int_{\Omega} k_0 \nabla \Phi \cdot \nabla w dx dt - \int_0^T \int_{\Omega} f'(u) \Phi w dx dt + \int_0^T \int_{\partial \Omega} k_0 \frac{\partial \Phi}{\partial n} w d\sigma dt = 0,$$

and

$$\begin{aligned} & \int_0^T \int_{\Omega} w_t \Phi dx dt + \int_0^T \int_{\Omega} k_0 \nabla w \cdot \nabla \Phi dx dt + \int_0^T \int_{\Omega} \chi_{\Omega/\omega_{\varepsilon}} p_{\varepsilon} w \Phi dx dt \\ &= \int_0^T \int_{\omega_{\varepsilon}} \tilde{k} \nabla u^{\varepsilon} \cdot \nabla \Phi dx dt + \int_0^T \int_{\omega_{\varepsilon}} f(u) \Phi dx dt. \end{aligned}$$

Summing up the two previous equations, we have

$$\begin{aligned} & \int_0^T \int_{\Omega} (w_t \Phi + \Phi_t w) dx dt - \int_0^T \int_{\Omega} f'(u) \Phi w dx dt + \int_0^T \int_{\partial \Omega} k_0 \frac{\partial \Phi}{\partial n} w d\sigma dt \\ &+ \int_0^T \int_{\Omega} \chi_{\Omega/\omega_{\varepsilon}} p_{\varepsilon} w \Phi dx dt = \int_0^T \int_{\omega_{\varepsilon}} \tilde{k} \nabla u^{\varepsilon} \cdot \nabla \Phi dx dt + \int_0^T \int_{\omega_{\varepsilon}} f(u) \Phi dx dt. \end{aligned} \quad (3.75)$$

Observe that the following identities hold

$$\int_0^T \int_{\Omega} (w_t \Phi + \Phi_t w) dx dt = \int_{\Omega} \int_0^T (w \Phi)_t dt dx = \int_{\Omega} (\Phi(\cdot, T) w(\cdot, T) - \Phi(\cdot, 0) w(\cdot, 0)) dx$$

and then, from (3.75) we infer

$$\begin{aligned} & \int_0^T \int_{\Omega} (\chi_{\Omega/\omega_\varepsilon} p_\varepsilon w \Phi - f'(u) \Phi w) dx dt + \int_0^T \int_{\partial\Omega} k_0 \frac{\partial \Phi}{\partial n} w d\sigma dt \\ &= \int_0^T \int_{\omega_\varepsilon} \tilde{k} \nabla u^\varepsilon \cdot \nabla \Phi dx dt + \int_0^T \int_{\omega_\varepsilon} f(u) \Phi dx dt. \end{aligned} \quad (3.76)$$

Moreover, on account of (3.38), we have

$$\begin{aligned} & \int_0^T \int_{\Omega} (\chi_{\Omega/\omega_\varepsilon} p_\varepsilon w \Phi - f'(u) \Phi w) dx dt \\ &= \int_0^T \int_{\Omega} (\chi_{\Omega/\omega_\varepsilon} p_\varepsilon w \Phi - \chi_{\Omega/\omega_\varepsilon} f'(u) \Phi w) dx dt - \int_0^T \int_{\omega_\varepsilon} f'(u) \Phi w dx dt \\ &= \int_0^T \int_{\Omega} \chi_{\Omega/\omega_\varepsilon} (p_\varepsilon - f'(u)) w \Phi dx dt + o(|\omega_\varepsilon|) = o(|\omega_\varepsilon|). \end{aligned} \quad (3.77)$$

The last equality in (3.77) is a consequence of the regularity of f (see (3.40), from which $|p_\varepsilon - f'(u)| \leq C|w|$ follows) and (3.38). Combining (3.76) and (3.77) we obtain

$$\int_0^T \int_{\partial\Omega} k_0 \frac{\partial \Phi}{\partial n} w d\sigma dt = |\omega_\varepsilon| \int_0^T \int_{\Omega} \left(\tilde{k} |\omega_\varepsilon|^{-1} \chi_{\omega_\varepsilon} \nabla u^\varepsilon \cdot \nabla \Phi + \chi_{\omega_\varepsilon} |\omega_\varepsilon|^{-1} f(u) \Phi \right) dx dt + o(|\omega_\varepsilon|).$$

And finally, by means of (3.70), (3.73) and (3.74), formula (3.59) holds. \square

Remark 3.1. We highlight that, with minor changes, the asymptotic expansion (3.59) extends to the case of piecewise smooth anisotropic conductivities of the form

$$\mathbb{K}_\varepsilon = \begin{cases} \mathbb{K}_0 & \text{in } \Omega \setminus \omega_\varepsilon, \\ \mathbb{K}_1 & \text{in } \omega_\varepsilon, \end{cases} \quad (3.78)$$

where $\mathbb{K}_0, \mathbb{K}_1 \in C^\infty(\Omega)$ are symmetric matrix valued functions satisfying

$$\alpha_0 |\xi|^2 \leq \xi^T \mathbb{K}_0(x) \xi \leq \beta_0 |\xi|^2, \quad \alpha_1 |\xi|^2 \leq \xi^T \mathbb{K}_1(x) \xi \leq \beta_1 |\xi|^2, \quad \forall \xi \in \mathbb{R}^3, \forall x \in \Omega,$$

with $0 < \alpha_1 < \beta_1 < \alpha_0 < \beta_0$. Then, the asymptotic formula (3.59) becomes

$$\int_0^T \int_{\partial\Omega} \mathbb{K}_0 \nabla \Phi \cdot n (u^\varepsilon - u) d\sigma dt = |\omega_\varepsilon| \int_0^T \int_{\Omega} \left(\mathcal{M}_{ij} (\mathbb{K}_0 - \mathbb{K}_1)_{ik} \frac{\partial u}{\partial x_k} \frac{\partial \Phi}{\partial x_j} + f(u) \Phi \right) d\mu dt + o(|\omega_\varepsilon|)$$

where Φ solves

$$\begin{cases} \Phi_t + \operatorname{div}(\mathbb{K}_0 \nabla \Phi) - f'(u) \Phi = 0, & \text{in } \Omega \times (0, T), \\ \Phi(T) = 0, & \text{in } \Omega, \end{cases} \quad (3.79)$$

and u is the background solution of

$$\begin{cases} u_t - \operatorname{div}(\mathbb{K}_0 \nabla u) + f(u) = 0, & \text{in } \Omega \times (0, T), \\ \mathbb{K}_0 \nabla u \cdot n = 0, & \text{on } \partial\Omega \times (0, T), \\ u(0) = 0, & \text{in } \Omega. \end{cases} \quad (3.80)$$

The matrix \mathcal{M} is called the polarization tensor associated to the inhomogeneity ω_ε . Indeed, all the results of the previous sections can be extended to the case of constant anisotropic coefficients using, for instance, the regularity results contained in [99].

Remark 3.2. Let us observe that the asymptotic expansion derived in Theorem 3.3 can be extended to the case of a finite number of small well-separated inhomogeneities. Compare Section 6 of [30] for the elliptic case.

3.5 A topological gradient-based reconstruction algorithm

We now take advantage of the asymptotic expansion (3.59) to set a numerical reconstruction procedure for the inverse problem of detecting a spherical inhomogeneity ω_ε from boundary measurements of the electric potential. Following the approach of [33],[52] but taking now into account the time-dependent nature of the problem, we introduce the mismatch functional

$$J(\omega_\varepsilon) = \frac{1}{2} \int_0^T \int_{\partial\Omega} (u^\varepsilon - u_{meas})^2 d\sigma dt, \quad (3.81)$$

where u^ε is the solution of the perturbed problem (3.5) in presence of an inclusion ω_ε satisfying hypotheses (3.3), (3.4). Then, the inverse problem can be reformulated as the following minimization problem

$$J(\omega_\varepsilon) \rightarrow \min \quad (3.82)$$

among all the small inclusions, well separated from the boundary. We introduce the following additional assumption on the exact inclusion

$$\omega_\varepsilon = z + \varepsilon D = \{x \in \Omega \text{ s.t. } x = z + \varepsilon d, d \in D\}, \quad (3.83)$$

where $z \in \Omega$ and D is an open, bounded, regular set containing the origin. We remark that we prescribe the geometry of the inclusion to be fixed throughout the whole observation time. The restriction of the functional J to the class of inclusions satisfying (3.83) is denoted by $j(\varepsilon; z)$. We can now define the *topological gradient* $G : \Omega \rightarrow \mathbb{R}$ of j as the first order term appearing in the asymptotic expansion of the cost functional with respect to ε , namely

$$j(\varepsilon; z) = j(0) + |\omega_\varepsilon| G(z) + o(|\omega_\varepsilon|), \quad \varepsilon \rightarrow 0, \quad (3.84)$$

where $j(0) = \int_0^T \int_{\partial\Omega} (u - u_{meas})^2 d\sigma dt$ and u is the solution of the unperturbed problem (3.1). Observe that $j(0)$ does not depend on z .

Under the assumptions that the exact inclusion has a small size and satisfies hypothesis (3.83), a reconstruction procedure consists in identifying the point $\bar{z} \in \Omega$ where the topological gradient G attains its minimum. Indeed, the cost functional achieves the smallest value when it is evaluated in the center of the exact inclusion. Thanks to the hypothesis of small size, we expect the reduction of the cost functional j to be correctly described by the first order term G , up to a remainder which is negligible with respect to ε .

Nevertheless, in order to define a reconstruction algorithm, the efficient evaluation of the topological gradient G is required. According to the definition above,

$$G(z) = \lim_{\varepsilon \rightarrow 0} \frac{j(\varepsilon; z) - j(0)}{|\omega_\varepsilon|}.$$

Evaluating G in a single point $z \in \Omega$ would require to solve the direct problem several times in presence of inclusions centered at z with decreasing volume. This procedure can be indeed avoided thanks to a useful *representation formula* that can be deduced from the asymptotic expansion (3.59). To show this latter, we need the following preliminary

Proposition 3.4. *Consider the problem*

$$\begin{cases} \Phi_t + k_0 \Delta \Phi - f'(u) \Phi = 0, & \text{in } \Omega \times (0, T), \\ \frac{\partial \Phi}{\partial n} = u^\varepsilon - u, & \text{on } \partial\Omega \times (0, T), \\ \Phi(T) = 0, & \text{in } \Omega. \end{cases} \quad (3.85)$$

Given a compact set $K \subset \Omega$ such that $d(K, \partial\Omega) \geq d_0 > 0$ the following estimate holds

$$\|\Phi\|_{L^1(0, T; W^{1, \infty}(K))} \leq C \|u^\varepsilon - u\|_{L^2(0, T; L^2(\partial\Omega))}. \quad (3.86)$$

Proof. Setting $Z(t) = \Phi(T - t)$, $t \in (0, T)$, we get an equivalent problem to (3.85)

$$\begin{cases} Z_t - k_0 \Delta Z + f'(u) Z = 0, & \text{in } \Omega \times (0, T), \\ \frac{\partial Z}{\partial n} = u^\varepsilon - u, & \text{on } \partial\Omega \times (0, T), \\ Z(0) = 0, & \text{in } \Omega. \end{cases} \quad (3.87)$$

We aim at proving that $Z \in L^2(0, T; H^3(K))$, in view of the continuous embedding of such space in $L^2(0, T; W^{1, \infty}(K))$ (hence in $L^1(0, T; W^{1, \infty}(K))$). Multiplying the first equation in (3.87) by Z , by Young's inequality it holds

$$\frac{1}{2} \frac{d}{dt} \|Z(\cdot, t)\|_{L^2(\Omega)}^2 + \frac{k_0}{2} \|\nabla Z(\cdot, t)\|_{L^2(\Omega)}^2 \leq C (\|Z(\cdot, t)\|_{L^2(\Omega)}^2 + \|(u^\varepsilon - u)(\cdot, t)\|_{L^2(\partial\Omega)}^2), \quad (3.88)$$

where $C = C(k_0, M_2, \Omega) > 0$. An application of Gronwall's lemma gives

$$\|Z(\cdot, t)\|_{L^2(\Omega)}^2 \leq C \|u^\varepsilon - u\|_{L^2(0, t; L^2(\partial\Omega))}^2, \quad t \in (0, T),$$

so that

$$\|Z\|_{L^\infty(0, T; L^2(\Omega))}^2 \leq C \|u^\varepsilon - u\|_{L^2(0, T; L^2(\partial\Omega))}^2 \quad (3.89)$$

and also

$$\|\nabla Z\|_{L^2(0, T; L^2(\Omega))}^2 \leq C \|u^\varepsilon - u\|_{L^2(0, T; L^2(\partial\Omega))}^2, \quad (3.90)$$

where C is a positive constant depending on k_0, M_2, Ω, T . We remark that, by standard regularity results, Z is smooth on $E \times [0, T]$, for any compact $E \subset \Omega$: indeed, via [99, Theorem 9.1, Chapter 4], $Z \in W_2^{2,1}(\Omega \times (0, T)) \subset C(\Omega \times (0, T))$. Consider now two compact sets K_1 and K_2 such that

$$K \subset K_2 \subset K_1 \subset \Omega, \quad d(K_1, \partial\Omega) \geq d_1 > 0.$$

It is possible to construct two functions ξ_1, ξ_2 and two constants b_1, b_2 satisfying

$$\xi_i \in C^2(\bar{\Omega}), \quad 0 \leq \xi_i \leq 1, \quad \xi_i(x) = 1 \quad \forall x \in K_i, \quad \xi_i(x) = 0 \quad \forall x \in B_i \quad i = 1, 2,$$

$$B_i = \{x \in \Omega : d(x, \partial\Omega) \leq b_i\}, \quad 0 < b_1 < b_2 < d_1, \quad K \subset \subset \text{Supp } \xi_2 \subset \subset K_1 \subset \text{Supp } \xi_1 \subset \Omega.$$

Let us multiply the first equation of (3.85) by $-\Delta Z$. Then it holds

$$\frac{d}{dt} \left(\frac{1}{2} |\nabla Z|^2 \right) + k_0 (\Delta Z)^2 - f'(u) Z \Delta Z = \text{div}(Z_t \nabla Z). \quad (3.91)$$

Multiplying (3.91) by ξ_1 , integrating on $\Omega \times (0, T)$ and using the definitions of Z , we get

$$\int_{\Omega} \frac{1}{2} |\nabla Z(\cdot, T)|^2 \xi_1 dx + k_0 \int_0^T \int_{\Omega} (\Delta Z)^2 \xi_1 dx dt = \int_0^T \int_{\Omega} f'(u) Z \Delta Z \xi_1 dx dt - \int_0^T \int_{\Omega} Z_t \nabla Z \cdot \nabla \xi_1 dx dt; \quad (3.92)$$

we remark that the integral terms are well defined thanks to the additional regularity $z \in W_2^{2,1}(\Omega \times (0, T)) \subset L^2(0, T; H^2(\Omega))$. Combining (3.92) and the first equation in (3.87), applying Young's inequality and taking into account (3.41) and the fact that $0 \leq \xi \leq 1$, we obtain

$$\int_{\Omega} |\nabla Z(\cdot, T)|^2 \xi_1 dx + k_0 \int_0^T \int_{\Omega} (\Delta Z)^2 \xi_1 dx dt \leq 2M_2 \int_0^T \int_{\Omega} Z^2 dx dt - 2 \int_0^T \int_{\Omega} (k_0 \Delta Z - f'(u) Z) \nabla Z \cdot \nabla \xi_1 dx dt.$$

Integrating by parts the term $\int_0^T \int_{\Omega} \Delta Z \nabla Z \cdot \nabla \xi_1 dx dt$, we easily deduce

$$\int_{\Omega} |\nabla Z(\cdot, T)|^2 \xi_1 dx + \int_0^T \int_{\Omega} (\Delta Z)^2 \xi_1 dx dt \leq C \left(\|Z\|_{L^2(0, T; L^2(\Omega))}^2 + \|\nabla Z\|_{L^2(0, T; L^2(\Omega))}^2 \right), \quad (3.93)$$

where C is a positive constant depending on M_2, k_0, ξ_1 . Hence, since $\xi_1 = 1$ in k_0 , we get

$$\|\Delta Z\|_{L^2(0, T; L^2(K_1))}^2 \leq C \left(\|Z\|_{L^2(0, T; L^2(\Omega))}^2 + \|\nabla Z\|_{L^2(0, T; L^2(\Omega))}^2 \right). \quad (3.94)$$

Observe that, replacing T by $t \in (0, T]$ in (3.93), we deduce also

$$\|\nabla Z\|_{L^\infty(0, T; L^2(K_1))} \leq C \left(\|Z\|_{L^2(0, T; L^2(\Omega))}^2 + \|\nabla Z\|_{L^2(0, T; L^2(\Omega))}^2 \right). \quad (3.95)$$

Combining (3.89), (3.94) and (3.95), we obtain

$$\|Z\|_{L^2(0, T; H^2(K_1))}^2 \leq C \|u^\varepsilon - u\|_{L^2(0, T; L^2(\partial\Omega))}^2, \quad (3.96)$$

where C is a positive constant depending on $k_0, M_2, \Omega, T, \xi_1$.

On account of the first equation in (3.87) and the previous estimates, we get

$$\|Z_t\|_{L^2(0, T; L^2(K_1))}^2 \leq C \left(\|Z\|_{L^2(0, T; L^2(\Omega))}^2 + \|\nabla Z\|_{L^2(0, T; L^2(\Omega))}^2 \right) \leq C \|u^\varepsilon - u\|_{L^2(0, T; L^2(\partial\Omega))}^2, \quad (3.97)$$

where C is a positive constant depending on $k_0, M_2, \Omega, T, \xi_1$.

Now, let us multiply the first equation of (3.87) by $-\Delta Z_t$. We obtain

$$-Z_t \Delta Z_t + \frac{k_0}{2} \frac{d}{dt} (\Delta Z)^2 - f'(u) Z \Delta Z_t = 0.$$

Multiplying the previous equation by ξ_2 and integrating on $\Omega \times (0, T)$, then a suitable integration by parts in space implies

$$\begin{aligned} & \int_0^T \int_{\Omega} |\nabla Z_t|^2 \xi_2 dx dt + \frac{k_0}{2} \int_0^T \int_{\Omega} \frac{d}{dt} (\Delta Z)^2 \xi_2 dx dt \\ & + \int_0^T \int_{\Omega} \xi_2 Z f''(u) \nabla u \cdot \nabla Z_t dx dt + \int_0^T \int_{\Omega} \xi_2 f'(u) \nabla Z \cdot \nabla Z_t dx dt \\ & = \int_0^T \int_{\Omega} \operatorname{div} \left(\frac{1}{2} \nabla((Z_t)^2) \right) \xi_2 dx dt + \int_0^T \int_{\Omega} \operatorname{div} \left(\nabla(f'(u) Z Z_t) dx dt - Z_t \nabla(f'(u) Z) \right) \xi_2 dx dt. \end{aligned}$$

Integrating by parts in time the second term of the left-hand side and by parts in space the terms in the right-hand side, by an application of Young's inequality we finally get

$$\int_0^T \int_{K_2} |\nabla Z_t|^2 dx dt \leq \int_0^T \int_{\Omega} |\nabla Z_t|^2 \xi_2 dx dt \leq C \left(\int_0^T \int_{\Omega} |Z|^2 dx dt + \int_0^T \int_{\Omega} |\nabla Z|^2 dx dt + \int_0^T \int_{K_1} (Z_t)^2 dx dt \right),$$

where the constant $C > 0$ depends on ξ_2, M_2 . A combination with (3.89), (3.90), (3.97) gives

$$\|\nabla Z_t\|_{L^2(0,T;L^2(K_2))}^2 \leq C \|u^\varepsilon - u\|_{L^2(0,T;L^2(\partial\Omega))}^2,$$

where the constant $C > 0$ depends on $k_0, M_2, \Omega, T, \xi_1, \xi_2$. In order to prove the desired regularity, we need to take into account also the third-order derivatives, in particular the operator $\nabla \Delta Z$. Observe that from the first equation in (3.87) we get

$$\nabla \Delta Z = \frac{1}{k_0} (\nabla Z_t + Z f''(u) \nabla u + f'(u) \nabla Z). \quad (3.98)$$

Hence, we can conclude

$$\|\nabla \Delta Z\|_{L^2(0,T;L^2(K_2))}^2 \leq C \|u^\varepsilon - u\|_{L^2(0,T;L^2(\partial\Omega))}^2,$$

where C is a positive constant depending on $k_0, \frac{1}{k_0}, M_2, \Omega, T, \xi_1, \xi_2$.

Recalling (3.96) and the fact that $K \subset K_2 \subset K_1$, standard regularity results imply

$$\|Z\|_{L^2(0,T;H^3(K))}^2 \leq C \|u^\varepsilon - u\|_{L^2(0,T;L^2(\partial\Omega))}^2. \quad (3.99)$$

Finally, from (3.96) and (3.99), by Sobolev immersion theorems, we get

$$\|Z\|_{L^1(0,T;W^{1,\infty}(K))}^2 \leq C(T) \|Z\|_{L^2(0,T;W^{1,\infty}(K))}^2 \leq C \|u^\varepsilon - u\|_{L^2(0,T;L^2(\partial\Omega))}^2, \quad (3.100)$$

where C is a positive constant depending on $k_0, \frac{1}{k_0}, M_2, \Omega, T, \xi_1, \xi_2$.

Recalling the relation between Z and Φ we get (3.86). \square

By Proposition 3.4, we deduce a representation formula for the topological gradient by introducing a suitable *adjoint problem*, according to the following

Proposition 3.5. *The topological gradient of the cost functional $j(\varepsilon, z)$ can be expressed by*

$$G(z) = \int_0^T \left(\tilde{k} \mathcal{M} \nabla u(z) \cdot \nabla W(z) + f(u(z)) W(z) \right) dt, \quad (3.101)$$

where W is the solution of the adjoint problem:

$$\begin{cases} W_t + k_0 \Delta W - f'(u) W = 0, & \text{in } \Omega \times (0, T), \\ k_0 \frac{\partial W}{\partial n} = u - u_{meas}, & \text{on } \partial\Omega \times (0, T), \\ W(T) = 0, & \text{in } \Omega. \end{cases} \quad (3.102)$$

Proof. Consider the difference

$$\begin{aligned} j(\varepsilon; z) - j(0) &= \frac{1}{2} \|u^\varepsilon - u_{meas}\|_{L^2(0,T;L^2(\partial\Omega))}^2 - \frac{1}{2} \|u - u_{meas}\|_{L^2(0,T;L^2(\partial\Omega))}^2 \\ &= \int_0^T \int_{\partial\Omega} (u^\varepsilon - u)(u - u_{meas}) d\sigma dt + \frac{1}{2} \|u^\varepsilon - u\|_{L^2(0,T;L^2(\partial\Omega))}^2. \end{aligned} \quad (3.103)$$

According to (3.59) and to the definition of the adjoint problem (3.102), we can express

$$\int_0^T \int_{\partial\Omega} (u^\varepsilon - u)(u - u_{meas}) d\sigma dt = |\omega_\varepsilon| \left\{ \int_0^T \int_\Omega \tilde{k} \mathcal{M} \nabla u \cdot \nabla W d\mu dt + \int_0^T \int_\Omega f(u) W d\mu dt + o(1) \right\}.$$

Since we assume (3.83), the measure μ associated to the inclusion is the Dirac mass δ_z centered in point z (see [47]). Hence

$$\int_0^T \int_{\partial\Omega} (u^\varepsilon - u)(u - u_{meas}) d\sigma dt = |\omega_\varepsilon| \int_0^T \left\{ \tilde{k} \mathcal{M} \nabla u(z) \cdot \nabla W(z) + f(u(z)) W(z) \right\} dt + o(|\omega_\varepsilon|). \quad (3.104)$$

Moreover, by (3.59), the second term in the left-hand side of (3.103) can be expressed as

$$\int_0^T \int_{\partial\Omega} (u^\varepsilon - u)(u^\varepsilon - u) d\sigma dt = |\omega_\varepsilon| \int_0^T \left\{ \tilde{k} \mathcal{M} \nabla u(z) \cdot \nabla \Phi(z) + f(u(z)) \Phi(z) \right\} dt + o(|\omega_\varepsilon|),$$

where Φ is the solution to (3.85). Thanks to regularity results on u (see Theorem 3.1) and using Proposition 3.4 with $K = \Omega_{d_0} = \{x \in \Omega \text{ s.t. } d(x, \partial\Omega) \geq d_0\}$, we obtain

$$\begin{aligned} \int_0^T \int_{\partial\Omega} (u^\varepsilon - u)(u^\varepsilon - u) d\sigma dt &\leq C |\omega_\varepsilon| \left\{ \int_0^T |\nabla \Phi(z)| dt + \int_0^T |\Phi(z)| dt \right\} + o(|\omega_\varepsilon|) \\ &\leq C |\omega_\varepsilon| \|u^\varepsilon - u\|_{L^2(0,T;L^2(\partial\Omega))} + o(|\omega_\varepsilon|) \leq C |\omega_\varepsilon| \|u^\varepsilon - u\|_{L^2(0,T;H^1(\Omega))} + o(|\omega_\varepsilon|) \\ &\leq C |\omega_\varepsilon|^{\frac{3}{2}} + o(|\omega_\varepsilon|) = o(|\omega_\varepsilon|). \end{aligned} \quad (3.105)$$

Replacing (3.104) and (3.105) in (3.103), we finally get

$$j(\varepsilon; z) - j(0) = |\omega_\varepsilon| \left\{ \int_0^T \tilde{k} \mathcal{M} \nabla u(z) \cdot \nabla W(z) dt + \int_0^T f(u(z)) W(z) dt \right\} + o(|\omega_\varepsilon|).$$

□

Thanks to the representation formula (3.101), evaluating the topological gradient of the cost functional requires just the solution of two initial and boundary value problems. This yields the definition of a *one-shot algorithm* for the identification of the center of a small inclusion satisfying hypothesis (3.83) (see Algorithm 4).

Guided by the application in electrophysiological we have in mind, we consider also the case of *partial boundary measurements* where the support of u_{meas} is given by a subset $\Gamma \subset \partial\Omega$. In this case, it is possible to formulate a slightly different optimization problem than (3.82), in which the mismatch $u^\varepsilon - u_{mean}$ is minimized just on the portion Γ of the boundary. The same reconstruction algorithm can be devised for this problem by simply considering non-homogeneous Neumann conditions in the adjoint problem (3.85) only on Γ .

Require: $u_0(x, 0) \forall x \in \Omega$, $u_{meas}(x, t) \forall x \in \partial\Omega$, $t \in (0, T)$.

Ensure: approximated centre of the inclusion, \bar{z}

1. compute u by solving (3.1);
2. compute W by solving (3.102);
3. determine G according to (3.101);
4. find \bar{z} s.t. $G(\bar{z}) \leq G(z) \quad \forall z \in \Omega$.

Algorithm 4: Reconstruction of a single inclusion of small dimensions

3.6 Numerical results

We rely on the Galerkin finite element method for the numerical approximation of the background problem (3.1) and the adjoint problem (3.102), as well as to compute the solution to the perturbed problem (3.5) in presence of the exact inclusion when considering synthetic data u_{meas} . The one-shot procedure makes the reconstruction algorithm very efficient, only requiring the solution of an adjoint problem for each acquired measurement over the time interval, without entailing any iterative (e.g. descent) method for numerical optimization.

3.6.1 Finite Element approximation

The background problem (3.1) can be cast in weak form as follows: $\forall t \in (0, T)$, find $u(t) \in V = H^1(\Omega)$ such that $u(0) = u_0$ and

$$\int_{\Omega} u_t v dx + \int_{\Omega} k_1 \nabla u \cdot \nabla v dx + \int_{\Omega} f(u) v dx = 0, \quad \forall v \in V. \quad (3.106)$$

By introducing a finite-dimensional subspace V_h of V , $\dim(V_h) = N_h < \infty$, the Galerkin (semi-discretized in space) formulation of problem (3.106) reads: $\forall t \in (0, T)$, find $u_h(t) \in V_h$ such that $u_h(0) = u_{h,0}$ and

$$\int_{\Omega} (u_h)_t v_h dx + b(u_h(t), v_h) + F(u_h(t), v_h) = 0, \quad \forall v_h \in V_h, \quad (3.107)$$

where $b(u, v) = \int_{\Omega} k_1 \nabla u \cdot \nabla v dx$, $F(u, v) = \int_{\Omega} f(u) v dx$, f is defined as in (3.2) and $u_{h,0}$ is the H^1 -projection of u_0 onto V_h .

To obtain a full discretization of the problem, we introduce a finite difference approximation in time. According to the strategy reported in [61], we rely on a semi-implicit scheme which allows an efficient treatment of the nonlinear terms. Let us consider an uniform partition $\{t^n\}_{n=0}^N$ of the time interval $[0, T]$ of step $\tau = \frac{T}{N}$ s.t. $t^0 = 0$, $t^N = T$. Then, the fully discrete formulation of (3.1) is given by: $\forall n = 0, \dots, N-1$, find $u_h^{n+1} \in V_h$ such that $u_h^0 = u_{0,h}$ and

$$\int_{\Omega} u_h^{n+1} v_h dx - \int_{\Omega} u_h^n v_h dx + \tau b(u_h^{n+1}, v_h) + \tau F(u_h^n, v_h) = 0, \quad \forall v_h \in V_h. \quad (3.108)$$

With the same discretization strategy one may describe a numerical scheme for the approximate solution of the perturbed problem, using the weak form reported in (3.13) and introducing the forms

$$b_{\varepsilon}(u, v) = \int_{\Omega} k_{\varepsilon} \nabla u \cdot \nabla v dx, \quad F_{\varepsilon}(u, v) = \int_{\Omega} \chi_{\Omega \setminus \omega_{\varepsilon}} f(u) v dx.$$

The adjoint problem, instead, requires the introduction of the form $dF(u, v; w) = \int_{\Omega} f'(w)uv dx$, which is bilinear with respect to u and v . Thanks to the linearity of the adjoint problem, we can consider a fully implicit Crank-Nicolson scheme: $\forall n = 0, \dots, N-1$, find $w_h^n \in V = H^1(\Omega)$ such that $w_h^N = 0$ and

$$\begin{aligned} \int_{\Omega} w_h^{n+1} v_h dx - \int_{\Omega} w_h^n v_h dx + \frac{\tau}{2} (b(w_h^{n+1}, v_h) + b(w_h^n, v_h)) + \\ dF(w_h^{n+1}, v_h; u_h^{n+1}) + dF(w_h^n, v_h; u_h^n) = \\ \frac{\tau}{2} \left(\int_{\partial\Omega} (u_h^{n+1} - u_{meas}(t^{n+1})) v_h d\sigma + \int_{\partial\Omega} (u_h^n - u_{meas}(t^n)) v_h d\sigma \right), \quad \forall v_h \in V_h. \end{aligned} \quad (3.109)$$

Existence and uniqueness of the solution to the fully-discrete problems (3.108) and (3.109) follow by the well-posedness of the continuous problems, since V_h is a subspace of $H^1(\Omega)$; see, e.g., [76], [127] and [61] for a detailed stability and convergence analysis of the proposed schemes.

The numerical setup for the simulation is represented in Figure 3.1. We consider an idealized geometry of the left ventricle (which has been object of several studies, see e.g. [61]), and define a tetrahedral tessellation \mathcal{T}_h of the domain. The discrete space V_h is the P1-Finite Element space over \mathcal{T}_h , i.e. the space of the continuous functions over Ω which are linear polynomials when restricted on each element $T \in \mathcal{T}_h$. The mesh we use for all the reported results consists of 24924 tetrahedral elements and $N_h = 5639$ nodes. We report also the anisotropic structure considered in all the reconstruction tests, according to [125, 118] and [61]. The conductivity matrix \mathbb{K}_0 for the monodomain equation is given by $\mathbb{K}_0(x) = \mathbb{K}^e(x)(\mathbb{K}^e(x) + \mathbb{K}^i(x))^{-1}\mathbb{K}^i(x)$, where \mathbb{K}^i and \mathbb{K}^e are orthotropic tensors with three constant positive real eigenvalues, namely

$$\begin{aligned} \mathbb{K}^e(x) &= k_f^e \vec{e}_f(x) \otimes \vec{e}_f(x) + k_t^e \vec{e}_t(x) \otimes \vec{e}_t(x) + k_r^e \vec{e}_r(x) \otimes \vec{e}_r(x) \\ \mathbb{K}^i(x) &= k_f^i \vec{e}_f(x) \otimes \vec{e}_f(x) + k_t^i \vec{e}_t(x) \otimes \vec{e}_t(x) + k_r^i \vec{e}_r(x) \otimes \vec{e}_r(x) \end{aligned}$$

The eigenvectors \vec{e}_f , \vec{e}_t and \vec{e}_r are associated to the three principal directions of conductivity in the heart tissue: respectively, the fiber centerline, the tangent direction to the heart sheets and the transmural direction (normal to the sheets).

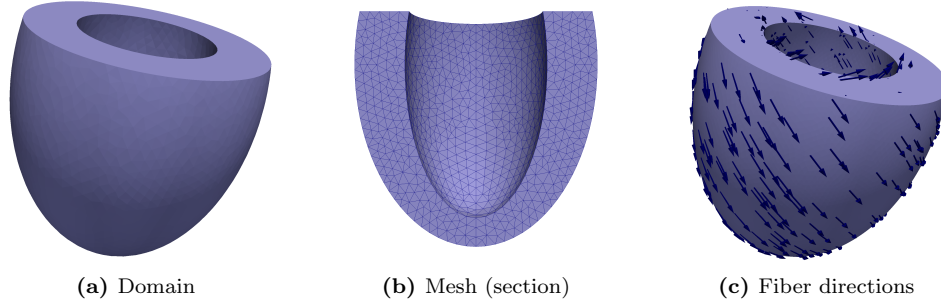


Figure 3.1: Setup of numerical test cases

For the direct problem simulations, we consider the formulation reported in (3.1), specifying realistic values for the parameters C_m and ν . We have rescaled the values of u_1 , u_2 , u_3 and A^2 in order to simulate the electric potential in the adimensional range $[0, 1]$. The rescaling is given by $\tilde{u} = (\alpha + u)/\beta$, where $\alpha = 0.085mV$ and $\beta = 0.125mV$, whereas for the sake of simplicity we will

still denote by u the rescaled variable \tilde{u} . We consider the initial datum u_0 to be positive on a band of the endocardium, representing the initial stimulus provided by the heart conducting system. The most relevant parameters, chosen according to [80], [132], are reported in Table 3.1.

ν	C_m	A^2	u_1	u_2	u_3	k_f^i	k_t^i	k_r^i	k_f^e	k_t^e	k_r^e
$500 \frac{m}{A}$	$0.1 \frac{mA \cdot ms}{cm^2}$	0.2	0	0.15	1	3	1	0.315	2	1.65	1.351

Table 3.1: Numerical values of physical coefficients

In Figure 3.2 we report the solution of the discrete background problem (3.108) at different time instants, comparing the isotropic and the anisotropic cases.

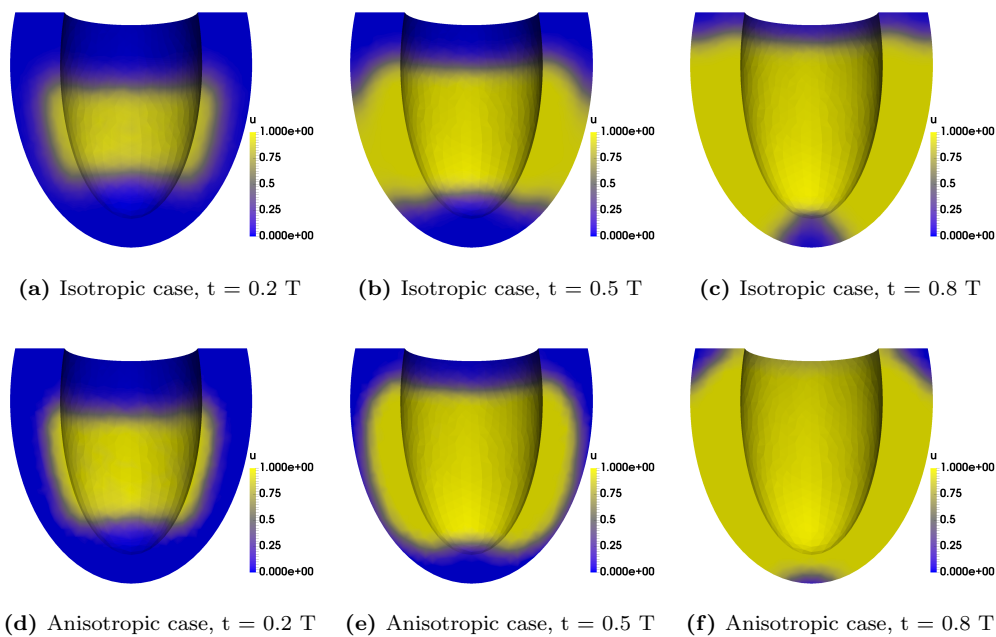


Figure 3.2: Background problem simulation: isotropic case (top) and anisotropic case (bottom) at different time instants

3.6.2 Reconstruction of small inclusions

We now tackle the problem of reconstructing the position of a small inhomogeneity using the knowledge of the electric potential on a portion Γ of the boundary. In particular, we assume that u_{meas} is known on the endocardium, i.e. the inner surface of the heart cavity. In each numerical experiment, we consider the presence of a spherical inclusion of small size (the ratio ρ_{isch}/ρ_{ventr} between the radius of the inhomogeneity and the radius of the horizontal section of the ventricle is 0.05) and consider a contrast of two orders of magnitude in the conductivity tensor between the ischemic and healthy tissue: $\mathbb{K}_1 = 0.01 \cdot \mathbb{K}_0$. We generate synthetic data on a more refined mesh and test the effectiveness of Algorithm 1 in the reconstruction of a small spherical inclusion in different

positions. In Figure 3.3 we report the value of the topological gradient and superimpose the exact inclusions (that is, the ones corresponding to the conductivity fields which have generated synthetic data): we observe a negative region in proximity of the position of the real inclusion. The algorithm precisely identifies the region where the inclusion is present, whereas the minimum may in general be found along the endocardium also when the center of the real inclusion is not located on the heart surface. Nevertheless, due to the domain thinness, the reconstructed position is found to be close to the real one.

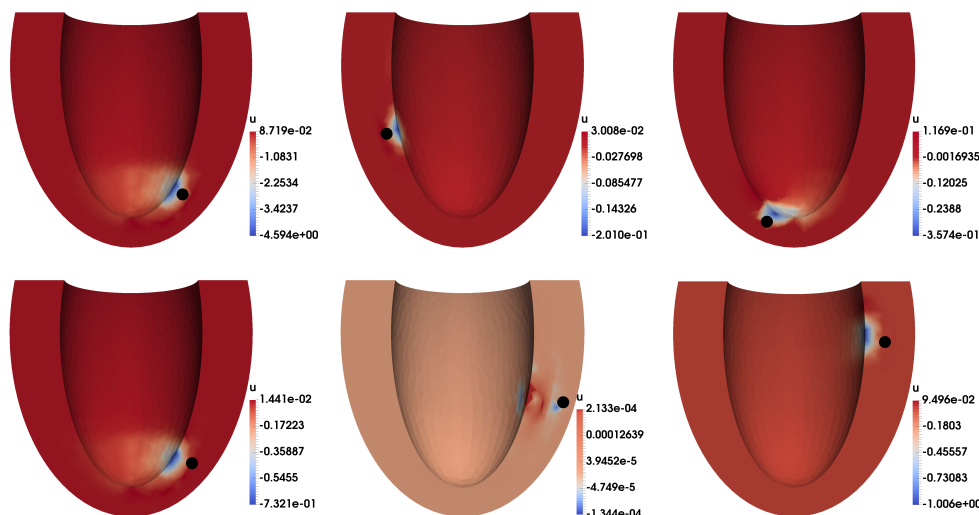


Figure 3.3: Reconstruction of small inclusions: topological gradient for different configurations

This slight loss in accuracy seems to be an intrinsic limit of the topological gradient strategy applied to the problem at hand. We point out that the reconstruction is performed by relying on a single measurement acquired on the boundary. This latter is a constraint imposed by the physical problem at hand, for which multiple measurements corresponding to different sources cannot be retrieved. As a matter of fact, all the techniques based on several measurements in order to increase the quality of the reconstruction are impracticable. A different strategy, as proposed in several works focusing on steady problems, may consist in introducing a modification to the cost functional J . In [11] and related works the authors introduce a cost functional inherited from imaging techniques, whereas in [52], [117] different strategies involving the Kohn-Vogelius functional or similar ones are explored. Nevertheless, the nonlinearity of the direct problem considered in this thesis prevents the possibility to apply these techniques, since the analytical expressions of the fundamental solution, single and double layer potentials would not be available in practice.

3.6.3 Reconstruction in presence of experimental noise

We then test the stability of the algorithm in presence of experimental noise on the measured data u_{meas} . We consider different noise levels, according to the formula

$$\tilde{u}_{meas}(x, t) = u_{meas}(x, t) + p\eta(x, t),$$

where $\eta(x, t)$ for each x, t is a Gaussian random variable with zero mean and standard deviation equal to $u_3 - u_1$, whereas $p \in [0, 1]$ is the noise level. In Figure 3.4 the results of the reconstruction in presence of different noise levels are compared. The algorithm shows to be robust with respect to large noise levels and increasingly accurate as the noise level reduces.

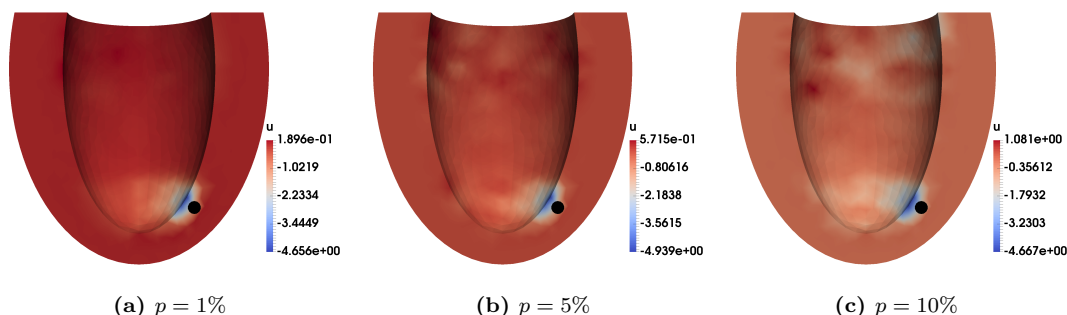


Figure 3.4: Reconstruction of small inclusions: results in presence of different noise levels

3.6.4 Reconstruction from partial discrete data

A further test case to assess at which extent the proposed procedure is effective deals with the reconstruction of small inclusions starting from the knowledge of partial data. These latter are provided by single measurements of the electric potential in a discrete set of points on the endocardium, possibly simulating the procedure of intracavitary electric measurements. Figure 3.5 shows that the algorithm is able to detect the presence of a small inclusion from the knowledge of the potential on $N_p = 246, 61, 15$ different points, shown in the bottom part of Figure 3.5. The position of the reconstructed inclusion is slightly affected by the reduction of sampling points; nevertheless, reliable reconstructions can be obtained even with a very small (compared to the number of mesh vertices lying on that boundary) number of points.

For the same purpose, we have tested the capability of the reconstruction procedure to avoid *false positives*: the algorithm is able to distinguish the case where inclusions are either present or absent, also in the case where the data are recovered only at a finite set of points and are affected by noise. We compare the value of the cost functional J and of the minimum of the topological gradient G obtained through Algorithm 4 on data generated when (i) a small inclusion is present or (ii) no inclusion is considered. The measurement is performed on a set of $N_p = 100$ points and is affected by different noise levels. The results are reported in Table 3.2.

The presence of a small noise on measured data causes a great increase of J : with 5% noise, e.g., the value of J is two orders of magnitude greater than the value assumed in presence of a small inclusion without noise. Nevertheless, the topological gradient G allows to distinguish the false positive cases, since (at least in the case of small noise level) the value attained by its minimum in presence of a small inclusion is considerably lower than the random oscillations of G due to noise.

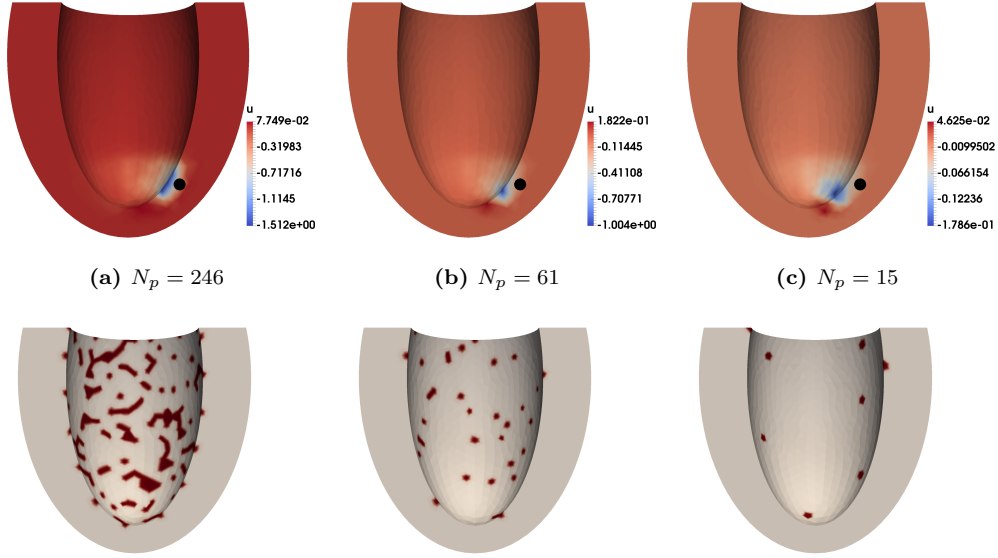


Figure 3.5: Reconstruction of small inclusions in presence of partial data. Top: topological gradient; bottom: mesh elements containing sampling points

Error	N_p	J	$min_{\Omega} G$	Error	N_p	J	$min_{\Omega} G$
0%	100	0.275	-0.5793	0%	100	0.000	0.000
1%	100	1.235	-0.589	1%	100	0.964	-0.044
2%	100	4.128	-0.530	2%	100	3.864	-0.105
5%	100	24.429	-0.589	5%	100	24.148	-0.189

(a) Results in presence of an inclusion

(b) Results with no inclusion present

Table 3.2: False positive test. Comparison between reconstructions obtained from data measured in presence of an inclusion (left table) and data measured with no inclusion present (right table). The null results in the first row of Table (b) are due to the usage of synthetic data.

3.6.5 Reconstruction of larger inclusions

We finally assess the performance of Algorithm 1, developed for the reconstruction of small inclusions well separated from the boundary, in detecting the position of extended inclusions. This case is of great potential interest in view of the problem of detecting ischemic regions*. The most important assumption on which the *one-shot* procedure above relies is that the variation of the cost functional when passing from the background case value ($J(0)$) to the value corresponding to the exact inclusion can be correctly described by the first order term of its asymptotic expansion, namely the topological gradient G . Removing the hypothesis of small size extension, we cannot rigorously assess the accuracy of the algorithm; however, the proposed procedure still allows us to identify the

*Total occlusion of a major coronary artery generally causes the entire thickness of the ventricular wall to become ischemic (transmural ischemia) or, alternatively, a significant ischemia only in the endocardium, that is, the inner layer of the myocardium (subendocardial ischemia). See, e.g., [60] for a detailed investigation of the interaction between the presence of moderate or severe subendocardial ischemic regions and the anisotropic structure of the cardiac muscle.

location of the inclusion.

We report the results of some numerical experiments conducted in presence of an inclusion of larger size, i.e., $\rho_{isch}/\rho_{ventr} = 0.25$, not even separated from the boundary. As depicted in Figure 3.6, the minimum of the topological gradient is close to the position of the inclusion and attains lower values with respect to the previously reported cases. When considering very extended ischemic regions (e.g. $\rho_{isch}/\rho_{ventr} = 0.5$), though, the information given by the topological gradient is less accurate – nevertheless, showing lower values close to the position of the inclusion.

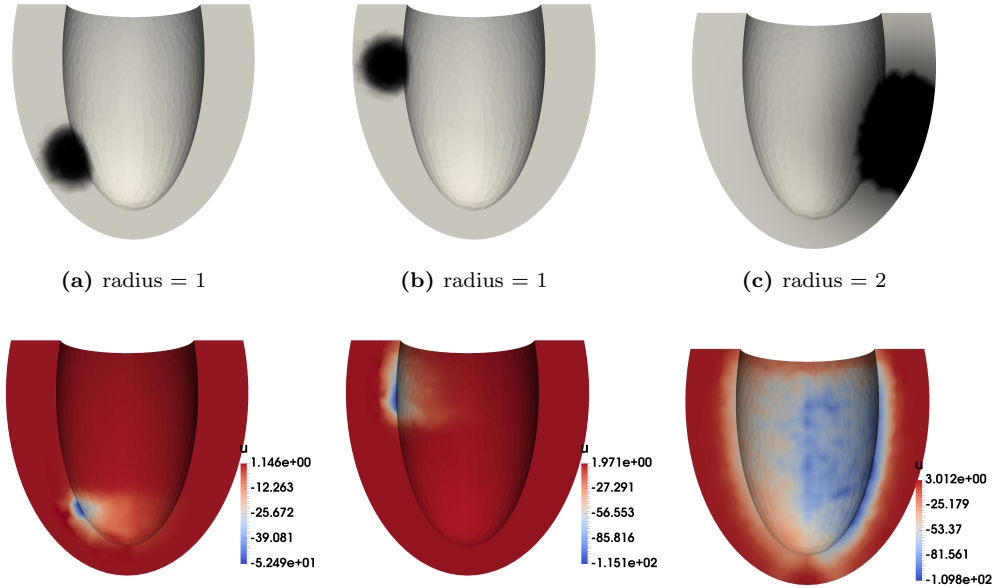


Figure 3.6: Reconstruction of larger inclusions, with $\rho_{isch}/\rho_{ventr} = 0.25$ (left and center plot), $\rho_{isch}/\rho_{ventr} = 0.5$ (right plot). Top: exact inclusion; bottom: topological gradient

Moreover, in Figure 3.7 we assess the stability of the reconstruction with respect to the presence of noisy data and partial measurements, as done in the case of small inclusions. Also in this case, reliable reconstructions can be obtained even in presence of noise, and/or data measured in a small number of points.

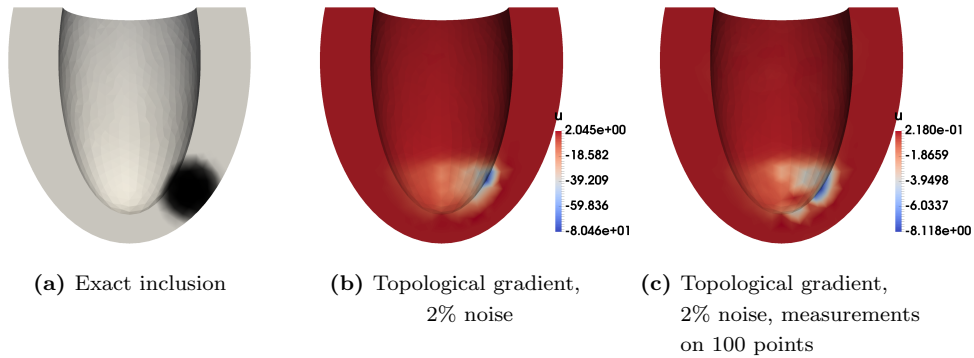


Figure 3.7: Larger ischemic regions: stability of the reconstruction

Chapter 4

A Shape Optimization approach for the reconstruction of large inclusions in a semilinear elliptic problem

This chapter tackles the problem of detecting large inhomogeneities in the coefficients of a semilinear elliptic equation by means of an approach inspired by the shape derivative technique. In particular, we consider the following Neumann problem, defined over $\Omega \subset \mathbb{R}^2$:

$$\begin{cases} -\operatorname{div}(k_\omega \nabla u) + \chi_{\Omega \setminus \omega} u^3 = f & \text{in } \Omega, \\ k_\omega \nabla u \cdot \nu = 0 & \text{on } \partial\Omega, \end{cases} \quad (4.1)$$

where

$$k_\omega(x) = \begin{cases} 1 & \text{if } x \in \omega \\ k & \text{if } x \in \Omega \setminus \omega, \end{cases} \quad k < 1.$$

We want to tackle the following inverse problem: knowing the source term f and the measured data u_{meas} on the boundary of Ω , determine the inclusion ω such that it holds: $u|_{\partial\Omega} = u_{meas}$, being u the solution of (4.1) with inclusion ω . This consists in a natural continuation of the purposes of Chapter 2: we rely on the same model tackled in that chapter, but removing the *regularization hypotheses* which allowed to perform an extended analysis. Namely, we do not assume that the inclusion to be identified is of small size.

As outlined in Section 1.3, even on the linear counterpart of the problem the purpose of reconstructing a piecewise constant coefficient from a finite number of measurements (or even a single one) entails severe issues unless further assumptions on the inclusion are introduced. Moreover, several reconstruction algorithms developed for the inverse conductivity problem fail to be applied in the nonlinear context at hand, except for a restricted selection of variational methods.

In particular, the task of this chapter is to rigorously introduce a shape derivative approach for the nonlinear inverse problem in consideration. This strategy allows to deal with the reconstruction

of a discontinuous parameter, by starting with a reasonable initial guess of the inclusion (i.e., the region in which the parameters assume a different value with respect to the reference one) and perturbing its boundary. In order to do so, we aim at minimizing a suitable misfit functional, endowed with a regularization term penalizing the perimeter of the inclusion. A deeper discussion both on the motivation and on the main results involved with the introduction of the regularization term can be found in Chapter 5. In order to study the sensitivity of the functional with respect to perturbations of an existing inclusion, it is necessary to rigorously derive an asymptotic expansions of suitable integral terms involving the boundary voltage. Finally, in view of these results and of the tools of the Shape Optimization theory, an iterative algorithm for the reconstruction of the inclusion is implemented.

The described strategy allows for the reconstruction of inclusions whose boundary is sufficiently smooth; nevertheless, it is possible to extend the same results also in the case of polygonal inclusions. In particular, we refer to [31] for the sensitivity analysis and to [34] for the shape-derivative based reconstruction algorithm.

The outline of the chapter is the following one: in Section 4.1 we provide an accurate asymptotic analysis of the solution of the direct problem associated to a large inclusion when small perturbations of the boundary are made. In Section 4.2, instead, we exploit those results within to formulate a reconstruction algorithm for the inverse problem based on the shape gradient of the cost functional.

4.1 Small perturbations of a large inclusion

As previously outlined, this chapter is focused on the reconstruction of inclusions of arbitrarily large size, removing the assumption of small size. Nevertheless, we still assume some *a priori* information regarding the solution we want to reconstruct: in particular, we look for inclusions ω which can be obtained as a smooth deformation of an initial shape ω_0 (such that the boundary $\partial\omega_0$ is of class C^2), and well separated from the boundary. More precisely, our analysis focuses on small regular perturbations ω_ε of a fixed inclusion ω_0 of the form:

$$\partial\omega_\varepsilon = \{y + \varepsilon h(y)\nu(y), y \in \partial\omega_0\}, \quad (4.2)$$

being $\varepsilon > 0$, $\nu(\cdot) : \partial\omega_0 \rightarrow \mathbb{R}^2$ the outward unit normal vector of $\partial\omega_0$ and $h(\cdot) \in C^2(\partial\omega_0; \mathbb{R})$. Large deformations of the original shape might be obtained by recursively applying small perturbations as the one reported in (4.2).

Notation: in the sequel, we will recall $\Delta\omega = \omega_0 \Delta\omega_\varepsilon$, $\varepsilon \setminus 0 = \omega_\varepsilon \setminus \omega_0$, $0 \setminus \varepsilon = \omega_0 \setminus \omega_\varepsilon$, $\Omega_r = \Omega \setminus (\omega_0 \cup \omega_\varepsilon)$, and the functions $\chi_0 = \chi_{\omega_0}$, $\chi_\varepsilon = \chi_{\omega_\varepsilon}$, $\chi_{\varepsilon \setminus 0} = \chi_{\omega_\varepsilon \setminus \omega_0}$, $\chi_{0 \setminus \varepsilon} = \chi_{\omega_0 \setminus \omega_\varepsilon}$, $\chi_r = \chi_{\Omega_r}$, $k_0 = 1 - (1 - k)\chi_0$, $k_\varepsilon = 1 - (1 - k)\chi_\varepsilon$.

4.1.1 The direct problem in presence of an inclusion: a review

The well-posedness of the direct problem in presence of ω_0 has already been investigated in Chapter 2, Proposition 2.1: indeed, no assumption on the size of the inclusion is required in the proof. Hence, the solution u_0 of (4.1) with $\omega = \omega_0$ exists and is unique in $H^1(\Omega)$. By the same argument, proceeding as in [30, equation (4.14)] we can also prove that $u_0 \in C^\alpha(\overline{\Omega})$.

We remark, as it will be useful in the sequel, that the following *transmission conditions* hold in a trace sense for u_0 :

$$\begin{aligned} u_0^i &= u_0^e & \text{on } \partial\omega_0, \\ \nabla_\tau u_0^i &= \nabla_\tau u_0^e & \text{on } \partial\omega_0, \\ k \nabla_\nu u_0^i &= \nabla_\nu u_0^e & \text{on } \partial\omega_0, \end{aligned} \tag{4.3}$$

where $u_0^e = u_0|_{\Omega \setminus \overline{\omega_0}}$, $u_0^i = u_0|_{\omega_0}$, $\nabla_\tau u = \nabla u \cdot \tau$, $\nabla_\nu u = \nabla u \cdot \nu$ and ν, τ are the (outward) normal and tangential unit versors of the boundary of ω_0 . The same conditions hold on u_ε across $\partial\omega_\varepsilon$. More refined interior regularity results can be obtained:

Lemma 4.1. *If the forcing term $f \in L^\infty(\Omega)$, then there exists a positive exponent $0 < \alpha < 1$ and a constant $C > 0$ independent of ε such that:*

$$\begin{aligned} \|u_0\|_{C^{1+\alpha}(\overline{\omega_0}) \cap C^{1+\alpha}(\Omega_\delta \setminus \omega_0)} &\leq C \\ \|u_\varepsilon\|_{C^{1+\alpha}(\overline{\omega_\varepsilon}) \cap C^{1+\alpha}(\Omega_\delta \setminus \omega_\varepsilon)} &\leq C, \end{aligned} \tag{4.4}$$

being $\Omega_\delta = \{x \in \Omega \text{ s.t. } \text{dist}(x, \partial\Omega) \geq \delta\}$, $\delta < d_0$.

Proof. From well-posedness results for the direct problem, we know that $u_0 \in H^1(\Omega)$ satisfies the equation:

$$-\text{div}(k_0 \nabla u_0) = f - (1 - \chi_0)u_0^3.$$

As previously outlined, by the same argument used in [30, formula (4.14)] for inclusions of small dimensions, we can exploit the interior estimates of [82, Theorem 8.24] to conclude that $\|u_0\|_{C^\alpha(\Omega)} \leq C$, where C depends on $\Omega, k, \|f\|_{L^p(\Omega)}$. In particular, the term $(1 - \chi_0)u_0^3$ belongs to $L^\infty(\Omega)$, hence we can apply the result from Li and Nirenberg (see [101], Theorem 1.1) to obtain

$$\begin{aligned} \|u_0\|_{C^{1+\alpha}(\overline{\omega_0})} &\leq C(\|u_0\|_{L^2(\Omega)} + \|f\|_{L^\infty(\Omega)} + \|u_0\|_{L^\infty(\Omega)}^3) \\ \|u_0\|_{C^{1+\alpha}(\Omega_\delta \setminus \omega_0)} &\leq C(\|u_0\|_{L^2(\Omega)} + \|f\|_{L^\infty(\Omega)} + \|u_0\|_{L^\infty(\Omega)}^3), \end{aligned}$$

where $C = C(k, \Omega, \omega_0, d_0, \alpha)$. Exploiting the bounds on the norm of u_0 in $C(\Omega)$ stated above, one may conclude that

$$\|u_0\|_{C^{1+\alpha}(\overline{\omega_0}) \cap C^{1+\alpha}(\Omega_\delta \setminus \omega_0)} \leq C$$

with $C = C(\Omega, k, \omega_0, d_0, \alpha, \|f\|_{L^\infty(\Omega)})$. \square

We point out that all the results stated in the present Section are valid also on ω_ε , since by the assumption (4.2) the boundary of the perturbed inclusion has the same regularity as the initial one.

4.1.2 Energy estimates

This section is devoted to some estimates involving the difference between u_ε and u_0 , which are useful for the proof of the fundamental results in the sequel. We first of all remark that, by trivial computation, it holds:

Lemma 4.2. *Defined ω_ε as in (4.2) and being $\Delta\omega = \omega_\varepsilon \Delta\omega_0$, there exists a positive constant C depending on h and ω_0 such that:*

$$|\Delta\omega| \leq C\varepsilon. \tag{4.5}$$

We now state and prove two important energy estimates regarding the difference $u_\varepsilon - u_0$.

Lemma 4.3.

$$\|u_\varepsilon - u_0\|_{H^1(\Omega)} \leq C|\Delta\omega|^{\frac{1}{2}} \quad (4.6)$$

Proof. Consider the problem which are solved by u_ε and u_0 :

$$\begin{aligned} -\operatorname{div}(k_\varepsilon \nabla u_\varepsilon) + (1 - \chi_\varepsilon)u_\varepsilon^3 &= f \\ -\operatorname{div}(k_0 \nabla u_0) + (1 - \chi_0)u_0^3 &= f; \end{aligned}$$

recalling $w_\varepsilon = u_\varepsilon - u_0$ and observing that $k_\varepsilon - k_0 = (k-1)\chi_{\varepsilon \setminus 0} + (1-k)\chi_{0 \setminus \varepsilon}$ and $1 - \chi_\varepsilon = \chi_r + \chi_{0 \setminus \varepsilon}$, $1 - \chi_0 = \chi_r + \chi_{\varepsilon \setminus 0}$, one obtains the following problem for w_ε :

$$-\operatorname{div}(k_\varepsilon \nabla w_\varepsilon) + \chi_r q_\varepsilon w_\varepsilon = -\operatorname{div}((1-k)\chi_{\varepsilon \setminus 0} \nabla u_0) + \chi_{\varepsilon \setminus 0} u_0^3 - \operatorname{div}((k-1)\chi_{0 \setminus \varepsilon} \nabla u_0) - \chi_{0 \setminus \varepsilon} u_\varepsilon^3, \quad (4.7)$$

where $q_\varepsilon = u_\varepsilon^2 + u_\varepsilon u_0 + u_0^2$. Using the strategy outlined in the Appendix of [30] in order to obtain a Poincarè inequality for w_ε , we write:

$$w_\varepsilon = \widetilde{w}_\varepsilon + a_\varepsilon, \quad a_\varepsilon = \frac{1}{\int_{\Omega_r} q_\varepsilon} \int_{\Omega_r} q_\varepsilon w_\varepsilon.$$

Hence, it follows that $\int_{\Omega_r} \widetilde{w}_\varepsilon q_\varepsilon = 0$, and it holds:

$$\|\widetilde{w}_\varepsilon\|_{L^2(\Omega)} \leq C_p \|\nabla \widetilde{w}_\varepsilon\|_{L^2(\Omega)} = C_p \|\nabla w_\varepsilon\|_{L^2(\Omega)}.$$

Moreover, exploiting the homogeneous Neumann boundary conditions satisfied by u_ε and u_0 , by the divergence theorem,

$$\int_{\Omega} \operatorname{div}(k_\varepsilon \nabla w_\varepsilon) = 0; \quad \int_{\Omega} \operatorname{div}(\chi_{\varepsilon \setminus 0} \nabla u_0) = \int_{\Omega} \operatorname{div}(\chi_{0 \setminus \varepsilon} \nabla u_0) = 0.$$

Thus, integrating equation (4.7) over Ω one obtains:

$$\int_{\Omega_r} q_\varepsilon w_\varepsilon = \int_{\varepsilon \setminus 0} u_0^3 - \int_{0 \setminus \varepsilon} u_\varepsilon^3,$$

and ultimately:

$$|a_\varepsilon| = \frac{1}{\left| \int_{\Omega_r} q_\varepsilon \right|} \left| \int_{\varepsilon \setminus 0} u_0^3 - \int_{0 \setminus \varepsilon} u_\varepsilon^3 \right| \leq Q \left(\|u_0\|_{L^6(\Omega)}^2 + \|u_\varepsilon\|_{L^6(\Omega)}^2 \right) |\Delta\omega|^{\frac{1}{2}},$$

being Q s.t. $\left| \int_{\Omega_r} q_\varepsilon \right| > \frac{1}{Q}$, which can be proved in the hypothesis that $f \geq m$ (according to the discussion in Chapter 2). This entails that the following inequality holds for w_ε :

$$\|w_\varepsilon\|_{H^1(\Omega)} \leq \|\widetilde{w}_\varepsilon\|_{H^1(\Omega)} + |a_\varepsilon| |\Omega| \leq (1 + C_p) \|\nabla w_\varepsilon\|_{L^2(\Omega)} + C_2 |\Delta\omega|^{\frac{1}{2}}. \quad (4.8)$$

In order to estimate $\|\nabla w_\varepsilon\|_{L^2(\Omega)}$, we integrate equation (4.7) using w_ε as a test function: after integration by parts, we obtain:

$$\int_{\Omega} k_\varepsilon |\nabla w_\varepsilon|^2 + \int_{\Omega_r} w_\varepsilon^2 q_\varepsilon = (k-1) \int_{0 \setminus \varepsilon} \nabla u_0 \cdot \nabla w_\varepsilon + (1-k) \int_{\varepsilon \setminus 0} \nabla u_0 \cdot \nabla w_\varepsilon + \int_{\varepsilon \setminus 0} u_0^3 - \int_{0 \setminus \varepsilon} \nabla u_\varepsilon^3.$$

$$\begin{aligned}
k\|\nabla w_\varepsilon\|_{L^2(\Omega)}^2 &\leq \int_{\Omega} k_\varepsilon |\nabla w_\varepsilon|^2 + \int_{\Omega_r} w_\varepsilon^2 q_\varepsilon \leq \text{(exploiting estimates (4.4))} \\
&\leq (1-k) \left(\|\nabla u_0\|_{L^\infty(\varepsilon\setminus 0)} \|\nabla w_\varepsilon\|_{L^2(\varepsilon\setminus 0)} + \|\nabla u_0\|_{L^\infty(0\setminus \varepsilon)} \|\nabla w_\varepsilon\|_{L^2(0\setminus \varepsilon)} \right) |\Delta\omega|^{\frac{1}{2}} + \\
&\quad \left(\|u_0^3\|_{L^\infty(\varepsilon\setminus 0)} \|w_\varepsilon\|_{L^2(\varepsilon\setminus 0)} + \|u_\varepsilon^3\|_{L^\infty(0\setminus \varepsilon)} \|w_\varepsilon\|_{L^2(0\setminus \varepsilon)} \right) |\Delta\omega|^{\frac{1}{2}} \leq \\
&\leq \left\{ (1-k) \|\nabla u_0\|_{L^\infty(\Delta\omega)} \|\nabla w_\varepsilon\|_{L^2(\Omega)} + \left(\|u_\varepsilon^3\|_{L^\infty(\Delta\omega)} + \|u_0^3\|_{L^\infty(\Delta\omega)} \right) \|w_\varepsilon\|_{L^2(\Omega)} \right\} |\Delta\omega|^{\frac{1}{2}}.
\end{aligned}$$

Hence, it holds (since $\|w_\varepsilon\|_{L^2(\Omega)} \leq \|w_\varepsilon\|_{H^1(\Omega)} \leq C_1 \|\nabla w_\varepsilon\|_{L^2(\Omega)} + C_2 |\Delta\omega|^{\frac{1}{2}}$):

$$A\|\nabla w_\varepsilon\|_{L^2(\Omega)}^2 - B|\Delta\omega|^{\frac{1}{2}}\|\nabla w_\varepsilon\|_{L^2(\Omega)} - C|\Delta\omega| \leq 0, \quad (4.9)$$

with A, B, C positive constants depending on $k, \|u_\varepsilon^3\|_{L^\infty(\Delta\omega)}, \|u_0^3\|_{L^\infty(\Delta\omega)}, \|\nabla u_0\|_{L^\infty(\Delta\omega)}$. Solving the second order inequality, one gets:

$$\|\nabla w_\varepsilon\|_{L^2(\Omega)} \leq \frac{B + \sqrt{B^2 - 4AC}}{2A} |\Delta\omega|^{\frac{1}{2}},$$

which can be inserted in (4.8) to obtain the thesis. \square

Lemma 4.4.

$$\|u_\varepsilon - u_0\|_{L^2(\Omega)} \leq C|\Delta\omega|^{\frac{1}{2}+\eta}, \quad \eta > 0. \quad (4.10)$$

Proof. As reported in the proof of Lemma 4.3, $w_\varepsilon \in H^1(\Omega)$ is the solution of problem (4.7) with homogeneous Neumann boundary conditions, whose weak formulation reads:

$$\begin{aligned}
\int_{\Omega} k_\varepsilon \nabla w_\varepsilon \cdot \nabla \varphi + \int_{\Omega_r} q_\varepsilon w_\varepsilon \varphi &= \int_{\varepsilon\setminus 0} ((1-k)\nabla u_0 \cdot \nabla \varphi + u_0^3 \varphi) \\
&\quad - \int_{0\setminus \varepsilon} ((1-k)\nabla u_0 \cdot \nabla \varphi + u_\varepsilon^3 \varphi) \quad \forall \varphi \in H^1(\Omega).
\end{aligned} \quad (4.11)$$

Moreover, we introduce \overline{w}_ε , the solution of the problem:

$$\int_{\Omega} k_\varepsilon \nabla \overline{w}_\varepsilon \cdot \nabla \varphi + \int_{\Omega_r} q_\varepsilon \overline{w}_\varepsilon \varphi = \int_{\Omega} w_\varepsilon \varphi \quad \forall \varphi \in H^1(\Omega). \quad (4.12)$$

By the same argument exposed in [30], problem (4.12) is well-posed and it holds

$$\|\overline{w}_\varepsilon\|_{H^1(\Omega)} \leq \|w_\varepsilon\|_{L^2(\Omega)}. \quad (4.13)$$

By Meyers inequalities ([107]), $\nabla \overline{w}_\varepsilon \in L^{p'}(\Delta\omega)$ and

$$\|\nabla \overline{w}_\varepsilon\|_{L^{p'}(\Delta\omega)} \leq C \left(\|\nabla \overline{w}_\varepsilon\|_{L^2(\widetilde{\Delta\omega})} + \|w_\varepsilon\|_{L^{p'}(\widetilde{\Delta\omega})} \right),$$

being $\widetilde{\Delta\omega} \supset \Delta\omega$. Using (4.13) and the Sobolev immersions we conclude that:

$$\|\nabla \overline{w}_\varepsilon\|_{L^{p'}(\Delta\omega)} \leq C \|w_\varepsilon\|_{H^1(\Omega)}. \quad (4.14)$$

Substituting $\varphi = \overline{w}_\varepsilon$ in (4.11) and $\varphi = w_\varepsilon$ in (4.12) and exploiting Hölder inequality (with $1 \leq p < 2$), one obtains:

$$\begin{aligned}
\int_{\Omega} w_\varepsilon^2 &= \int_{\varepsilon\setminus 0} ((1-k)\nabla u_0 \cdot \nabla \overline{w}_\varepsilon + u_0^3 \overline{w}_\varepsilon) - \int_{0\setminus \varepsilon} ((1-k)\nabla u_0 \cdot \nabla \overline{w}_\varepsilon + u_\varepsilon^3 \overline{w}_\varepsilon) \\
&\leq C \left(\|\nabla u_0\|_{L^p(\Delta\omega)} \|\nabla \overline{w}_\varepsilon\|_{L^{p'}(\Delta\omega)} + \left(\|u_0^3\|_{L^p(\Delta\omega)} + \|u_\varepsilon^3\|_{L^p(\Delta\omega)} \right) \|\overline{w}_\varepsilon\|_{L^{p'}(\Delta\omega)} \right).
\end{aligned} \quad (4.15)$$

Thanks to Lemma 4.1, we can ensure that $\|\nabla u_0\|_{L^\infty(\Delta\omega)}$, $\|u_0^3\|_{L^\infty(\Delta\omega)}$ and $\|u_\varepsilon^3\|_{L^\infty(\Delta\omega)}$ are controlled by a positive constant C . Hence,

$$\|\nabla u_0\|_{L^p(\Delta\omega)}, \|u_0^3\|_{L^p(\Delta\omega)}, \|u_\varepsilon^3\|_{L^p(\Delta\omega)} \leq C|\Delta\omega|^{\frac{1}{p}}. \quad (4.16)$$

Thanks to Sobolev immersions,

$$\|\overline{w_\varepsilon}\|_{L^{p'}(\Delta\omega)} \leq \|\overline{w_\varepsilon}\|_{L^{p'}(\Omega)} \leq C\|\overline{w_\varepsilon}\|_{H^1(\Omega)},$$

and exploiting (4.13)

$$\|\overline{w_\varepsilon}\|_{L^{p'}(\Delta\omega)} \leq C\|w_\varepsilon\|_{H^1(\Omega)} \quad (4.17)$$

Hence, thanks to (4.16), (4.17), (4.14), we conclude from (4.15):

$$\|w_\varepsilon\|_{L^2(\Omega)}^2 \leq C|\Delta\omega|^{\frac{1}{p}}\|w_\varepsilon\|_{H^1(\Omega)} \leq C|\Delta\omega|^{\frac{1}{p}+\frac{1}{2}}$$

which entails that

$$\|w_\varepsilon\|_{L^2(\Omega)} \leq C|\Delta\omega|^{\frac{1}{2}+\eta},$$

with $\eta = \frac{2-p}{4p} > 0$. □

Lemma 4.5. *The following estimates hold on the boundary of ω_ε :*

$$\begin{aligned} \|\nabla(u_\varepsilon^e - u_0^e)\|_{L^\infty(\partial\omega_\varepsilon \cap \omega_0)} + \|\nabla(u_\varepsilon^e - u_0^e)\|_{L^\infty(\partial\omega_\varepsilon \setminus \omega_0)} &\leq C\varepsilon^{\frac{\alpha}{2\alpha+2}} \\ \|u_\varepsilon^3 - u_0^3\|_{L^\infty(\partial\omega_\varepsilon \cap \omega_0)} + \|u_\varepsilon^3 - u_0^3\|_{L^\infty(\partial\omega_\varepsilon \setminus \omega_0)} &\leq C\varepsilon^{\frac{1}{4}} \end{aligned} \quad (4.18)$$

Proof. The function $w_\varepsilon = u_\varepsilon - u_0$ is the solution of (4.7), which means that in $\Omega_r = \Omega \setminus (\omega_0 \cup \omega_\varepsilon)$ it satisfies:

$$-\Delta w_\varepsilon + q_\varepsilon w_\varepsilon = 0 \quad \text{in } \Omega_r,$$

whereas its gradient $\theta = \nabla w_\varepsilon$ satisfies:

$$-\Delta \theta + q_\varepsilon \theta = -w_\varepsilon \nabla q_\varepsilon \quad \text{in } \Omega_r.$$

Exploiting the local estimates in [82, Theorem 8.17], we obtain that in $\Omega_r^d = \{x \in \Omega_r : \text{dist}(x, \partial\Omega_r) > d\}$ it holds:

$$\|\nabla w_\varepsilon\|_{L^\infty(\Omega_r^d)} \leq Cd^{-1} \left(\|w_\varepsilon\|_{L^2(\Omega)} + \|q_\varepsilon\|_{H^1(\Omega)} \|w_\varepsilon\|_{L^2(\Omega)} \right)$$

and, exploiting the energy estimate (4.6), we obtain:

$$\|\nabla w_\varepsilon\|_{L^\infty(\Omega_r^d)} \leq Cd^{-1}\varepsilon^{\frac{1}{2}}. \quad (4.19)$$

Consider now $y \in \partial\omega_\varepsilon \setminus \omega_0$ and let y_d be the point of Ω_r^d which is closest to y : thanks to the Hölder continuity of the restriction ∇u_ε^e of ∇u_ε in $\Omega_\delta \setminus \omega_\varepsilon$ and to the regularity of ∇u_0^e (see Lemma 4.1), we can ensure:

$$\begin{aligned} |\nabla u_\varepsilon^e(y) - \nabla u_\varepsilon^e(y_d)| &\leq Cd^\alpha, \\ |\nabla u_0^e(y) - \nabla u_0^e(y_d)| &\leq Cd^\alpha; \end{aligned}$$

hence:

$$\begin{aligned} |\nabla u_\varepsilon^e(y) - \nabla u_0^e(y)| &\leq |\nabla u_\varepsilon^e(y) - \nabla u_\varepsilon^e(y_d)| + |\nabla u_\varepsilon^e(y_d) - \nabla u_0^e(y_d)| + |\nabla u_0^e(y) - \nabla u_0^e(y_d)| \\ &\leq Cd^\alpha + d^{-1}\varepsilon^{\frac{1}{2}}. \end{aligned}$$

One may choose $d = \varepsilon^\beta$, $\beta > 0$: substituting in the previous inequality, we obtain that $|\nabla u_\varepsilon^e(y) - \nabla u_0^e(y)| \leq C\varepsilon^\sigma$, being $\sigma = \min\{\alpha\beta, \frac{1}{2} - \beta\}$. We select $d = \varepsilon^{\frac{1}{2\alpha+2}}$, which entails that:

$$|\nabla u_\varepsilon^e(y) - \nabla u_0^e(y)| \leq C\varepsilon^{\frac{\alpha}{2\alpha+2}} \quad (4.20)$$

for every $y \in \partial\omega_\varepsilon \setminus \omega_0$. Similar arguments allow to conclude that the same inequality holds on $\partial\omega_\varepsilon \cap \omega_0$. The proof of the other inequalities is similar, exploiting the interior estimates for w_ε :

$$\|w_\varepsilon\|_{L^\infty(\Omega_r^d)} \leq Cd^{-1}\|w_\varepsilon\|_{L^2(\Omega)} \leq Cd^{-1}\varepsilon^{\frac{1}{2}}$$

(we remark that the result could be improved by considering $\varepsilon^{\frac{1}{2}+\eta}$, but it will not be useful in the sequel). Moreover, as $u_\varepsilon^e, u_0^e \in C^{1+\alpha}(\Omega_\delta \setminus \omega_0)$,

$$\begin{aligned} |\nabla u_\varepsilon^e(y) - \nabla u_\varepsilon^e(y_d)| &\leq Cd \\ |\nabla u_0^e(y) - \nabla u_0^e(y_d)| &\leq Cd; \end{aligned}$$

hence

$$\|w_\varepsilon\|_{L^\infty(\partial\omega_\varepsilon \setminus \omega_0)} \leq C(d + d^{-1}\varepsilon^{\frac{1}{2}}) \leq C\varepsilon^{\frac{1}{4}}.$$

With analogous arguments it is possible to show that the same inequality holds on $\partial\omega_\varepsilon \cap \omega_0$. \square

4.1.3 Asymptotic expansion

The main achievement of this Section is the following asymptotic expansion, which will be a crucial result for the introduction of a shape-gradient based reconstruction algorithm.

Proposition 4.1. *For every $g \in L^p(\partial\Omega)$, $p \geq 2$, it holds:*

$$\int_{\partial\Omega} g(u_\varepsilon - u_0) = \varepsilon \int_{\partial\omega_0} \left\{ (1-k)[\nabla_\tau u_0^e \cdot \nabla_\tau w^e + \frac{1}{k} \nabla_\nu u_0^e \cdot \nabla_\nu w^e] + u_0^3 w \right\} h + o(\varepsilon), \quad (4.21)$$

being w the solution of the auxiliary problem:

$$\begin{cases} -\operatorname{div}(k_0 \nabla w) + 3\chi_{\Omega \setminus \omega_0} u_0^2 w = 0 & \text{in } \Omega \\ \partial_\nu w = g & \text{on } \partial\Omega. \end{cases} \quad (4.22)$$

Proof. We first remark that the results in Lemma 4.1 and Lemma 4.5 can be extended to w .

Exploiting the expression of the auxiliary problem, we write:

$$\begin{aligned} \int_{\partial\Omega} (u_\varepsilon - u_0)g &= \int_{\Omega} k_0 \nabla(u_\varepsilon - u_0)w + \int_{\Omega} 3(1 - \chi_0)u_0^2(u_\varepsilon - u_0)w = \\ &= - \int_{\Omega} (k_\varepsilon - k_0) \nabla u_\varepsilon \cdot \nabla w + \int_{\Omega} k_\varepsilon \nabla u_\varepsilon \cdot \nabla w - \int_{\Omega} k_0 \nabla u_0 \cdot \nabla w \\ &\quad + \int_{\Omega} 3(1 - \chi_0)u_0^2(u_\varepsilon - u_0)w. \end{aligned}$$

Moreover, being $3u_0^2(u_\varepsilon - u_0) = u_\varepsilon^3 - u_0^3 - 3u_0(u_\varepsilon - u_0)^2 - (u_\varepsilon - u_0)^3$,

$$\begin{aligned} \int_{\partial\Omega} (u_\varepsilon - u_0)g &= - \int_{\Omega} (k_\varepsilon - k_0)\nabla u_\varepsilon \cdot \nabla w + \int_{\Omega} k_\varepsilon \nabla u_\varepsilon \cdot \nabla w - \int_{\Omega} k_0 \nabla u_0 \cdot \nabla w \\ &\quad + \int_{\Omega} (1 - \chi_0)(u_\varepsilon^3 - u_0^3)w - \int_{\Omega} (1 - \chi_0)3u_0(u_\varepsilon - u_0)^2w - \int_{\Omega} (1 - \chi_0)(u_\varepsilon - u_0)^3w. \end{aligned}$$

Thanks to estimate 4.4 and 4.2, we can assess that

$$\begin{aligned} \int_{\Omega} (1 - \chi_0)3u_0(u_\varepsilon - u_0)^2w &\leq 3\|u_0\|_{L^\infty(\Omega)}\|w\|_{L^\infty(\Omega)}\|u_\varepsilon - u_0\|_{L^2(\Omega)}^2 = O(\varepsilon^{1+2\eta}) = o(\varepsilon) \\ \int_{\Omega} (1 - \chi_0)(u_\varepsilon - u_0)^3w &\leq \|(u_\varepsilon - u_0)^3\|_{L^p(\Omega)}\|w\|_{L^{p'}(\Omega)} \leq C\|u_\varepsilon - u_0\|_{L^{3p}(\Omega)}^3 \\ &\leq C\|u_\varepsilon - u_0\|_{H^1(\Omega)}^3 = O(\varepsilon^{\frac{3}{2}}) = o(\varepsilon). \end{aligned}$$

Exploiting the expression of the state equation,

$$\int_{\Omega} k_\varepsilon \nabla u_\varepsilon \cdot \nabla w + \int_{\Omega} (1 - \chi_\varepsilon)u_\varepsilon^3 = \int_{\Omega} fw = \int_{\Omega} k_0 \nabla u_0 \cdot \nabla w + \int_{\Omega} (1 - \chi_0)u_0^3.$$

Hence, we obtain:

$$\int_{\partial\Omega} (u_\varepsilon - u_0)g = - \int_{\Omega} (k_\varepsilon - k_0)\nabla u_\varepsilon \cdot \nabla w + \int_{\Omega} (\chi_\varepsilon - \chi_0)(u_\varepsilon^3)w + o(\varepsilon). \quad (4.23)$$

In order to analyze the right hand side of (4.23), we follow the strategy described in [10]. Since $(k_\varepsilon - k_0) = (k - 1)\chi_{\varepsilon \setminus 0} + (1 - k)\chi_{0 \setminus \varepsilon}$, we have:

$$\int_{\Omega} (k_\varepsilon - k_0)\nabla u_\varepsilon \cdot \nabla w = \int_{\varepsilon \setminus 0} (k - 1)\nabla u_\varepsilon^i \cdot \nabla w^e + \int_{0 \setminus \varepsilon} (1 - k)\nabla u_\varepsilon^e \cdot \nabla w^i. \quad (4.24)$$

Consider the first term in (4.24): recalling $\partial\omega_0^+ = \partial\omega_0 \cap \{h > 0\}$

$$\begin{aligned} &\int_{\varepsilon \setminus 0} (k - 1)\nabla u_\varepsilon^i \cdot \nabla w^e = \\ &\text{(via Lemma 4.1)} = \int_0^\varepsilon \int_{\partial\omega_0^+} (k - 1)h \nabla u_\varepsilon^i(x_\varepsilon) \cdot \nabla w^e(x_\varepsilon) + O(\varepsilon^{1+2\alpha}) \\ &\quad \text{(via (4.3))} = \int_0^\varepsilon \int_{\partial\omega_0^+} (k - 1)h \left[\nabla_\tau u_\varepsilon^e(x_\varepsilon) \cdot \nabla_\tau w^e(x_\varepsilon) + \frac{1}{k} \nabla_\nu u_\varepsilon^e(x_\varepsilon) \cdot \nabla_\nu w^e(x_\varepsilon) \right] + o(\varepsilon) \\ &\text{(via Lemma 4.5)} = \int_0^\varepsilon \int_{\partial\omega_0^+} (k - 1)h \left[\nabla_\tau u_0^e(x_\varepsilon) \cdot \nabla_\tau w^e(x_\varepsilon) + \frac{1}{k} \nabla_\nu u_0^e(x_\varepsilon) \cdot \nabla_\nu w^e(x_\varepsilon) \right] + O(\varepsilon^{1+\frac{2\alpha}{2\alpha+2}}) \\ &\text{(via Lemma 4.1)} = \varepsilon \int_{\partial\omega_0^+} (k - 1)h \left[\nabla_\tau u_0^e(x) \cdot \nabla_\tau w^e(x) + \frac{1}{k} \nabla_\nu u_0^e(x) \cdot \nabla_\nu w^e(x) \right] + o(\varepsilon). \end{aligned}$$

Through the same computation, one may obtain, for the second term in (4.24):

$$\int_{0 \setminus \varepsilon} (1 - k)\nabla u_\varepsilon^e \cdot \nabla w^i = - \int_0^\varepsilon \int_{\partial\omega_0^-} (1 - k)h \left[\nabla_\tau u_0^e(x) \cdot \nabla_\tau w^e(x) + \frac{1}{k} \nabla_\nu u_0^e(x) \cdot \nabla_\nu w^e(x) \right] + o(\varepsilon),$$

where $\partial\omega_0^- = \partial\omega_0 \cap \{h < 0\}$, on which it holds that $|h| = -h$. Hence, it holds

$$\begin{aligned} \int_{\Omega} (k_{\varepsilon} - k_0) \nabla u_{\varepsilon} \cdot \nabla w &= \varepsilon \int_{\partial\omega_0^+} (k-1)h \left[\nabla_{\tau} u_0^e(x) \cdot \nabla_{\tau} w^e(x) + \frac{1}{k} \nabla_{\nu} u_0^e(x) \cdot \nabla_{\nu} w^e(x) \right] \\ &\quad - \varepsilon \int_{\partial\omega_0^-} (1-k)h \left[\nabla_{\tau} u_0^e(x) \cdot \nabla_{\tau} w^e(x) + \frac{1}{k} \nabla_{\nu} u_0^e(x) \cdot \nabla_{\nu} w^e(x) \right] + o(\varepsilon) \\ &= -\varepsilon \int_{\partial\omega_0} (1-k)h \left[\nabla_{\tau} u_0^e(x) \cdot \nabla_{\tau} w^e(x) + \frac{1}{k} \nabla_{\nu} u_0^e(x) \cdot \nabla_{\nu} w^e(x) \right] + o(\varepsilon). \end{aligned} \quad (4.25)$$

Next, we have to prove a similar result for the second term in the right hand side of (4.23). By an analogous procedure, we consider:

$$\int_{\Omega} (\chi_{\varepsilon} - \chi_0) u_{\varepsilon}^3 w = \int_{\varepsilon \setminus 0} u_{\varepsilon}^3 w - \int_{0 \setminus \varepsilon} u_{\varepsilon}^3 w. \quad (4.26)$$

The first term in (4.26) can be rewritten as:

$$\begin{aligned} \int_{\varepsilon \setminus 0} u_{\varepsilon}^3 w &= \\ (\text{through Lemma 4.1})^* &= \int_0^{\varepsilon} \int_{\partial\omega_0^+} u_{\varepsilon}^3(x_{\varepsilon}) w(x_{\varepsilon}) h + O(\varepsilon^2) \\ (\text{using Lemma 4.5}) &= \int_0^{\varepsilon} \int_{\partial\omega_0^+} u_0^3(x_{\varepsilon}) w(x_{\varepsilon}) h + O(\varepsilon^{\frac{3}{2}}) \\ (\text{again via Lemma 4.1}) &= \varepsilon \int_{\partial\omega_0^+} u_0^3(x) w(x) h + o(\varepsilon). \end{aligned}$$

With the same argument we can find a similar expression for the second term in (4.26), where $|h| = -h$. Thus, from (4.26) we recover the expression:

$$\int_{\Omega} (\chi_{\varepsilon} - \chi_0) u_{\varepsilon}^3 w = \varepsilon \int_{\partial\omega_0} u_0^3(x) w(x) h + o(\varepsilon). \quad (4.27)$$

Substituting the expressions (4.25) and (4.27) in (4.23) we obtain the thesis. \square

Remark 4.1. The first term of the asymptotic expansion in the right-hand side of (4.21) can be rewritten as

$$\int_{\partial\omega_0} \{(1-k)M(y) \nabla u_0^e(y) \cdot \nabla w^e(y) + u_0(y)^3 w(y)\} h(y) d\sigma(y),$$

where for each $y \in \partial\omega_0$ $M(y)$ is a symmetric positive definite matrix with eigenvalues 1 and $\frac{1}{k}$ associated respectively to eigenvectors $\tau(y)$ and $\nu(y)$, the tangent and outward normal unit vectors of $\partial\omega_0$ in y . This formula reveals several similarity to the one derived in Chapter 2 for the perturbation of the boundary voltage when a small inclusion is inserted.

As a corollary of 4.1, we get the following estimate:

Lemma 4.6.

$$\|u_{\varepsilon} - u_0\|_{L^2(\Omega)}^2 = o(\varepsilon) \quad (4.28)$$

*One should consider that $u_{\varepsilon}(x_t) \leq u_{\varepsilon}(x_{\varepsilon}) + C\varepsilon \Rightarrow u_{\varepsilon}^3(x_t) \leq u_{\varepsilon}^3(x_{\varepsilon}) + O(\varepsilon)$

Proof. Let W_ε be the solution of

$$\begin{cases} -\operatorname{div}(k_0(x)\nabla W_\varepsilon) + 3\chi_{\Omega \setminus \omega_0} u_0^2 W_\varepsilon = 0 & \text{in } \Omega \\ \partial_\nu W_\varepsilon = u_\varepsilon - u_0 & \text{on } \partial\Omega. \end{cases} \quad (4.29)$$

Hence, in $\Omega \setminus \overline{\omega_0}$, W_ε satisfies

$$-\Delta W_\varepsilon + 3u_0^2 W_\varepsilon = 0,$$

whereas $\mu = \nabla W_\varepsilon$ satisfies

$$-\Delta \mu + 3u_0^2 \mu = -6W_\varepsilon u_0 \nabla u_0.$$

In both cases, it is possible to use the interior regularity estimates as in the proof of Lemma 4.5 (see [82], Theorem 8.17): being $d > 0$ and $\Omega^d = \{x \in \Omega \text{ s.t. } \operatorname{dist}(x, \partial(\Omega \setminus \overline{\omega_0})) > d\}$ then

$$\begin{aligned} \|W_\varepsilon\|_{L^\infty(\Omega^d)} &\leq Cd^{-1} \|W_\varepsilon\|_{L^2(\Omega)} \\ \|\nabla W_\varepsilon\|_{L^\infty(\Omega^d)} &\leq Cd^{-1} (\|\nabla W_\varepsilon\|_{L^2(\Omega)} + \|6u_0 W_\varepsilon \nabla u_0\|_{L^2(\Omega)}) \leq Cd^{-1} \|W_\varepsilon\|_{H^1(\Omega)}. \end{aligned}$$

Since W_ε is the solution of (4.29), it holds that

$$\|W_\varepsilon\|_{H^1(\Omega)} \leq \frac{1}{k} \|u_\varepsilon - u_0\|_{L^2(\partial\Omega)} \leq C \|u_\varepsilon - u_0\|_{H^1(\Omega)} \leq C\varepsilon^{\frac{1}{2}};$$

hence, $\|W_\varepsilon\|_{L^\infty(\Omega^d)}, \|\nabla W_\varepsilon\|_{L^\infty(\Omega^d)} \leq Cd^{-1} \varepsilon^{\frac{1}{2}} \forall d > 0$. Moreover, exploiting Li-Nirenberg regularity estimates (see [101], Theorem 1.1), we have (for every $\delta > 0$, being $\Omega_\delta = \{x \in \Omega \text{ s.t. } \operatorname{dist}(x, \partial\Omega) > \delta\}$)

$$\|W_\varepsilon\|_{C^{1+\alpha}(\Omega_\delta \setminus \omega_0)} \leq C.$$

Thus, chosen $\delta = d$ and defined, for each $y \in \partial\omega_0$, $y_d = \arg \min \operatorname{dist}(y, \Omega_d)$,

$$\begin{aligned} |W_\varepsilon(y)| &\leq |W_\varepsilon(y_d)| + Cd \quad (\text{thanks to Lipschitz-continuity of } W_\varepsilon) \\ &\leq Cd^{-1} \varepsilon^{\frac{1}{2}} + Cd \end{aligned}$$

and, chosen $d = \varepsilon^{\frac{1}{4}}$, one obtains $\|W_\varepsilon\|_{L^\infty(\partial\omega_0)} \leq C\varepsilon^{\frac{1}{4}}$. Instead, by the Hölder-continuity of ∇W_ε ,

$$|W_\varepsilon^e(y)| \leq |\nabla W_\varepsilon(y_d)| + Cd^\alpha \leq Cd^{-1} \varepsilon^{\frac{1}{2}} + Cd^\alpha,$$

and chosen $d = \varepsilon^{\frac{1}{2(\alpha+1)}}$, one obtains $\|\nabla W_\varepsilon^e\|_{L^\infty(\partial\omega_0)} \leq C\varepsilon^{\frac{\alpha}{2(\alpha+1)}}$. Hence, exploiting Proposition 4.1,

$$\begin{aligned} \|u_\varepsilon - u_0\|_{L^2(\partial\Omega)}^2 &= \int_{\partial\Omega} (u_\varepsilon - u_0)(u_\varepsilon - u_0) \\ &= \varepsilon \int_{\partial\omega_0} \left\{ (1-k)[\nabla_\tau u_0^e \cdot \nabla_\tau W_\varepsilon^e + \frac{1}{k} \nabla_\nu u_0^e \cdot \nabla_\nu W_\varepsilon^e] + u_0^3 W_\varepsilon \right\} h + o(\varepsilon) \\ &= \varepsilon (C\varepsilon^{\frac{\alpha}{2(\alpha+1)}}) \tilde{C} + o(\varepsilon) \quad (\text{with } \tilde{C} = \tilde{C}(\|h\|_{C(\partial\omega_0)}, \|u_0\|_{C^{1+\alpha}(\Omega_d \setminus \omega_0)}, |\partial\omega_0|)). \end{aligned}$$

□

4.2 A shape-derivative based reconstruction algorithm

In this section we describe how the results previously outlined can be employed in order to formulate a reconstruction algorithm for the inverse problem based on techniques from shape optimization. We start introducing the following cost functional associated with the reconstruction problem:

$$J(\Omega_\varepsilon) = \int_{\partial\Omega} (u_\varepsilon - u_{meas})^2, \quad (4.30)$$

where u_ε is the solution of problem (4.1) with inclusion ω_ε . We thus consider the constraint optimization problem of finding the minimum of the functional J among the possible deformations of the initial guess ω_0 . We remark that, although all the computations are performed on the initial guess ω_0 and on its perturbations ω_ε , they can be easily replicated on a general domain ω of class C^2 , whose boundary is perturbed as in (4.2).

We attain an iterative method for the solution of the optimization problem, which relies on the definition of the *shape derivative* of the functional J , defined as:

$$DJ(\Omega_0)[h] = \lim_{\varepsilon \rightarrow 0} \frac{J(\Omega_\varepsilon) - J(\Omega_0)}{\varepsilon}. \quad (4.31)$$

We define the *shape gradient* as the function $\nabla_S J(\Omega_0)$ which allows to write:

$$DJ(\Omega_0)[h] = \int_{\partial\omega_0} \nabla_S J(\Omega_0) h \quad \forall h \in C^2(\partial\omega_0; \mathbb{R}). \quad (4.32)$$

The computation of the shape gradient $\nabla_S J$ allows to perform an approximated reconstruction of the position, size and shape of the inclusion through an iterative algorithm which will be described in the sequel.

4.2.1 Representation formula for the shape gradient

Taking advantage of Proposition 4.1, we derive a representation formula for the shape gradient, which allows to easily compute it, circumventing the fact that definition (4.32) is not constructive.

Proposition 4.2. *The following representation formula holds for the shape gradient of J evaluated in Ω_0 :*

$$\nabla_S J(\Omega_0) = (1 - k)[\nabla_\tau u_0^e \cdot \nabla_\tau W^e + \frac{1}{k} \nabla_\nu u_0^e \cdot \nabla_\nu W^e] + u_0^3 W \quad (4.33)$$

being W the solution of the adjoint problem:

$$\begin{cases} -\operatorname{div}(k_0(x)\nabla W) + \chi_{\Omega \setminus \omega_0} u_0^2 W = 0 & \text{in } \Omega \\ \partial_\nu W = u_0 - u_{meas} & \text{on } \partial\Omega. \end{cases} \quad (4.34)$$

Proof of Proposition 4.2. It holds that:

$$\begin{aligned} J(\Omega_\varepsilon) - J(\Omega_0) &= \frac{1}{2} \|u_\varepsilon - u_{meas}\|_{L^2(\partial\Omega)}^2 - \|u_0 - u_{meas}\|_{L^2(\partial\Omega)}^2 \\ &= \frac{1}{2} \|u_\varepsilon\|_{L^2(\partial\Omega)}^2 - \int_{\partial\Omega} u_\varepsilon u_{meas} - \frac{1}{2} \|u_0\|_{L^2(\partial\Omega)}^2 + \int_{\partial\Omega} u_0 u_{meas} \\ &= \frac{1}{2} \|u_\varepsilon - u_0\|_{L^2(\partial\Omega)}^2 - \|u_0\|_{L^2(\partial\Omega)}^2 + \int_{\partial\Omega} u_\varepsilon u_0 - \int_{\partial\Omega} u_\varepsilon u_{meas} + \int_{\partial\Omega} u_0 u_{meas} \\ &= \frac{1}{2} \|u_\varepsilon - u_0\|_{L^2(\partial\Omega)}^2 + \int_{\partial\Omega} (u_\varepsilon - u_0)(u_0 - u_{meas}). \end{aligned}$$

The first term of the last summation, thanks to Lemma 4.6, is $o(\varepsilon)$, whereas the second term can be described through formula (4.21) with $g = (u_0 - u_{meas})$, which leads to the definition of the adjoint problem as in (4.34) and ultimately entails the thesis. \square

Remark 4.2. As it will be outlined in Chapter 5, the minimization problem associated to (4.30) shows severe stability issues; namely, small perturbations in the boundary data u_{meas} might imply large deviations in the associated solutions ω . This can be avoided by adding a regularization term to the functional, penalizing the perimeter of the inclusion to be identified. For a fixed parameter $\lambda > 0$, the expression of the regularized cost functional is the following one:

$$J_{reg}(\Omega_\varepsilon) = \int_{\partial\Omega} (u_\varepsilon - u_{meas})^2 + \lambda |\partial\omega_\varepsilon|. \quad (4.35)$$

Under the assumption that the boundary of the inclusion is of class C^2 , it is possible to obtain a representation formula analogous to the one in (4.33), taking into account the penalization term:

$$\nabla_S J_{reg}(\Omega_0) = (1 - k) \left(\nabla_\tau u_0^e \cdot \nabla_\tau W^e + \frac{1}{k} \nabla_\nu u_0^e \cdot \nabla_\nu W^e \right) + u_0^3 W + \lambda \mathcal{H}, \quad (4.36)$$

where \mathcal{H} is the curvature of the boundary $\partial\omega_0$. A detailed proof can be found in Section 9.4.3 in [67].

4.2.2 Algorithm formulation and implementation

Exploiting the representation formula for the shape gradient, it is possible to devise an algorithm which allows to find a critical point of the cost functional. We focus in particular to the minimization of J_{reg} with a fixed regularization parameter $\lambda > 0$. Inspired by the concept of minimizing movements introduced by De Giorgi in [65], we aim at modifying the initial guess of the inclusion according to the a gradient flow, driven by the expression of the shape gradient. In particular, we define a sequence of inclusions $\{\omega_k\}$ obtained as follows: fix an initial ω_0 s.t. $\partial\omega_0$ is of class C^2 and, for $k \geq 0$, take

$$\begin{aligned} h_k &= -\nabla_S J_{reg}(\Omega_k); \\ \partial\omega_{k+1} &= \{y + \tau_k h_k(y) \nu_k(y), y \in \partial\omega_k\}. \end{aligned} \quad (4.37)$$

We define a *local descent direction* for the functional J_{reg} in a configuration Ω_k each scalar field $h : \partial\omega_k \rightarrow \mathbb{R}$ such that $DJ_{reg}(\Omega_k)[h] \leq 0$: thence, we easily verify that $-\nabla_S J_{reg}(\Omega_k)$ is a descent direction. Indeed, inserting $h = -\nabla_S J_{reg}(\Omega_k)$ in the expression of the shape differential of J_{reg} , computed in Ω_k (which is analogous to the one for J in Ω_0 reported in (4.32)), we get:

$$DJ_{reg}(\Omega_k)[-\nabla_S J_{reg}(\Omega_k)] = \int_{\partial\omega_k} -|\nabla_S J_{reg}(\Omega_k)|^2 \leq 0.$$

Since we only prescribe that the first-order variation of the cost functional is non-positive, such a descent direction is only local: by continuity of the functional we can ensure that there exists a positive τ_k such that $\forall \tau \geq \tau_k$, defining Ω_{k+1} as in (4.37), then $J_{reg}(\Omega_{k+1}) \leq J_{reg}(\Omega_k)$. The following

backtracking strategy allows to find a suitable value for τ_k :

Data: Inclusion Ω_k , descent direction h_k , reference step $\bar{\tau}$
Result: Ω_{k+1} such that $J_{reg}(\Omega_{k+1}) \leq J_{reg}(\Omega_k)$; u_{k+1} associated to Ω_{k+1}
 Set $\tau_k = \bar{\alpha}$; $J_{reg}(\Omega_*) = +\infty$;
while $J_{reg}(\Omega_*) > J(\Omega_k)$ **do**
 Reduce the step $\tau_k = \tau_k/2$;
 Perturb $\partial\omega_* = \{y + \tau_k h_k(y) \nu_k(y), y \in \partial\omega_k\}$;
 Compute u_* solving (4.1) with $\omega = \omega_*$;
end
 Set $\Omega_{k+1} = \Omega_*$.

Algorithm 5: Backtracking strategy

This finally allows to write a complete algorithm for the search of a critical point of the functional J_{reg} :

Data: Initial guess for the inclusion ω_0 , measured boundary data u_{meas}
Result: $\bar{\Omega}$, the limit of the discrete gradient flow
 Set $k = 0$; $convergence_criterion = +\infty$;
 Compute u_0 solving the direct problem (4.1) with $\omega = \omega_0$;
while $convergence_criterion \geq tolerance$ **do**
 Compute W_k solving (4.34) with $\omega = \omega_k$;
 Select a local descent direction h^k as $h_k = -\nabla_S J_{reg}(\Omega_k)$, using (4.36) ;
 Backtracking (see Algorithm 5): obtain Ω_{k+1} and u_{k+1} ;
end
 Set $\bar{\Omega} = \Omega_{k+1}$.

Algorithm 6: Descent algorithm

4.2.3 Numerical results

When implementing Algorithm 6, we resort to a Finite Element scheme for the solution both of the direct and the adjoint problems, see Chapter 2. In particular, in order to accurately capture the discontinuous behavior of the gradient across the interface $\partial\omega_k$, we aim to include a finite set of points discretizing the boundary $\partial\omega_k$ within the vertices of the mesh. This entails some implementation issues for Algorithm 6: in particular, when computing an updated version of the inclusion ω_{k+1} , we need to ensure that also the new boundary can be approximated by means of a suitable number of vertices of the mesh. The strategy we adopt in order to overcome this difficulty is to create a new mesh at each iteration, considering $\partial\omega_{k+1}$ as an inner boundary.

In this Section, we report some results of the application of the algorithm based on the shape derivative. In all the simulations reported, the initial guess is a disc centered in the origin with radius 0.2. As in the case of Chapter 2, we take advantage of $N_f = 2$ measurements, associated to the source terms $f_1(x, y) = x$ and $f_2(x, y) = y$. The iterative algorithm stops when the following criterion is fulfilled:

$$\|\chi_{\omega_{k+1}} - \chi_{\omega_k}\|_{L^1(\Omega)} = |\omega_{k+1} \Delta \omega_k| \leq tol.$$

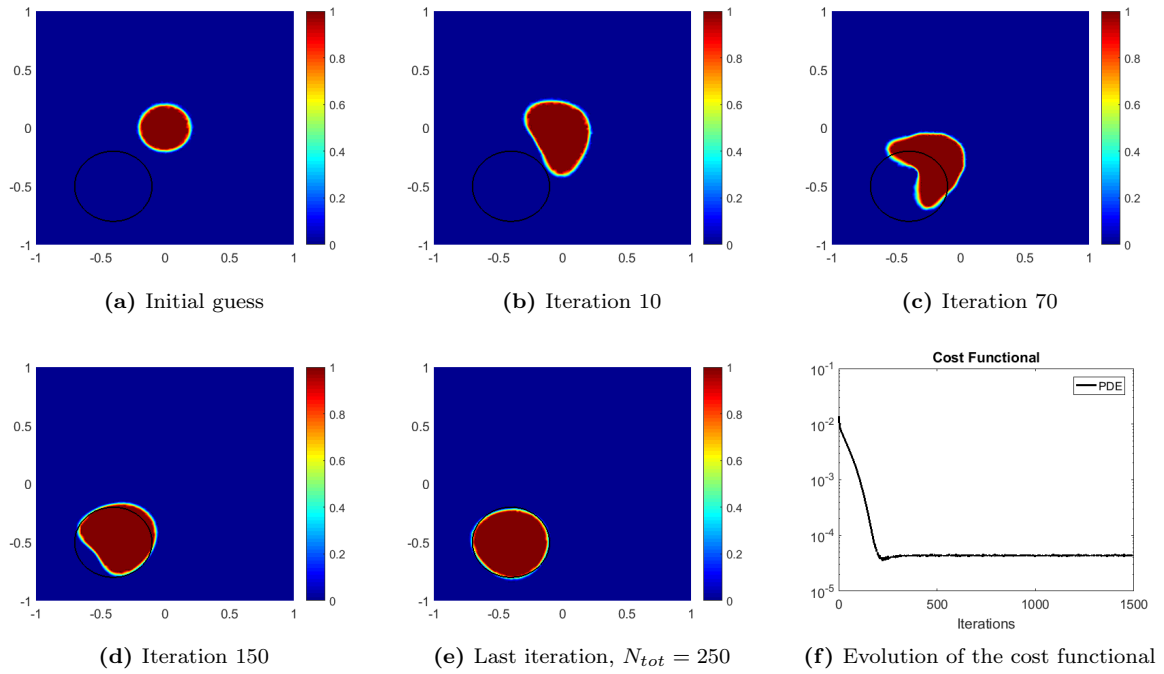
The main parameters of this set of simulations are reported in Table 4.1

In Figure 4.1 and 4.2 we show the quality of the reconstruction with the shape gradient algorithm both in the case of a circular and an elliptical inclusion. The boundary of the exact shape is outlined

λ	$\bar{\tau}$	tol
10^{-3}	10^{-3}	10^{-6}

Table 4.1: Values of the main parameters

in black, whereas in order to illustrate the inclusions ω_k in selected iterations we report the contour plot of their indicator functions.

**Figure 4.1:** Shape gradient algorithm: result comparison

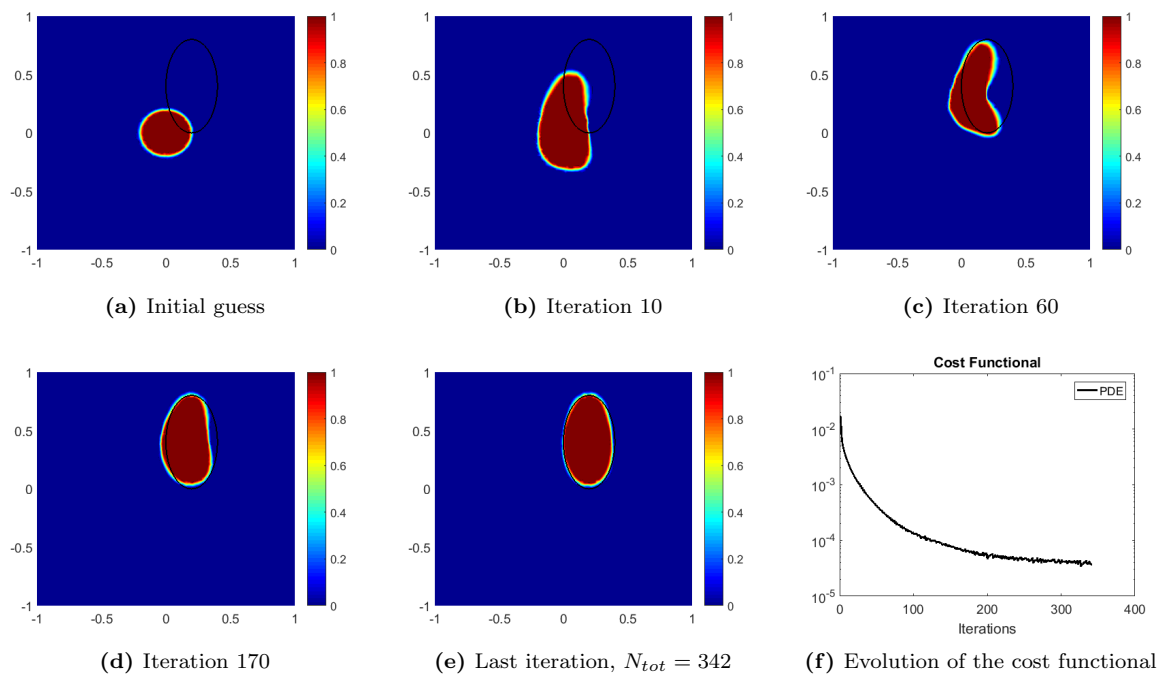


Figure 4.2: Shape gradient algorithm: result comparison

Chapter 5

A phase-field approach for the identification of arbitrary inclusions in a semilinear elliptic boundary value problem

This chapter is devoted to the analysis of the same inverse problem as the one introduced in Chapter 2, although in a more general framework and with different purposes. We briefly report the boundary value problem which is the object of study, which is set in $\Omega \subset \mathbb{R}^2$

$$\begin{cases} -\operatorname{div}(k_\omega \nabla u) + \chi_{\Omega \setminus \omega} u^3 = f & \text{in } \Omega \\ k_\omega \nabla u \cdot \nu = 0 & \text{on } \partial\Omega, \end{cases} \quad (5.1)$$

where $\chi_{\Omega \setminus \omega}$ is the indicator function of $\Omega \setminus \omega$ and

$$k_\omega(x) = \begin{cases} k & \text{if } x \in \omega \\ 1 & \text{if } x \in \Omega \setminus \omega, \end{cases}$$

being $0 < k < 1$ and $f \in L^2(\Omega)$. The homogeneous Neumann problem (5.1) consists of a semilinear diffusion-reaction equation with discontinuous coefficients across the interface of an inclusion $\omega \subset \Omega$, in which the conducting properties are different from the background medium. The value of the coefficient k is supposed to be known. We refer to the determination of the solution u from the knowledge of the inclusion ω as the *direct problem*; whereas the *inverse problem* consists in determining the inclusion associated to the measurements u_{meas} on the boundary of Ω . More precisely, given the measured data u_{meas} on the boundary, we search for $\omega \subset \Omega$ such that the corresponding solution u of (5.1) satisfies

$$u|_{\partial\Omega} = u_{meas}. \quad (5.2)$$

In Chapter 2 we tackled the same problem by introducing a strong *regularization hypothesis*, namely that the size of ω is significantly smaller than the size of the domain Ω . Although this assumption

allowed to obtain both theoretical results and an effective reconstruction algorithm, motivated by the biological application, we now aim at removing the hypothesis of small size and investigate the problem of reconstructing arbitrarily large inclusions ω . In Chapter 4, we already developed a rigorous analysis for the case in which the small-size assumption is removed, but the shape-gradient based strategy proposed there is only capable of reconstructing inclusions ω which consists in a smooth deformation of an original shape ω_0 . Thence, some *a priori* knowledge is still required regarding the topology and the regularity of the inclusion to be identified. Conversely, throughout this chapter, we assume a different approach, which allows to tackle the inverse problem (5.2) with minimal assumptions on ω .

In order to give a sense of the theoretical and numerical issues related to this approach, it is useful to recall the results which can be achieved in the context of the *inverse conductivity problem*, or *Calderón problem*, as in Section 1.3. When dealing with the reconstruction of a piecewise constant coefficient, from [71], [92], [6] and references therein we know that infinitely measurements are needed to ensure the uniqueness of the solution, as well as its (Lipschitz) dependence from the boundary data. A finite number of measurements is sufficient to determine uniquely and with Lipschitz stability the inclusion only introducing additional information either on the shape of the inclusion or on its size.

Several reconstruction algorithms have been developed for the solution of the inverse conductivity problem, and it is beyond the purposes of this introduction to provide an exhaustive overview of the topic. When dealing with the reconstruction of arbitrary inclusions in the linear case, several variational algorithms are available. A shape-optimization approach, with suitable regularization, is explored in [97] [87], [2] and [10]; in [88] this approach is coupled with topology optimization; whereas the level set technique has been applied in [128] and in [44]. Recently, several specific schemes have been employed to deal with the minimization of misfit functional endowed with a Total-Variation regularization: along this line, we mention the Levenberg-Marquardt and Landweber algorithms in [22], the augmented Lagrangian approach in [55] and the regularized level set technique in [53]. Finally, the phase field approach has been explored for the linear inverse conductivity problem e.g. in [124] and recently in [66].

Concerning inverse problems related to nonlinear PDEs, only a few theoretical results and numerical strategies are available, especially regarding the electrophysiological problem of interest. We remark that the level-set method has been implemented for the reconstruction of extended inclusions in the nonlinear problem of cardiac electrophysiology (see [112] and [54]), by evaluating the sensitivity of the cost functional with respect to a selected set of parameters involved in the full discretization of the shape of the inclusion.

In this chapter, we propose a rigorous reconstruction algorithm of inclusions of *arbitrary* shape and position by relying on the minimization of a suitable functional, enhanced with a perimeter penalization term, and by following a relaxation strategy relying on the phase field approach. The outline of the chapter is as follows: in Section 5.1 we recall some results regarding the direct problem, extending them (when necessary) to the case of large inclusions in consideration. In Section 5.2 we introduce an optimization problem related to the inverse problem and analyze the issue of stability, concluding for the necessity to introduce a suitable regularization term. Section 5.3 is devoted to the phase-field relaxation, discussing its well-posedness, the Γ -convergence of the relaxed

functional to the original one, and the derivation of necessary optimality conditions. In Section 5.4 we propose an iterative reconstruction algorithm allowing for the numerical approximation of the solution and prove its convergence properties. The power of this approach is twofold: on the one hand, it allows to consider conductivity inclusions of arbitrary shape and position which is the case of interest for our application and, on the other, it leads to good reconstructions as shown in the numerical experiments in Section 5.5. Finally, the last two Sections are devoted to the comparison between the proposed approach and to two different techniques which can be considered as alternative approaches. In particular, in Section 5.6 we compare our technique to the shape optimization based approach introduced in Chapter 4: after showing that the optimality conditions derived for the relaxed problem converge to the ones corresponding to the sharp interface case, we show numerical results obtained by applying both the algorithms on the same benchmark cases. In Section 5.7, instead, a Lagrangian approach is considered for the optimization problem introduced in Section 5.2, yielding the introduction of a correlated saddle-point problem which can be tackled with an Uzawa-type algorithm: a formal expression of such algorithm is reported, and we compare its effectiveness with the phase-field relaxation strategy.

5.1 Direct problem analysis

In this Section, the analysis of the well-posedness of the direct problem is reported in details, and consists in an extension of the results previously obtained in [30]. We formulate the boundary value problem (5.1) in terms of the indicator function of the inclusion, $\chi = \chi_\omega$. We assume a minimal *a priori* hypothesis on the inclusion, namely that it is a subset of Ω of finite perimeter: χ belongs to $BV(\Omega) = \{v \in L^1(\Omega) : TV(v) < \infty\}$, being

$$TV(v) = \sup \left\{ \int_{\Omega} v \operatorname{div}(\phi); \quad \phi \in C_0^1(\Omega; \mathbb{R}^2), \|\phi\|_{L^\infty} \leq 1 \right\},$$

endowed with the norm $\|\cdot\|_{BV} = \|\cdot\|_{L^1} + TV(\cdot)$. Moreover, we formulate particular restrictions on the inclusion and on the source f .

Assumption 2. Given a positive number d_0 we assume that

$$\chi \in X_{0,1} = \{\chi \in BV(\Omega) : \chi(x) \in \{0, 1\} \text{ a.e. in } \Omega, \chi = 0 \text{ a.e. in } \Omega^{d_0}\}, \quad (5.3)$$

where $\Omega^{d_0} = \{x \text{ s.t. } \operatorname{dist}(x, \partial\Omega) \leq d_0\}$.

This also entails that the inclusion is well separated from the boundary $\partial\Omega$. Moreover,

Assumption 3. Given a positive constant m , we require

$$f \geq m \quad \text{a.e. in } \Omega. \quad (5.4)$$

The weak formulation of the direct problem (5.1) in terms of χ reads: find u in $H^1(\Omega)$ s.t., $\forall \varphi \in H^1(\Omega)$,

$$\int_{\Omega} a(\chi) \nabla u \nabla \varphi + \int_{\Omega} b(\chi) u^3 \varphi = \int_{\Omega} f \varphi, \quad (5.5)$$

being $a(\chi) = 1 - (1 - k)\chi$ and $b(\chi) = 1 - \chi$. Define $S : X_{0,1} \rightarrow H^1(\Omega)$ the *solution map*: for all $\chi \in X_{0,1}$, $S(\chi) = u$ is the solution to problem (5.5) with indicator function χ .

Recall the generalized Poincaré inequality:

Lemma 5.1. $\exists C > 0, C = C(\Omega, d_0)$ s.t., $\forall w \in H^1(\Omega)$,

$$\|w\|_{H^1(\Omega)}^2 \leq C \left(\|\nabla w\|_{L^2(\Omega)}^2 + \|w\|_{L^2(\Omega^{d_0})}^2 \right). \quad (5.6)$$

The proof of the Lemma 5.1 is given in the Appendix of [30] and follows by Theorem 8.11 in [102].

Thanks to Lemma 5.1, we can prove the following well-posedness result for the direct problem.

Proposition 5.1. *Consider $f \in (H^1(\Omega))^*$ and a function $\chi \in X_{0,1}$. Then there exists an unique solution $S(\chi) \in H^1(\Omega)$ of*

$$\int_{\Omega} a(\chi) \nabla S(\chi) \cdot \nabla v + \int_{\Omega} b(\chi) S(\chi)^3 v = \int_{\Omega} f v \quad \forall v \in H^1(\Omega),$$

where $a(\chi) = 1 - (1 - k)\chi$ and $b(\chi) = 1 - \chi$.

Proof. The proof is analogous to the analysis performed in [30, Theorem 4.1], but generalizes that result to the case of inclusions of finite perimeter. The strategy consists in applying the Minty-Browder theorem on the direct operator $T : H^1(\Omega) \rightarrow (H^1(\Omega))^*$ s.t.

$$\langle T(S), v \rangle_* = \int_{\Omega} a(\chi) \nabla S \cdot \nabla v + \int_{\Omega} b(\chi) S^3 v,$$

which shows to be continuous, coercive and strictly monotone. In particular

- Local Lipschitz continuity:

$$\begin{aligned} |\langle T(S) - T(S_0), v \rangle_*| &= \left| \int_{\Omega} a(\chi) \nabla(S - S_0) \cdot \nabla v + \int_{\Omega} b(\chi)(S - S_0) q v \right| \\ &\leq \|\nabla(S - S_0)\|_{L^2} \|\nabla v\|_{L^2} + \|S - S_0\|_{L^6} \|q\|_{L^3} \|v\|_{L^2}, \end{aligned}$$

(being $q = S^2 + SS_0 + S_0^2$). If S and S_0 belong to a bounded subset of $H^1(\Omega)$, then (thanks to the Sobolev Embedding of $H^1(\Omega)$ in $L^6(\Omega)$) we can assess that $\|q\|_{L^3} \leq M$ and moreover $\exists K = K(\chi) > 0$ s.t.

$$|\langle T(S) - T(S_0), v \rangle_*| \leq K \|S - S_0\|_{H^1} \|v\|_{H^1} \quad \forall v \in H^1(\Omega).$$

- Coercivity: we show that $\langle T(S), S \rangle_* \rightarrow +\infty$ as $\|S\|_{H^1(\Omega)} \rightarrow +\infty$. Since $\chi = 0$ a.e. in Ω^{d_0} , $b(\chi) \geq \chi_{\Omega^{d_0}}$, the indicator function of Ω^{d_0} . Then,

$$\begin{aligned} \langle T(S), S \rangle_* &\geq k \int_{\Omega} |\nabla S|^2 + \int_{\Omega^{d_0}} S^4 \geq k \|\nabla S\|_{L^2(\Omega)}^2 + \frac{1}{|\Omega|} \|S\|_{L^2(\Omega^{d_0})}^4 \\ &= k \left(\|\nabla S\|_{L^2(\Omega)}^2 + \|S\|_{L^2(\Omega^{d_0})}^2 \right) + R, \end{aligned}$$

where $R = \frac{1}{|\Omega|} \|S\|_{L^2(\Omega^{d_0})}^4 - k \|S\|_{L^2(\Omega^{d_0})}^2$ can be bounded by below independently of S : $R \geq -\frac{k^2 |\Omega|}{4}$. Together with Poincaré inequality in Lemma 5.1, we conclude that

$$\langle T(S), S \rangle_* \geq \frac{k}{C} \|S\|_{H^1(\Omega)}^2 - \frac{k^2 |\Omega|}{4}.$$

- (Strict) monotonicity: we claim that $\langle T(S) - T(R), S - R \rangle_* \geq 0$ and $\langle T(S) - T(R), S - R \rangle_* = 0 \Leftrightarrow S = R$. Indeed,

$$\langle T(S) - T(R), S - R \rangle_* \geq \int_{\Omega} k |\nabla(S - R)|^2 + \int_{\Omega^{d_0}} (S^2 + SR + R^2)(S - R)^2 \geq 0.$$

Moreover, since $S^2 + SR + R^2 \geq \frac{1}{4}(S - R)^2$,

$$\langle T(S) - T(R), S - R \rangle_* = 0 \Rightarrow \|\nabla(S - R)\|_{L^2(\Omega)} = 0 \text{ and } \int_{\Omega^{d_0}} (S - R)^4 = 0,$$

and from the latter equality it follows that $S = R$ a.e. in Ω^{d_0} , hence also $\|S - R\|_{L^2(\Omega^{d_0})} = 0$, and via Lemma 5.1 $\|S - R\|_{H^1(\Omega)} = 0$.

□

It is possible to prove additional properties of the solution $S(\chi)$ of the direct problem. In particular, we provide an uniform bound on $\|S(\chi)\|_{H^1(\Omega)}$ independent of χ .

Proposition 5.2. *There exists a constant $C = C(\Omega, d_0, k)$ s.t., $\forall \chi \in X_{0,1}$,*

$$\|S(\chi)\|_{H^1(\Omega)} \leq C \left(\|f\|_{L^2(\Omega)} + \|f\|_{L^2(\Omega)}^3 \right). \quad (5.7)$$

This can be proved as in [30, Proposition 4.1], where we take advantage of the bound

$$\|S(\chi)\|_{L^2(\Omega^{d_0})}^4 \leq |\Omega^{d_0}| \int_{\Omega^{d_0}} S(\chi)^4 \leq |\Omega| \int_{\Omega} b(\chi) S(\chi)^4,$$

and hence the constant appearing in (5.7) only depends on Ω , d_0 , k .

Moreover, we prove a Hölder regularity result on $S(\chi)$:

Proposition 5.3. *Let $S(\chi)$ be the solution of (5.5) associated to $\chi \in X_{0,1}$ and let $f \in L^2(\Omega)$. Then, $S(\chi) \in C^\alpha(\bar{\Omega})$ and*

$$\|S(\chi)\|_{C^\alpha(\bar{\Omega})} \leq C(\Omega, k, \|f\|_{L^2(\Omega)}, d_0).$$

Proof. The proof is analogous to the one in [30]. An application of [82, Theorem 8.24] ensures that

$$\forall \Omega' \subset\subset \Omega, \quad \|S(\chi)\|_{C^\alpha(\bar{\Omega}')} \leq C \left(\|S(\chi)\|_{L^2(\Omega)} + \|S(\chi)\|_{L^6(\Omega)}^3 + \|f\|_{L^2(\Omega)} \right) \leq C,$$

where $C = C(\bar{\Omega}', k, \|f\|_{L^2(\Omega)})$. By taking $\Omega' \supset \Omega^{d_0}$, since the conductivity is constant in Ω^{d_0} and the normal derivative on the boundary is zero, we can apply standard regularity results up to the boundary, obtaining:

$$\|S(\chi)\|_{C^\alpha(\bar{\Omega})} \leq C = C(\Omega, d_0, k, \|f\|_{L^2(\Omega)}).$$

□

Finally, we prove an estimate which occurs many times in the proof of various results.

Proposition 5.4. *Suppose that $f \in L^2(\Omega)$ s.t. $f \geq m > 0$ a.e. in Ω . Consider $S(\chi)$ the solution of problem (5.5) associated to $\chi \in X_{0,1}$. Then, $S(\chi) \geq m^{1/3}$.*

The proof is an immediate consequence of the following Lemma:

Lemma 5.2. *Let S_1 and S_2 be a sub- and supersolution of (5.5) with $\chi \in X_{0,1}$, namely $S_1, S_2 \in H^1(\Omega)$ s.t., $\forall \varphi \in H^1(\Omega)$, $\varphi \geq 0$ a.e., it holds:*

$$\int_{\Omega} a(\chi) \nabla S_1 \cdot \nabla \varphi + \int_{\Omega} b(\chi) S_1^3 \varphi - \int_{\Omega} f \varphi \leq 0, \quad (5.8)$$

$$\int_{\Omega} a(\chi) \nabla S_2 \cdot \nabla \varphi + \int_{\Omega} b(\chi) S_2^3 \varphi - \int_{\Omega} f \varphi \geq 0. \quad (5.9)$$

Then, $S_1 \leq S_2$ a.e. in Ω .

Proof. Subtract the equations (5.9) - (5.8) and define $W = S_2 - S_1$: it holds, $\forall \varphi \in H^1(\Omega)$, $\varphi \geq 0$ a.e.,

$$\int_{\Omega} a(\chi) \nabla W \cdot \nabla \varphi + \int_{\Omega} b(\chi) Q W \varphi \geq 0,$$

where $Q = (S_1^2 + S_1 S_2 + S_2^2) \geq 0$. Take $\varphi = W^-$, the negative part of W . We remark that $W^+ = \max\{0, W\}$, $W^- = \max\{0, -W\}$, $W = W^+ - W^-$; moreover $W^+, W^- \in H^1(\Omega)$, $W^+ W^- = 0$, and in view of [75, Theorem 4.4] we refer to ∇W^- as the gradient of the negative part W^- or equivalently as the vector of the negative parts of the components of ∇W . Thus, it holds

$$\int_{\Omega} a(\chi) \nabla W^- \cdot \nabla W^- + \int_{\Omega} b(\chi) Q (W^-)^2 \leq 0,$$

which implies that $S_2 \geq S_1$ a.e. Indeed, $k \|\nabla W^-\|_{L^2(\Omega)} \leq 0$ implies $\nabla W^- = 0$ a.e. in Ω ; moreover, both S_1 and S_2 are continuous, and hence also W and W^- , which entails $W^- = c$, $c \geq 0$ by definition. In order to guarantee that $W^- = \max\{0, -W\} = c$ is continuous, either $c = 0$ or $W = -c < 0$ in Ω . The latter case, though, would imply that $S_2 = S_1 - c$ and, by simple computation, $Q = 3S_1^2 - 3cS_1 + c^2 \geq \frac{c^2}{4}$, which is incompatible with $\int_{\Omega} b(\chi) Q (W^-)^2 \leq 0$. Hence $W^- = 0$, and so $W = W^+ \geq 0$. \square

Proof of Proposition 5.4. Taking $S_2 = S(\chi)$ and $S_1 = m^{1/3}$ (which is a subsolution since $b(\chi)m - f \leq 0$), we obtain the uniform bound $S(\chi) \geq m^{1/3}$. \square

Remark 5.1. We could extend all the previous results to a class of more general functions f , namely f not vanishing in Ω^{d_0} , but that would entail that the lower bound in Proposition 5.4 might depend on χ . On the other hand, when applying the previous estimates in the proofs of following results (in particular, Proposition 5.5, 5.14, 5.19 and Lemma 5.3), we always invoke Proposition 5.4 on a fixed indicator function χ .

Another crucial property satisfied by the solution map S is the continuity with respect to the L^1 norm, which requires an accurate treatment due to the nonlinearity of the direct problem.

Proposition 5.5. *Let $f \in L^2(\Omega)$ satisfy assumption (5.4). If $\{\chi_n\} \subset X_{0,1}$ s.t. $\chi_n \xrightarrow{L^1} \chi \in X_{0,1}$, then $S(\chi_n)|_{\partial\Omega} \xrightarrow{L^2(\partial\Omega)} S(\chi)|_{\partial\Omega}$.*

Proof. Define $w_n = S(\chi_n) - S(\chi)$; then, subtracting (5.5) evaluated at χ_n and the same one evaluated at χ , w_n is the solution of:

$$\int_{\Omega} a(\chi_n) \nabla w_n \nabla \varphi + \int_{\Omega} b(\chi_n) q_n w_n \varphi = \int_{\Omega} (1-k)(\chi_n - \chi) \nabla S(\chi) \nabla \varphi - \int_{\Omega} (\chi_n - \chi) S(\chi)^3 \varphi, \quad (5.10)$$

where $q_n = S(\chi_n)^2 + S(\chi_n)S(\chi) + S(\chi)^2$. Considering $\varphi = w_n$ and taking advantage of the fact that $a(\chi_n) \geq k$ and (by simple computation) $q_n \geq \frac{3}{4}S(\chi)^2$, we can show, via Cauchy-Schwarz inequality, that

$$\begin{aligned} k \|\nabla w_n\|_{L^2(\Omega)}^2 + \frac{3}{4} \int_{\Omega} b(\chi_n) S(\chi)^2 w_n^2 &\leq (1-k) \|(\chi_n - \chi) \nabla S(\chi)\|_{L^2(\Omega)} \|\nabla w_n\|_{L^2(\Omega)} \\ &\quad + \|(\chi_n - \chi) S(\chi)^3\|_{L^2(\Omega)} \|w_n\|_{L^2(\Omega)}. \end{aligned}$$

We remark that $(\chi_n - \chi) S(\chi)^3 \in L^2(\Omega)$ since $S(\chi) \in H^1(\Omega) \subset\subset L^6(\Omega)$. Moreover, as $b(\chi_n) \geq \chi_{\Omega^{d_0}}$ and using Proposition 5.4,

$$\begin{aligned} k \|\nabla w_n\|_{L^2(\Omega)}^2 + \frac{3}{4} \int_{\Omega^{d_0}} m^{2/3} w_n^2 &\leq (1-k) \|(\chi_n - \chi) \nabla S(\chi)\|_{L^2(\Omega)} \|\nabla w_n\|_{L^2(\Omega)} \\ &\quad + \|(\chi_n - \chi) S(\chi)^3\|_{L^2(\Omega)} \|w_n\|_{L^2(\Omega)}, \end{aligned}$$

from which we deduce

$$k \|\nabla w_n\|_{L^2(\Omega)}^2 + \frac{3}{4} m^{2/3} \|w_n\|_{L^2(\Omega^{d_0})}^2 \leq (q_1 + q_2) \|w_n\|_{H^1(\Omega)},$$

where $q_1 = \|(\chi_n - \chi) \nabla S(\chi)\|_{L^2(\Omega)}$ and $q_2 = \|(\chi_n - \chi) S(\chi)^3\|_{L^2(\Omega)}$, which implies, thanks to the Poincaré inequality in Lemma 5.1,

$$\|w_n\|_{H^1(\Omega)} \leq C(q_1 + q_2),$$

being $C = C(d_0, \Omega, m, k)$. Consider

$$q_1 = \left(\int_{\Omega} (\chi_n - \chi)^2 |\nabla S(\chi)|^2 \right)^{\frac{1}{2}};$$

since $\chi_n \xrightarrow{L^1} \chi$, then (up to a subsequence) $\chi_n \rightarrow \chi$ pointwise almost everywhere. Thus also the integrand $(\chi_n - \chi)^2 |\nabla S(\chi)|^2$ converges to 0. Moreover, $|\chi_n - \chi| \leq 1$, hence $\forall n$ $(\chi_n - \chi)^2 |\nabla S(\chi)|^2 \leq |\nabla S(\chi)|^2 \in L^1(\Omega)$, and thanks to Lebesgue convergence theorem, we conclude that $q_1 \rightarrow 0$. Analogously, $q_2 \rightarrow 0$ and eventually $\|w_n\|_{H^1(\Omega)} \rightarrow 0$, i.e. $S(\chi_n) \xrightarrow{H^1} S(\chi)$ and by the trace inequality also $S(\chi_n)|_{\partial\Omega} \xrightarrow{L^2(\partial\Omega)} S(\chi)|_{\partial\Omega}$. \square

Remark 5.2. Being $X_{0,1}$ a closed subspace of the Banach space $BV(\Omega)$, it is compact with respect to its weak topology; moreover, the weak BV convergence implies the strong L^1 convergence, and in view of Proposition 5.5 we can assess that the map $F = \tau \circ S$, τ being the trace operator in $H^1(\Omega)$, is compact from $X_{0,1}$ to $L^2(\partial\Omega)$. It is immediate to conclude that, if the inverse F^{-1} exists, it cannot be continuous: hence, the inverse problem (5.11) is ill-posed.

For example, consider the inclusions $\omega = B_1(0) = \{(r, \vartheta) : 0 \leq \vartheta \leq 2\pi, 0 \leq r \leq 1\}$ and $\omega_n = \{(r, \vartheta) :$

$0 \leq \vartheta \leq 2\pi, 0 \leq r \leq 1 + \frac{1}{n} \sin(n\vartheta)$ and define $\chi = \chi_\omega$, $\chi_n = \chi_{\omega_n}$. Then, it holds that $\chi_n \xrightarrow{L^1} \chi$, and hence $S(\chi_n) \xrightarrow{H^1} S(\chi)$ and $S(\chi_n)|_{\partial\Omega} \xrightarrow{L^2(\partial\Omega)} S(\chi)|_{\partial\Omega}$, but $\chi_n \not\xrightarrow{BV} \chi$. Indeed,

$$\begin{aligned} \|\chi_n - \chi\|_{L^1(\Omega)} &= \int_0^{2\pi} \int_1^{1+\frac{1}{n}|\sin(n\vartheta)|} \rho d\rho d\vartheta = \int_0^{2\pi} \left(\frac{1}{2n^2} \sin^2(n\vartheta) + \frac{1}{n} |\sin(n\vartheta)| \right) d\vartheta \\ &= \frac{\pi}{2n^2} + \frac{4}{n} \rightarrow 0 \text{ as } n \rightarrow +\infty, \end{aligned}$$

whereas

$$\begin{aligned} TV(\chi_n) &= P(\omega_n) = \int_0^{2\pi} \sqrt{1 + \cos^2(n\vartheta)} d\vartheta = \sqrt{2} \int_0^{2\pi} \sqrt{1 - \frac{1}{2} \sin^2(n\vartheta)} d\vartheta \\ &= 2\pi\sqrt{2} \left(\frac{1}{2\pi} \int_0^{2\pi} \sqrt{1 - \frac{1}{2} \sin^2 t} dt \right) \rightarrow 2\pi\sqrt{2} \frac{1}{2\pi} \int_0^{2\pi} \sqrt{1 - \frac{1}{2} \sin^2 t} dt = \sqrt{2} E \left(2\pi, \frac{1}{2} \right), \end{aligned}$$

where $E(2\pi, \frac{1}{2})$ is an elliptic integral of second kind and $\sqrt{2} E(2\pi, \frac{1}{2}) \neq 2\pi = TV(\chi)$, hence surely $\chi_n \not\xrightarrow{BV} \chi$.

5.2 Optimization problem and its regularization

When reformulated in terms of the indicator function χ , the inverse problem (5.2) becomes:

$$\text{find } \chi \in X_{0,1} \text{ s.t. } S(\chi)|_{\partial\Omega} = u_{meas}. \quad (5.11)$$

We now introduce the following constraint optimization problem:

$$\arg \min_{\chi \in X_{0,1}} J(\chi); \quad J(\chi) = \frac{1}{2} \|S(\chi) - u_{meas}\|_{L^2(\partial\Omega)}^2, \quad (5.12)$$

which shares the same property of non-stability and (possibly) non-uniqueness as problem (5.11). Nevertheless, a well-known strategy to recover well-posedness for problem (5.12) is available and consists in introducing a Tikhonov regularization term in the functional to minimize, e.g. a penalization term for the perimeter of the inclusion. The regularized problem reads:

$$\arg \min_{\chi \in X_{0,1}} J_{reg}(\chi); \quad J_{reg}(\chi) = \frac{1}{2} \|S(\chi) - u_{meas}\|_{L^2(\partial\Omega)}^2 + \alpha TV(\chi), \quad (5.13)$$

For the regularized problem (5.13), it is possible to prove several desirable properties:

- for every $\alpha > 0$ there exists at least one solution to (5.13) (existence);
- small perturbations on the data u_{meas} in $L^2(\partial\Omega)$ -norm imply small perturbation on the solutions of (5.13) in BV -intermediate convergence (stability);
- the sequence of solutions of problem (5.13) associated to the regularization parameters $\{\alpha_k\}$ (s.t. $\alpha_k \rightarrow 0$) converges in the BV -intermediate convergence to a minimum-variation solution of problem (5.12).

We recall that a sequence $\{\chi_n\} \subset BV(\Omega)$ converges to $\chi \in BV(\Omega)$ in the sense of the intermediate convergence iff $\chi_n \xrightarrow{L^1} \chi$ and $TV(\chi_n) \rightarrow TV(\chi)$. The proof of the previous properties follows from a careful application of the results in [72, Chapter 10]. Since $BV(\Omega)$ is a non-reflexive Banach space, we believe it is useful to report a detailed version of such proofs.

Proposition 5.6. *For every $\alpha > 0$ there exists a solution of (5.13)*

Proof. Let $\{\chi_n\}$ be a minimizing sequence: then $\{S(\chi_n)|_{\partial\Omega}\}$ is bounded in $L^2(\partial\Omega)$ and $\{\chi_n\}$ is bounded in $BV(\Omega)$ (since $\{TV(\chi_n)\}$ is bounded and $\|\chi_n\|_{L^1(\Omega)} \leq |\Omega|$ for all $\chi_n \in X_{0,1}$). Thanks to the result of compactness for the BV space (see [9], Theorem 3.23), there exists a subsequence χ_{n_k} weakly converging to an element $\bar{\chi} \in BV(\Omega)$. Moreover, being $\mathcal{D}(S)$ weakly closed, $\bar{\chi} \in \mathcal{D}(S)$. Since the weak BV -convergence implies the L^1 -convergence, thanks to Proposition 5.5 we can assess that $S(\chi_{n_k}) \rightarrow S(\bar{\chi})$ in $H^1(\Omega)$ and in $L^2(\partial\Omega)$. Eventually, this proves that $\|S(\chi_{n_k}) - u_{meas}\|_{L^2(\partial\Omega)} \rightarrow \|S(\bar{\chi}) - u_{meas}\|_{L^2(\partial\Omega)}$. Analogously, by semi-continuity of the total variation with respect to the weak convergence in BV , $TV(\bar{\chi}) \leq \liminf_k TV(\chi_{n_k})$, and it is possible to conclude that

$$\frac{1}{2}\|S(\bar{\chi}) - u_{meas}\|_{L^2(\partial\Omega)}^2 + \alpha TV(\bar{\chi}) \leq \liminf_k \left(\frac{1}{2}\|S(\chi_{n_k}) - u_{meas}\|_{L^2(\partial\Omega)}^2 + \alpha TV(\chi_{n_k}) \right),$$

thus $\bar{\chi}$ is a minimum of the functional. \square

Even if the existence of the solution is ensured by the previous result, uniqueness cannot be guaranteed since the functional is neither linear nor convex (in general). We now investigate the stability of the minimizer of the regularized cost functional with respect to small perturbations of the boundary data. We point out that, due to the non-reflexivity of the Banach space BV , it is not possible to formulate a stability result with respect to the strong BV convergence; nevertheless, we can perform the analysis with respect to the *intermediate convergence* of BV functions.

Proposition 5.7. *Fix $\alpha > 0$ and consider a sequence $\{u_k\} \subset L^2(\partial\Omega)$ such that $u_k \rightarrow u_{meas}$ in $L^2(\partial\Omega)$. Consider the sequence $\{\chi_k\}$, where χ_k is a solution of (5.13) with datum u_k . Then there exists a subsequence $\{\chi_{k_n}\}$ which converges to a minimizer $\bar{\chi}$ of (5.13) with datum u_{meas} in the sense of the intermediate convergence.*

Proof. For every χ_k , we have that

$$\frac{1}{2}\|S(\chi_k) - u_k\|_{L^2(\partial\Omega)}^2 + \alpha TV(\chi_k) \leq \frac{1}{2}\|S(\chi) - u_k\|_{L^2(\partial\Omega)}^2 + \alpha TV(\chi) \quad \forall \chi \in \mathcal{D}(S).$$

Hence, $\{\|S(\chi_k)\|_{L^2(\partial\Omega)}\}$ and $\{TV(\chi_k)\}$ (and therefore $\{\|\chi_k\|_{BV(\Omega)}\}$) are bounded, and there exists a subsequence $\{\chi_{k_n}\}$ such that both $\chi_{k_n} \rightharpoonup \bar{\chi}$ in $BV(\Omega)$ and $S(\chi_{k_n}) \rightarrow S(\bar{\chi})$ in $L^2(\partial\Omega)$. Thanks to the continuity of the map S with respect to the convergence (in L^1) of χ_{k_n} and to the weak lower semi-continuity of the $BV(\Omega)$ norm,

$$\begin{aligned} \frac{1}{2}\|S(\bar{\chi}) - u_{meas}\|_{L^2(\partial\Omega)}^2 + \alpha TV(\bar{\chi}) &\leq \liminf_n \left(\frac{1}{2}\|S(\chi_{k_n}) - u_{k_n}\|_{L^2(\partial\Omega)}^2 + \alpha TV(\chi_{k_n}) \right) \\ &\leq \lim_n \left(\frac{1}{2}\|S(\chi) - u_{k_n}\|_{L^2(\partial\Omega)}^2 + \alpha TV(\chi) \right) \quad \forall \chi \in \mathcal{D}(S) \quad (5.14) \\ &= \frac{1}{2}\|S(\chi) - u_{meas}\|_{L^2(\partial\Omega)}^2 + \alpha TV(\chi) \quad \forall \chi \in \mathcal{D}(S). \end{aligned}$$

Hence, $\bar{\chi}$ is a solution of problem (5.13). In order to prove that also $TV(\chi_{k_n}) \rightarrow TV(\bar{\chi})$, first consider that, according to (5.14),

$$\begin{aligned} J_{reg}(\bar{\chi}) &\leq \liminf_n \left(\frac{1}{2} \|S(\chi_{k_n}) - u_{k_n}\|_{L^2(\partial\Omega)}^2 + \alpha TV(\chi_{k_n}) \right) \\ &\leq \lim_n \left(\frac{1}{2} \|S(\chi_{k_n}) - u_{k_n}\|_{L^2(\partial\Omega)}^2 + \alpha TV(\chi_{k_n}) \right) = J_{reg}(\bar{\chi}), \end{aligned}$$

hence

$$\lim_n \left(\frac{1}{2} \|S(\chi_{k_n}) - u_{k_n}\|_{L^2(\partial\Omega)}^2 + \alpha TV(\chi_{k_n}) \right) = \frac{1}{2} \|S(\bar{\chi}) - u_{meas}\|_{L^2(\partial\Omega)}^2 + \alpha TV(\bar{\chi}).$$

In addition, thanks to the continuity of S , the first term in the sum admits a limit, i.e.:

$$\lim_n \frac{1}{2} \|S(\chi_{k_n}) - u_{k_n}\|_{L^2(\partial\Omega)}^2 = \frac{1}{2} \|S(\bar{\chi}) - u_{meas}\|_{L^2(\partial\Omega)}^2,$$

which eventually implies that also $TV(\chi_{k_n}) \rightarrow TV(\bar{\chi})$. \square

We finally state and prove the following result regarding asymptotic behavior of the minimum of J_{reg} when $\alpha \rightarrow 0$.

Proposition 5.8. *Consider a sequence $\{\alpha_k\}$ s.t. $\alpha_k \rightarrow 0$, and define the sequence $\{\chi_k\}$ of the solutions of (5.13) with the same datum u_{meas} but different weights α_k . Suppose there exists (at least) one solution of the inverse problem (5.11). Then, $\{\chi_k\}$ admits a convergent subsequence with respect to the $L^1(\Omega)$ norm and the limit χ is a minimum-variation solution of the inverse problem, i.e. $S(\chi)|_{\partial\Omega} = u_{meas}$ and $TV(\chi) \leq TV(\tilde{u}) \forall \tilde{\chi}$ s.t. $S(\tilde{\chi})|_{\partial\Omega} = u_{meas}$.*

Proof. Let χ^\dagger be a solution of the inverse problem. By definition of χ_k ,

$$\frac{1}{2} \|S(\chi_k) - u_{meas}\|_{L^2(\partial\Omega)}^2 + \alpha_k TV(\chi_k) \leq \frac{1}{2} \|S(\chi^\dagger) - u_{meas}\|_{L^2(\partial\Omega)}^2 + \alpha_k TV(\chi^\dagger) = \alpha_k TV(\chi^\dagger).$$

Hence, $\{TV(\chi_k)\}$ is bounded, and since $\|\chi_k\|_{L^1(\Omega)} \leq |\Omega|$, χ_k is also bounded in $BV(\Omega)$ and there exists a subsequence (still denoted as χ_k) and $\chi \in X_{0,1}$ s.t. $\chi_k \xrightarrow{BV} \chi$. Moreover, it holds $\|S(\chi_k)|_{\partial\Omega} - u_{meas}\|_{L^2(\partial\Omega)} \rightarrow 0$, which implies that χ is a solution of the inverse problem (5.11), and

$$TV(\chi_k) \leq TV(\chi^\dagger) \quad \Rightarrow \quad \limsup_k TV(\chi_k) \leq TV(\chi^\dagger).$$

The lower semicontinuity of the BV norm with respect to the weak convergence, together with the continuity of the L^1 norm, implies that

$$TV(\chi) \leq \liminf_k TV(\chi_k) \leq \limsup_k TV(\chi_k) \leq TV(\chi^\dagger)$$

for each solution χ^\dagger of the inverse problem, which eventually implies that χ is a minimum-variation solution. \square

Notice that, if the minimum-variation solution of problem (5.12) is unique, then the sequence $\{\chi_k\}$ converges to it.

The latter result can be improved by considering small perturbation of the data. By similar arguments as in proof of Proposition 5.8, one can prove the following

Proposition 5.9. *Let $u^\delta \in L^2(\partial\Omega)$ s.t. $\|u^\delta - u_{meas}\|_{L^2(\partial\Omega)} \leq \delta$ and let $\alpha(\delta)$ be such that $\alpha(\delta) \rightarrow 0$ and $\frac{\delta^2}{\alpha(\delta)} \rightarrow 0$ as $\delta \rightarrow 0$. Suppose there exists at least one solution of the inverse problem (5.11). Then, every sequence $\{\chi_{\alpha_k}^{\delta_k}\}$, with $\delta_k \rightarrow 0$, $\alpha_k = \alpha(\delta_k)$ and $\chi_{\alpha_k}^{\delta_k}$ solution of (5.13) corresponding to α_k and u^{δ_k} , has a converging subsequence with respect to the $L^1(\Omega)$ norm. The limit χ of every convergent subsequence is a minimum-variation solution of the inverse problem.*

Proof. Consider a solution χ^\dagger of the inverse problem. By definition of $\chi_{\alpha_k}^{\delta_k}$,

$$\frac{1}{2} \|S(\chi_{\alpha_k}^{\delta_k}) - u^{\delta_k}\|_{L^2(\partial\Omega)}^2 + \alpha_k TV(\chi_{\alpha_k}^{\delta_k}) \leq \frac{1}{2} \|S(\chi^\dagger) - u^{\delta_k}\|_{L^2(\partial\Omega)}^2 + \alpha_k TV(\chi^\dagger) \leq \delta_k^2 + \alpha_k TV(\chi^\dagger) \quad (5.15)$$

In particular,

$$TV(\chi_{\alpha_k}^{\delta_k}) \leq \frac{\delta_k^2}{\alpha_k} + TV(\chi^\dagger), \quad (5.16)$$

hence $\{\chi_{\alpha_k}^{\delta_k}\}$ is bounded in $BV(\Omega)$ and admits a subsequence (denoted by the same index k) such that $\exists \chi \in X_{0,1}$: $\chi_{\alpha_k}^{\delta_k} \xrightarrow{BV} \chi$. Passing to the limit in (5.15) as $k \rightarrow +\infty$,

$$\|S(\chi_{\alpha_k}^{\delta_k}) - u^{\delta_k}\|_{L^2(\partial\Omega)}^2 \rightarrow 0,$$

hence also

$$\|S(\chi_{\alpha_k}^{\delta_k}) - u_{meas}\|_{L^2(\partial\Omega)}^2 \leq \|S(\chi_{\alpha_k}^{\delta_k}) - u^{\delta_k}\|_{L^2(\partial\Omega)}^2 + \|u^{\delta_k} - u_{meas}\|_{L^2(\partial\Omega)}^2 \rightarrow 0$$

and by continuity of the solution map, we have that $S(\chi)|_{\partial\Omega} = u_{meas}$, which implies that χ is a solution of the inverse problem. By lower semi continuity of the BV norm (hence of the total variation) with respect the weak convergence and from inequality (5.16),

$$TV(\chi) \leq \liminf_k TV(\chi_{\alpha_k}^{\delta_k}) \leq \limsup_k TV(\chi_{\alpha_k}^{\delta_k}) \leq TV(\chi^\dagger),$$

which allows to conclude that χ is also a minimum-variation solution of the inverse problem. \square

5.3 Relaxation: a phase-field approach

According to the results of the previous Section, a good approximation of a minimum-variation solution of the inverse problem (5.11) can be achieved by solving the regularized constraint minimization problem (5.13) with a sufficiently small parameter $\alpha > 0$. Although the stability of the problem is guaranteed, its numerical solution may raise difficulties, namely the non-convexity both of the functional J_{reg} and of the space $X_{0,1}$, as well as the non-differentiability of the functional. To overcome these difficulties, in this Section we propose a phase-field relaxation of the optimization problem (5.13) inspired by [66], with the additional difficulty of the nonlinearity of the direct problem. The relaxation strategy consists in defining a minimization problem in a space of more regular functions, associated to a differentiable cost functional (which in our case is achieved by replacing the Total Variation term with a Modica-Mortola functional, representing a Ginzburg-Landau energy).

Consider $\chi \in \mathcal{K} = \{\chi \in H^1(\Omega) : 0 \leq \chi \leq 1 \text{ a.e. in } \Omega, \chi = 0 \text{ a.e. in } \Omega^{d_0}\}$ and, for every $\varepsilon > 0$, introduce the optimization problem:

$$\arg \min_{\chi \in \mathcal{K}} J_\varepsilon(\chi); \quad J_\varepsilon(\chi) = \frac{1}{2} \|S(\chi) - u_{meas}\|_{L^2(\partial\Omega)}^2 + \alpha \int_\Omega \left(\varepsilon |\nabla \chi|^2 + \frac{1}{\varepsilon} \chi(1 - \chi) \right). \quad (5.17)$$

The well-posedness result for the direct problem in Proposition 5.1, together with the additional stability and regularity results can be easily extended to the case $\chi \in \mathcal{K}$. In the next two propositions, we prove existence and stability of the solutions of the relaxed minimization problem (5.17) for fixed ε .

Proposition 5.10. *For every fixed $\varepsilon > 0$, the minimization problem (5.17) has a solution $\chi_\varepsilon \in \mathcal{K}$.*

Proof. Fix $\varepsilon > 0$ and consider a minimizing sequence for the functional J_ε , $\{\chi_k\} \subset \mathcal{K}$ (we omit the dependence of χ_k on ε). By definition of minimizing sequence, $J_\varepsilon(\chi_k) \leq M$ independently of k , which implies that also $\|\nabla\chi_k\|_{L^2(\Omega)}^2$ is bounded. Moreover, being $\chi_k \in \mathcal{K}$, $0 \leq \chi_k \leq 1$ a.e., thus $\|\chi_k\|_{L^2(\Omega)}$ and $\|\chi_k\|_{H^1(\Omega)}$ are bounded independently of k . Thanks to weak compactness of H^1 , there exist $\chi_\varepsilon \in H^1(\Omega)$ and a subsequence $\{\chi_{k_n}\}$ s.t. $\chi_{k_n} \xrightarrow{H^1} \chi_\varepsilon$, hence $\chi_{k_n} \xrightarrow{L^2} \chi_\varepsilon$. The strong L^2 convergence implies (up to a subsequence) pointwise convergence a.e., which allows to conclude (together with the Lebesgue's dominated convergence theorem, since $\chi_{k_n}(1 - \chi_{k_n}) \leq 1/2$) that

$$\int_{\Omega} \chi_{k_n}(1 - \chi_{k_n}) \rightarrow \int_{\Omega} \chi_\varepsilon(1 - \chi_\varepsilon).$$

Moreover, by the lower semicontinuity of the H^1 norm with respect to the weak convergence, and by the compact embedding in L^2 ,

$$\begin{aligned} \|\chi_\varepsilon\|_{H^1(\Omega)}^2 &\leq \liminf_n \|\chi_{k_n}\|_{H^1(\Omega)}^2 \\ \|\chi_\varepsilon\|_{L^2(\Omega)}^2 + \|\nabla\chi_\varepsilon\|_{L^2(\Omega)}^2 &\leq \liminf_n \|\chi_{k_n}\|_{L^2(\Omega)}^2 + \liminf_n \|\nabla\chi_{k_n}\|_{L^2(\Omega)}^2 \\ \|\nabla\chi_\varepsilon\|_{L^2(\Omega)}^2 &\leq \liminf_n \|\nabla\chi_{k_n}\|_{L^2(\Omega)}^2. \end{aligned}$$

Moreover, using the continuity of the solution map S with respect to the L^1 convergence, we can conclude that

$$J_\varepsilon(\chi_\varepsilon) \leq \liminf_n J_\varepsilon(\chi_{k_n}).$$

Finally, by pointwise convergence, $0 \leq \chi_\varepsilon \leq 1$ a.e. and $\chi_\varepsilon = 0$ a.e. in Ω^{d_0} , hence χ_ε is a minimum of J_ε in \mathcal{K} . \square

Proposition 5.11. *Fix $\alpha, \varepsilon > 0$ and consider a sequence $\{u^k\} \subset L^2(\partial\Omega)$ such that $u^k \xrightarrow{L^2(\partial\Omega)} u_{meas}$. For each k , let χ_ε^k be a solution of (5.17), where u_{meas} is replaced by u^k . Then, up to a subsequence, $\chi_\varepsilon^k \xrightarrow{H^1} \chi_\varepsilon$, where χ_ε is a solution of (5.17).*

Proof. Consider a solution χ^* of (5.17): by definition of χ_ε^k , it holds

$$\begin{aligned} &\frac{1}{2} \|S(\chi_\varepsilon^k) - u^k\|_{L^2(\partial\Omega)}^2 + \alpha\varepsilon \|\nabla\chi_\varepsilon^k\|_{L^2(\Omega)}^2 + \frac{\alpha}{\varepsilon} \int_{\Omega} \chi_\varepsilon^k(1 - \chi_\varepsilon^k) \\ &\leq \frac{1}{2} \|S(\chi^*) - u^k\|_{L^2(\partial\Omega)}^2 + \alpha\varepsilon \|\nabla\chi^*\|_{L^2(\Omega)}^2 + \frac{\alpha}{\varepsilon} \int_{\Omega} \chi^*(1 - \chi^*) \\ &\leq \frac{1}{2} \|u_{meas} - u^k\|_{L^2(\partial\Omega)}^2 + \frac{1}{2} J_\varepsilon(\chi^*). \end{aligned}$$

Hence $\|\nabla\chi_\varepsilon^k\|_{L^2(\Omega)}$ is bounded independently of k , and so is $\|\chi_\varepsilon^k\|_{L^2(\Omega)}$ (since $\chi_\varepsilon^k \in \mathcal{K}$). This implies that, up to a subsequence, $\chi_\varepsilon^k \xrightarrow{H^1} \chi_\varepsilon \in H^1(\Omega)$, from which it follows that $\chi_\varepsilon^k \xrightarrow{L^2} \chi_\varepsilon$ and in

particular $S(\chi_\varepsilon^k) \xrightarrow{H^1} S(\chi_\varepsilon)$ (thanks to Proposition 5.5) and $\chi_\varepsilon^k \rightarrow \chi_\varepsilon$ almost everywhere in Ω , and by Lebesgue's convergence theorem also $\int_\Omega \chi_\varepsilon^k(1 - \chi_\varepsilon^k) \rightarrow \int_\Omega \chi_\varepsilon(1 - \chi_\varepsilon)$. Finally, by lower semi-continuity of the H^1 norm with respect to the weak convergence, we conclude that

$$\begin{aligned} J_\varepsilon(\chi_\varepsilon) &\leq \liminf_k \left(\frac{1}{2} \|S(\chi_\varepsilon^k) - u^k\|_{L^2(\partial\Omega)}^2 + \alpha\varepsilon \|\nabla \chi_\varepsilon^k\|_{L^2(\Omega)}^2 + \frac{\alpha}{\varepsilon} \int_\Omega \chi_\varepsilon^k(1 - \chi_\varepsilon^k) \right) \\ &\leq J_\varepsilon(\chi^*) + \frac{1}{2} \lim_k \|u_{meas} - \chi^k\|_{L^2(\partial\Omega)}^2, \end{aligned}$$

hence $J_\varepsilon(\chi_\varepsilon) = J_\varepsilon(\chi^*)$ and χ_ε is a solution of (5.17). Moreover, this implies that $\|\nabla \chi_\varepsilon\|_{L^2(\Omega)} = \lim_k \|\nabla \chi_\varepsilon^k\|_{L^2(\Omega)}$; and since H^1 is an Hilbert space, together with the weak convergence, this implies that $\chi_\varepsilon^k \xrightarrow{H^1} \chi_\varepsilon$. \square

The asymptotic behavior of the phase-field relaxation when $\varepsilon \rightarrow 0$ is reported in the next two propositions and is related to the notion of Γ -convergence.

Proposition 5.12. *Consider the space X of the Lebesgue-measurable functions over Ω endowed with the $L^1(\Omega)$ norm and the following extension of the cost functionals on X*

$$\tilde{J}(\chi) = \begin{cases} J_{reg}(\chi) & \text{if } \chi \in X_{0,1} \\ \infty & \text{otherwise,} \end{cases} \quad \tilde{J}_\varepsilon(\chi) = \begin{cases} J_\varepsilon(\chi) & \text{if } \chi \in \mathcal{K} \\ \infty & \text{otherwise.} \end{cases}$$

Then, the functionals $\tilde{J}_{\varepsilon_k}$ associated to $\{\varepsilon_k\}$ s.t. $\varepsilon_k \rightarrow 0$ converge to \tilde{J} in X in the sense of the Γ -convergence.

We proceed as in [66, Theorem 2.2]. After decomposing the cost functionals $\tilde{J}_\varepsilon(\chi) = G(\chi) + F_\varepsilon(\chi)$ and $\tilde{J}(\chi) = G(\chi) + F(\chi)$, being $G(\chi) = \frac{1}{2} \|S(\chi) - u_{meas}\|_{L^2(\Omega)}^2$, the main task is to prove that $F_\varepsilon \xrightarrow{\Gamma} F$ in X , which is done in [66, Theorem 6.1].

Finally, from the compactness result in [23, Proposition 4.1] and applying the definition of Γ -convergence, it is easy to prove the following convergence result for the solutions of (5.17).

Proposition 5.13. *Consider a sequence $\{\varepsilon_k\}$ s.t. $\varepsilon_k \rightarrow 0$ and let $\{\chi_{\varepsilon_k}\}$ be the sequence of the respective minimizers of the functionals $\{J_{\varepsilon_k}\}$. Then, there exists a subsequence, still denoted as $\{\varepsilon_k\}$ and a function $\chi \in X_{0,1}$ such that $\chi_{\varepsilon_k} \rightarrow \chi$ in L^1 and u is a solution of (5.13).*

Proof. Thanks to the compactness result exposed in Proposition 4.1 in [23], it is possible to extract a subsequence (still denoted as $\{\varepsilon_k\}$) s.t. $\chi_{\varepsilon_k} \xrightarrow{L^1} \chi \in X$. Thanks to the definition of the Γ convergence, it is easy to prove that χ is a minimum of the sharp functional \tilde{J} : indeed, consider a generic $\xi \in X$; then by the Γ convergence,

$$\exists \{\xi_k\} \subset X \text{ s.t. } \xi_k \xrightarrow{L^1} \xi \text{ and } \lim_n \tilde{J}_{\varepsilon_k}(\xi_k) = \tilde{J}(\xi).$$

For each k , by definition of the minimizers χ_{ε_k} , $\tilde{J}_{\varepsilon_k}(\chi_{\varepsilon_k}) \leq \tilde{J}_{\varepsilon_k}(\xi_k)$, and passing to the limit, again by definition of Γ convergence,

$$\tilde{J}(\chi) \leq \liminf_k \tilde{J}_{\varepsilon_k}(\chi_{\varepsilon_k}) \leq \lim_k \tilde{J}_{\varepsilon_k}(\xi_k) = \tilde{J}(\xi),$$

and since this holds for each $\xi \in X$, we conclude that the limit χ is a minimizer of \tilde{J} . Moreover, clearly $\tilde{J}(\chi) < \infty$, hence $\chi \in X_{0,1}$ and is indeed a solution of the optimization problem (5.13). \square

5.3.1 Optimality conditions

We can now provide an expression for the optimality condition associated with the minimization problem (5.17), which is formulated as a variational inequality involving the Fréchet derivative of J_ε .

Proposition 5.14. *Consider the solution map $S : \mathcal{K} \rightarrow H^1(\Omega)$ and let $f \in L^2(\Omega)$ satisfy assumption (5.4): for every $\varepsilon > 0$, the operators S and J_ε are Fréchet-differentiable on $\mathcal{K} \subset L^\infty(\Omega) \cap H^1(\Omega)$ and a minimizer χ_ε of J_ε satisfies the variational inequality:*

$$J'_\varepsilon(\chi_\varepsilon)[\xi - \chi_\varepsilon] \geq 0 \quad \forall \xi \in \mathcal{K}, \quad (5.18)$$

being

$$J'_\varepsilon(\chi)[\vartheta] = \int_\Omega (1-k)\vartheta \nabla S(\chi) \cdot \nabla p + \int_\Omega \vartheta S(\chi)^3 p + 2\alpha\varepsilon \int_\Omega \nabla \chi \cdot \nabla \vartheta + \frac{\alpha}{\varepsilon} \int_\Omega (1-2\chi)\vartheta; \quad (5.19)$$

where $\vartheta \in \mathcal{K} - \chi = \{\xi \text{ s.t. } \chi + \xi \in \mathcal{K}\}$ and p is the solution of the adjoint problem:

$$\int_\Omega a(\chi) \nabla p \cdot \nabla \psi + \int_\Omega 3b(\chi) S(\chi)^2 p \psi = \int_{\partial\Omega} (S(\chi) - u_{meas}) \psi \quad \forall \psi \in H^1(\Omega). \quad (5.20)$$

Proof. First of all we need to prove that S is Fréchet differentiable in $L^\infty(\Omega)$: in particular, we claim that for $\vartheta \in L^\infty(\Omega) \cap (\mathcal{K} - \chi)$ it holds that $S'(\chi)[\vartheta] = S_*$, where S_* is the solution in $H^1(\Omega)$ of

$$\int_\Omega a(\chi) \nabla S_* \nabla \varphi + \int_\Omega b(\chi) 3S(\chi)^2 S_* \varphi = \int_\Omega (1-k)\vartheta \nabla S \nabla \varphi + \int_\Omega \vartheta S(\chi)^3 \varphi \quad \forall \varphi \in H^1(\Omega), \quad (5.21)$$

namely, that

$$\|S(\chi + \vartheta) - S(\chi) - S_*\|_{H^1(\Omega)} = o(\|\vartheta\|_{L^\infty(\Omega)}). \quad (5.22)$$

First we show that if $\vartheta \in L^\infty(\Omega) \cap (\mathcal{K} - \chi)$, then $\|S(\chi + \vartheta) - S(\chi)\|_{H^1(\Omega)} \leq C\|\vartheta\|_{L^\infty(\Omega)}$. Indeed, the difference $w = S(\chi + \vartheta) - S(\chi)$ satisfies

$$\begin{aligned} \int_\Omega a(\chi + \vartheta) \nabla w \nabla \varphi + \int_\Omega b(\chi + \vartheta) q w \varphi &= - \int_\Omega (a(\chi + \vartheta) - a(\chi)) \nabla S(\chi) \nabla \varphi \\ &\quad - \int_\Omega (b(\chi + \vartheta) - b(\chi)) S(\chi)^3 \varphi \quad \forall \varphi \in H^1(\Omega), \end{aligned} \quad (5.23)$$

with $q = S(\chi + \vartheta)^2 + S(\chi)S(\chi + \vartheta) + S(\chi)^2$. Substituting $a(\chi + \vartheta) - a(\chi) = -(1-k)\vartheta$ and $b(\chi + \vartheta) - b(\chi) = -\vartheta$, and taking $\varphi = w$ in (5.23), as in the proof of Proposition 5.5, we obtain

$$k\|\nabla w\|_{L^2}^2 + \frac{3}{4} \int_\Omega b(\chi + \vartheta) S(\chi)^2 w^2 \leq \|\vartheta\|_{L^\infty} \|\nabla S(\chi)\|_{L^2} \|\nabla w\|_{L^2} + \|S(\chi)^3\|_{L^2} \|w\|_{L^2} \|\vartheta\|_{L^\infty}$$

and again by Proposition 5.4

$$k\|\nabla w\|_{L^2}^2 + \frac{3}{4} m^{2/3} \|w\|_{L^2(\Omega^{a_0})}^2 \leq \|\vartheta\|_{L^\infty} \|\nabla S(\chi)\|_{L^2} \|\nabla w\|_{L^2} + \|\vartheta\|_{L^\infty} \|S(\chi)^3\|_{L^2} \|w\|_{L^2}.$$

By (5.6) and the Sobolev inequality, eventually

$$\|w\|_{H^1(\Omega)}^2 \leq C \|S(\chi)\|_{H^1(\Omega)} \|w\|_{H^1(\Omega)} \|\vartheta\|_{L^\infty},$$

hence $\|S(\chi + \vartheta) - S(\chi)\|_{H^1(\Omega)} = O(\|\vartheta\|_{L^\infty(\Omega)})$.

Take now (5.23) and subtract (5.21). Define $r = S(\chi + \vartheta) - S(\chi) - S_*$: it holds that

$$\begin{aligned} \int_{\Omega} a(\chi) \nabla r \nabla \varphi + \int_{\Omega} b(\chi) 3S(\chi)^2 r \varphi &= \int_{\Omega} (a(\chi + \vartheta) - a(\chi)) \nabla w \cdot \nabla \varphi \\ &+ \int_{\Omega} (b(\chi + \vartheta) q - 3b(\chi) S(\chi)^2) w \varphi \quad \forall \varphi \in H^1(\Omega). \end{aligned}$$

The second integral in the latter sum can be split as follows:

$$\int_{\Omega} (b(\chi + \vartheta) q - 3b(\chi) S(\chi)^2) w \varphi = \int_{\Omega} (b(\chi + \vartheta) - b(\chi)) q w \varphi + \int_{\Omega} (q - 3S(\chi)^2) b(\chi) w \varphi,$$

and in particular $q - 3S(\chi)^2 = S(\chi + \vartheta)^2 + S(\chi + \vartheta)S(\chi) - 2S(\chi)^2 = hw$, where $h = S(\chi + \vartheta) + 2S(\chi) \in H^1(\Omega)$. Hence, chosen $\varphi = r$ and exploiting again Proposition 5.4, the Poincaré inequality in Lemma 5.1 and the Hölder inequality:

$$\begin{aligned} \frac{1}{C} \|r\|_{H^1}^2 &\leq k \|\nabla r\|_{L^2}^2 + m^{2/3} \|r\|_{L^2(\Omega^{d_0})}^2 \leq (1-k) \|\vartheta\|_{L^\infty} \|\nabla w\|_{L^2} \|\nabla r\|_{L^2} \\ &+ \|\vartheta\|_{L^\infty} \|q\|_{L^4} \|w\|_{L^2} \|r\|_{L^4} + \|h\|_{L^4} \|w\|_{L^4}^2 \|r\|_{L^4} \\ &\leq \left((1-k) \|\vartheta\|_{L^\infty} \|w\|_{H^1} + \|q\|_{H^1} \|\vartheta\|_{L^\infty} \|w\|_{H^1} + \|h\|_{H^1} \|w\|_{H^1}^2 \right) \|r\|_{H^1}. \end{aligned}$$

It follows eventually that $\|r\|_{H^1(\Omega)} \leq C \|\vartheta\|_{L^\infty}^2 = o(\|\vartheta\|_{L^\infty})$, which guarantees that $S_* = S'(\chi)[\vartheta]$.

The last step is to provide an expression of the Fréchet derivative of J_ε . Exploiting the fact that S is differentiable, we can compute the expression of $J'_\varepsilon(\chi)$ through the *chain rule*:

$$J'_\varepsilon(\chi)[\vartheta] = \int_{\partial\Omega} (S(\chi) - u_{meas}) S'(\chi)[\vartheta] + \alpha \int_{\Omega} \left(2\varepsilon \nabla \chi \nabla \vartheta + \frac{1}{\varepsilon} (1 - 2\chi) \vartheta \right). \quad (5.24)$$

Finally, thanks to the expression of the adjoint problem,

$$\begin{aligned} \int_{\partial\Omega} (S(\chi) - u_{meas}) S'(\chi)[\vartheta] &= \int_{\partial\Omega} (S(\chi) - u_{meas}) S_* = \int_{\Omega} a(\chi) \nabla p \cdot \nabla S_* + \int_{\Omega} 3S(\chi)^2 p S_* = \\ &(by\ definition\ of\ S_*) = \int_{\Omega} (1-k) \vartheta \nabla S(\chi) \cdot \nabla p + \int_{\Omega} \vartheta S(\chi)^3 p, \end{aligned}$$

and hence:

$$J'_\varepsilon(\chi)[\vartheta] = \int_{\Omega} (1-k) \vartheta \nabla S(\chi) \cdot \nabla p + \int_{\Omega} \vartheta S(\chi)^3 p + \alpha \int_{\Omega} \left(2\varepsilon \nabla \chi \cdot \nabla \vartheta + \frac{1}{\varepsilon} (1 - 2\chi) \vartheta \right).$$

Finally, it is a standard argument that, being J_ε a continuous and Fréchet differentiable functional on a convex subset \mathcal{K} of the Banach space $H^1(\Omega)$, the optimality conditions for the optimization problem (5.17) are expressed by the variational inequality (5.18). \square

5.4 Discrete framework and reconstruction algorithm

For a fixed $\varepsilon > 0$, we now introduce a Finite Element formulation of problem (5.17) in order to define a numerical reconstruction algorithm and compute an approximated solution of the inverse problem.

In what follows, we consider Ω to be polygonal, in order to avoid a discretization error involving the geometry of the domain. Let \mathcal{T}_h be a shape regular triangulation of Ω and define $V_h \subset H^1(\Omega)$:

$$V_h = \{v_h \in C(\bar{\Omega}), v_h|_K \in \mathbb{P}_1(K) \ \forall K \in \mathcal{T}_h\}; \quad \mathcal{K}_h = V_h \cap \mathcal{K}.$$

For every fixed $h > 0$, we define the solution map $S_h : \mathcal{K} \rightarrow V_h$, where $S_h(\chi)$ solves

$$\int_{\Omega} a(\chi) \nabla S_h(\chi) \nabla v_h + \int_{\Omega} b(\chi) S_h(\chi)^3 v_h = \int_{\Omega} f v_h \quad \forall v_h \in V_h.$$

5.4.1 Convergence analysis as $h \rightarrow 0$

The present section is devoted to the numerical analysis of the discretized problem: the convergence of the approximated solution of the direct problem is studied, taking into account the difficulties implied by the nonlinear term. Moreover, the existence and convergence of minimizers of the discrete cost functional is analyzed. The following result, which is preliminary for the proof of the convergence of the approximated solutions to the exact one, can be proved by resorting to the techniques of [57, Theorem 2.1].

Lemma 5.3. *Let $f \in L^2(\Omega)$ satisfy assumption (5.4); then, for every $\chi \in \mathcal{K}$, $S_h(\chi) \rightarrow S(\chi)$ strongly in $H^1(\Omega)$.*

Proof. As in the proof of Proposition 5.1, for a fixed $\chi \in \mathcal{K}$ we define the operator $T : H^1(\Omega) \rightarrow (H^1(\Omega))^*$ such that

$$\langle T(u), \varphi \rangle = \int_{\Omega} a(\chi) \nabla u \nabla \varphi + \int_{\Omega} b(\chi) u^3 \varphi;$$

then $u_h = S_h(\chi)$ and $u = S(\chi)$ are respectively the solutions of the equations

$$\langle T(u_h), \varphi_h \rangle = \int_{\Omega} f \varphi_h \quad \forall \varphi_h \in V_h; \quad \langle T(u), \varphi \rangle = \int_{\Omega} f \varphi \quad \forall \varphi \in H^1(\Omega). \quad (5.25)$$

The ellipticity of the operator T follows by Lemma 5.1 and Proposition 5.4, indeed:

$$\begin{aligned} \langle T(u_h) - T(u), u_h - u \rangle &= \int_{\Omega} a(\chi) |\nabla(u_h - u)|^2 + \int_{\Omega} b(\chi) (u_h - u)^2 (u_h^2 + u_h u + u^2) \\ &\geq k \|\nabla(u_h - u)\|_{L^2(\Omega)}^2 + \frac{3}{4} m^{2/3} \|u_h - u\|_{L^2(\Omega^{d_0})}^2 \geq C \|u_h - u\|_{H^1(\Omega)}^2, \end{aligned}$$

where $C = C(k, m, \Omega, d_0)$ is independent of h . Consider now an arbitrary $w_h \in V_h$ and exploit the orthogonality $\langle T(u_h) - T(u), \varphi_h \rangle = 0 \ \forall \varphi_h \in V_h$, which follows by (5.25).

$$\begin{aligned} C \|u_h - u\|_{H^1}^2 &\leq \langle T(u_h) - T(u), u_h - u \rangle = \langle T(u_h) - T(u), w_h - u \rangle \\ &\leq K \|w_h - u\|_{H^1} \|u_h - u\|_{H^1}, \end{aligned}$$

where K is the Lipschitz constant of T (see Proposition 5.1). We point out that, in view of Proposition 5.2, the constant K does not depend on u nor on h , but only on $\|f\|_{L^2(\Omega)}$, Ω , d_0 , k . Hence:

$$\|u_h - u\|_{H^1} \leq \frac{K}{C} \|w_h - u\|_{H^1},$$

and since the latter inequality holds for each $w_h \in H^1(\Omega)$, it holds:

$$\|u_h - u\|_{H^1(\Omega)} \leq \frac{K}{C} \inf_{w_h \in V_h} \|w_h - u\|_{H^1(\Omega)},$$

and the thesis follows by the interpolation estimates of $H^1(\Omega)$ functions in V_h . \square

The convergence of the solution of the discrete direct problem to the continuous one is an immediate consequence of Lemma 5.3 and of the continuity of the map S_h in the space V_h , which can be assessed analogously to the proof of Proposition 5.5.

Proposition 5.15. *Let $\{h_k\}, \{\chi_k\}$ be two sequences such that $h_k \rightarrow 0$, $\chi_k \in \mathcal{K}_{h_k}$ and $\chi_k \xrightarrow{L^1} \chi \in \mathcal{K}$. Then $S_{h_k}(\chi_k) \xrightarrow{H^1} S(\chi)$.*

Define the discrete cost functional, $J_{\varepsilon,h} : \mathcal{K}_h \rightarrow \mathbb{R}$

$$J_{\varepsilon,h}(\chi_h) = \frac{1}{2} \|S_h(\chi_h) - u_{meas,h}\|_{L^2(\partial\Omega)}^2 + \alpha \int_{\Omega} \left(\varepsilon |\nabla \chi_h|^2 + \frac{1}{\varepsilon} \chi_h (1 - \chi_h) \right), \quad (5.26)$$

being $u_{meas,h}$ the $L^2(\Omega)$ -projection of the boundary datum u_{meas} in the space of the traces of V_h functions. The existence of minimizers of the discrete functionals $J_{\varepsilon,h}$ is stated in the following proposition, together with an asymptotic analysis as $h \rightarrow 0$. Taking advantage of Proposition 5.15, the proof is analogous to the one of [66, Theorem 3.2].

Proposition 5.16. *For each $h > 0$, there exists $\chi_h \in \mathcal{K}_h$ such that $J_{\varepsilon,h}(\chi_h) = \min_{\xi_h \in \mathcal{K}_h} J_{\varepsilon,h}(\xi_h)$. Every sequence $\{\chi_{h_k}\}$ s.t. $\lim_{k \rightarrow \infty} h_k = 0$ admits a subsequence that converges in $H^1(\Omega)$ to a minimum of the cost functional J_{ε} .*

The strategy we adopt in order to minimize the discrete cost functional $J_{\varepsilon,h}$ is to search for a function χ_h satisfying discrete optimality conditions, which can be obtained as in section 5.3.1:

$$J'_{\varepsilon,h}(\chi_h)[\xi_h - \chi_h] \geq 0 \quad \forall \xi_h \in \mathcal{K}_h \quad (5.27)$$

where for each $\theta_h \in \mathcal{K}_h - \chi_h := \{\theta_h = \xi_h - \chi_h; \xi_h \in \mathcal{K}_h\}$ it holds

$$\begin{aligned} J'_{\varepsilon,h}(\chi_h)[\vartheta_h] &= \int_{\Omega} (1-k) \vartheta_h \nabla S_h(\chi_h) \cdot \nabla p_h + \int_{\Omega} \vartheta_h S_h(u_h)^3 p_h + 2\alpha \varepsilon \int_{\Omega} \nabla \chi_h \cdot \nabla \vartheta_h \\ &\quad + \frac{\alpha}{\varepsilon} \int_{\Omega} (1-2\chi_h) \vartheta_h, \end{aligned} \quad (5.28)$$

where p_h is the solution in V_h of the adjoint problem (5.20) associated to χ_h .

It is finally possible to prove the convergence of critical points of the discrete functionals $J_{\varepsilon,h}$ (i.e., functions in \mathcal{K}_h satisfying (5.27)) to a critical point of the continuous one, J_{ε} . The proof can be adapted from the one of [66, Theorem 3.2].

Proposition 5.17. *Consider a sequence $\{h_k\}$ s.t. $h_k \rightarrow 0$ and for every k denote as χ_k a solution of the discrete variational inequality (5.27). Then there exists a subsequence of $\{\chi_k\}$ that converges a.e and in $H^1(\Omega)$ to a solution χ of the continuous variational inequality (5.19)*

5.4.2 Reconstruction algorithm: a Parabolic Obstacle Problem approach

The necessary optimality conditions that have been stated in Proposition 5.14, together with the expression of the Fréchet derivative of the cost functional reported in (5.19) allow to define a Parabolic Obstacle problem, which consists of a very common strategy in order to search for a solution of optimization problems in a phase-field approach. In this section, we give a continuous

formulation of the problem and provide a formal proof of its desired properties. We then introduce a numerical discretization of the problem and rigorously prove the main convergence results.

The core of the proposed approach is to rely on a parabolic problem whose solution $\chi(\cdot, t)$ converges, as the fictitious time variable tends to $+\infty$, to an asymptotic state χ_∞ satisfying the continuous optimality conditions (5.19). The problem can be formulated as follows, for a fixed $\varepsilon > 0$: let χ be the solution of

$$\begin{cases} \int_{\Omega} \partial_t \chi(\xi - \chi) + J'_\varepsilon(\chi)[\xi - \chi] \geq 0 & \forall \xi \in \mathcal{K}, \quad t \in (0, +\infty) \\ \chi(\cdot, 0) = \chi_0 \in \mathcal{K}. \end{cases} \quad (5.29)$$

The theoretical analysis of the latter problem is beyond the purposes of this work, and would require to deal with the severe nonlinearity of the expression of $J'_\varepsilon(\chi)$; consequently, we provide a complete discretization of the Parabolic Obstacle Problem and assess its convergence properties. This is performed by setting (5.29) in the discrete spaces \mathcal{K}_h and V_h , and by considering a semi-implicit one-step scheme for the time updating, as in [66]: i.e., by treating explicitly the nonlinear terms and implicitly the linear ones. We obtain that the approximate solution $\{\chi_h^n\}_{n \in \mathbb{N}} \subset V_h$, $\chi_h^n \approx \chi(\cdot, t^n)$ is computed as:

$$\begin{cases} \chi_h^0 = \chi_0 \in \mathcal{K}_h & (a \text{ prescribed initial datum}) \\ \chi_h^{n+1} \in \mathcal{K}_h : \int_{\Omega} (\chi_h^{n+1} - \chi_h^n)(\xi_h - \chi_h^{n+1}) + \tau_n \int_{\Omega} (1 - k) \nabla S_h(\chi_h^n) \cdot \nabla p_h^n (\xi_h - \chi_h^{n+1}) \\ \quad + \tau_n \int_{\Omega} S_h(\chi_h^n)^3 p_h^n (\xi_h - \chi_h^{n+1}) + 2\tau_n \alpha \varepsilon \int_{\Omega} \nabla \chi_h^{n+1} \cdot \nabla (\xi_h - \chi_h^{n+1}) \\ \quad + \tau_n \alpha \frac{1}{\varepsilon} \int_{\Omega} (1 - 2\chi_h^n)(\xi_h - \chi_h^{n+1}) \geq 0 & \forall \xi_h \in \mathcal{K}_h, \quad n = 0, 1, \dots \end{cases} \quad (5.30)$$

The following preliminary result is necessary for the proof of the convergence of the algorithm:

Lemma 5.4. *For each $n > 0$, there exists a positive constant $\mathcal{B}_n = \mathcal{B}_n(\Omega, h, k, \|p_h^n\|_{H^1}, \|u_h^n\|_{H^1}, \|u_h^{n+1}\|_{H^1})$ such that, provided that $\tau_n \leq \mathcal{B}_n$ it holds that:*

$$\|\chi_h^{n+1} - \chi_h^n\|_{L^2}^2 + J_{\varepsilon, h}(\chi_h^{n+1}) \leq J_{\varepsilon, h}(\chi_h^n) \quad n > 0. \quad (5.31)$$

Proof. In the expression of the discrete parabolic obstacle problem (5.30), consider $\xi_h = \chi_h^n$: via simple computation, we can point out that

$$\begin{aligned} & \frac{1}{\tau_n} \|\chi_h^{n+1} - \chi_h^n\|_{L^2}^2 + J(\chi_h^{n+1}) - J(\chi_h^n) + \alpha \varepsilon \|\nabla(\chi_h^{n+1} - \chi_h^n)\|_{L^2}^2 + \frac{\alpha}{\varepsilon} \|\chi_h^{n+1} - \chi_h^n\|_{L^2}^2 \\ & \leq \int_{\Omega} (a(\chi_h^{n+1}) - a(\chi_h^n)) \nabla u_h^n \nabla p_h^n + \int_{\Omega} (b(\chi_h^{n+1}) - b(\chi_h^n)) (u_h^n)^3 p_h^n \\ & \quad + \frac{1}{2} \|u_h^{n+1} - u_h^n\|_{L^2(\partial\Omega)}^2 + \int_{\partial\Omega} (u_h^{n+1} - u_h^n)(u_h^{n+1} - u_{meas, h}), \end{aligned}$$

where $u_h^n = S_h(\chi_h^n)$ and $u_h^{n+1} = S_h(\chi_h^{n+1})$. Moreover, by the expression of the adjoint problem,

$$RHS = \frac{1}{2} \|u_h^{n+1} - u_h^n\|_{L^2(\partial\Omega)}^2 + \textcircled{\text{I}} + \textcircled{\text{II}},$$

where

$$\begin{aligned}
\textcircled{\text{I}} &= \int_{\Omega} (a(\chi_h^{n+1}) - a(\chi_h^n)) \nabla u_h^n \cdot \nabla p_h^n + \int_{\Omega} a(\chi_h^n) \nabla p_h^n \cdot \nabla (u_h^{n+1} - u_h^n) \\
&= \int_{\Omega} (a(\chi_h^n) - a(\chi_h^{n+1})) \nabla (u_h^{n+1} - u_h^n) \cdot \nabla p_h^n + \int_{\Omega} a(\chi_h^{n+1}) \nabla u_h^{n+1} \cdot \nabla p_h^n \\
&\quad - \int_{\Omega} a(\chi_h^n) \nabla u_h^n \cdot \nabla p_h^n; \\
\textcircled{\text{II}} &= \int_{\Omega} (b(\chi_h^{n+1}) - b(\chi_h^n)) (u_h^n)^3 p_h^n + 3 \int_{\Omega} b(\chi_h^n) (u_h^n)^2 p_h^n (u_h^{n+1} - u_h^n) = \\
&= \int_{\Omega} b(\chi_h^{n+1}) ((u_h^n)^3 - (u_h^{n+1})^3) p_h^n + 3 \int_{\Omega} b(\chi_h^n) (u_h^n)^2 p_h^n (u_h^{n+1} - u_h^n) \\
&\quad + \int_{\Omega} b(\chi_h^{n+1}) (u_h^{n+1})^3 p_h^n - \int_{\Omega} b(\chi_h^n) (u_h^n)^3 p_h^n = \\
&\quad \text{(by the expansion } (u_h^{n+1})^3 = (u_h^n + (u_h^{n+1} - u_h^n))^3 \text{)} \\
&= 3 \int_{\Omega} (b(\chi_h^n) - b(\chi_h^{n+1})) (u_h^n)^2 p_h^n (u_h^{n+1} - u_h^n) - 3 \int_{\Omega} b(\chi_h^{n+1}) (\chi_h^n) p_h^n (u_h^{n+1} - u_h^n)^2 \\
&\quad - \int_{\Omega} b(\chi_h^{n+1}) p_h^n (u_h^{n+1} - u_h^n)^3 + \int_{\Omega} b(\chi_h^{n+1}) (u_h^{n+1})^3 p_h^n - \int_{\Omega} b(\chi_h^n) (u_h^n)^3 p_h^n.
\end{aligned}$$

Collecting the terms and taking advantage of the expression of the direct problem, we conclude that

$$\begin{aligned}
RHS &= \frac{1}{2} \|u_h^{n+1} - u_h^n\|_{L^2(\partial\Omega)}^2 + \int_{\Omega} (a(\chi_h^n) - a(\chi_h^{n+1})) \nabla (u_h^{n+1} - u_h^n) \cdot \nabla p_h^n \\
&\quad + 3 \int_{\Omega} (b(\chi_h^n) - b(\chi_h^{n+1})) (u_h^n)^2 p_h^n (u_h^{n+1} - u_h^n) \\
&\quad - 3 \int_{\Omega} b(\chi_h^{n+1}) (u_h^n) p_h^n (u_h^{n+1} - u_h^n)^2 - \int_{\Omega} b(\chi_h^{n+1}) p_h^n (u_h^{n+1} - u_h^n)^3.
\end{aligned}$$

We now employ the Cauchy-Schwarz inequality and the regularity of the solutions of the discrete direct and adjoint problems (in particular the equivalence of the $W^{1,\infty}$ and H^1 norm in V_h : $\|u_h\|_{W^{1,\infty}} \leq C_1 \|u_h\|_{H^1}$, $C_1 = C_1(\Omega, h)$):

$$RHS \leq C_2 \|\chi_h^{n+1} - \chi_h^n\|_{L^2} \|u_h^{n+1} - u_h^n\|_{H^1} + C_3 \|u_h^{n+1} - u_h^n\|_{H^1}^2$$

with $C_2 = (1-k)C_1 \|p_h^n\|_{H^1} + C_1 \|u_h^n\|_{H^1} \|p_h^n\|_{H^1}$ and $C_3 = 3C_1^2 \|u_h^n\|_{H^1} \|p_h^n\|_{H^1} + C_1^3 \|p_h^n\|_{H^1} (\|u_h^n\|_{H^1} + \|u_h^{n+1}\|_{H^1}) + \frac{1}{2} C_{tr}^2$, being C_{tr} the constant of the trace inequality in $H^1(\Omega)$. Eventually, similarly to the computation included in the proof of Proposition 5.14, one can assess that

$$\|u_h^{n+1} - u_h^n\|_{H^1} \leq C_4 \|\chi_h^{n+1} - \chi_h^n\|_{L^2},$$

with $C_4 = C_4(k, C_1, \|u_h^n\|_{H^1}, \Omega)$. Hence, we can conclude that there exists a positive constant $\mathcal{C}_n = C_2 C_4 + C_3 C_4^2$ such that

$$\frac{1}{\tau_n} \|\chi_h^{n+1} - \chi_h^n\|_{L^2}^2 + J(\chi_h^{n+1}) - J(\chi_h^n) \leq \mathcal{C}_n \|\chi_h^{n+1} - \chi_h^n\|_{L^2}^2,$$

and choosing $\tau_n < \mathcal{B}_n := \frac{1}{1+\mathcal{C}_n}$ we can conclude the thesis. \square

We are finally able to prove the following convergence result for the fully discretized Parabolic Obstacle Problem:

Proposition 5.18. *Consider a starting point $\chi_h^0 \in \mathcal{K}_h$. Then, there exists a collection of timesteps $\{\tau_n\}$ s.t. $0 < \gamma \leq \tau_n \leq \mathcal{B}_n \forall n > 0$. Corresponding to $\{\tau_n\}$, the sequence $\{\chi_h^n\}$ generated by (5.30) has a converging subsequence (which we still denote with χ_h^n) such that $\chi_h^n \xrightarrow{W^{1,\infty}} \chi_h \in V_h$, which satisfies the discrete optimality conditions (5.27).*

Proof. Consider a generic collection of timesteps $\tilde{\tau}_n$ satisfying $\tilde{\tau}_n \leq \mathcal{B}_n \forall n > 0$. Hence, by Lemma 5.4,

$$\sum_{n=0}^{\infty} \|\chi_h^{n+1} - \chi_h^n\|_{L^2}^2 \leq J_{\varepsilon,h}(\chi_h^0) \quad \text{and} \quad \sup_n J_{\varepsilon,h}(\chi_h^n) \leq J_{\varepsilon,h}(\chi_h^0)$$

which implies that $\|\chi_h^{n+1} - \chi_h^n\|_{L^2} \rightarrow 0$ and hence χ_h^n is bounded in $H^1(\Omega)$, and this implies that also $\{u_h^n\}$ and $\{p_h^n\}$ are bounded in $H^1(\Omega)$. According to the definition of the constants \mathcal{C}_n and \mathcal{B}_n reported in the proof of Lemma 5.4, this entails that there exists a constant $M > 0$ such that $\mathcal{C}_n \leq M \forall n > 0$, and equivalently there exists a positive constant γ s.t. $\gamma \leq \mathcal{B}_n$. Hence, it is possible to choose, for each $n > 0$, $\gamma \leq \tau_n \leq \mathcal{B}_n$.

Eventually, we conclude that there exists $\chi_h \in \mathcal{K}_h$ such that, up to a subsequence, $\chi_h^n \rightarrow \chi_h$ a.e. and in $W^{1,\infty}(\Omega)$ (and $u_h^n \rightarrow u_h := S_h(\chi_h)$, $p_h^n \rightarrow p_h$ in H^1 and in $W^{1,\infty}$ as well, as in the discrete space V_h the L^∞ norm is equivalent to the $L^2(\Omega)$). We exploit the expression of the discrete Parabolic Obstacle Problem (5.30) to show that

$$\begin{aligned} & \int_{\Omega} (1-k) \nabla u_h^n \cdot \nabla p_h^n (\xi_h - \chi_h^{n+1}) + \int_{\Omega} (u_h^n)^3 p_h^n (\xi_h - \chi_h^{n+1}) + 2\alpha\varepsilon \int_{\Omega} \nabla \chi_h^{n+1} \cdot \nabla (\xi_h - \chi_h^{n+1}) \\ & + \alpha \frac{1}{\varepsilon} \int_{\Omega} (1 - 2\chi_h^n) (\xi_h - \chi_h^{n+1}) \geq -\frac{1}{\tau_n} \int_{\Omega} (\chi_h^{n+1} - \chi_h^n) (\xi_h - \chi_h^{n+1}) \quad \forall \xi_h \in \mathcal{K}_h, \end{aligned}$$

and since $-\frac{1}{\tau_n} > -\frac{1}{\gamma} \forall n$, when taking the limit as $n \rightarrow \infty$, the right-hand side converges to 0, which entails that u_h satisfies the discrete optimality conditions (5.27). \square

In order to solve (5.30) we resort the Primal-Dual Active Set method, introduced in [37]. Thus, the final formulation of the reconstruction algorithm is the following:

- 1: Set $n = 0$ and $\chi_h^0 = \chi_0$, the initial guess for the inclusion ;
- 2: **while** $\|\chi_h^n - \chi_h^{n-1}\|_{L^\infty(\Omega)} > \text{tol}_{POP}$ **do**
- 3: solve the direct problem (5.5) with $\chi = \chi_h^n$;
- 4: solve the adjoint problem (5.20) with $\chi = \chi_h^n$;
- 5: compute χ_h^{n+1} solving (5.30) via PDAS algorithm ;
- 6: update $n = n + 1$;
- 7: **end while**
- 8: **return** χ_h^n

Algorithm 7: Solution of the discrete Parabolic Obstacle Problem

Remark 5.3. It is a common practice to increase the performance of a reconstruction algorithm taking advantage of multiple measurements. In this context, it is possible to suppose the knowledge of N_f different measurements of the electric potential on the boundary, $u_{meas,j}$ $j = 1, \dots, N_f$, associated to different source terms f_j . Therefore, instead of tackling the optimization of the mismatch functional J as in (5.12), it is possible to introduce the averaged cost functional $J^{TOT}(\chi) = \frac{1}{N_f} \sum_{j=1}^{N_f} J^j(\chi)$, where $J^j(\chi) = \frac{1}{2} \|S_j(\chi) - u_{meas,j}\|_{L^2(\partial\Omega)}^2$, being $S_j(\chi)$ the solution of the direct

problem (5.5) with source term $f = f_j$. The process of regularization, relaxation and computation of the optimality conditions is exactly the same as for J , and yields the same reconstruction algorithm as in Algorithm 7, where at each timestep the solution of N^f direct and adjoint problem must be computed.

5.5 Numerical results

In this section we report various results obtained applying Algorithm 7. In all the numerical experiments, we consider $\Omega = (-1, 1)^2$ and we introduce an uniform and shape regular tessellation \mathcal{T}_h of triangles. Due to the lack of experimental measures of the boundary datum u_{meas} , we make use of synthetic data, i.e., we simulate the direct problem via the Finite Element method, considering the presence of an ischemic region of prescribed geometry, and extract the value on the boundary of the domain. In order to avoid to incur an inverse crime (i.e. the performance of the reconstruction algorithm are improved by the fact that the exact data are synthetically generated with the same numerical scheme adopted in the algorithm) we introduce a more refined mesh \mathcal{T}_h^{ex} on which the exact problem is solved, and interpolate the resulting datum u_{meas} on the mesh \mathcal{T}_h .

5.5.1 Reconstruction of inclusions of arbitrary shape and topology

In the following test cases, we apply Algorithm 7 for the reconstruct inclusions of different geometries, in order to investigate the effectiveness of the introduced strategy. We use the same computational mesh \mathcal{T}_h (mesh size $h = 0.04$, nearly 6000 elements) for the numerical solution of the boundary value problems involved in the procedure, except for the generation of each synthetic data which is performed on different finer meshes \mathcal{T}_h^{ex} . According to Remark 5.3, we make use of $N_f = 2$ different measurements, associated to the source terms $f_1(x, y) = x$ and $f_2(x, y) = y$. The main parameters for all the simulations lie in the ranges reported in Table 5.1. We make use of the same relationship between ε and τ as in [66]. The initial guess for each simulation is $u_0 \equiv 0$.

α	ε	τ	tol_{POP}
$10^{-4} \div 10^{-3}$	$1/(8\pi)$	$(0.01 \div 0.1)/\varepsilon$	10^{-4}

Table 5.1: Range of the main parameters

In Figure 5.1 we report some of the iterations of Algorithm 7 for the reconstruction of a circular inclusion ($\alpha = 0.0001$, $\tau = 0.01/\varepsilon$). The boundary $\partial\omega$ is marked with a black line, which is superimposed to the contour plot of the approximation of the indicator function u_h^n at different timesteps n . The algorithm converged after $N_{tot} = 568$ iterations, corresponding to a final (fictitious) time $T_{tot} = 1427.54$. In Figure 5.2 we investigate the effectiveness of the algorithm to reconstruct inclusions of rather complicated geometry. For each test case, we show the contour plot of the final iteration of the reconstruction (the total number of iterations N and the final time T are reported in the caption), and the boundary of the exact inclusion is overlaid in black line. Moreover, each result is equipped with the graphic (in semilogarithmic scale) of the evolution of the cost functional J_ε , split into the components $J_{PDE}(\chi) = \frac{1}{2}\|S(\chi) - u_{meas}\|_{L^2(\partial\Omega)}^2$ and $J_{regularization}(\chi) = \alpha\varepsilon\|\nabla\chi\|_{L^2(\Omega)}^2 + \frac{\alpha}{\varepsilon}\int_\Omega \chi(1 - \chi)$. The reported results consist in approximations of minimizers of J_ε

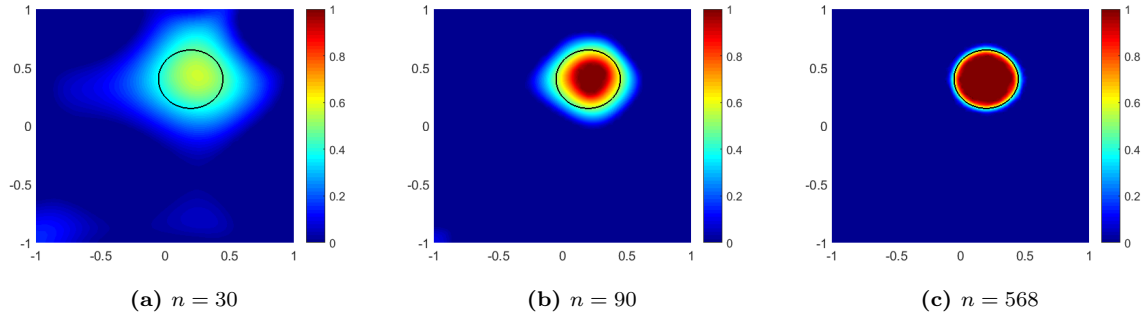


Figure 5.1: Reconstruction of a circular inclusion: successive iterations

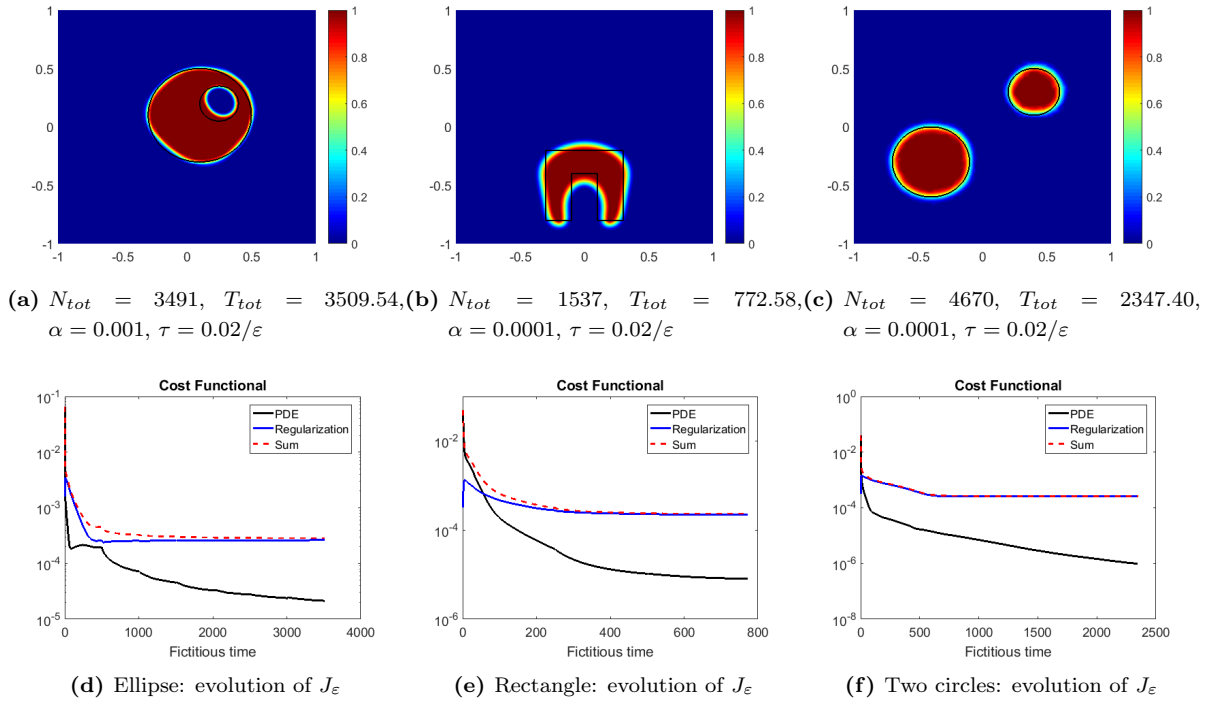


Figure 5.2: Reconstruction of various inclusions

in \mathcal{K} : they are smooth function and range between 0 and 1. They show large regions in which they attain the limit values 0 and 1, and a region of *diffuse interface* between them, whose thickness is about $\varepsilon/2$. As Figures 5.1 and 5.2 show, the algorithm is able to reconstruct inclusion of rather complicated geometry. The identification of smooth inclusion is performed with higher precision, whereas it seems that the accuracy is low in presence of sharp corners. We point out that we do not need to have any *a priori* knowledge on the topology of the inclusion ω , i.e., the number of connected components is correctly identified.

5.5.2 Initial guess

We now assess that the final result of the reconstruction is independent of the initial guess imposed as a starting point of the Parabolic Obstacle problem. In Figure 5.3 we compare the behavior of the algorithm applied to the reconstruction of a circular inclusion (the same as in Figure 5.1), where we impose a different initial datum with respect to the constant zero function. In the first experiment, we start from an initial datum which is the indicator function of an arbitrarily chosen region. In the second one, we impose as a starting point the indicator function of a sublevel of the *topological gradient* of the cost functional J . As investigated in [33], the topological gradient is a powerful tool for the detection of small-size inclusions, which yield a small perturbation in the cost functional with respect to the background (unperturbed) case. The position of a small inclusion is easily identified by searching for the point where the topological gradient of J attains its (negative) minimum. As the information given by the topological gradient G has shown to be useful even in the case of large-size inclusions (see, e.g., [28], [49]), we take advantage of it by computing G (see Theorem 3.1 in [33]), setting a threshold G_{thr} and defining $u_0 = \chi_{\{G \leq G_{thr}\}}$. The results reported in Figure 5.3 show the

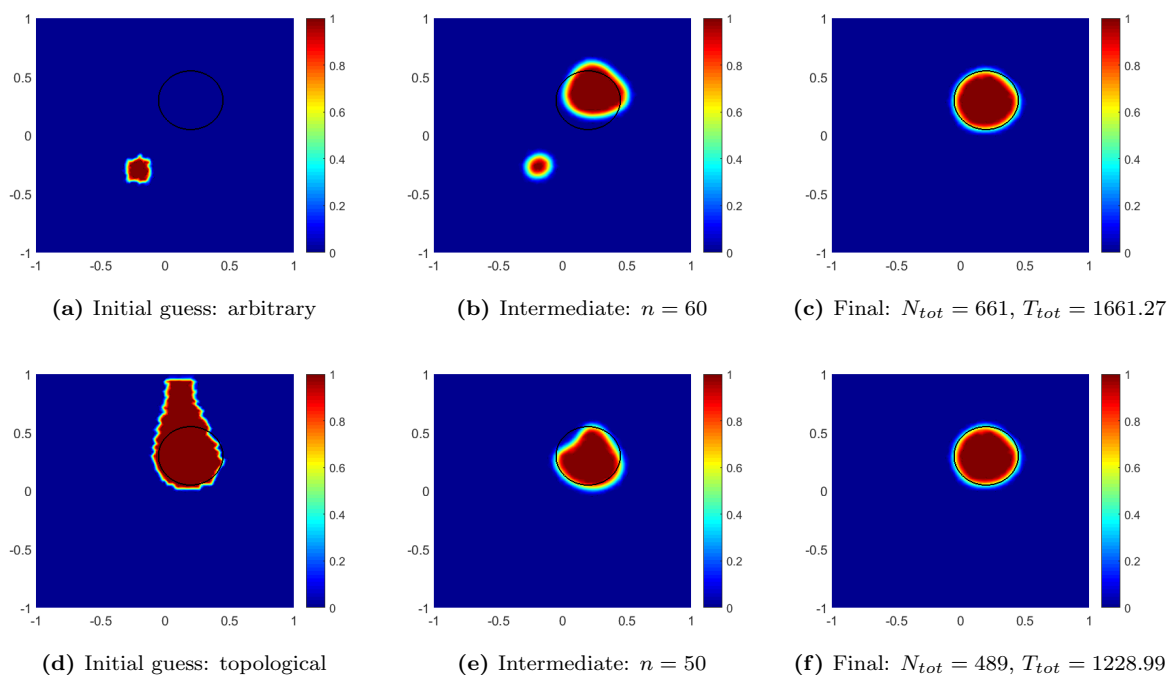


Figure 5.3: Reconstruction of a circular inclusion with different initial conditions

starting point of the algorithm, an intermediate iteration and the final reconstruction. In both cases we set $\alpha = 0.001$, $\varepsilon = 1/(8\pi)$ and $\tau = 0.1/\varepsilon$. We underline that the result in each case is similar to the one depicted in Figure 5.1, but through the second strategy it was possible to perform a smaller number of iterations.

5.5.3 Mesh size and adaptation

Another interesting investigation is the comparison of the results obtained when perturbing the relaxation parameter ε . In Figure 5.4 we report the final reconstruction of an ellipse-shaped inclusion when setting $\varepsilon = \frac{1}{4\pi}, \frac{1}{8\pi}, \frac{1}{16\pi}$. As expected, it is possible to remark that the thickness of the diffuse

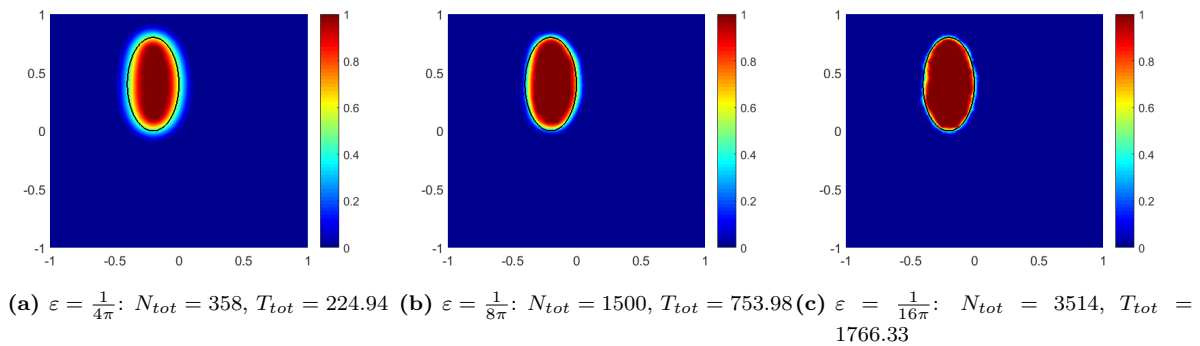


Figure 5.4: Reconstruction of a circular inclusion with different ε

interface region decreases as ε decreases. Nevertheless, one must take into account the size of the computational mesh \mathcal{T}_h : in the last test of Figure 5.4, the thickness of the region in which the final iteration $\chi_h^{N_{tot}}$ increases from 0 to 1 is of the same order of magnitude as h_{max} . This is rather likely the reason why the edge of the reconstructed inclusion appears to be irregular and jagged. A natural strategy to avoid the problem would be to make use of a finer mesh, e.g., ensuring that $h_{max} < \varepsilon/10$; however, that could result in an extremely high computational effort. It is possible to overcome this drawback by introducing an adaptive mesh refinement strategy, i.e., by locally refining the mesh close to the region of the detected edges. In Figure 5.5 we compare the result obtained when approximating a rectangular and a circular inclusion with $\varepsilon = \frac{1}{16\pi}$ on the reference mesh or through a process of mesh adaptation. We invoked a goal-oriented mesh adaptation algorithm each $N_{adapt} = 50$ iterations, requiring for a higher refinement of the grid in proximity to higher values of $|\nabla \chi_h^n|$ and for a lower refinement in the regions where χ_h^n is approximately constant. This allows to have more precise reconstruction even for small ε , almost without increasing the global number of elements of the mesh. In Figure 5.5, we also report the final configuration of the refined computational mesh.

5.5.4 Robustness with respect to measurements

We finally verify the stability result obtained in Proposition 5.11, by testing the reconstruction algorithm when the measured boundary data are perturbed by a small amount of noise. In particular, we consider $u_\eta = u_{meas} + \eta\zeta$, being ζ a Gaussian random variable with null mean and standard deviation equal to $\max_\Omega u_{meas} - \min_\Omega u_{meas}$ and $\eta \in [0, 1]$ the noise level. In Figure 5.6 we report the final results of the reconstruction algorithm when applied to the boundary measurements related to an elliptical inclusion perturbed with different noise level. For each simulation, we fix $\alpha = 0.001$ and $\varepsilon = \frac{1}{8\pi}$. In Figure 5.7, instead, we investigate the effect of the regularization parameter α in

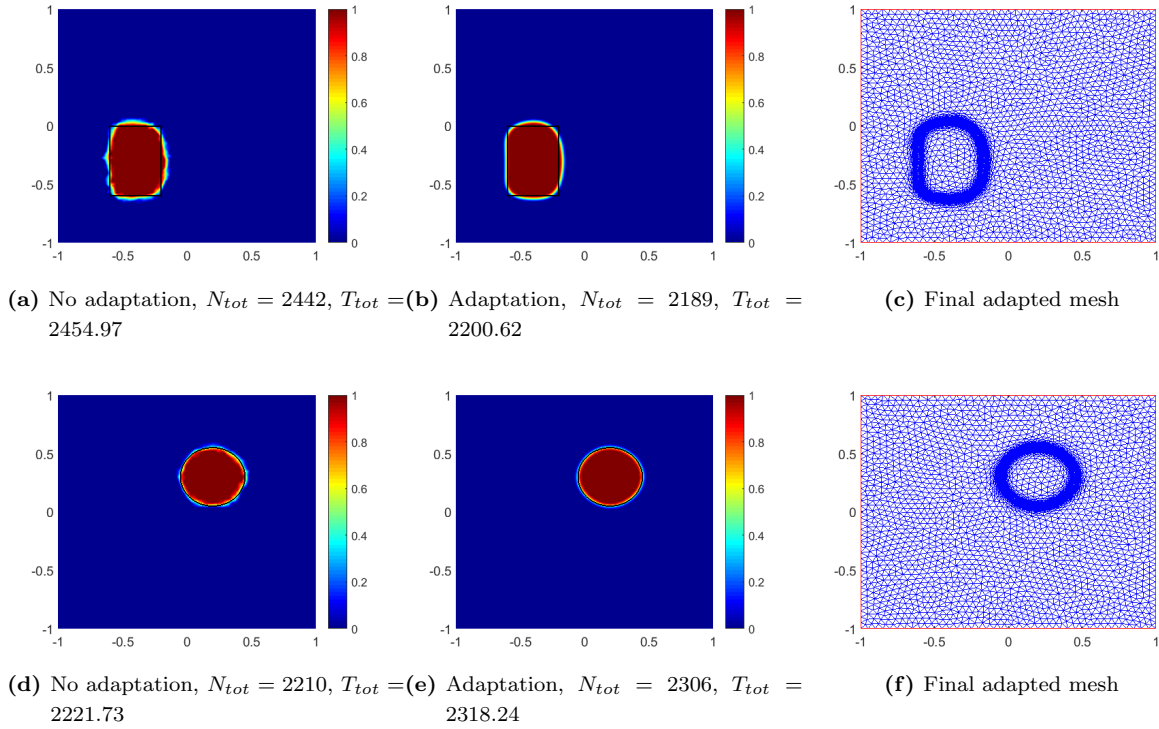


Figure 5.5: Mesh adaptation: result comparison

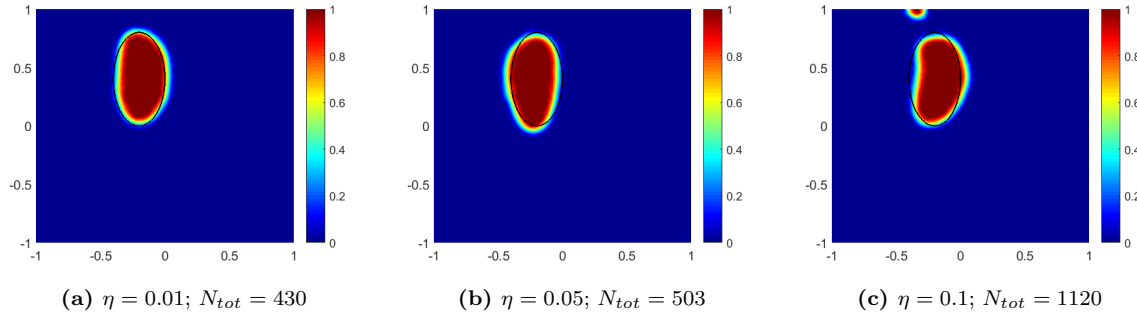


Figure 5.6: Reconstruction of an elliptical inclusion with noisy measurements

the reconstruction from noisy data, fixing $\eta = 0.1$. We observe that a higher value of α may help in filtering the information coming from the noise, avoiding to let it spoil the reconstruction, although it might result in an overall loss of precision.

5.6 Comparison with the Shape Derivative approach

In the previous sections, we have analyzed in detail the phase-field relaxation of the minimization problem expressed in (5.13). We now aim at describing the relationship between this method and

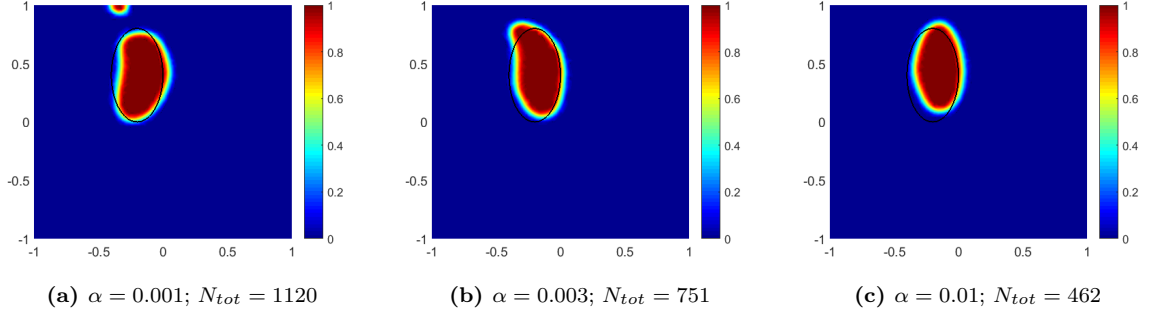


Figure 5.7: Reconstruction of an elliptical inclusion with noisy measurements

a shape derivative based approach analogous to the one proposed in Chapter 4, which consists in updating the shape of the inclusion to be reconstructed by perturbing its boundary along the directions of the vector field which causes the greatest descent of the cost functional. Such a direction can be deduced by computing the shape derivative of the functional itself. In this section, we first theoretically investigate the relationship between the shape derivative of the cost functional J_{reg} and the Fréchet derivative of J_ε and then report a comparison between the numerical results of the two algorithms in a set of benchmark cases.

5.6.1 Sharp interface limit of the Optimality Conditions

In order to study the relationship between the optimality conditions in the phase-field approach and the ones derived in the sharp case, we follow an analogous approach as in [38]. First of all, in Proposition 5.19 we introduce the necessary optimality condition for the sharp problem (5.13), taking advantage of the computation of the material derivative of the cost functional. Such a derivative consists in a generalization of the one computed in Chapter 4. We then define in Proposition 5.21 similar optimality conditions for the relaxed problem (5.17), which are related but not equivalent to the one stated in (5.18)-(5.19) through the Fréchet derivative. In Proposition 5.22 we finally assess the convergence of the phase-field optimality condition to the sharp one when $\varepsilon \rightarrow 0$.

For the sake of simplicity, in this section, we will refer to J_{reg} as J . Consider the minimization problem (as in (5.13)):

$$\arg \min_{\chi \in X_{0,1}} J(\chi); \quad J(\chi) = \frac{1}{2} \|S(\chi) - u_{meas}\|_{L^2(\partial\Omega)}^2 + \alpha TV(\chi). \quad (5.32)$$

Since $\chi \in X_{0,1}$ implies that $\chi = \chi_\omega$, being ω a finite-perimeter subset of Ω , we can perturb χ by means of a vector field $\phi_t : \Omega \rightarrow \mathbb{R}^2$, $\phi_t(x) = x + tV(x)$, being

$$V \in C^1(\Omega) \text{ s.t. } V(x) = 0 \text{ in } \Omega^{d_0} = \{x \in \Omega \text{ s.t. } \text{dist}(x, \partial\Omega) \leq d_0\}. \quad (5.33)$$

Consider the family of functions $\{\chi_t\}$: $\chi_t = \chi \circ \phi_t^{-1}$: we can compute the shape derivative of the functional J in χ along the direction V (see [67]) as

$$DJ(\chi)[V] := \lim_{t \rightarrow 0} \frac{J(\chi_t) - J(\chi)}{t}, \quad (5.34)$$

where $J(\chi_t)$ is the cost functional evaluated in the deformed domain $\Omega_t = \phi_t(\Omega)$ but, according to (5.33), Ω_t and Ω are the same set, thus we do not adopt a different notation. We prove the following result:

Proposition 5.19. *If χ is a solution of (5.32) and $f \in L^2(\Omega)$ satisfies assumption (5.4), then*

$$DJ(\chi)[V] = 0 \quad \text{for all the smooth vector fields } V. \quad (5.35)$$

The shape derivative is given by:

$$DJ(\chi)[V] = \int_{\partial\Omega} (S(\chi) - u_{meas}) \dot{S}(\chi)[V] + \int_{\Omega} (\operatorname{div} V - DV\nu \cdot \nu) d|D\chi|, \quad (5.36)$$

where $d|D\chi| = \delta_{\partial\omega} dx$, ν is the generalized unit normal vector (see [83]) and $\dot{S}(\chi)[V] =: \dot{S}$, the material derivative of the solution map, solves

$$\begin{aligned} \int_{\Omega} a(\chi) \nabla \dot{S} \cdot \nabla v + \int_{\Omega} b(\chi) 3S(\chi)^2 \dot{S} v = - \int_{\Omega} a(\chi) \mathcal{A} \nabla S(\chi) \cdot \nabla v - \int_{\Omega} b(\chi) S(\chi)^3 v \operatorname{div} V + \\ \int_{\Omega} \operatorname{div}(fV) v \quad \forall v \in H^1(\Omega), \end{aligned} \quad (5.37)$$

being $\mathcal{A} = \operatorname{div} V - (DV + DV^T)$.

Proof. We start by deriving the formula of the material derivative of the solution map. Define $S_0 = S(\chi)$ and $S_t : \Omega \rightarrow \mathbb{R}$, $S_t = S(\chi_t) \circ \phi_t$. Then, applying the change of variables induced by the map ϕ_t , it holds that

$$\int_{\Omega} a(\chi) A(t) \nabla S_t \cdot \nabla v + \int_{\Omega} b(\chi) S_t^3 v |\det D\phi_t| = \int_{\Omega} (f \cdot \phi_t) v |\det D\phi_t| \quad \forall v \in H^1(\Omega), \quad (5.38)$$

where $A(t) = D\phi_t^{-T} D\phi_t^{-1} |\det D\phi_t|$. By computation,

$$\frac{d}{dt} A(t) = \mathcal{A} = (\operatorname{div} V)I - (DV^t + DV) \quad \text{and} \quad \frac{d}{dt} |\det D\phi_t| = \operatorname{div} V.$$

Subtract (5.5) from (5.38) and divide by t : then $w_t = \frac{S_t - S_0}{t}$ is the solution of

$$\begin{aligned} \int_{\Omega} a(\chi) A(t) \nabla w_t \cdot \nabla v + \int_{\Omega} b(\chi) q_t w_t v |\det(D\phi_t)| = - \int_{\Omega} a(\chi) \frac{A(t) - I}{t} \nabla S_0 \cdot \nabla v \\ - \int_{\Omega} \frac{|\det(D\phi_t)| - 1}{t} b(\chi) S_0^3 v + \int_{\Omega} \frac{1}{t} (f \circ \phi_t) v |\det(D\phi_t)| - \int_{\Omega} \frac{1}{t} f v \end{aligned} \quad (5.39)$$

$\forall v \in H^1(\Omega)$, where the norm of the right-hand side in the dual space of $H^1(\Omega)$ is bounded by

$$\begin{aligned} \left\| \frac{A - I}{t} \right\|_{L^\infty(\Omega)} \|S_0\|_{H^1(\Omega)} + \left\| \frac{|\det(D\phi_t)| - 1}{t} \right\|_{L^\infty(\Omega)} \|S_0\|_{H^1(\Omega)} \\ + \left\| \frac{|\det(D\phi_t)| - 1}{t} \right\|_{L^\infty(\Omega)} \|f\|_{L^2(\Omega)} + C(\|V\|_{C(\Omega)}) \|f\|_{H^1(\Omega)} \leq C_F, \end{aligned}$$

being C_F independent of t . Moreover, the matrix $A(t)$ is symmetric positive definite: $(A(t)y) \cdot y \geq \frac{1}{2} \|y\|^2 \quad \forall y \in \mathbb{R}^2, \forall t$. Together with the property that $q_t = \chi_t^2 + \chi_t \chi + \chi^2 \geq \frac{3}{4} \chi^2$, and thanks to Proposition 5.4 and to the Poincaré inequality in Lemma 5.1,

$$\|w_t\|_{H^1}^2 \leq C \left(k \|\nabla w_t\|_{L^2}^2 + \frac{3}{4} m^{2/3} \|w_t\|_{L^2(\Omega^{d_0})}^2 \right) \leq C_F \|w_t\|_{H^1}.$$

Thus, $\|w_t\|_{H^1}$ is bounded independently of t , from which it follows that $\|S_t - S_0\|_{H^1(\Omega)} \leq Ct$ and that every sequence $\{w_n\} = \{w_{t_n}, t_n \rightarrow 0\}$ is bounded in $H^1(\Omega)$, thus $w_t \xrightarrow{H^1} w \in H^1(\Omega)$. We aim at proving that w is also the limit of w_t in the strong convergence, which entails that

$$\dot{S}(\chi)[V] := \lim_{t \rightarrow 0} \frac{S_t - S_0}{t} = w.$$

First of all, we show that w is the solution of problem (5.37). It follows from (5.39), since $q_t w_t = \frac{1}{t}(S_t^3 - S_0^3) = \frac{1}{t}((S_0 + t w_t)^3 - S_0^3) = 3S_0^2 w_t + 3t S_0 w_t^2 + t^2 w_t^3$, that

$$\begin{aligned} & \int_{\Omega} a(\chi) A(t) \nabla w_t \cdot \nabla v + \int_{\Omega} b(\chi) 3S_0^2 w_t v |det D\phi_t| = - \int_{\Omega} a(\chi) \frac{A(t) - I}{t} \nabla S_0 \cdot \nabla v \\ & - \int_{\Omega} \frac{|det D\phi_t| - 1}{t} b(\chi) S_0^3 v - \int_{\Omega} b(\chi) 3t S_0 w_t^2 v |det D\phi_t| - \int_{\Omega} b(\chi) t^2 w_t^3 v |det D\phi_t| \\ & + \int_{\Omega} (f \circ \phi_t) \frac{|det D\phi_t| - 1}{t} v - \int_{\Omega} \frac{(f \circ \phi_t) - f}{t} v \quad \forall v \in H^1(\Omega). \end{aligned} \quad (5.40)$$

Taking the limit as $t \rightarrow 0$ and by the weak convergence of w_t in H^1 , we recover the same expression as in (5.37). One may eventually show that $w_t \xrightarrow{H^1} w$. In order to do this we start proving that

$$\int_{\Omega} a(\chi) A(t) |\nabla w_t|^2 + \int_{\Omega} b(\chi) |det D\phi_t| 3S_0^2 w_t^2 \rightarrow \int_{\Omega} a(\chi) |\nabla w|^2 + \int_{\Omega} b(\chi) 3S_0^2 w^2. \quad (5.41)$$

Indeed, take (5.40) and substitute $v = w_t$: using the weak convergence of w_t in the right-hand side, we obtain that

$$\begin{aligned} & \int_{\Omega} a(\chi) A(t) |\nabla w_t|^2 + \int_{\Omega} b(\chi) |det D\phi_t| 3S_0^2 w_t^2 \rightarrow - \int_{\Omega} a(\chi) \mathcal{A} \nabla S_0 \cdot \nabla w - \int_{\Omega} div V b(\chi) S_0^3 w \\ & + \int_{\Omega} f w div V - \int_{\Omega} \nabla f \cdot V w \stackrel{(5.37)}{=} \int_{\Omega} a(\chi) |\nabla w|^2 + \int_{\Omega} b(\chi) 3S_0^2 w^2. \end{aligned}$$

We then compute:

$$\begin{aligned} & \int_{\Omega} a(\chi) A(t) |\nabla(w_t - w)|^2 + \int_{\Omega} b(\chi) 3S_0^2 (w_t - w)^2 |det D\phi_t| = \\ & \int_{\Omega} a(\chi) A(t) |\nabla w_t|^2 + \int_{\Omega} a(\chi) A(t) |\nabla w|^2 - 2 \int_{\Omega} a(\chi) A(t) \nabla w_t \cdot \nabla w \\ & + \int_{\Omega} b(\chi) 3S_0^2 w_t^2 |det D\phi_t| + \int_{\Omega} b(\chi) 3S_0^2 w^2 |det D\phi_t| - 2 \int_{\Omega} b(\chi) 3S_0^2 w_t w |det D\phi_t|. \end{aligned} \quad (5.42)$$

Using (5.41), the convergence of A to I and of $|det D\phi_t|$ to 1, and the fact that $w_t \xrightarrow{H^1} w$, we derive that

$$\int_{\Omega} a(\chi) |\nabla(w_t - w)|^2 + \int_{\Omega} b(\chi) 3S_0^2 (w_t - w)^2 \rightarrow 0$$

A combination of the Proposition 5.4 and of the Poincaré inequality in Lemma 5.1 allows to conclude that also $\|w_t - w\|_{H^1} \rightarrow 0$.

We now prove the necessary optimality conditions for the optimization problem (5.32). The derivative of the quadratic part of the cost functional J can be easily computed by means of the

material derivative of the solution map:

$$\begin{aligned}
& \lim_{t \rightarrow 0} \frac{1}{2} \int_{\partial\Omega} \frac{(S(\chi_t) - u_{meas})^2 |det(D\phi_t)| - (S_0 - u_{meas})^2}{t} \quad (\text{since } S(\chi_t) = S_t \text{ on } \partial\Omega) \\
&= \lim_{t \rightarrow 0} \frac{1}{2} \int_{\partial\Omega} (S_t - u_{meas})^2 \frac{|det(D\phi_t)| - 1}{t} + \lim_{t \rightarrow 0} \frac{1}{2} \int_{\partial\Omega} \frac{(S_t - u_{meas})^2 - (S_0 - u_{meas})^2}{t} \quad (5.43) \\
&= \frac{1}{2} \int_{\partial\Omega} (S_0 - u_{meas})^2 div V + \int_{\partial\Omega} \dot{S}(\chi)[V](S_0 - u_{meas}),
\end{aligned}$$

and the first integral in the latter expression vanishes since $V = 0$ on Ω_{d_0} . On the other hand, using Lemma 10.1 of [83] and the remark 10.2, we recover the expression for the derivative of the Total Variation of χ , which is the same reported in (5.36). \square

The optimality conditions reported in (5.35) are, at the best of our knowledge, the most general result which can be obtained in this case, i.e. by simply assuming that $\chi = \chi_\omega$ and ω is a set of finite perimeter. We point out that, assuming more *a priori* information on χ , it is possible to recover from (5.36) the expression of the *shape gradient* of the cost functional J . By assuming that $\partial\omega$ is of class C^2 , we come back to the main result proved in Chapter 4:

Proposition 5.20. *Suppose that $\omega \subset \Omega$ is open, connected, well separated from the boundary $\partial\Omega$ and regular ($\partial\omega$ is at least of class C^2), and $\chi = \chi_\omega$. Then, the expression of the shape derivative of the cost functional J along a smooth vector field V is:*

$$DJ(\chi)[V] = \int_{\partial\omega} \left[(1-k) \left(\nabla_\tau S(\chi) \cdot \nabla_\tau w + \frac{1}{k} \nabla_\nu S(\chi)^e \cdot \nabla_\nu w^e \right) + S(\chi)^3 w + \mathcal{H} \right] V \cdot \nu, \quad (5.44)$$

where w is the solution of the adjoint problem (see (5.20)). The gradients $\nabla S(\chi)$ and ∇w are decomposed in the normal and tangential component with respect to the boundary $\partial\omega$, and due to the transmission condition of the direct problem their normal components are discontinuous across $\partial\omega$: the valued assumed in $\Omega \setminus \omega$ is marked as $\nabla_\nu S(\chi)^e$. The term \mathcal{H} is instead the curvature of the boundary.

For the sake of completeness, we point out that the latter result can be easily generalized to the case in which ω is the union of N_c disjoint, well separated, components, each of them satisfying the expressed hypotheses. Thanks to the results recently obtained in [31], we expect formula (5.44) to be valid also under milder assumption, in particular for polygons.

We aim at demonstrating that the expression of the shape derivative reported in (5.35) is the limit, as $\varepsilon \rightarrow 0$, of the shape derivative of the relaxed cost functional J_ε (defined as in (5.34), replacing χ by χ_ε and J by J_ε). In order to accomplish this result, we need to introduce necessary optimality conditions for the relaxed problem (5.17) which are different from the ones reported in Proposition 5.14 and can be derived by the same technique as in Proposition 5.19 as shown in the following result.

Proposition 5.21. *If χ_ε is a solution of (5.17), then*

$$DJ_\varepsilon(\chi_\varepsilon)[V] = 0 \quad \text{for all the smooth vector fields } V, \quad (5.45)$$

The expression of the derivative is given by:

$$\begin{aligned} DJ_\varepsilon(\chi_\varepsilon)[V] &= \int_{\partial\Omega} (S(\chi_\varepsilon) - u_{meas}) \dot{S}(\chi_\varepsilon)[V] + \alpha\varepsilon \int_{\Omega} |\nabla\chi_\varepsilon|^2 \operatorname{div}V \\ &\quad - 2\alpha\varepsilon \int_{\Omega} DV \nabla\chi_\varepsilon \cdot \nabla\chi_\varepsilon + \frac{\alpha}{\varepsilon} \int_{\Omega} \chi_\varepsilon(1 - \chi_\varepsilon) \operatorname{div}V \end{aligned} \quad (5.46)$$

where $\dot{S}(\chi_\varepsilon)[V]$ solves the same problem as in (5.37), replacing χ with χ_ε .

Proof. The same strategy as in the proof of Proposition 5.19 can be adapted to compute $\dot{S}(\chi_\varepsilon)[V]$ and the derivative of the first term of the cost functional. We now derive with the same computational rules the relaxed penalization term. Recall

$$F_\varepsilon(\chi_\varepsilon) = \alpha\varepsilon \int_{\Omega} |\nabla\chi_\varepsilon|^2 + \frac{\alpha}{\varepsilon} \int_{\Omega} \psi(\chi_\varepsilon),$$

being $\psi : \mathbb{R} \rightarrow \mathbb{R}$, $\psi(x) = x(1 - x)$. After the deformation from χ_ε to $\chi_\varepsilon \circ \phi_t^{-1}$ and applying the change of variables induced by ϕ_t ,

$$F_\varepsilon(\chi_\varepsilon \circ \phi_t^{-1}) = \alpha\varepsilon \int_{\Omega} A(t) \nabla\chi_\varepsilon \cdot \nabla\chi_\varepsilon + \frac{\alpha}{\varepsilon} \int_{\Omega} \psi \circ \chi_\varepsilon \circ \phi_t^{-1}.$$

Hence,

$$\begin{aligned} \dot{F}_\varepsilon(\chi_\varepsilon)[V] &= \lim_{t \rightarrow 0} \frac{F_\varepsilon(\chi_\varepsilon \circ \phi_t^{-1}) - F_\varepsilon(\chi_\varepsilon)}{t} = \alpha\varepsilon \int_{\Omega} \mathcal{A} \nabla\chi_\varepsilon \cdot \nabla\chi_\varepsilon + \alpha\varepsilon \frac{\alpha}{\varepsilon} \int_{\Omega} \psi(\chi_\varepsilon) \operatorname{div}V = \\ &= \alpha\varepsilon \int_{\Omega} |\nabla\chi_\varepsilon|^2 \operatorname{div}V - \alpha\varepsilon \int_{\Omega} (DV + DV^T) \nabla\chi_\varepsilon \cdot \nabla\chi_\varepsilon + \frac{\alpha}{\varepsilon} \int_{\Omega} \chi_\varepsilon(1 - \chi_\varepsilon) \operatorname{div}V, \end{aligned}$$

which is the same expression as in (5.46), since $DV^T \nabla v \cdot \nabla v = DV \nabla v \cdot \nabla v$. \square

We point out that the optimality conditions deduced in the latter proposition are not equivalent to the ones expressed in Proposition 5.14 via the Fréchet derivative of J_ε . Nevertheless, if χ_ε satisfies (5.18)-(5.19), then it also satisfies (5.45) (it is sufficient to consider in (5.18) $v = \chi_\varepsilon \circ \phi_t^{-1}$, which belongs to \mathcal{K} thanks to the regularity of V), whereas the contrary is not valid in general. In particular, due to the regularity of the perturbation fields V , the optimality conditions (5.45) do not take into account possible topological changes of the inclusion: for example, the number of connected components of ω cannot change. We remark that this holds also for the optimality conditions (5.35) for the sharp problem, and consists in a limitation for the effectiveness of the reconstruction via a shape derivative approach: the initial guess of the reconstruction algorithm and the exact inclusion must be diffeomorphic.

We are now able to show the sharp interface limit of the expression of the shape derivative of the relaxed cost functional J_ε as $\varepsilon \rightarrow 0$, which is done in the following proposition.

Proposition 5.22. *Consider a family $\bar{\chi}_\varepsilon$ s.t. $\bar{\chi}_\varepsilon \in \mathcal{K} \forall \varepsilon > 0$ and $\bar{\chi}_\varepsilon \xrightarrow{L^1} \bar{\chi} \in BV(\Omega)$ as $\varepsilon \rightarrow 0$. Then,*

$$DJ_\varepsilon(\bar{\chi}_\varepsilon)[V] \rightarrow DJ(\bar{\chi})[V] \quad \text{for every smooth vector field } V.$$

Proof. We follow a similar argument as in the proof of [38, Theorem 21]. Thanks to Proposition 5.5, $\bar{\chi}_\varepsilon \xrightarrow{L^1} \bar{\chi} \Rightarrow S(\bar{\chi}_\varepsilon) \xrightarrow{H^1} S(\bar{\chi})$. Also $\dot{S}(\bar{\chi}_\varepsilon)[V] \xrightarrow{H^1} \dot{S}(\bar{\chi})[V]$: the proof is done by subtracting the equations of which $\dot{S}(\bar{\chi}_\varepsilon)[V]$ and $\dot{S}(\bar{\chi})[V]$ and verifying that the norm of their difference is controlled by the norm of $S(\bar{\chi}_\varepsilon) - S(\bar{\chi})$ in $H^1(\Omega)$. Thanks to these results, surely

$$\int_{\Omega} (S(\chi_\varepsilon) - u_{meas}) \dot{S}(\bar{\chi}_\varepsilon)[V] \rightarrow \int_{\Omega} (S(\chi) - u_{meas}) \dot{S}(\bar{\chi})[V].$$

Eventually, the convergence

$$\alpha\varepsilon \int_{\Omega} |\nabla \bar{\chi}_\varepsilon|^2 \operatorname{div} V - 2\alpha\varepsilon \int_{\Omega} DV \nabla \bar{\chi}_\varepsilon \cdot \nabla \bar{\chi}_\varepsilon + \frac{\alpha}{\varepsilon} \int_{\Omega} \bar{\chi}_\varepsilon (1 - \bar{\chi}_\varepsilon) \operatorname{div} V \rightarrow \int_{\Omega} (\operatorname{div} V - DV \nu \cdot \nu) d|D\bar{\chi}|$$

is proved in [79], Theorem 4.2 (see also annotations in [38], proof of Theorem 21). \square

In particular, we point out that this implies, together with Proposition 5.13, that the expression of the optimality condition for the phase field problem converges, as $\varepsilon \rightarrow 0$, to the one in the sharp case.

5.6.2 Comparison with the shape derivative algorithm

In this section, we report some results of the application of the algorithm based on the shape derivative. In the implementation, we take advantage of the Finite Element method to solve the direct and adjoint problems and compute the shape gradient as in (5.44). We consider an initial guess for the inclusion (in all the simulations reported, the initial guess is a disc centered in the origin with radius 0.02) and discretize its boundary with a finite number of points, which always coincide with vertices of the numerical mesh. We iteratively perturb the inclusion by moving the boundary with a normal vector field V which is the projection in the Finite Element space of the shape gradient reported in (5.44) (see e.g. [69] for more details). After the descent direction is determined, a backtracking scheme is implemented (see [114]), in order to guarantee the decrease of the cost functional J at each iteration. As in the case of Algorithm 7, we start from the initial guess $\chi^0 \equiv 0$ and take advantage of $N_f = 2$ measurements, associated to the same source terms. The main parameters of this set of simulations are reported in Table 5.2.

α	<i>maxstep</i>	<i>tol</i>
10^{-3}	10	10^{-6}

Table 5.2: Values of the main parameters

In Figure 5.8 we report the results of the reconstruction with the shape gradient algorithm compared to the ones of the Parabolic Obstacle problem (with $\varepsilon = \frac{1}{16\pi}$ and with mesh adaptation). Each result is endowed with a plot of the evolution of the cost functional throughout time (in particular, of $J_{PDE}(u) = \frac{1}{2} \|S(u) - u_{meas}\|_{L^2(\partial\Omega)}$). The reconstruction achieved by the shape gradient algorithm is qualitatively as accurate as the phase-field one. The first method is less expensive in terms of number of iterations. Nevertheless, it requires *a priori* knowledge about the topology of the unknown inclusion.

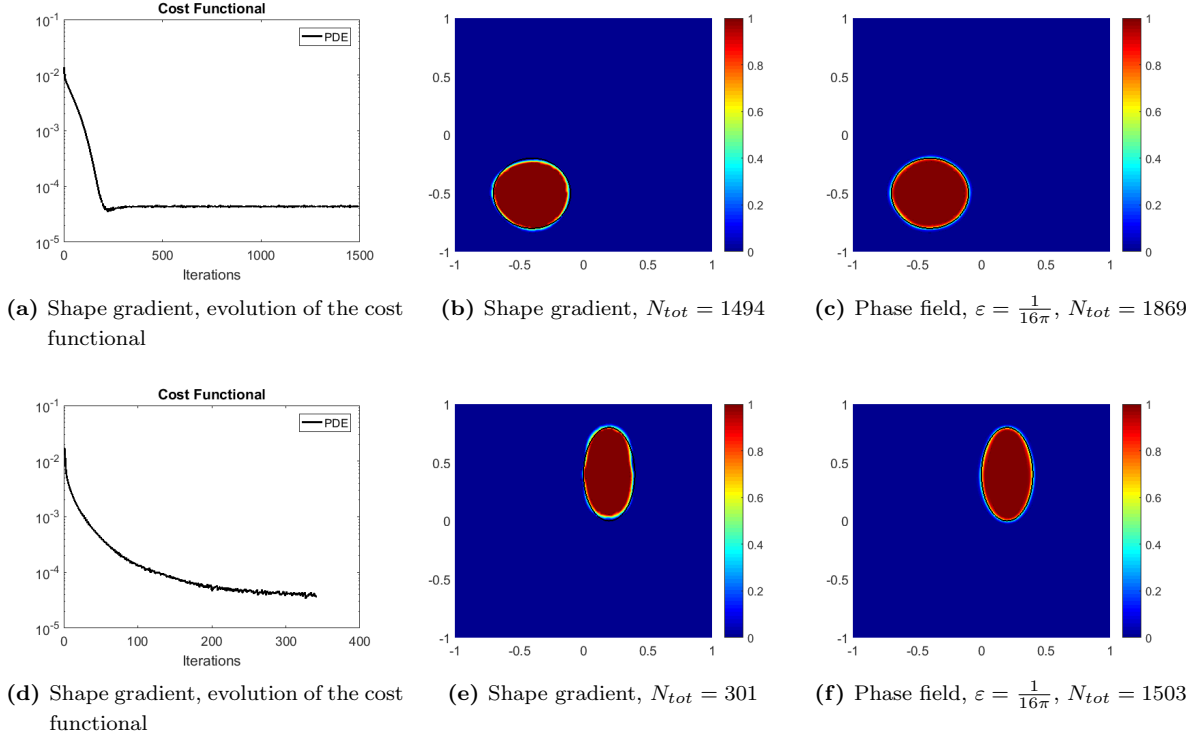


Figure 5.8: Shape gradient algorithm: result comparison

5.7 Alternative: a saddle-point problem

In this section, we present a reconstruction algorithm for the solution of the inverse problem which consists in an alternative with respect to the phase-field approach. We develop an algorithm for the minimization of the cost functional J_{reg} , see (5.13), which involves the Lagrangian strategy reported in [26, Chapter 10] for an image reconstruction problem. As expressed in Section 5.3, the main difficulties which required the introduction of a relaxation of the cost functional are the non-convexity of the space $X_{0,1}$ and the non-differentiability of J_{reg} (especially the TV-part). An alternative, which is explored in this section, is to look for a minimizer of J_{reg} within the space $BV(\Omega, [0, 1])$, which is indeed convex. In order to overcome the non-differentiability of J_{reg} , we exploit the definition of the Total Variation of a BV-function to formulate the minimization problem (5.13) in an alternative way: since

$$TV(\chi) = \sup \left\{ \int_{\Omega} \chi \operatorname{div}(p) : p \in C_C^1(\Omega; \mathbb{R}^d), \|p\|_{L^\infty} \leq 1 \right\},$$

we introduce the Lagrangian functional $L(\chi, p)$:

$$L(\chi, p) = \frac{1}{2} \|S(\chi) - y_{meas}\|_{L^2(\partial\Omega)}^2 + \int_{\Omega} \chi \operatorname{div}(p). \quad (5.47)$$

We consider $\chi \in BV(\Omega; [0, 1])$ and $p \in \mathcal{P} = \{q \text{ s.t. } q \in L^2(\Omega; \mathbb{R}^d), \operatorname{div}(q) \in L^2(\Omega), p \cdot \nu = 0 \text{ on } \partial\Omega, |p| \leq 1 \text{ a.e.}\}$; \mathcal{P} is the closure of $C_C^1(\Omega; \mathbb{R}^d)$ with respect to the norm $\|\cdot\|_{L^2} + \|\operatorname{div}(\cdot)\|_{L^2}$.

After introducing L , instead of searching for a minimum point $\chi \in BV(\Omega; [0, 1])$ of J_{reg} we might look for a couple $(\chi, p) \in BV(\Omega; [0, 1]) \times \mathcal{P}$ which solves the following *saddle-point problem*:

$$\text{find } (\chi, p) \in BV(\Omega; [0, 1]) \times \mathcal{P} \text{ s.t. } \begin{cases} L(\chi, p) \leq L(\xi, p) & \forall \xi \in BV(\Omega; [0, 1]) \\ L(\chi, p) \geq L(\chi, q) & \forall q \in \mathcal{P} \end{cases} \quad (5.48)$$

5.7.1 Reconstruction algorithm: Uzawa Total Variation flow

In order to define a numerical algorithm for the approximation of the solution of (5.48), we introduce a discretization of the spaces in which the problem is set: defined a tessellation \mathcal{T}_h of the domain Ω , we look for $\chi_h \in \mathcal{K}_h$, being \mathcal{K}_h the Finite Element space introduced in Section 5.4; whereas $p_h \in P_h$, the space of vectorial functions which are element-wise constant on \mathcal{T}_h and such that $|p_h| \leq 1$. The discretized Lagrangian can be rewritten as

$$L_h(\chi_h, p_h) = \frac{1}{2} \|S(\chi_h) - u_{meas,h}\|_{L^2(\partial\Omega)}^2 + \int_{\Omega} \nabla \chi_h \cdot p_h. \quad (5.49)$$

The numerical algorithm for the research of a saddle point of L_h in $\mathcal{K}_h \times P_h$ that we propose is an Uzawa iterative algorithm, allowing to define a sequence of approximations (χ_h^k, p_h^k) which consists in a descent flow for L_h with respect to χ and in an ascent flow for L_h with respect to p .

$$\begin{cases} \chi_h^0, p_h^0 \text{ given. For } k = 0, 1, \dots, \\ \text{find } \chi_h^{k+1} \text{ s.t. } (\chi_h^{k+1} - \chi_h^k, \xi_h - \chi_h^{k+1}) + \partial_{\chi} L_h(\chi_h^k, p_h^k)[\xi_h - \chi_h^{k+1}] \geq 0 & \forall \xi_h \in \mathcal{K}_h \\ \text{find } p_h^{k+1} \text{ s.t. } (p_h^{k+1} - p_h^k, q_h - p_h^{k+1}) - \partial_p L_h(\chi_h^{k+1}, p_h^{k+1})[q_h - p_h^{k+1}] \geq 0 & \forall p_h \in P_h. \end{cases} \quad (5.50)$$

where $\partial_{\chi} L_h$ and $\partial_p L_h$ are the Fréchet derivatives of the Lagrangian functional with respect to its first and second variable respectively. We remark that, in the first variational inequality, we would prefer to evaluate $\partial_{\chi} L_h$ in $(\chi_h^{k+1}, p_h^{k+1})$, but that would yield the presence of terms which are highly non linear with respect to χ_h^{k+1} and would require expensive algorithm for the solution. Indeed, the expression of the derivative is deduced by formal computations and is the following one:

$$\begin{aligned} \partial_{\chi} L_h(\chi_h, p_h)[\vartheta_h] &= 2S'(\chi_h)[\vartheta_h] + \int_{\Omega} p_h \cdot \nabla \vartheta_h \\ \partial_p L_h(\chi_h, p_h)[\psi_h] &= \int_{\Omega} \psi_h \cdot \nabla \chi_h, \end{aligned}$$

where the expression of the Fréchet derivative of the solution map $S'(\chi_h)[\vartheta_h]$ can be derived, as in (5.19), by introducing an adjoint problem.

This allows to formulate an algorithm for the implementation of the Uzawa iterations: as explained before, we avoid a full-implicit scheme, and treat explicitly all the (non-linear) terms within $S'(\chi_h)$. Moreover, we decouple the update of χ_h^{k+1} and p_h^{k+1} : we first compute χ_h^{k+1} making use of χ_h^k and p_h^k , then we exploit also χ_h^{k+1} for the computation of p_h^{k+1} . For the latter step, it is possible to give an explicit expression of the update, since the condition in (5.50) is equivalent to minimizing a quadratic functional in the L^{∞} -unitary ball: as in [26], Remark 10.11,

$$p_h^{k+1} = \frac{p_h^k + \tau \nabla \chi_h^{k+1}}{\max\{1, |p_h^k + \tau \nabla \chi_h^{k+1}|\}}. \quad (5.51)$$

Instead, the variational inequality for the update of χ_h^{k+1} is

$$\begin{aligned} & \int_{\Omega} (\chi_h^{k+1} - \chi_h^k)(\xi_h - \chi_h^{k+1}) + \tau \int_{\Omega} (1 - k) \nabla S(\chi_h^k) \cdot \nabla p(\chi_h^k)(\xi_h - \chi_h^{k+1}) \\ & + \tau \int_{\Omega} S(\chi_h^k)^3 p(\chi_h^k)(\xi_h - \chi_h^{k+1}) + \tau \int_{\Omega} p_h^k \cdot \nabla (\xi_h - \chi_h^{k+1}) \geq 0 \quad \forall \xi_h \in \mathcal{K}_h, \end{aligned} \quad (5.52)$$

where $p(\chi_h)$ is the solution of the adjoint problem (5.20) with $\chi = \chi_h$. The solution of the inequality is performed via a PDAS strategy as in Algorithm 7, in order to fulfill the requirement that $0 \leq \chi_h^{k+1} \leq 1$. We remark that this results in a fully explicit evolution step, which entails more restrictive bounds on the choice of the timestep τ in order to preserve stability. Eventually, we implement the following Algorithm:

Data: Initial guess for the inclusion u_h^0

Set $k = 0$;

while $\|\chi_h^k - \chi_h^{k-1}\|_{\infty} > tol$ **do**

compute $S(\chi_h^k)$ solving the direct problem (5.5);
 compute $p(\chi_h^k)$ solving the adjoint problem (5.20);
 update χ_h^{k+1} solving (5.52) via PDAS Algorithm;
 update p_h^{k+1} according to (5.51);
 set $k = k + 1$;

end

Algorithm 8: Uzawa algorithm for the minimization of J_{reg}

5.7.2 Numerical results and comparison with the phase-field relaxation

We now report some results of the application of Algorithm 8, which implements the Uzawa flow for the research of the saddle point of the Lagrangian functional. This allows also to perform a comparison with the main proposed algorithm, which is based on a phase-field approach to the problem and motivates future further investigation in this field. Indeed, the identification of the ischemic region seems to be effective. The parameters for this set of simulations are reported in Table 5.3 We considered $N_f = 2$ different measurements associated to $f_1 = x$ and $f_2 = y$ and the

α	τ	tol_{PDAS}	tol_{POP}
10^{-4}	1	10^{-16}	10^{-4}

Table 5.3: Values of the main parameters

starting guess is $u_0 \equiv 0$. In Figure 5.9 we report the results of the reconstruction with the Uzawa flow compared to the ones of the Parabolic Obstacle problem (on the same mesh, with $\varepsilon = \frac{\pi}{4}$ and $\varepsilon = \frac{\pi}{8}$) in two different configurations. The reconstruction achieved by the saddle-point method seems to be as accurate as the phase-field one, and even more sharp in presence of non-smooth geometry. The computational cost of the former, indeed, is considerably higher than the one of the latter, as depicted by the total number of iterations required.

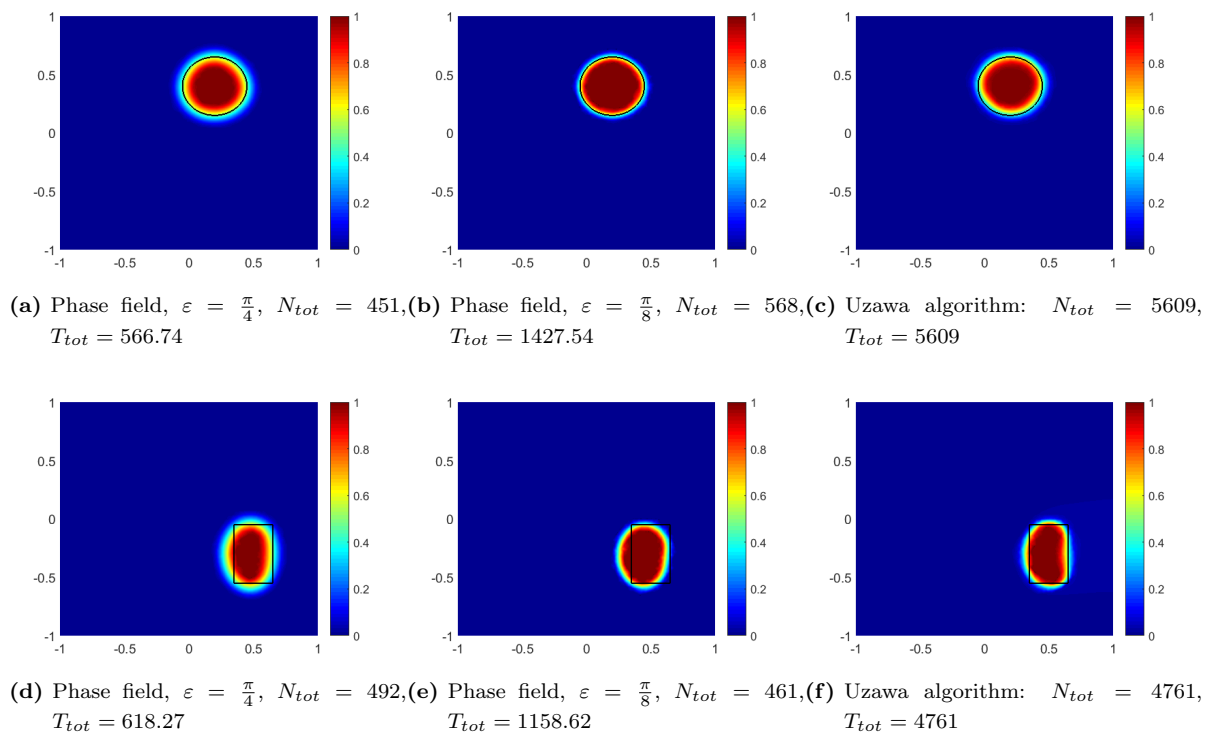


Figure 5.9: Uzawa algorithm: result comparison

Chapter 6

Well-posedness results for the monodomain problem

This chapter is entirely devoted to the extension of the results regarding existence, uniqueness and regularity of the solutions of the monodomain problem. Particular attention is given both to the unperturbed case (i.e., when no ischemia is present) and to the perturbed one. The results obtained in this chapter are of crucial importance in order to extend to the monodomain case the methods developed in the previous chapters of the thesis for reconstructing discontinuous coefficients in semilinear elliptic and parabolic equations.

The well-posedness analysis of the monodomain system has been the object of several studies, mainly as a by-product of the discussion on the more complicated bidomain model: we refer to [61, Chapter 3] for a general overview. Existence and uniqueness of weak solutions of the system have been tackled via various techniques: in [62], e.g., such results have been obtained on the Fitz-Hugh Nagumo model (see Chapter 1 for the expression of f, g) by applying a theory for abstract evolution inequalities based on semi-discretization in time, *a-priori* error estimates and compactness properties. In [41] a result of existence and uniqueness of weak solution is proved for the Fitz-Hugh Nagumo, the Aliev Panfilov and the Rogers MacCulloch models by means of a Faedo-Galerkin argument. A result of existence of strong solutions, local in time, is also derived. In [136], instead, results of well-posedness are obtained on a wider range of models, by resorting on a fixed point argument.

Regarding the regularity of the solutions of the monodomain problem, we report a result in [64] for Fitz-Hugh Nagumo, Aliev Panfilov and Rogers MacCulloch models: if the coefficient of the system are sufficiently regular, thanks to arguments from [131] and [86], existence and uniqueness of solutions of the monodomain system in a classical sense is guaranteed, locally in time. A comparison principle is also provided, by means of the tool of invariant sets, allowing for the extension to global solutions. We also report a result of local existence of classical solutions for the bidomain model, recently obtained in [81].

The aim of this chapter is to first state and prove a result of existence and uniqueness of classical solutions of the monodomain problem in the case of regular coefficients. In order to do so, we design a strategy (according to the approach contained in [116]) which enables us to derive such a result

together with a comparison principle, which can be extended to a wider class of models. In the case of discontinuous coefficients, we prove that the Faedo-Galerkin strategy developed in [41] is valid, although the switch-off of the nonlinear reaction term within the ischemic region. We hence derive a result of existence of weak solutions, global in time. Regarding the uniqueness argument, we resort on the technique developed by [98], which is suitable to be extended to a wider class of models. As a conclusion, we prove a result ensuring more regularity (namely, Hölder continuity) of the weak solutions even in the case of the perturbed coefficient, by relying on a suitable approximating sequence.

All the results proved in this chapter are referred to Aliev Panfilov model. We report as a remark the minimal hypotheses required for the proof of each proposition.

6.1 Assumptions and statement of the main results

The initial and boundary value problem associated to the monodomain system in a healthy heart is the following one:

$$\begin{cases} \partial_t u - \operatorname{div}(K_0 \nabla u) + f(u, w) = 0 & \text{in } \Omega \times (0, T), \\ K_0 \nabla u \cdot \nu = 0 & \text{on } \partial\Omega \times (0, T), \\ \partial_t w + g(u, w) = 0 & \text{in } \Omega \times (0, T), \\ u(\cdot, 0) = u_0 \quad w(\cdot, 0) = w_0 & \text{in } \Omega. \end{cases} \quad (6.1)$$

In presence of an ischemia ω , we consider the following system:

$$\begin{cases} \partial_t u - \operatorname{div}(K(\chi_\omega) \nabla u) + (1 - \chi_\omega) f(u, w) = 0 & \text{in } \Omega \times (0, T), \\ K(\chi_\omega) \nabla u \cdot \nu = 0 & \text{on } \partial\Omega \times (0, T), \\ \partial_t w + g(u, w) = 0 & \text{in } \Omega \times (0, T), \\ u(\cdot, 0) = u_0 \quad w(\cdot, 0) = w_0 & \text{in } \Omega, \end{cases} \quad (6.2)$$

where χ_ω is the indicator function of ω and $K(\chi_\omega) = K_0 - (K_0 - K_1)\chi_\omega$.

Assumption 4. We specify the following requirements for the coefficients and source terms:

- $K_0 \in C^{1+\alpha}(\bar{\Omega})$. Hence, define the differential operator $L = \sum_{j,l=1}^n a_{jl} \frac{\partial^2}{\partial x_j \partial x_l} + \sum_{j=1}^n b_j \frac{\partial}{\partial x_j}$ s.t. $Lu = \operatorname{div}(K_0 \nabla u)$: we ensure that implies that $a_{jl} = [K_0]_{jl}$ and $b_j = \sum_{l=1}^n \frac{\partial [K_0]_{lj}}{\partial x_l}$ are both of class $C^\alpha(\bar{\Omega})$;
- K_0 is strongly elliptic: $\exists \lambda > 0 : (K_0 \xi) \cdot \xi \geq \lambda |\xi|^2$ for all $\xi \in \mathbb{R}^3$. This implies that K_0 is definite positive;
- K_0 is symmetric and $K_0|_{\partial\Omega}$ admits the unit normal outward vector ν as an eigenvector. This allows to consider the oblique boundary condition in (6.1) as an homogeneous Neumann condition on u : $K_0 \nabla u \cdot \nu = \nabla u \cdot K_0 \nu = \lambda_1 \nabla u \cdot \nu = \lambda_1 \partial_\nu u$. As explained in Chapter 1, these hypotheses are surely satisfied by typical tensors involved in physiological application;
- K_1 , the conductivity tensor within the ischemia, satisfies the same hypotheses on K_0 . Moreover, pointwise in Ω , the three positive eigenvalues of K_1 , $\lambda_1^{(1)} < \lambda_2^{(1)} < \lambda_3^{(1)}$ are associated to

the same eigenvectors as the eigenvalues $\lambda_1^{(0)} < \lambda_2^{(0)} < \lambda_3^{(0)}$ of K_0 respectively. It also holds that $k_1 := \lambda_1^{(1)} \leq \lambda_1^{(0)}$ and $k_{max} := \lambda_3^{(0)}$;

- $\partial\Omega \in C^{2+\alpha}$;
- $u_0 \in C^{2+\alpha}(\bar{\Omega})$, $w_0 \in C^\alpha(\bar{\Omega})$, and the compatibility condition holds: $K_0 \nabla u_0 \cdot \nu = 0$ on the boundary of Ω ;
- the functions f, g are the ones from the Aliev Panfilov model, namely:

$$f(u, w) = Au(u - a)(u - 1) + uw \quad g(u, w) = \epsilon(Au(u - 1 - a) + w). \quad (6.3)$$

In particular, the function f, g (as well as many nonlinear terms associated to phenomenological monodomain models) have a particular property. Indeed, there exists a rectangle $S := [\underline{u}, \bar{u}] \times [\underline{w}, \bar{w}]$ such that f, g satisfy the *Nagumo condition* on S : let \vec{p} be a generalized outward normal on ∂S (for $\xi_0 \in \partial S$, $\vec{p}(\xi_0)$ s.t. $\vec{p}(\xi_0) \cdot \xi_0 \geq \vec{p}(\xi_0) \cdot \xi \forall \xi \in S$): then,

$$\vec{p}(\xi_0) \cdot \begin{pmatrix} -f(\xi_0) \\ -g(\xi_0) \end{pmatrix} \leq 0 \quad \forall \xi_0 \in \partial S; \quad (6.4)$$

We easily verify that f, g defined as in (6.3) satisfy the Nagumo condition (6.4) for example on the rectangle $S = [0, 1] \times [0, \frac{A(a+1)^2}{4}]$:

- on the left side, (6.4) prescribes $f(\underline{u}, w) \leq 0 \forall w \in [\underline{w}, \bar{w}]$, and this is true since $f(0, w) = 0 \forall w$;
- on the lower side, (6.4) prescribes $g(u, \underline{w}) \leq 0 \forall u \in [\underline{u}, \bar{u}]$, and this is true since $g(u, 0) = \epsilon Au(u - 1 - a)$ and $u \in [0, 1] \Rightarrow u(u - 1 - a) \leq 0$;
- on the right side, (6.4) prescribes $f(\bar{u}, w) \geq 0 \forall w \in [\underline{w}, \bar{w}]$, and this is true since $f(1, w) = w$ and $w \in [0, \frac{A(a+1)^2}{4}] \Rightarrow w \geq 0$;
- on the upper side, (6.4) prescribes $g(u, \bar{w}) \geq 0 \forall u \in [\underline{u}, \bar{u}]$, and this is true because $g(u, \frac{A(a+1)^2}{4}) = \epsilon(Au(u - 1 - a) + \frac{A(a+1)^2}{4}) \geq 0$ as we can immediately verify that the minimum of the parabola $Au(u - 1 - a)$ is attained at its vertex and has value $-\frac{A(a+1)^2}{4}$.

Moreover, by the expression in (6.3), we stress the fact that the functions f, g are Lipschitz continuous on S with constants $M_f, M_g \leq M$.

We now outline the main results of the chapter, reporting also the minimal assumptions under which we may deduce them.

Theorem 6.1. *Let the hypotheses of Assumption 4 hold, and suppose the initial data are such that, $\forall x \in \bar{\Omega}$, $(u_0(x), w_0(x)) \in S$, being S a rectangle satisfying (6.4). Then, the unperturbed problem (6.1) admits a unique classical solution (u, w) , namely $u \in C^{2+\alpha, 1+\alpha/2}(\bar{Q}_T)$, $w \in C^{\alpha, 1+\alpha/2}(\bar{Q}_T)$. Moreover, $(u(x, t), w(x, t)) \in S$ for each $x, t \in \bar{Q}_T$.*

Remark 6.1. This result can be proven by assuming any expression for the functions f, g satisfying the Nagumo conditions (6.4) on a rectangle S and such that f, g are Lipschitz continuous on S .

Regarding the perturbed problem, we first introduce the following definition of weak solutions:

Definition 6.1. A couple (u, w) , $u \in L^2(0, T; H^1(\Omega)) \cap L^\infty(0, T, L^2(\Omega))$, $u \in L^4(Q_T^*)$, $w \in L^\infty(0, T, L^2(\Omega))$, with distributional derivatives $\partial_t u \in L^2(0, T; H^*) + L^{4/3}(Q_T)$, $\partial_t w \in L^1(0, T; L^2(\Omega))$ (being $Q_T^* = \Omega^* \times (0, T) = (\Omega \setminus \omega) \times (0, T)$) is a *weak solution* of (6.2) if, $\forall \varphi \in H^1(\Omega), \psi \in L^2(\Omega)$,

$$\begin{aligned} \langle \partial_t u, \varphi \rangle_* + \int_{\Omega} K(\chi_\omega) \nabla u \cdot \nabla \varphi + \int_{\Omega} (1 - \chi_\omega) f(u, w) \varphi &= 0, \\ \int_{\Omega} \partial_t w \psi + \int_{\Omega} g(u, w) \psi &= 0 \end{aligned} \quad (6.5)$$

are satisfied in $\mathcal{D}'(0, T)$ and $u(\cdot, 0) = u_0$, $w(\cdot, 0) = w_0$.

We denote by $\langle \cdot, \cdot \rangle_*$ the duality pairing between $H^* = (H^1(\Omega))^*$ and $H^1(\Omega)$, whereas $\langle \cdot, \cdot \rangle$ denotes the pairing between a distribution and a test function in $\mathcal{D}(0, T)$. It is now possible to state the following result:

Theorem 6.2. *Under Assumption 4, there exists a unique weak solution (u, w) of the perturbed problem (6.2).*

Remark 6.2. For the Aliev-Panfilov model, existence of weak solutions can be proved also by the weaker assumption that $u_0 \in L^2(\Omega)$, $w_0 \in L^2(\Omega)$ and disregarding the compatibility conditions at the initial time. In order to obtain a uniqueness result, we need to require at least $w_0 \in L^3(\Omega)$. Analogous results can be obtained for the Fitz-Hugh Nagumo and the Rogers MacCulloch models.

The final result we report infers additional regularity for the weak solutions previously defined, in particular:

Theorem 6.3. *Let the hypotheses of Assumption 4 hold, and suppose the initial data are such that, $\forall x \in \overline{\Omega}$, $(u_0(x), w_0(x)) \in S$, being S a rectangle satisfying (6.4). Then, the unique weak solution (u, w) of (6.2) is such that $u \in C^{\alpha, \alpha/2}(\overline{Q_T})$, $w \in C^{\alpha, \alpha/2}(\overline{Q_T})$ and $(u(x, t), w(x, t)) \in S$ for each $x, t \in \overline{Q_T}$.*

6.2 Proof of Theorem 6.1

The strategy we adopt to prove Theorem 6.1 is based on the results of [116, Chapter 8, Sections 9 and 11].

Consider a couple of functions (\tilde{f}, \tilde{g}) which are Lipschitz globally on \mathbb{R}^2 with constants respectively M_f and M_g and such that

$$\tilde{f}(u, w) = f(u, w), \quad \tilde{g}(u, w) = g(u, w) \quad \forall (u, w) \in S. \quad (6.6)$$

Of course there exist more than one couple (\tilde{f}, \tilde{g}) satisfying (6.6): nevertheless, we select one of them and show that the argument of the proof is independent of that choice. Replace \tilde{f}, \tilde{g} in (6.1)

and define (\tilde{u}, \tilde{w}) as the solution of the following system:

$$\begin{cases} \partial_t \tilde{u} - \operatorname{div}(K_0 \nabla \tilde{u}) + \tilde{f}(\tilde{u}, \tilde{w}) = 0 & \text{in } Q_T, \\ K_0 \nabla \tilde{u} \cdot \nu = 0 & \text{on } \partial\Omega \times (0, T), \\ \partial_t \tilde{w} + \tilde{g}(\tilde{u}, \tilde{w}) = 0 & \text{in } \Omega \times (0, T), \\ \tilde{u}(\cdot, 0) = u_0 \quad \tilde{w}(\cdot, 0) = w_0 & \text{in } \Omega. \end{cases} \quad (6.7)$$

Consider now the change of variable: $v_1 = e^{-\gamma t} \tilde{u}$, $v_2 = e^{-\gamma t} \tilde{w}$, with $\gamma > 0$. Then, (v_1, v_2) solves the problem:

$$\begin{cases} \partial_t v_1 - \operatorname{div}(K_0 \nabla v_1) + \gamma v_1 + f^*(v_1, v_2) = 0 & \text{in } Q_T, \\ K_0 \nabla v_1 \cdot \nu = 0 & \text{on } \partial\Omega \times (0, T), \\ \partial_t v_2 + \gamma v_2 + g^*(v_1, v_2) = 0 & \text{in } \Omega \times (0, T), \\ v_1(\cdot, 0) = u_0 \quad v_2(\cdot, 0) = w_0 & \text{in } \Omega, \end{cases} \quad (6.8)$$

where $f^*(v_1, v_2) = e^{-\gamma t} \tilde{f}(e^{\gamma t} v_1, e^{\gamma t} v_2)$ and $g^*(v_1, v_2) = e^{-\gamma t} \tilde{g}(e^{\gamma t} v_1, e^{\gamma t} v_2)$. Observe that, for each $(v_1, v_2), (v'_1, v'_2) \in \mathbb{R}^2$,

$$\begin{aligned} |f^*(v_1, v_2) - f^*(v'_1, v'_2)| &\leq e^{-\gamma t} |\tilde{f}(e^{\gamma t} v_1, e^{\gamma t} v_2) - \tilde{f}(e^{\gamma t} v'_1, e^{\gamma t} v'_2)| \\ &\leq e^{-\gamma t} M (|e^{\gamma t} v_1 - e^{\gamma t} v'_1| + |e^{\gamma t} v_2 - e^{\gamma t} v'_2|) = M (|v_1 - v'_1| + |v_2 - v'_2|), \end{aligned}$$

hence f^* is globally Lipschitz continuous with constant less than or equal to M , and the same holds for g^* .

In order to study the well-posedness of (6.8), we introduce the sequence $\{\underline{v}^{(k)}\}$ defined by the following iterative scheme:

$$\begin{cases} \partial_t v_1^{(k)} - \operatorname{div}(K_0 \nabla v_1^{(k)}) + \gamma v_1^{(k)} = -f^*(v_1^{(k-1)}, v_2^{(k-1)}) & \text{in } \Omega \times (0, T), \\ K_0 \nabla v_1^{(k)} \cdot \nu = 0 & \text{on } \partial\Omega \times (0, T), \\ \partial_t v_2^{(k)} + \gamma v_2^{(k)} = -g^*(v_1^{(k-1)}, v_2^{(k-1)}) & \text{in } \Omega \times (0, T), \\ v_1^{(k)}(\cdot, 0) = u_0 \quad v_2^{(k)}(\cdot, 0) = w_0 & \text{in } \Omega, \end{cases} \quad (6.9)$$

which can be written in operatorial form as follows:

$$\mathcal{A} \underline{v}^{(k)} = \mathcal{F}(\underline{v}^{(k-1)}), \quad (6.10)$$

being $\underline{v}^{(k)} = \begin{pmatrix} v_1^{(k)} \\ v_2^{(k)} \end{pmatrix}$, $\mathcal{F}(\underline{v}) = \begin{pmatrix} -f^*(v_1, v_2) \\ -g^*(v_1, v_2) \end{pmatrix}$, $\mathcal{A} = \begin{pmatrix} A_1 & 0 \\ 0 & A_2 \end{pmatrix}$,

$$A_1 : v_1 \mapsto \partial_t v_1 - L v_1 + \gamma v_1, \quad A_2 : v_2 \mapsto \partial_t v_2 + \gamma v_2.$$

The domains of the functionals A_1 and A_2 are defined as follows:

$$\begin{aligned} \mathcal{D}(A_1) &= \left\{ v_1 \in C^{2+\alpha, 1+\alpha/2}(\overline{Q_T}) : v_1(\cdot, 0) = u_0 \text{ in } \Omega, \quad K_0 \nabla v_1 = 0 \text{ on } \partial\Omega \times (0, T) \right\}, \\ \mathcal{D}(A_2) &= \left\{ v_2 \in C^{\alpha, 1+\alpha/2}(\overline{Q_T}) : v_2(\cdot, 0) = w_0 \text{ in } \Omega \right\}, \\ \mathcal{D}(\mathcal{A}) &= \mathcal{D}(A_1) \times \mathcal{D}(A_2). \end{aligned}$$

We consider problem (6.10) in the functional space $\mathcal{X} = X_1 \times X_1$, being $X_1 = C^{\alpha, \alpha/2}(\overline{Q_T})$. In particular, we immediately notice that \mathcal{F} maps \mathcal{X} into itself, since the composition of a Hölder continuous function (of exponent α) with a Lipschitz one is a Hölder continuous function with the same exponent. In order to prove that problem (6.10) is well-posed it is sufficient to verify that for each $\underline{b} \in \mathcal{X}$ there exists a unique $\underline{v} \in \mathcal{D}(\mathcal{A})$ such that $\mathcal{A}\underline{v} = \underline{b}$. Since \mathcal{A} is diagonal, we study the two equations separately:

$$\text{find } v_1 \in \mathcal{D}(A_1) \quad \text{s.t.} \quad A_1 v_1 = b_1, \quad (6.11)$$

$$\text{find } v_2 \in \mathcal{D}(A_2) \quad \text{s.t.} \quad A_2 v_2 = b_2. \quad (6.12)$$

According to the definition of $\mathcal{D}(A_1)$, (6.11) is equivalent to finding a classical solution $v_1 \in C^{2+\alpha, 1+\alpha/2}(\overline{Q_T})$ of the following initial boundary value problem:

$$\begin{cases} \partial_t v_1 - Lv_1 + \gamma v_1 = b_1 & \text{in } Q_T, \\ K_0 \nabla v_1 \cdot \nu = 0 & \text{on } \partial\Omega \times (0, T), \\ v_1(\cdot, 0) = u_0 & \text{in } \Omega. \end{cases}$$

The existence of v_1 is ensured by [104, Theorem 5.1.20], which we can apply to our problem in view of the regularity of the coefficients in L , the $C^{2+\alpha}$ regularity of the initial datum, the compatibility condition on it and the fact that $b_1 \in X_1 = C^{\alpha, \alpha/2}(\overline{Q_T})$. Hence (6.11) admits a unique solution $\forall b_1 \in X_1$. Problem (6.12) is instead equivalent to finding a solution $v_2 \in C^{\alpha, 1+\alpha/2}(\overline{Q_T})$ of the following initial value problem:

$$\begin{cases} \partial_t v_2 + \gamma v_2 = b_2 & \text{in } Q_T, \\ v_2(\cdot, 0) = w_0 & \text{in } \Omega; \end{cases}$$

in particular, the solution can be expressed in closed form, i.e.

$$v_2(x, t) = e^{-\gamma t} w_0(x) + \int_0^t e^{-\gamma(t-s)} b_2(x, s) ds.$$

We immediately verify that since $b_2 \in C^{\alpha, \alpha/2}(\overline{Q_T})$ and $w_0 \in C^\alpha(\overline{\Omega})$, then $v_2 \in C^{\alpha, \alpha/2}(\overline{Q_T})$. Moreover, by

$$\partial_t v_2(x, t) = -\gamma e^{-\gamma t} w_0(x) - \gamma \int_0^t e^{-\gamma(t-s)} b_2(x, s) ds + b_2(x, t),$$

we can easily conclude that $v_2 \in C^{\alpha, 1+\alpha/2}(\overline{Q_T})$; whence problem (6.11) admits a unique solution $\forall b_2 \in X_1$. In conclusion, \mathcal{A} is a bijective operator from $\mathcal{D}(\mathcal{A})$ to \mathcal{X} , and the inverse operator \mathcal{A}^{-1} is well defined in \mathcal{X} . Equation (6.10) can be rewritten as

$$\underline{v}^{(k)} = \mathcal{A}^{-1} \mathcal{F}(\underline{v}^{(k-1)}), \quad (6.13)$$

where $\mathcal{A}^{-1} \mathcal{F}$ is a well defined operator from \mathcal{X} to $\mathcal{D}(\mathcal{A}) \subset \mathcal{X}$.

It is now possible to prove that $\mathcal{A}^{-1} \mathcal{F}$ is a contraction in \mathcal{X} with respect to the norm $\|\underline{v}\|_0 = \|v_1\|_0 + \|v_2\|_0 = \max\{v_1(x, t) : (x, t) \in \overline{Q_T}\} + \max\{v_2(x, t) : (x, t) \in \overline{Q_T}\}$. First of all notice that, by the properties of f^*, g^* and by the definition of \mathcal{F} ,

$$\|\mathcal{F}(\underline{v}) - \mathcal{F}(\underline{v}')\|_0 \leq M \|\underline{v} - \underline{v}'\|_0 \quad \forall \underline{v}, \underline{v}' \in \mathcal{X}. \quad (6.14)$$

Moreover, we want to verify that

$$\|\mathcal{A}^{-1}\underline{v} - \mathcal{A}^{-1}\underline{v}'\|_0 \leq \frac{1}{\gamma}\|\underline{v} - \underline{v}'\|_0 \quad \forall \underline{v}, \underline{v}' \in \mathcal{X}. \quad (6.15)$$

This is equivalent to prove that

$$\|\mathcal{A}\underline{v} - \mathcal{A}\underline{v}'\|_0 \geq \gamma\|\underline{v} - \underline{v}'\|_0 \quad \forall \underline{v}, \underline{v}' \in \mathcal{D}(A_1) \times \mathcal{D}(A_2). \quad (6.16)$$

Observe that by the diagonal expression of \mathcal{A} , if

$$\|A_1 v_1 - A_1 v'_1\|_0 \geq \gamma\|v_1 - v'_1\|_0 \quad \forall v_1, v'_1 \in \mathcal{D}(A_1), \quad (6.17)$$

$$\|A_2 v_2 - A_2 v'_2\|_0 \geq \gamma\|v_2 - v'_2\|_0 \quad \forall v_2, v'_2 \in \mathcal{D}(A_2), \quad (6.18)$$

then (6.16) is satisfied. Both (6.17) and (6.18) can be proved by [116, Chapter 8, Lemma 9.1] and [116, Chapter 8, Lemma 11.1] respectively.

Proof of (6.17): define $w = v_1 - v'_1$ and take x_0, t_0 such that $\|w\|_0 = |w(x_0, t_0)|$. Then, we claim that if $x_0 \in \Omega$, it holds

$$w(x_0, t_0) (\partial_t w - Lw)(x_0, t_0) \geq 0. \quad (6.19)$$

Property (6.19) is trivially verified if $w(x_0, t_0) = 0$: otherwise, (x_0, t_0) is a positive maximum point or a negative minimum point for w . For sure, $t_0 > 0$ (because $v_1(\cdot, 0) = v'_1(\cdot, 0) = u_0$): hence $\partial_t w(x_0, t_0)w(x_0, t_0) \geq 0$ is verified (since $w \in C^1(\overline{Q_T})$, the Kuhn-Tucker optimality condition holds). Moreover, if $x_0 \in \Omega$, $w(x_0, t_0)(Lw)(x_0, t_0) \leq 0$: indeed, $Lw = K_0 : \mathcal{H}(w) + \text{div}(K_0) \cdot \nabla w$ (where $\mathcal{H}(w)$ is the Hessian matrix of w , $\text{div}(K_0)$ must be intended row-wise and we considered the Frobenius scalar product between matrices :). Being (x_0, t_0) a local internal extreme point, $\nabla w(x_0, t_0) = 0$ and $(w\mathcal{H}(w))(x_0, t_0)$ is negative definite, hence, since K_0 is positive definite, we conclude $w(x_0, t_0)(Lw)(x_0, t_0) \leq 0$. The case $x_0 \in \partial\Omega$ is more delicate; nevertheless, for each $\varepsilon > 0$ it is possible to find a point $(x_\varepsilon, t_\varepsilon) \in Q_T$ such that

$$\begin{aligned} w(x_0, t_0)\partial_t w(x_\varepsilon, t_\varepsilon) &\geq -\frac{\varepsilon}{3}\|w\|_0^2, \\ w(x_0, t_0)\sum_{j=1}^n b_j \partial_{x_j} w(x_\varepsilon, t_\varepsilon) &\leq \frac{\varepsilon}{3}\|w\|_0^2, \\ w(x_0, t_0)\sum_{j,l=1}^n a_{jl} \partial_{x_j, x_l} w(x_\varepsilon, t_\varepsilon) &\leq \frac{\varepsilon}{3}\|w\|_0^2, \end{aligned}$$

whence

$$\forall \varepsilon > 0, \exists (x_\varepsilon, t_\varepsilon) : \quad w(x_0, t_0) (\partial_t w - Lw)(x_\varepsilon, t_\varepsilon) \geq -\varepsilon\|w\|_0^2. \quad (6.20)$$

In both cases, if (6.19) or (6.20) is verified, we can conclude (6.17), since

$$\|w\|_0 \|A_1 v_1 - A_1 v'_1\|_0 \geq |w(x_0, t_0) (\partial_t w - Lw + \gamma w)(x_0, t_0)| \geq \gamma\|w\|_0^2.$$

Proof of (6.18): define $w = v_2 - v'_2$ and take x_0, t_0 such that $\|w\|_0 = w(x_0, t_0)$. If $w(x_0, t_0) \neq 0$, then $t_0 > 0$ and by Kuhn-Tucker optimality condition $w(x_0, t_0)\partial_t w(x_0, t_0) \geq 0$, hence it holds that $|w(x_0, t_0)(\partial_t w(x_0, t_0) + \gamma w(x_0, t_0))| \geq \gamma w(x_0, t_0)^2$, and this concludes (6.18).

Via (6.14) and (6.15), we assess that the operator $\mathcal{A}^{-1}\mathcal{F}$ is Lipschitz continuous in \mathcal{X} with respect to $\|\cdot\|_0$, with constant $\frac{M}{\gamma}$. Choosing $\gamma > M$, the operator is a contraction in \mathcal{X} with respect to $\|\cdot\|_0$. This easily entails that $\{v^{(k)}\} \subset \mathcal{X}$ is a Cauchy sequence, with respect to $\|\cdot\|_0$: thus, $\exists v^* \in C(\overline{Q_T}) \times C(\overline{Q_T})$. This does not immediately allow to conclude that v^* is a fixed point solution of (6.9), since it might not belong to \mathcal{X} . We now apply some results from the analytic semigroup theory for parabolic equations from [104] to recover the desired regularity. First of all, being $v_1^{(k)}$ the solution of the first equation in (6.9), it admits the following representation:

$$v_1^{(k)}(\cdot, t) = e^{t\mathcal{L}}u_0 + \int_0^t e^{(t-s)\mathcal{L}}f^*(v_1^{(k-1)}(\cdot, s), v_2^{(k-1)}(\cdot, s))ds,$$

where $\mathcal{L}u = Lu - \gamma u = \operatorname{div}(K_0\nabla u) - \gamma u$. Since $v_1^{(k)} \rightarrow v_1^*$, $v_2^{(k)} \rightarrow v_2^*$ uniformly in $\overline{Q_T}$, also $f(v_1^{(k)}, v_2^{(k)}) \rightarrow f(v_1^*, v_2^*)$ uniformly. Define now $v_{\#} \in C(\overline{Q_T})$ such that

$$v_{\#}(\cdot, t) = e^{t\mathcal{L}}u_0 + \int_0^t e^{(t-s)\mathcal{L}}f^*(v_1^*(\cdot, s), v_2^*(\cdot, s))ds;$$

by linearity,

$$v_1^{(k)}(\cdot, t) - v_{\#}(\cdot, t) = \int_0^t e^{(t-s)\mathcal{L}}(f^*(v_1^{(k-1)}(\cdot, s), v_2^{(k-1)}(\cdot, s)) - f^*(v_1^*(\cdot, s), v_2^*(\cdot, s)))ds,$$

and according to [104, equation (4.1.3)] (which relies on equation (4.0.2) and Proposition 2.2.9 therein), we can ensure that for $0 \leq t \leq T$

$$\left\|v_1^{(k)}(\cdot, t) - v_{\#}(\cdot, t)\right\|_{C(\overline{\Omega})} \leq M_0 \int_0^t \left\|f^*(v_1^{(k-1)}(\cdot, s), v_2^{(k-1)}(\cdot, s)) - f^*(v_1^*(\cdot, s), v_2^*(\cdot, s))\right\|_{C(\overline{\Omega})},$$

whence

$$\left\|v_1^{(k)} - v_{\#}\right\|_0 \leq M_0 T \left\|f^*(v_1^{(k-1)}, v_2^{(k-1)}) - f^*(v_1^*, v_2^*)\right\|_0.$$

Eventually, we conclude that $v_1^{(k)} \rightarrow v_{\#}$ uniformly in $\overline{Q_T}$, and by the uniqueness of the uniform limit we have that $v_1^* = v_{\#}$ and also

$$v_1^*(\cdot, t) = e^{t\mathcal{L}}u_0 + \int_0^t e^{(t-s)\mathcal{L}}f^*(v_1^*(\cdot, s), v_2^*(\cdot, s))ds. \quad (6.21)$$

An application of [104, Theorem 5.1.17, point *ii*] guarantees that $v_1^* \in C^{\alpha, \alpha/2}(\overline{Q_T})$.

Consider now the equation for v_2^* : each $v_2^{(k)}$ admits the representation

$$v_2^{(k)}(x, t) = e^{t\gamma}w_0(x) + \int_0^t e^{(t-s)\gamma}g^*(v_1^{(k-1)}(x, s), v_2^{(k-1)}(x, s)),$$

and passing to the limit, thanks to the continuity of g^* , v_2^* satisfies

$$v_2^*(x, t) = e^{t\gamma}w_0(x) + \int_0^t e^{(t-s)\gamma}g^*(v_1^*(x, s), v_2^*(x, s)). \quad (6.22)$$

From (6.22), we compute the expression of time derivative:

$$\partial_t v_2^*(x, t) = -\gamma \left(e^{t\gamma}w_0(x) + \int_0^t e^{(t-s)\gamma}g^*(v_1^*(x, s), v_2^*(x, s)) \right) + g^*(v_1^*(x, t), v_2^*(x, t))$$

and we can conclude that $\partial_t v_2^* \in C(\overline{Q_T})$ by the assumptions on w_0 and g^* . We now show that v_2^* is Hölder continuous with respect to the space variable x with coefficient α : for every $(x_1, t), (x_2, t) \in \overline{Q_T}$,

$$\begin{aligned} & e^{-\gamma t} |v_2^*(x_1, t) - v_2^*(x_2, t)| \\ & \leq |w_0(x_1) - w_0(x_2)| + \int_0^t e^{-\gamma s} |g^*(v_1^*(x_1, s), v_2^*(x_1, s)) - g^*(v_1^*(x_2, s), v_2^*(x_2, s))| ds \\ & \leq c_0 |x_1 - x_2|^\alpha + \int_0^t M e^{-\gamma s} |v_1^*(x_1, s) - v_1^*(x_2, s)| ds + \int_0^t M e^{-\gamma s} |v_2^*(x_1, s) - v_2^*(x_2, s)| ds \\ & \leq c_0 |x_1 - x_2|^\alpha + c_1 |x_1 - x_2|^\alpha \int_0^t M e^{-\gamma s} ds + \int_0^t M e^{-\gamma s} |v_2^*(x_1, s) - v_2^*(x_2, s)| ds \\ & \leq \left(c_0 + \frac{M}{\gamma} c_1 (1 - e^{-\gamma t}) \right) |x_1 - x_2|^\alpha + \int_0^t M e^{-\gamma s} |v_2^*(x_1, s) - v_2^*(x_2, s)| ds. \end{aligned}$$

By an application of Gronwall's inequality,

$$e^{-\gamma t} |v_2^*(x_1, t) - v_2^*(x_2, t)| \leq e^{Mt} \left(c_0 + \frac{M}{\gamma} c_1 (1 - e^{-\gamma t}) \right) |x_1 - x_2|^\alpha,$$

and we can conclude the uniform estimate

$$|v_2^*(x_1, t) - v_2^*(x_2, t)| \leq e^{(M+\gamma)T} \left(c_0 + \frac{M}{\gamma} c_1 (1 - e^{-\gamma T}) \right) |x_1 - x_2|^\alpha.$$

Even though these regularity results are sufficient to continue the proof, we remark that v_2^* is also of class $C^{\alpha, 1+\alpha/2}$ since $\partial_t v_2^*$ is Hölder continuous with respect to t with coefficient $\frac{\alpha}{2}$. Indeed, $\partial_t v_2^* = -\gamma v_2^* + g^*(v_1^*, v_2^*)$, being v_2 a differentiable function w.r.t. the variable t , g^* Lipschitz continuous and v_1^* Hölder continuous with coefficient $\alpha/2$.

In conclusion, we have proved that for every initial guess $\underline{v}^{(0)} \in \mathcal{X}$ the sequence recursively defined in (6.13) uniformly converges to a unique \underline{v}^* , which in principle would only belong to $C(\overline{Q_T}) \times C(\overline{Q_T})$. We have moreover shown additional regularity on \underline{v}^* , and in particular that it belongs to \mathcal{X} : this allows to conclude that \underline{v}^* is a fixed point solution of (6.13), i.e.,

$$\underline{v}^* = \mathcal{A}^{-1} \mathcal{F}(\underline{v}^*),$$

and this immediately entails that $\underline{v}^* \in \mathcal{D}(\mathcal{A})$ and hence is a classical solution of (6.8). We point out that such a solution is unique: otherwise, taking another classical solution \underline{v}' of (6.8), then it would necessarily be also a fixed point for $\mathcal{A}^{-1} \mathcal{F}$, and satisfy

$$\|\underline{v}^* - \underline{v}'\|_0 = \|\mathcal{A}^{-1} \mathcal{F}(\underline{v}^*) - \mathcal{A}^{-1} \mathcal{F}(\underline{v}')\|_0 \leq \frac{M}{\gamma} \|\underline{v}^* - \underline{v}'\|_0,$$

which implies (since $\gamma > M$) that $\underline{v}^* = \underline{v}'$.

We now aim at showing that the solution of problem (6.8) does not depend on the extension of \tilde{f} and \tilde{g} , by proving that it stays within the set S throughout time. In order to do so, it is necessary to define another iterative scheme associated to (6.8): starting from $\underline{w}^{(0)} \in \mathcal{X}$, for each $k \geq 1$ introduce

$\underline{w}^{(k)} = (w_1^{(k)}, w_2^{(k)})$ such that

$$\left\{ \begin{array}{ll} \partial_t w_1^{(k)} - \operatorname{div}(K_0 \nabla w_1^{(k)}) + \gamma w_1^{(k)} + M w_1^{(k)} = M w_1^{(k-1)} - f^*(w_1^{(k-1)}, w_2^{(k-1)}) & \text{in } \Omega \times (0, T), \\ K_0 \nabla w_1^{(k)} \cdot \nu = 0 & \text{on } \partial\Omega \times (0, T), \\ \partial_t w_2^{(k)} + \gamma w_2^{(k)} + M w_2^{(k)} = M w_2^{(k-1)} - g^*(w_1^{(k-1)}, w_2^{(k-1)}) & \text{in } \Omega \times (0, T), \\ w_1^{(k)}(\cdot, 0) = u_0 \quad w_2^{(k)}(\cdot, 0) = w_0 & \text{in } \Omega, \end{array} \right. \quad (6.23)$$

which can be written in operatorial form as: find $\underline{w}^{(k)} \in \mathcal{D}(\mathcal{B})$ such that

$$\mathcal{B}\underline{w}^{(k)} = \mathcal{G}(\underline{w}^{(k-1)}), \quad (6.24)$$

being $\mathcal{G}(\underline{w}) = \begin{pmatrix} M w_1 - f^*(w_1, w_2) \\ M w_2 - g^*(w_1, w_2) \end{pmatrix}$, $\mathcal{B} = \begin{pmatrix} B_1 & 0 \\ 0 & B_2 \end{pmatrix}$,

$$B_1 : w_1 \mapsto \partial_t w_1 - L w_1 + \gamma w_1 + M w_1, \quad B_2 : w_2 \mapsto \partial_t w_2 + \gamma w_2 + M w_2,$$

and $\mathcal{D}(\mathcal{B}) = \mathcal{D}(\mathcal{A})$. Analogously to the analysis performed on $\mathcal{A}^{-1}\mathcal{F}$, we may prove that the operator \mathcal{B} is invertible from $\mathcal{D}(\mathcal{B})$ to \mathcal{X} , and that $\mathcal{B}^{-1}\mathcal{G} : \mathcal{X} \rightarrow \mathcal{X}$ is a Lipschitz operator with respect to the norm $\|\cdot\|_0$ with constant $\frac{2M}{M+\gamma}$. Hence, we can guarantee that, $\forall \underline{w}^{(0)} \in \mathcal{X}$, the sequence $\{\underline{w}^{(k)}\}$ uniformly converges in $C(\overline{Q_T}) \times C(\overline{Q_T})$. We can immediately prove that the limit is exactly \underline{v}^* , the classical solution of (6.8), since for sure \underline{v}^* satisfies $\underline{v}^* = \mathcal{B}^{-1}\mathcal{G}(\underline{v}^*)$, and this implies that

$$\|\underline{w}^{(k)} - \underline{v}^*\|_0 = \|\mathcal{B}^{-1}\mathcal{G}(\underline{w}^{(k)}) - \mathcal{B}^{-1}\mathcal{G}(\underline{v}^*)\|_0 \leq \frac{2M}{M+\gamma} \|\underline{w}^{(k-1)} - \underline{v}^*\|_0 \leq \left(\frac{2M}{M+\gamma}\right)^k \|\underline{w}^{(0)} - \underline{v}^*\|_0,$$

and since $\frac{2M}{M+\gamma} < 1$ we conclude that $\underline{w}^{(k)} \rightarrow \underline{v}^*$ uniformly in $\overline{Q_T}$. Take now the sequence $\{\underline{w}^{(k)}\}$ with starting point $\underline{w}^{(0)} = (e^{-\gamma t} u_0, e^{-\gamma t} w_0)$, and perform the change of variables $\{\underline{z}^{(k)}\} = e^{\gamma t} \{\underline{w}^{(k)}\}$: we immediately remark that $\underline{z}^{(k)}$ uniformly converges to $\underline{z}^* = e^{\gamma t} \underline{v}^*$, and \underline{z}^* is a solution of (6.7) in a classical sense. Such a solution is also unique: indeed, being \underline{z}^* , \underline{z}' two solution of (6.7), then $e^{\gamma t} \underline{z}^*$ and $e^{\gamma t} \underline{z}'$ are solutions of (6.7), thus they must coincide. Moreover, each $\underline{z}^{(k)}$ is the solution of the following problem:

$$\left\{ \begin{array}{ll} \partial_t z_1^{(k)} - \operatorname{div}(K_0 \nabla z_1^{(k)}) + M z_1^{(k)} = M z_1^{(k-1)} - \tilde{f}(z_1^{(k-1)}, z_2^{(k-1)}) & \text{in } \Omega \times (0, T), \\ K_0 \nabla z_1^{(k)} \cdot \nu = 0 & \text{on } \partial\Omega \times (0, T), \\ \partial_t z_2^{(k)} + M z_2^{(k)} = M z_2^{(k-1)} - \tilde{g}(z_1^{(k-1)}, z_2^{(k-1)}) & \text{in } \Omega \times (0, T), \\ z_1^{(k)}(\cdot, 0) = u_0 \quad z_2^{(k)}(\cdot, 0) = w_0 & \text{in } \Omega. \end{array} \right. \quad (6.25)$$

We now show that

$$\forall k, \quad \underline{z}^{(k)}(x, t) \in S \quad \forall (x, t) \in \overline{Q_T}. \quad (6.26)$$

According to the choice of $\underline{z}^{(0)}(x, t) = e^{\gamma t} \underline{w}^{(0)}(x, t) = (u_0(x), w_0(x))$, property (6.26) is surely valid for $k = 0$ thanks to Assumption 4. Suppose now by induction hypothesis that $\underline{z}^{(k-1)} \in S$. We shall now make use of the Nagumo property (see (6.4)), which we assume is valid for (f, g) but holds true also for any possible extension (\tilde{f}, \tilde{g}) since they coincide with (f, g) on S . On the

right-hand side of ∂S , $\{(\bar{u}, w), \underline{w} \leq w \leq \bar{w}\}$, the Nagumo condition (6.4) can be rewritten as $\tilde{f}(\bar{u}, w) = f(\bar{u}, w) \geq 0$, $\forall w \in [\underline{w}, \bar{w}]$. Define $z_1^+ = \bar{u} - z_1^{(k)}$: since \bar{u} is constant, we have

$$\partial_t \bar{u} - \operatorname{div}(K_0 \nabla \bar{u}) \geq -\tilde{f}(\bar{u}, w),$$

and subtracting the first equation in (6.25) we get that

$$\partial_t z_1^+ - \operatorname{div}(K_0 \nabla z_1^+) \geq M z_1^{(k)} - M z_1^{(k-1)} + \tilde{f}(z_1^{(k-1)}, z_2^{(k-1)}) - \tilde{f}(\bar{u}, w) \quad \text{in } \Omega \times (0, T) \quad \forall w \in [\underline{w}, \bar{w}].$$

Take in particular $w = z_2^{(k-1)}$: by Lipschitz continuity of \tilde{f} ,

$$\tilde{f}(z_1^{(k-1)}, z_2^{(k-1)}) - \tilde{f}(\bar{u}, z_2^{(k-1)}) \geq -M |z_1^{(k-1)} - \bar{u}| = -M(\bar{u} - z_1^{(k-1)}),$$

where we exploited the induction hypothesis on $z_1^{(k-1)}$. It follows that

$$\partial_t z_1^+ - \operatorname{div}(K_0 \nabla z_1^+) + M z_1^+ \geq 0 \quad \text{in } \Omega \times (0, T). \quad (6.27)$$

Moreover, $z_1^+(\cdot, 0) = \bar{u} - u_0 \geq 0$ and this, together with (6.27) and [116, Chapter 2, Lemma 2.1] allows to conclude that $z_1^+ \geq 0$, hence $z_1^{(k)} \leq \bar{u}$ in $\overline{Q_T}$. Analogously one can prove that $z_1^{(k)} \geq \underline{u}$. Consider instead the upper side of ∂S , $\{(u, \bar{w}), \underline{u} \leq u \leq \bar{u}\}$: the Nagumo condition (6.4) in this case reduces to $\tilde{g}(u, \bar{w}) = g(u, \bar{w}) \geq 0$, $\forall u \in [\underline{u}, \bar{u}]$. Define $z_2^+ = \bar{w} - z_2^{(k)}$: since $\partial_t \bar{w} = 0$, by the third equation in (6.25) we get that

$$\partial_t z_2^+ \geq M z_2^{(k)} - M z_2^{(k-1)} + \tilde{g}(z_1^{(k-1)}, z_2^{(k-1)}) - \tilde{g}(u, \bar{w}) \quad \text{in } \Omega \times (0, T)$$

holds $\forall u \in [\underline{u}, \bar{u}]$. Take in particular $u = z_1^{(k-1)}$: by Lipschitz continuity of \tilde{g} ,

$$\partial_t z_2^+ + M z_2^+ \geq 0 \quad \text{in } \Omega \times (0, T). \quad (6.28)$$

Taking advantage of the fact that $z_2^+ = \bar{w} - w_0 \geq 0$ and applying the Gronwall inequality on (6.28), we conclude that $z_2^+ \geq 0$, hence $z_2^{(k)} \leq \bar{w}$ in $\overline{Q_T}$. Analogously, one can prove that $z_2^{(k)} \geq \underline{w}$: in conclusion, property (6.26) is verified via induction. Since $\underline{z}^{(k)} \rightarrow \underline{z}^*$ uniformly in $\overline{Q_T}$, we can also ensure that $\underline{z}^* \in S \forall (x, t) \in \overline{Q_T}$, but this implies, together with (6.6), that $\tilde{f}(z_1^*(x, t), z_2^*(x, t)) = f(z_1^*(x, t), z_2^*(x, t))$ and $\tilde{g}(z_1^*(x, t), z_2^*(x, t)) = g(z_1^*(x, t), z_2^*(x, t))$ for each (x, t) in $\overline{Q_T}$. Hence, \underline{z}^* is also a solution (in classical sense) of the original system (6.1). The solution is unique because otherwise (6.7) would not have unique solution; we point out that the whole procedure is independent of the choice of the Lipschitz extensions \tilde{f}, \tilde{g} .

6.3 Proof of Theorem 6.2

We first observe that the bilinear form $\int_{\Omega} K(\chi_{\omega}) \nabla u \cdot \nabla v$ is not coercive in $H^1(\Omega)$, but it is weakly coercive. We hence introduce

$$\mathcal{B}(u, v) = \int_{\Omega} K(\chi_{\omega}) \nabla u \cdot \nabla v + k_1 \int_{\Omega} uv,$$

which is coercive with constant $k_1 > 0$, being k_1 the minimum eigenvalue of the tensor K_1 . According to the spectral theory of the compact self-adjoint operators (see [121, Theorem 6.2-1]), there

exists an orthonormal basis of $L^2(\Omega)$, orthonormal with respect to the $L^2(\Omega)$ norm, composed by eigenfunctions of \mathcal{B} , $\{\Psi_i\}_{i \in \mathbb{N}}$ associated to positive eigenvalues $\{\lambda_i\}_{i \in \mathbb{N}}$.

Before applying the Faedo-Galerkin technique, we need to prove some preliminary results involving upper and lower bounds on the nonlinear terms f, g . We make use of the following Young-type estimates:

$$x^{n-1} \leq \frac{n-1}{n}x^n + \frac{1}{n} \quad \forall n > 1, \quad \forall x > 0; \quad (6.29)$$

$$x^{n-1} \leq \varepsilon \frac{n-1}{n}x^n + \frac{1}{n\varepsilon^{n-1}} \quad \forall n > 1, \quad \forall x > 0, \quad \forall \varepsilon > 0. \quad (6.30)$$

The following estimates hold, as in [41]:

- the term $f(u, w)$ is bounded from above,

$$\begin{aligned} |f(u, w)| &\leq A|u|^3 + A(a+1)|u|^2 + Aa|u| + |u||w| \\ &\leq A|u|^3 + A(a+1)|u|^2 + \frac{1}{2}Aa|u|^2 + \frac{1}{2}Aa + \frac{1}{3}|u|^3 + \frac{2}{3}|w|^{3/2} \\ &= \left(A + \frac{1}{3}\right)|u|^3 + \left(\frac{3}{2}Aa + A\right)|u|^2 + \frac{1}{2}Aa + \frac{2}{3}|w|^{3/2} \\ &\leq \left[A + \frac{1}{3} + \frac{3}{4}\left(\frac{3}{2}Aa + A\right)\right]|u|^3 + \frac{1}{4}\left(\frac{3}{2}Aa + A\right) + \frac{1}{2}Aa + \frac{2}{3}|w|^{3/2} \\ &\leq A_1|u|^3 + A_2 + A_3|w|^{3/2}, \end{aligned} \quad (6.31)$$

and this also allows to conclude that, if $u(\cdot, t) \in L^4(\Omega)$ and $w(\cdot, t) \in L^2(\Omega)$,

$$\begin{aligned} \|f(u(\cdot, t), w(\cdot, t))\|_{L^{4/3}(\Omega)} &\leq A_1 \| |u(\cdot, t)|^3 \|_{L^{4/3}(\Omega)} + A_2 |\Omega|^{3/4} + A_3 \| |w(\cdot, t)|^{3/2} \|_{L^{4/3}(\Omega)} \\ &\leq A_1 \|u(\cdot, t)\|_{L^4(\Omega)}^3 + A_2 |\Omega|^{3/4} + A_3 \|w(\cdot, t)\|_{L^2(\Omega)}^{3/2}; \end{aligned} \quad (6.32)$$

- the term $g(u, w)$ is bounded from above,

$$\begin{aligned} |g(u, w)| &\leq \varepsilon A|u|^2 + \varepsilon A(1+a)|u| + \varepsilon|w| \\ &\leq \left[\varepsilon A + \frac{1}{2}\varepsilon A(1+a)\right]|u|^2 + \frac{1}{2}\varepsilon A(1+a) + \varepsilon|w| \\ &\leq B_1|u|^2 + B_2 + B_3|w|, \end{aligned} \quad (6.33)$$

and this also allows to conclude that, if $u \in L^4(\Omega)$ and $w \in L^2(\Omega)$,

$$\begin{aligned} \|g(u(\cdot, t), w(\cdot, t))\|_{L^2(\Omega)} &\leq B_1 \| |u(\cdot, t)|^2 \|_{L^2(\Omega)} + B_2 |\Omega|^{1/2} + B_3 \|w(\cdot, t)\|_{L^2(\Omega)} \\ &\leq B_1 \|u(\cdot, t)\|_{L^4(\Omega)}^2 + B_2 |\Omega|^{1/2} + B_3 \|w(\cdot, t)\|_{L^2(\Omega)}; \end{aligned} \quad (6.34)$$

- if $u \in L^4(\Omega)$ and $w \in L^2(\Omega)$, the following estimate from below holds

$$\begin{aligned}
uf(u, w) + wg(u, w) &\geq A|u|^4 - A(1+a)|u|^3 + Aa|u|^2 - |u|^2|w| \\
&\quad - \epsilon A|u|^2|w| - \epsilon A(1+a)|u||w| + \epsilon|w|^2 \\
&\geq A|u|^4 - A(1+a) \left[\frac{3\epsilon_1}{4}|u|^4 + \frac{1}{n\epsilon_1^3} \right] + Aa|u|^2 \\
&\quad - (1+\epsilon A) \left[\frac{\epsilon_2}{2}|u|^4 + \frac{1}{2\epsilon_2}|w|^2 \right] - (1+a)A\epsilon \left[\frac{\epsilon_3}{2}|u|^2 + \frac{1}{2\epsilon_3}|w|^2 \right] \\
&\geq \left[A - A(1+a)\frac{3\epsilon_1}{4} - (1+\epsilon A)\frac{\epsilon_2}{2} \right] |u|^4 + \left[Aa - \frac{1}{2}(1+a)A\epsilon_3 \right] |u|^2 \\
&\quad + \left[\epsilon - (1+\epsilon A)\frac{1}{2\epsilon_2} - (1+a)A\epsilon\frac{1}{2\epsilon_3} \right] |w|^2 - \frac{A(1+a)}{n\epsilon_1^3},
\end{aligned}$$

and with a suitable choice of ϵ_1 , ϵ_2 and ϵ_3 , it is possible to conclude that

$$uf(u, w) + wg(u, w) \geq C_1|u|^4 - C_2 - C_3(|u|^2 + |w|^2). \quad (6.35)$$

Consider the following change of variables: $\tilde{u} = e^{-k_1 t} u$ (which implies $\partial_t \tilde{u} = e^{-k_1 t} \partial_t u - k_1 \tilde{u}$). The weak formulation of (6.2) thus becomes what follows:

$$\begin{aligned}
\langle \partial_t \tilde{u}, \varphi \rangle_* + \mathcal{B}(\tilde{u}, \varphi) + \int_{\Omega} (1 - \chi_{\omega}) \tilde{f}(\tilde{u}, w) \varphi &= 0 \quad \forall \varphi \in H^1(\Omega), \\
\int_{\Omega} \partial_t w \psi + \int_{\Omega} \tilde{g}(\tilde{u}, w) \psi &= 0 \quad \forall \psi \in L^2(\Omega),
\end{aligned} \quad (6.36)$$

where $\tilde{f}(\tilde{u}, w) = e^{-Kt} f(e^{Kt} \tilde{u}, w)$ and $\tilde{g}(\tilde{u}, w) = g(e^{Kt} \tilde{u}, w)$. The same estimates as in (6.32), (6.34) and (6.35) hold for \tilde{f} with small modifications; indeed,

$$\begin{aligned}
|\tilde{f}(\tilde{u}, w)| &= |e^{-k_1 t} f(e^{k_1 t} \tilde{u}, w)| \leq A_1 e^{2k_1 t} |\tilde{u}|^3 + A_2 e^{-k_1 t} + A_3 e^{-k_1 t} |w|^{3/2}, \\
|\tilde{g}(\tilde{u}, w)| &= |g(e^{k_1 t} \tilde{u}, w)| \leq B_1 e^{2k_1 t} |\tilde{u}|^2 + B_2 + B_3 |w|,
\end{aligned}$$

and also

$$\begin{aligned}
\tilde{u} \tilde{f}(\tilde{u}, w) + w \tilde{g}(\tilde{u}, w) &= e^{-k_1 t} \tilde{u} f((\tilde{u} e^{k_1 t}), w) + wg((\tilde{u} e^{k_1 t}), w) \\
&\geq e^{-2k_1 t} (e^{k_1 t} \tilde{u} f(e^{k_1 t} \tilde{u}, w) + wg((\tilde{u} e^{k_1 t}), w)) \\
&\geq e^{2k_1 t} C_1 |\tilde{u}|^4 - e^{-2k_1 t} C_2 - C_3 (|\tilde{u}|^2 + |w|^2).
\end{aligned}$$

When considering a switch-off of the nonlinear term f within the ischemic region ω , the following modifications must be considered: if $\tilde{u}(\cdot, t) \in L^4(\Omega)$, $w(\cdot, t) \in L^2(\Omega)$, then

$$\begin{aligned}
\left\| (1 - \chi_{\omega}) \tilde{f}(\tilde{u}(\cdot, t), w(\cdot, t)) \right\|_{L^{4/3}(\Omega)} &\leq A_1 e^{2k_1 t} \|\tilde{u}(\cdot, t)\|_{L^4(\Omega^*)}^3 + A_2 e^{-k_1 t} |\Omega|^{3/4} + A_3 e^{-k_1 t} \|w(\cdot, t)\|_{L^2(\Omega)}^{3/2}, \\
\|\tilde{g}(\tilde{u}(\cdot, t), w(\cdot, t))\|_{L^2(\Omega)} &\leq B_1 e^{2k_1 t} \|\tilde{u}(\cdot, t)\|_{L^4(\Omega)}^2 + B_2 |\Omega|^{3/4} + B_3 \|w(\cdot, t)\|_{L^2(\Omega)},
\end{aligned} \quad (6.37)$$

and also

$$\begin{aligned}
(1 - \chi_{\omega}) \tilde{u} \tilde{f}(\tilde{u}, w) + w \tilde{g}(\tilde{u}, w) &\geq (1 - \chi_{\omega}) (\tilde{u} \tilde{f}(\tilde{u}, w) + w \tilde{g}(\tilde{u}, w)) \\
&\geq (1 - \chi_{\omega}) (e^{2k_1 t} C_1 |\tilde{u}|^4 - e^{-2k_1 t} C_2 - C_3 (|\tilde{u}|^2 + |w|^2)) \\
&\geq (1 - \chi_{\omega}) e^{2k_1 t} C_1 |\tilde{u}|^4 - e^{-2k_1 t} C_2 - C_3 (|\tilde{u}|^2 + |w|^2).
\end{aligned} \quad (6.38)$$

We follow the Faedo-Galerkin procedure. In particular, the steps 1-4 are analogous to the ones in [41] (with careful handling of the vanishing nonlinear term in ω). Steps 5 and 6 are obtained by analogous arguments as in [98].

1) Discrete problems

Consider a basis $\{\Psi_i\}_{i \in \mathbb{N}}$ of eigenfunctions of \mathcal{B} corresponding to positive eigenvalues $\{\lambda_i\}_{i \in \mathbb{N}}$ and fix a positive $m \in \mathbb{N}$. Define $V_m = \text{span}\{\Psi_i, i = 1, \dots, m\} \subset H^1(\Omega)$ and the orthogonal projection operator $P_m : H^1(\Omega) \rightarrow V_m$

$$P_m : v \mapsto v_m, \quad v_m = \sum_{i=1}^m v_i \Psi_i \quad v_i = \int_{\Omega} v \Psi_i.$$

One can easily prove that $\|P_m v\|_{L^2(\Omega)} \leq \|v\|_{L^2(\Omega)}$, $\|P_m v\|_{H^1(\Omega)} \leq \left(1 + \frac{k_{max}}{k_1}\right) \|v\|_{H^1(\Omega)}$, where k_{max} is the maximum between the eigenvalues of K_0 and K_1 . Introduce the functions $\tilde{u}_m, w_m \in V_m$ such that

$$\tilde{u}_m(x, t) = \sum_{i=1}^m \tilde{u}_{im}(t) \Psi_i(x) \quad w_m(x, t) = \sum_{i=1}^m w_{im}(t) \Psi_i(x)$$

where the components $\tilde{u}_{im}, w_{im} : \mathbb{R} \rightarrow \mathbb{R}$ are the solutions of the system of ordinary differential equations:

$$\begin{cases} \dot{\tilde{u}}_{im}(t) + \lambda_i \tilde{u}_{im}(t) + \int_{\Omega} (1 - \chi_{\omega}) \tilde{f}(\tilde{u}_m(\cdot, t), w_m(\cdot, t)) \Psi_i = 0 & i = 1, \dots, m \\ \dot{w}_{im}(t) + \int_{\Omega} \tilde{g}(\tilde{u}_m(\cdot, t), w_m(\cdot, t)) \Psi_i = 0 & i = 1, \dots, m \\ \tilde{u}_m(0) = P_m(\tilde{u}_0) \quad w_m(0) = P_m(w_0). \end{cases} \quad (6.39)$$

The integral terms in the system are well defined due to properties (6.37) and since it holds that $\tilde{u}_m(\cdot, t), w_m(\cdot, t) \in V_m \subset H^1(\Omega)$. According to Cauchy-Peano local existence theorem, since \tilde{f} and \tilde{g} are continuous functions with respect to \tilde{u} and w , the solution of system (6.39) exists unique in $C^1(0, t_m)$, where t_m may depend on m . In order to conclude that $t_m \geq T \forall m$, we need to show that $\tilde{u}_m(\cdot, t)$ and $w_m(\cdot, t)$ are bounded in $L^\infty(0, T; L^2)$ independently of m , which will be done in the next step.

2) *A priori* estimates

We state and prove the following *a priori* estimates regarding \tilde{u}_m and w_m ; i.e., if their components are solutions of system (6.39), they satisfy

$$\|\tilde{u}_m\|_{L^\infty(0, T; L^2)}, \|w_m\|_{L^\infty(0, T; L^2)} \leq c_1, \quad (6.40)$$

$$\|\tilde{u}_m\|_{L^2(0, T; H^1)}, \|\tilde{u}_m\|_{L^4(Q_T^*)} \leq c_2, \quad (6.41)$$

$$\|\dot{\tilde{u}}_m\|_{L^2(0, T; H^*) + L^{4/3}(Q_T)} \leq c_3, \quad (6.42)$$

$$\|\dot{w}_m\|_{L^1(0, T; L^2(\Omega))} \leq c_4, \quad (6.43)$$

where $\dot{\tilde{u}}_m = \sum_{i=1}^m \dot{\tilde{u}}_{im} \psi_i$, $\dot{w}_m = \sum_{i=1}^m \dot{w}_{im} \psi_i$ and c_1, c_2, c_3, c_4 are positive constants depending on $|\Omega|, T, k_1, f, g, \|u_0\|_{L^2(\Omega)}, \|w_0\|_{L^2(\Omega)}$. In order to prove them, take the $2m$ equations in

(6.39), multiply them times \tilde{u}_{im} (the first m components) and times w_{im} (the others) and sum together. Exploiting the eigenvalue and eigenvector properties, we obtain:

$$\begin{aligned} & \frac{1}{2} \frac{d}{dt} \|\tilde{u}_m(\cdot, t)\|_{L^2(\Omega)} + \frac{1}{2} \frac{d}{dt} \|w_m(\cdot, t)\|_{L^2(\Omega)} + \mathcal{B}(\tilde{u}_m(\cdot, t), \tilde{u}_m(\cdot, t)) \\ & + \int_{\Omega} (1 - \chi_{\omega}) \tilde{f}(\tilde{u}_m(\cdot, t), w_m(\cdot, t)) \tilde{u}_m(\cdot, t) + \int_{\Omega} \tilde{g}(\tilde{u}_m(\cdot, t), w_m(\cdot, t)) w_m(\cdot, t) = 0. \end{aligned} \quad (6.44)$$

Taking advantage of the coercivity of \mathcal{B} , of the estimate from below (6.38), and eventually the fact that $e^{k_1 s} \geq 1$, we get

$$\begin{aligned} & \frac{1}{2} \frac{d}{dt} \|\tilde{u}_m(\cdot, t)\|_{L^2(\Omega)}^2 + \frac{1}{2} \frac{d}{dt} \|w_m(\cdot, t)\|_{L^2(\Omega)}^2 + k_1 \|\tilde{u}_m(\cdot, t)\|_{H^1(\Omega)}^2 + C_1 \int_{\Omega^*} |\tilde{u}_m|^4 \\ & \leq C_2 e^{-2k_1 t} |\Omega| + C_3 (\|\tilde{u}_m(\cdot, t)\|_{L^2(\Omega)}^2 + \|w_m(\cdot, t)\|_{L^2(\Omega)}^2); \end{aligned}$$

integrating from 0 to $t \leq T$ and using the fact that $\int_0^t e^{-2k_1 s} ds = \frac{1 - e^{-2k_1 t}}{2k_1} \leq \frac{1}{2k_1}$, $\|\tilde{u}_m(\cdot, 0)\|_{L^2(\Omega)} = \|P_m(u_0)\|_{L^2(\Omega)} \leq \|u_0\|_{L^2(\Omega)}$ and $\|w_m(\cdot, 0)\|_{L^2(\Omega)} = \|P_m(w_0)\|_{L^2(\Omega)} \leq \|w_0\|_{L^2(\Omega)}$, we obtain the following important estimate:

$$\begin{aligned} & \frac{1}{2} \|\tilde{u}_m(\cdot, t)\|_{L^2(\Omega)}^2 + \frac{1}{2} \|w_m(\cdot, t)\|_{L^2(\Omega)}^2 + k_1 \int_0^t \|\tilde{u}_m(\cdot, s)\|_{H^1(\Omega)}^2 + C_1 \int_0^t \|\tilde{u}_m(\cdot, s)\|_{L^4(\Omega^*)}^4 \\ & \leq C_2 \frac{|\Omega|}{2k_1} + C_3 \int_0^t (\|\tilde{u}_m(\cdot, s)\|_{L^2(\Omega)}^2 + \|w_m(\cdot, s)\|_{L^2(\Omega)}^2) + \frac{1}{2} \|u_0\|_{L^2(\Omega)}^2 + \frac{1}{2} \|w_0\|_{L^2(\Omega)}^2. \end{aligned} \quad (6.45)$$

As a consequence of (6.45), it holds

$$\begin{aligned} \|\tilde{u}_m(\cdot, t)\|_{L^2(\Omega)}^2 + \|w_m(\cdot, t)\|_{L^2(\Omega)}^2 & \leq \left(C_2 \frac{|\Omega|}{k_1} + \|u_0\|_{L^2(\Omega)}^2 + \|w_0\|_{L^2(\Omega)}^2 \right) \\ & + 2C_3 \int_0^t (\|\tilde{u}_m(\cdot, s)\|_{L^2(\Omega)}^2 + \|w_m(\cdot, s)\|_{L^2(\Omega)}^2) \end{aligned}$$

and thanks to Gronwall's inequality

$$\|\tilde{u}_m(\cdot, t)\|_{L^2(\Omega)}^2 + \|w_m(\cdot, t)\|_{L^2(\Omega)}^2 \leq \left(C_2 \frac{|\Omega|}{k_1} + \|u_0\|_{L^2(\Omega)}^2 + \|w_0\|_{L^2(\Omega)}^2 \right) e^{2C_3 T} := c_1, \quad (6.46)$$

which proves (6.40).

Moreover, taking (6.45) with $t = T$, via (6.46) we have

$$k_1 \|\tilde{u}_m\|_{L^2(0, T; H^1)}^2 + C_1 \|\tilde{u}_m\|_{L^4(Q_T^*)}^4 \leq C_2 \frac{|\Omega|}{2k_1} + C_3 T c_1 + \frac{1}{2} \|u_0\|_{L^2(\Omega)}^2 + \frac{1}{2} \|w_0\|_{L^2(\Omega)}^2 =: \tilde{c}_2,$$

hence (6.41) holds with $c_2 = \max(\sqrt{\frac{\tilde{c}_2}{k_1}}, \sqrt[4]{\frac{\tilde{c}_2}{C_1}})$.

Instead, in order to prove (6.42), we need to consider $\partial_t \dot{\tilde{u}}(\cdot, t)$ as a sum of two operators: one in the dual of $H^1(\Omega)$ a.e. in $(0, T)$ (and with square integrable H^* -norm), and one in the dual of $L^4(Q_T)$. Let $v \in H^1(\Omega)$:

$$\langle \dot{\tilde{u}}_m(\cdot, t), v \rangle_* = \sum_{i=1}^m \langle \dot{\tilde{u}}_{im}(t) \Psi_i, v \rangle_* = \sum_{im=1}^m \int_{\Omega} \dot{\tilde{u}}_{im}(t) \Psi_i v = \sum_{i=1}^m \dot{\tilde{u}}_{im}(t) v_i,$$

and since the vectors $\{\Psi_i\}_{i=1}^m$ are orthogonal, the latter expression is equivalent to $\int_{\Omega} \dot{\tilde{u}}_m(\cdot, t)v_m$, where $v_m = P_m v$. Taking the first m equations of (6.39), multiplying each of them by v_i and summing up, we obtain

$$\int_{\Omega} \dot{\tilde{u}}_m(\cdot, t)v_m = -\mathcal{B}(\tilde{u}_m(\cdot, t), v_m) - \int_{\Omega^*} \tilde{f}(\tilde{u}_m(\cdot, t), w_m(\cdot, t))v_m;$$

Consider now $\dot{\tilde{u}}_m^{(1)}$ such that $\langle \dot{\tilde{u}}_m^{(1)}(\cdot, t), v \rangle_* = -\mathcal{B}(\tilde{u}_m(\cdot, t), v_m)$:

$$|\langle \dot{\tilde{u}}_m^{(1)}(\cdot, t), v \rangle_*| = |\mathcal{B}(\tilde{u}_m(\cdot, t), v_m)| \leq k_{max} \|\tilde{u}_m(\cdot, t)\|_{H^1(\Omega)} \left(1 + \frac{k_{max}}{k_1}\right) \|v\|_{H^1(\Omega)},$$

hence $\left\| \dot{\tilde{u}}_m^{(1)} \right\|_{L^2(0, T; H^*)}$ is controlled by $\|\tilde{u}\|_{L^2(0, T; H^1)}$. Instead, consider $\dot{\tilde{u}}_m^{(2)}$ such that $\langle \dot{\tilde{u}}_m^{(2)}(\cdot, t), v \rangle_* = -\int_{\Omega^*} \tilde{f}(\tilde{u}_m(\cdot, t), w_m(\cdot, t))v_m$: for each $v \in H^1(\Omega)$, $\Phi \in \mathcal{D}(0, T)$,

$$\left| \langle \dot{\tilde{u}}_m^{(2)}(\cdot, t), v \rangle_*, \Phi(t) \right| = \left| \int_{Q_T^*} \tilde{f}(\tilde{u}_m, w_m)v_m \Phi \right| \leq \left\| \tilde{f}(\tilde{u}_m, w_m) \right\|_{L^{4/3}(Q_T^*)} \|v_m \Phi\|_{L^4(Q_T)}.$$

Hence, using also (6.37) and the fact that $e^{-k_1 t} \leq 1$,

$$\begin{aligned} \left\| \dot{\tilde{u}}_m^{(2)} \right\|_{L^{4/3}(Q_T)} &\leq \left(1 + \frac{k_{max}}{k_1}\right) \left\| \tilde{f}(\tilde{u}_m, w_m) \right\|_{L^{4/3}(Q_T^*)} = c \left(\int_0^T \left\| \tilde{f}(\tilde{u}_m, w_m) \right\|_{L^{4/3}(\Omega^*)}^{4/3} dt \right)^{3/4} \\ &\leq c \left(\int_0^T \left(A_1 e^{2k_1 t} \|\tilde{u}_m(\cdot, t)\|_{L^4(\Omega^*)}^3 + A_2 |\Omega|^{3/4} + A_3 \|w_m(\cdot, t)\|_{L^2(\Omega)}^{3/2} \right)^{4/3} dt \right)^{3/4} \\ &\leq a_1 e^{2k_1 T} \|\tilde{u}_m\|_{L^4(Q_T^*)}^3 + a_2 |\Omega|^{3/4} T + a_3 \|w_m\|_{L^2(Q_T)}^{3/2} \\ &\leq a_1 e^{2k_1 T} c_2^3 + a_2 |\Omega|^{3/4} T + a_3 T c_1^{3/2}. \end{aligned}$$

We hence conclude that $\dot{\tilde{u}}_m \in L^2(0, T; H^*) + L^{4/3}(Q_T)$ and that (6.42) is verified with a suitable c_4 . Eventually, by analogous arguments, we have that $\forall \psi \in L^2(\Omega)$

$$\int_{\Omega} \dot{w}_m(\cdot, t)\psi = - \int_{\Omega} g(e^{Kt}u_m(\cdot, t), w_m(\cdot, t))\psi_m,$$

with $\psi_m = P_m \psi$. Hence, in view of (6.34),

$$\|\dot{w}_m(\cdot, t)\|_{L^2(\Omega)} \leq B_1 e^{2k_1 t} \|\tilde{u}_m(\cdot, t)\|_{L^4(\Omega)}^2 + B_2 |\Omega|^{3/4} + B_3 \|w_m(\cdot, t)\|_{L^2(\Omega)}$$

and

$$\|\dot{w}_m\|_{L^1(0, T; L^2(\Omega))} \leq B_1 e^{2k_1 T} \|\tilde{u}_m\|_{L^2(0, T; H^1(\Omega))}^2 + B_2 T |\Omega|^{3/4} + B_3 T^{1/2} \|w\|_{L^2(Q_T)}.$$

3) Convergence to a weak solution

According to estimate (6.40), the solution of the discrete problem (6.39) is well defined globally in $C^1(0, T; \mathbb{R}^{2m})$ for each m . Thanks to the provided *a priori* estimates, we know that the sequences $\{\tilde{u}_m\}$, $\{\dot{\tilde{u}}_m\}$, $\{w_m\}$, $\{\dot{w}_m\}$ are bounded (uniformly in m) in the spaces $L^2(0, T; H^1) \cap L^4(Q_T^*)$, $L^2(0, T; H^*) + L^{4/3}(Q_T)$, $L^2(Q_T)$ and $L^1(0, T; L^2(\Omega))$, respectively. According to compactness

results, we know that $\exists \tilde{u} \in L^2(0, T; H^1) \cap L^4(Q_T^*)$, $\tilde{u}^* \in L^2(0, T; H^*) + L^{4/3}(Q_T)$, $w \in L^2(Q_T)$ such that

$$\tilde{u}_m \xrightarrow{L^2(0, T; H^1)} \tilde{u}, \quad \dot{\tilde{u}}_m \xrightarrow{L^2(0, T; H^*) + L^{4/3}(Q_T)} \tilde{u}^*, \quad w_m \xrightarrow{L^2(Q_T)} w.$$

Moreover, since $L^2(0, T; H^*) + L^{4/3}(Q_T) \subset L^{4/3}(0, T; H^*)$, $\{\tilde{u}_m\}$ is such that $\|\tilde{u}_m\|_{L^2(0, T; H^1)}$ and $\|\partial_t \tilde{u}_m\|_{L^{4/3}(0, T; H^*)}$ are bounded independently of m , and by [103, Theorem 5.1, Chapter 1] this implies that, up to a subsequence, $\tilde{u}_m \xrightarrow{L^2(Q_T)} \tilde{u}$.

We now study the limit as $m \rightarrow +\infty$ of each term of the equations

$$\begin{aligned} \langle \dot{\tilde{u}}_m(\cdot, t), v \rangle_* + \mathcal{B}(\tilde{u}_m(\cdot, t), v) + \int_{\Omega} (1 - \chi_{\omega}) \tilde{f}(\tilde{u}_m(\cdot, t), w_m(\cdot, t)) v &= 0, \\ \int_{\Omega} \dot{w}_m(\cdot, t) \psi + \int_{\Omega} \tilde{g}(\tilde{u}_m(\cdot, t), w_m(\cdot, t)) \psi &= 0, \end{aligned} \quad (6.47)$$

which are equivalent to (6.39) if $v, \psi \in V_m$.

- Consider $v \in H^1(\Omega)$, $\Phi \in \mathcal{D}(0, T)$

$$\begin{aligned} \langle \lim_{m \rightarrow \infty} \langle \dot{\tilde{u}}_m(\cdot, t), v \rangle_*, \Phi \rangle &= \langle \lim_{m \rightarrow \infty} \int_{\Omega} \left(\sum_{i=1}^m \dot{\tilde{u}}_{im}(t) \Psi_i \right) v, \Phi \rangle = - \langle \lim_{m \rightarrow \infty} \int_{\Omega} \left(\sum_{i=1}^m \tilde{u}_{im}(t) \Psi_i \right) v, \Phi' \rangle \\ &= - \langle \int_{\Omega} \tilde{u} v, \Phi' \rangle = \langle \langle \partial_t \tilde{u}, v \rangle_*, \Phi \rangle, \end{aligned}$$

which implies that $\lim_{m \rightarrow \infty} \langle \dot{\tilde{u}}_m, v \rangle_* = \langle \partial_t \tilde{u}, v \rangle_*$ in a distributional sense. Moreover, since $v \Phi \in L^2(0, T; H^1) \cap L^4(Q_T^*)$ we also have

$$\lim_{m \rightarrow \infty} \langle \langle \dot{\tilde{u}}_m, v \rangle_*, \Phi \rangle = \langle \langle u^*, v \rangle_*, \Phi \rangle,$$

hence in addition $\partial_t \tilde{u} = u^* \in L^2(0, T; H^*) + L^{4/3}(Q_T)$.

- Consider $v \in H^1(\Omega)$ and $\Phi \in \mathcal{D}(0, T)$: by weak convergence,

$$\lim_{m \rightarrow \infty} \langle \mathcal{B}(\tilde{u}_m, v), \Phi \rangle = \int_0^T \lim_{m \rightarrow \infty} \mathcal{B}(\tilde{u}_m, v \Phi) = \int_0^T \mathcal{B}(\tilde{u}, v \Phi) = \langle \mathcal{B}(\tilde{u}, v), \Phi \rangle.$$

- Recalling the expression $\tilde{f}(\tilde{u}, w) = e^{2k_1 t} A \tilde{u}^3 - (1+a)e^{k_1 t} A \tilde{u}^2 + a A \tilde{u} + \tilde{u} w$, we prove separately that

$$\begin{aligned} \int_0^T \int_{\Omega} (1 - \chi_{\omega}) (e^{2k_1 t} A \tilde{u}_m^3 - (1+a)e^{k_1 t} A \tilde{u}_m^2 + a A \tilde{u}_m) v \phi &\rightarrow \\ \int_0^T \int_{\Omega} (1 - \chi_{\omega}) (e^{2k_1 t} A \tilde{u}^3 - (1+a)e^{k_1 t} A \tilde{u}^2 + a A \tilde{u}) v \phi & \end{aligned} \quad (6.48)$$

and

$$\int_0^T \int_{\Omega} (1 - \chi_{\omega}) \tilde{u}_m w_m v \phi \rightarrow \int_0^T \int_{\Omega} (1 - \chi_{\omega}) (\tilde{u} w) v \phi. \quad (6.49)$$

The limit in (6.48) is proved by Lebesgue dominated convergence theorem: since $\tilde{u}_m \xrightarrow{L^2(Q_T)} \tilde{u}$, $\tilde{u}_m \rightarrow \tilde{u}$ a.e. in Q_T , and hence the pointwise convergence of the integrand is guaranteed

almost everywhere. Moreover,

$$\begin{aligned} \|(1 - \chi_\omega)(e^{2k_1 t} A \tilde{u}_m^3 - (1 + a)e^{k_1 t} A \tilde{u}_m^2 + aA \tilde{u}_m) v \Phi\|_{L^1(Q_T^*)} &\leq \left\| \left(\tilde{A}_1 |\tilde{u}_m|^3 + \tilde{A}_2 \right) v \Phi \right\|_{L^1(Q_T^*)} \\ &\leq \left\| \tilde{A}_1 |\tilde{u}_m|^3 + \tilde{A}_2 \right\|_{L^{4/3}(Q_T^*)} \|v \Phi\|_{L^4(Q_T^*)} \leq \left(\tilde{A}_1 \|\tilde{u}_m\|_{L^4(Q_T^*)}^{3/4} + \tilde{A}_2 |\Omega|^{3/4} \right) \|v \Phi\|_{L^4(Q_T^*)}, \end{aligned}$$

which is bounded independently of m . Instead, regarding (6.49),

$$\int_{Q_T^*} (1 - \chi_\omega)(\tilde{u}_m w_m - \tilde{u} w) v \Phi = \int_{Q_T^*} (1 - \chi_\omega)(w_m - w) \tilde{u} v \Phi + \int_{Q_T^*} (1 - \chi_\omega)(\tilde{u}_m - \tilde{u}) w_m v \Phi \rightarrow 0;$$

the first term of the right-hand side vanishes thanks to the weak convergence of w_m (since $\tilde{u} \in L^4(Q_T^*)$ and also $v \Phi$). Regarding the second one, it holds that

$$\|(1 - \chi_\omega)(\tilde{u}_m - \tilde{u}) w_m v \Phi\|_{L^1(Q_T^*)} \leq \|(\tilde{u}_m - \tilde{u}) v \Phi\|_{L^2(Q_T^*)} \|w_m\|_{L^2(Q_T)},$$

and in particular $\|w_m\|_{L^2(Q_T)}$ is uniformly bounded, whereas and the other term, which can be expressed as

$$\|(\tilde{u}_m - \tilde{u}) v \Phi\|_{L^2(Q_T^*)}^2 = \int_{Q_T^*} (\tilde{u}_m - \tilde{u})^2 v^2 \Phi^2,$$

tends to 0 via Lebesgue's dominated convergence theorem. Indeed the integrand pointwise converges to 0 a.e. and the uniform bound holds

$$\|(\tilde{u}_m - \tilde{u})^2 v^2 \Phi^2\|_{L^1(Q_T^*)} \leq (c_2 + \|\tilde{u}\|_{L^4(Q_T^*)}) \|v \Phi\|_{L^4(Q_T^*)}.$$

- Analogously to the previous points, one shows that $\forall \psi \in L^2(\Omega)$, $\forall \Phi \in \mathcal{D}(0, T)$

$$\left\langle \lim_{m \rightarrow \infty} \int_{\Omega} \dot{w}_m(\cdot, t) \psi, \Phi \right\rangle = - \left\langle \lim_{m \rightarrow \infty} \int_{\Omega} w_m(\cdot, t) \psi, \Phi' \right\rangle = - \left\langle \int_{\Omega} w(\cdot, t) \psi, \Phi' \right\rangle = \left\langle \int_{\Omega} \partial_t w(\cdot, t) \psi, \Phi \right\rangle,$$

By now, we can only say that $\partial_t w(\cdot, t) \in \mathcal{D}'(0, T)$, but further regularity will be inherited in the sequel.

- Finally, recalling the expression $\tilde{g}(\tilde{u}, w) = \epsilon A e^{2k_1 t} \tilde{u}^2 - \epsilon A (1 + a) e^{k_1 t} \tilde{u} + \epsilon w$, we prove separately that

$$\int_{Q_T} (\epsilon A e^{2k_1 t} \tilde{u}_m^2 - \epsilon A (1 + a) e^{k_1 t} \tilde{u}_m) \psi \Phi \rightarrow \int_{Q_T} (\epsilon A e^{2k_1 t} \tilde{u}^2 - \epsilon A (1 + a) e^{k_1 t} \tilde{u}) \psi \Phi \quad (6.50)$$

and

$$\int_0^T \int_{\Omega} \epsilon w_m \psi \Phi \rightarrow \int_0^T \int_{\Omega} \epsilon w \psi \Phi. \quad (6.51)$$

The limit (6.50) is proved as before by Lebesgue's dominated convergence theorem, taking advantage of the (a.e.) pointwise convergence of \tilde{u}_m and of the bound

$$\begin{aligned} \|(e^{2k_1 t} \epsilon A \tilde{u}_m^2 - \epsilon A (1 + a) e^{k_1 t} \tilde{u}_m) \psi \Phi(t)\|_{L^1(Q_T)} &\leq \int_0^T \int_{\Omega} (C_1 \tilde{u}_m^2 + C_2) \psi \Phi \\ &\leq \|\psi\|_{L^2(\Omega)} \|\Phi\|_{L^\infty(0, T)} \int_0^T \|C_1 \tilde{u}_m^2(\cdot, t) + C_2\|_{L^2(\Omega)} \\ &\leq \|\psi\|_{L^2(\Omega)} \|\Phi\|_{L^\infty(0, T)} \left(C_1 \int_0^T \|\tilde{u}_m(\cdot, t)\|_{L^4(\Omega)}^2 + C_2 T \right) \\ &\leq \|\psi\|_{L^2(\Omega)} \|\Phi\|_{L^\infty(0, T)} \left(C_1 \|\tilde{u}_m\|_{L^2(0, T; H^1)}^2 + C_2 T \right). \end{aligned}$$

The limit in (6.51) immediately follows by the weak convergence of w_m .

Combining all the results that are previously listed, according to (6.47) we obtain that (\tilde{u}, w) satisfies distributionally in time

$$\begin{aligned} \langle \partial_t \tilde{u}(\cdot, t), v \rangle_* + \mathcal{B}(\tilde{u}(\cdot, t), v) + \int_{\Omega} (1 - \chi_{\omega}) \tilde{f}(\tilde{u}(\cdot, t), w(\cdot, t)) v &= 0, \\ \int_{\Omega} \partial_t w(\cdot, t) \psi + \int_{\Omega} \tilde{g}(\tilde{u}(\cdot, t), w(\cdot, t)) \psi &= 0, \end{aligned}$$

for all $v, \psi \in V_m$, $\forall m$, and since $\{\Psi_m\}$ is a basis both for $H^1(\Omega)$ and $L^2(\Omega)$, the equation is satisfied for all $v \in H^1(\Omega)$, $\psi \in L^2(\Omega)$. Eventually, since

$$\int_{\Omega} \partial_t w(\cdot, t) \psi = - \int_{\Omega} \tilde{g}(\tilde{u}(\cdot, t), w(\cdot, t)) \psi \quad \forall \psi \in L^2(\Omega),$$

then, taking $\psi = \partial_t w(\cdot, t)$ (which belongs to $L^2(\Omega)$ for a.e. t),

$$\|\partial_t w(\cdot, t)\|_{L^2(\Omega)} \leq \|\tilde{g}(\tilde{u}(\cdot, t), w(\cdot, t))\|_{L^2(\Omega)} \leq B_1 + B_2 \|\tilde{u}(\cdot, t)\|_{L^4(\Omega)}^2 + B_3 \|w(\cdot, t)\|_{L^2(\Omega)}$$

and hence $\|\dot{w}\|_{L^1(0, T; L^2(\Omega))}$ is bounded. This finally allows to conclude, after the change of variable $u = e^{Kt} \tilde{u}$, that (u, w) is a weak solution of problem (6.2) in the sense of Definition 6.1.

4) Gain of regularity on u and w

We first prove that $u \in C([0, T]; L^2(\Omega))$: indeed, it holds that $\langle \partial_t u, u \rangle_* = \frac{1}{2} \frac{d}{dt} \|u(\cdot, t)\|_{L^2(\Omega)}^2$ in the sense of distributions, and hence

$$\frac{1}{2} \frac{d}{dt} \|u(\cdot, t)\|_{L^2(\Omega)}^2 = - \int_{\Omega} K(\chi_{\omega}) |\nabla u|^2 - \int_{\Omega} (1 - \chi_{\omega}) f(u, w) u,$$

where the right-hand side surely belongs to $L^1(0, T)$. By the fundamental theorem of calculus, one obtains that $u \in C([0, T]; L^2(\Omega))$. Analogously, we show that $\frac{1}{2} \frac{d}{dt} \|w\|_{L^2(\Omega)} = \int_{\Omega} g(u, w) w \in L^1(0, T)$: indeed,

$$\begin{aligned} \int_0^T \left| \int_{\Omega} g(u(x, t), w(x, t)) w(x, t) dx \right| dt &\leq \int_0^T \|g(u(\cdot, t), w(\cdot, t))\|_{L^2(\Omega)} \|w(\cdot, t)\|_{L^2(\Omega)} dt \\ &\leq \|w\|_{L^\infty(0, T; L^2(\Omega))} \int_0^T \left(B_1 \|u(\cdot, t)\|_{L^4(\Omega)}^2 + B_2 |\Omega|^{1/2} + B_3 \|w(\cdot, t)\|_{L^2(\Omega)} \right) dt \\ &\leq \|w\|_{L^\infty(0, T; L^2(\Omega))} \left(B_1 \|u\|_{L^2(0, T; H^1(\Omega))} + B_2 T |\Omega|^{1/2} + B_3 T \|w\|_{L^\infty(0, T; L^2(\Omega))} \right), \end{aligned}$$

whence $w \in C([0, T]; L^2(\Omega))$. By the explicit expression of the solution of the third line in (6.2),

$$w(x, t) = e^{-ct} w_0(x) + \epsilon A e^{-ct} \int_0^t ((1+a)u - u^2) e^{\epsilon s} ds. \quad (6.52)$$

If we assume that $w_0 \in L^3(\Omega)$, we obtain that $w \in L^\infty(0, T; L^3(\Omega))$:

$$\begin{aligned} \|w(\cdot, t)\|_{L^3(\Omega)} &\leq \|w_0\|_{L^3(\Omega)} + c \left(\int_{\Omega} \left(\int_0^t |u(x, s)| + |u(x, s)|^2 \right)^3 \right)^{\frac{1}{3}} \\ &\leq \|w_0\|_{L^3(\Omega)} + c \int_0^t \left(\int_{\Omega} |u(x, s)|^3 + \int_{\Omega} |u(x, s)|^6 \right)^{\frac{1}{3}} ds \\ &\leq \|w_0\|_{L^3(\Omega)} + c \|u\|_{L^1(0, T; L^3(\Omega))} + c \|u\|_{L^2(0, T; L^6(\Omega))}^2 \\ &\leq \|w_0\|_{L^3(\Omega)} + c \|u\|_{L^2(0, T; H^1(\Omega))} + c \|u\|_{L^2(0, T; H^1(\Omega))}^2, \end{aligned} \quad (6.53)$$

where we have used the generalized Minkowski inequality, proved e.g. in [141, Chapter 1, formula 9.12].

5) Further *a priori* estimates

Consider now the weak formulation of (6.2) as in (6.5) and use $\varphi = u$, $\psi = w$ as test functions:

$$\begin{aligned} \frac{1}{2} \frac{d}{dt} (\|u(\cdot, t)\|_{L^2(\Omega)}^2 + \|w(\cdot, t)\|_{L^2(\Omega)}^2) + \int_{\Omega} K(\chi_{\omega}) |\nabla u(\cdot, t)|^2 + \int_{\Omega^*} f(u(\cdot, t), w(\cdot, t)) u(\cdot, t) \\ + \int_{\Omega} g(u(\cdot, t), w(\cdot, t)) w(\cdot, t) = 0 \end{aligned}$$

and by the estimates from below

$$\begin{aligned} \frac{1}{2} \frac{d}{dt} (\|u(\cdot, t)\|_{L^2(\Omega)}^2 + \|w(\cdot, t)\|_{L^2(\Omega)}^2) + k_1 \|u(\cdot, t)\|_{H^1(\Omega)}^2 + C_1 \int_{\Omega^*} |u(\cdot, t)|^4 \\ \leq C_2 + (C_3 + k_1) (\|u(\cdot, t)\|_{L^2(\Omega)}^2 + \|w(\cdot, t)\|_{L^2(\Omega)}^2). \end{aligned}$$

Since both $\frac{d}{dt} \|u(\cdot, t)\|_{L^2(\Omega)}^2$ and $\frac{d}{dt} \|w(\cdot, t)\|_{L^2(\Omega)}^2$ belong to $L^1(0, T)$, we may apply the fundamental theorem of calculus and obtain

$$\begin{aligned} \frac{1}{2} (\|u(\cdot, t)\|_{L^2(\Omega)}^2 + \|w(\cdot, t)\|_{L^2(\Omega)}^2) + \int_0^t k_1 \|u(\cdot, s)\|_{H^1(\Omega)}^2 ds + C_1 \int_{Q_T^*} |u|^4 \\ \leq (\|u_0\|_{L^2(\Omega)}^2 + \|w_0\|_{L^2(\Omega)}^2) + C_2 t + (C_3 + k_1) \int_0^s (\|u(\cdot, s)\|_{L^2(\Omega)}^2 + \|w(\cdot, s)\|_{L^2(\Omega)}^2) ds. \end{aligned}$$

By Gronwall inequality, we have

$$\frac{1}{2} (\|u(\cdot, t)\|_{L^2(\Omega)}^2 + \|w(\cdot, t)\|_{L^2(\Omega)}^2) \leq (\|u_0\|_{L^2(\Omega)}^2 + \|w_0\|_{L^2(\Omega)}^2 + C_2 t) e^{(C_3 + k_1)t},$$

hence $\|u\|_{L^\infty(0, T; L^2(\Omega))}$ is bounded by a constant depending on $\|u_0\|_{L^2(\Omega)}^2$, $\|w_0\|_{L^2(\Omega)}^2$, T, Ω, f, g and k_1 only. Analogous bounds can be proved for $\|u\|_{L^2(0, T; H^1(\Omega))}$ and $\|u\|_{L^4(Q_T^*)}$. This implies that also the bound in (6.53) only depends on $\|u_0\|_{L^2(\Omega)}^2$, $\|w_0\|_{L^2(\Omega)}^2$, T, Ω, f, g and k_1 .

6) Uniqueness

We now follow the argument of [98, Theorem 1.1]. Consider two weak solutions (u_1, w_1) and (u_2, w_2) of (6.2) in the sense of Definition 6.1. Testing both the equations for u_1 and u_2 with $\varphi = u_1 - u_2$ and subtracting, we get:

$$\begin{aligned} \frac{1}{2} \frac{d}{dt} \|u_1 - u_2\|_{L^2(\Omega)}^2 + k_1 \|u_1 - u_2\|_{H^1(\Omega)}^2 + \int_{\Omega} (1 - \chi_{\omega}) (f(u_1, w_1) - f(u_2, w_2)) (u_1 - u_2) \\ \leq k_1 \|u_1 - u_2\|_{L^2(\Omega)}^2 \end{aligned}$$

Moreover, according to the expression of f in the Aliev Panfilov model (6.3), it holds

$$\begin{aligned} f(u_1, w_1) - f(u_2, w_2) = (u_1 - u_2)(u_1^2 + u_1 u_2 + u_2^2 - (a + 1)(u_1 + u_2) + a) \\ + (u_1 - u_2)w_1 + u_2(w_1 - w_2) \end{aligned}$$

and eventually, since $|1 - \chi_{\omega}| \leq 1$,

$$\begin{aligned} \frac{1}{2} \frac{d}{dt} \|u_1 - u_2\|_{L^2(\Omega)}^2 + k_1 \|u_1 - u_2\|_{H^1(\Omega)}^2 \leq k_1 \|u_1 - u_2\|_{L^2(\Omega)}^2 \\ + (a + 1) \int_{\Omega} |u_1 + u_2| (u_1 - u_2)^2 + \int_{\Omega} |w_1| (u_1 - u_2)^2 + \int_{\Omega} |u_2| |u_1 - u_2| |w_1 - w_2| \end{aligned} \tag{6.54}$$

Consider the second term at right-hand side: via Young inequality (with coefficient ε_1 which might depend on time)

$$\begin{aligned} \int_{\Omega} |u_1 + u_2|(u_1 - u_2)^2 &\leq c\varepsilon_1(t) \|(u_1 - u_2)(u_1 + u_2)\|_{L^2(\Omega)}^2 + \frac{c}{\varepsilon_1(t)} \|u_1 - u_2\|_{L^2(\Omega)}^2 \\ &\leq c\varepsilon_1(t) \|(u_1 - u_2)\|_{L^4(\Omega)}^2 \|(u_1 + u_2)\|_{L^4(\Omega)}^2 + \frac{c}{\varepsilon_1(t)} \|u_1 - u_2\|_{L^2(\Omega)}^2 \\ &\leq c\varepsilon_1(t) (1 + \|u_1\|_{L^4(\Omega)}^2 + \|u_2\|_{L^4(\Omega)}^2) \|(u_1 - u_2)\|_{L^4(\Omega)}^2 + \frac{c}{\varepsilon_1(t)} \|u_1 - u_2\|_{L^2(\Omega)}^2. \end{aligned}$$

Selecting $\varepsilon_1(t) = \frac{\varepsilon_1}{1 + \|u_1\|_{L^4(\Omega)}^2 + \|u_2\|_{L^4(\Omega)}^2}$ we can conclude that

$$\begin{aligned} \int_{\Omega} |u_1 + u_2|(u_1 - u_2)^2 &\leq \frac{c}{\varepsilon_1} (1 + \|u_1\|_{L^4(\Omega)}^2 + \|u_2\|_{L^4(\Omega)}^2) \|u_1 - u_2\|_{L^2(\Omega)}^2 \\ &\quad + c\varepsilon_1 \|(u_1 - u_2)\|_{L^4(\Omega)}^2. \end{aligned} \quad (6.55)$$

Consider now the following term in (6.54): applying Hölder and Young inequalities,

$$\begin{aligned} \int_{\Omega} |w_1|(u_1 - u_2)^2 &= \int_{\Omega} \left(w_1^{2/3}(u_1 - u_2) \right) \left(w_1^{1/3}(u_1 - u_2) \right) \\ &\leq c\varepsilon_2 \left(\int_{\Omega} w_1^{4/3}(u_1 - u_2)^2 \right) + \frac{c}{\varepsilon_2} \left(\int_{\Omega} w_1^{2/3}(u_1 - u_2)^2 \right) \\ &\leq c\varepsilon_2 \left(\int_{\Omega} w_1^{8/3} \right)^{\frac{1}{2}} \|u_1 - u_2\|_{L^4(\Omega)}^2 + \frac{c}{\varepsilon_2} \left(\int_{\Omega} w_1^{4/3}(u_1 - u_2)^2 \right)^{\frac{1}{2}} \|u_1 - u_2\|_{L^2(\Omega)} \\ &\leq c\varepsilon_2 \|w_1\|_{L^{8/3}(\Omega)}^{4/3} \|u_1 - u_2\|_{L^4(\Omega)}^2 + \\ &\quad \frac{c}{\varepsilon_2} \left[\tilde{\varepsilon}_2 \|w_1\|_{L^{8/3}(\Omega)}^{4/3} \|u_1 - u_2\|_{L^4(\Omega)}^2 + \frac{1}{\tilde{\varepsilon}_2} \|u_1 - u_2\|_{L^2(\Omega)}^2 \right] \\ &\leq c \left(\varepsilon_2 + \frac{\tilde{\varepsilon}_2}{\varepsilon_2} \right) \|w_1\|_{L^\infty(0,T;L^3(\Omega))}^{4/3} \|u_1 - u_2\|_{L^4(\Omega)}^2 + \frac{c}{\varepsilon_2 \tilde{\varepsilon}_2} \|u_1 - u_2\|_{L^2(\Omega)}^2. \end{aligned} \quad (6.56)$$

Regarding the last term in (6.54), we derive

$$\begin{aligned} \int_{\Omega} (w_1 - w_2)u_2(u_1 - u_2) &\leq c\varepsilon_3(t) \int_{\Omega} (u_2)^2(u_1 - u_2)^2 + \frac{c}{\varepsilon_3(t)} \|w_1 - w_2\|_{L^2(\Omega)}^2 \leq \\ &\leq c\varepsilon_3(t) \|u_2\|_{L^4(\Omega)}^2 \|u_1 - u_2\|_{L^4(\Omega)}^2 + \frac{c}{\varepsilon_3(t)} \|w_1 - w_2\|_{L^2(\Omega)}^2 \end{aligned}$$

and selecting $\varepsilon_3(t) = \frac{\varepsilon_3}{1 + \|u_2\|_{L^4(\Omega)}^2}$, we conclude

$$\int_{\Omega} (w_1 - w_2)u_2(u_1 - u_2) \leq c\varepsilon_3 \|u_1 - u_2\|_{L^4(\Omega)}^2 + \frac{c}{\varepsilon_4} (1 + \|u_2\|_{L^4(\Omega)}^2) \|w_1 - w_2\|_{L^2(\Omega)}^2. \quad (6.57)$$

Collecting (6.55), (6.56) and (6.57) in (6.54),

$$\begin{aligned} \frac{1}{2} \frac{d}{dt} \|u_1 - u_2\|_{L^2(\Omega)}^2 + k_1 \|u_1 - u_2\|_{H^1(\Omega)}^2 &\leq k_1 \|u_1 - u_2\|_{L^2(\Omega)}^2 \\ &\quad + c \left(\varepsilon_1 + \left(\varepsilon_2 + \frac{\varepsilon_2}{\tilde{\varepsilon}_2} \right) \|w_1\|_{L^\infty(0,T;L^3(\Omega))} + \varepsilon_3 \right) \|u_1 - u_2\|_{L^4(\Omega)}^2 \\ &\quad + c \left(\frac{1}{\varepsilon_1} (1 + \|u_1\|_{L^4(\Omega)}^2 + \|u_2\|_{L^4(\Omega)}^2) + \frac{1}{\varepsilon_2 \tilde{\varepsilon}_2} \right) \|u_1 - u_2\|_{L^2(\Omega)}^2 \\ &\quad + \frac{c}{\varepsilon_3} (1 + \|u_2\|_{L^4(\Omega)}^2) \|w_1 - w_2\|_{L^2(\Omega)}^2, \end{aligned}$$

and selecting $\varepsilon_1, \varepsilon_2, \tilde{\varepsilon}_2$ and ε_3 such that $c \left(\varepsilon_1 + \left(\varepsilon_2 + \frac{\varepsilon_2}{\tilde{\varepsilon}_2} \right) \|w_1\|_{L^\infty(0,T;L^3(\Omega))} + \varepsilon_3 \right) = \frac{k_1}{2}$ (which is possible also thanks to the fact that the estimate in (6.53) does not depend on w_1 as previously proved), we conclude

$$\begin{aligned} \frac{d}{dt} \|u_1 - u_2\|_{L^2(\Omega)}^2 + k_1 \|u_1 - u_2\|_{H^1(\Omega)}^2 \\ \leq c(1 + \|u_1\|_{L^4(\Omega)}^2 + \|u_2\|_{L^4(\Omega)}^2) (\|u_1 - u_2\|_{L^2(\Omega)}^2 + \|w_1 - w_2\|_{L^2(\Omega)}^2). \end{aligned} \quad (6.58)$$

Analogously to what done in (6.54), testing both the equations for w_1 and w_2 with $\psi = w_1 - w_2$ and subtracting, we obtain

$$\begin{aligned} \frac{1}{2} \frac{d}{dt} \|w_1 - w_2\|_{L^2(\Omega)}^2 &= \epsilon \|w_1 - w_2\|_{L^2(\Omega)}^2 + \epsilon A(1+a) \int_{\Omega} (u_1 - u_2)(w_1 - w_2) \\ &\quad - \epsilon A \int_{\Omega} (u_1 + u_2)(u_1 - u_2)(w_1 - w_2) \\ &\leq c \|w_1 - w_2\|_{L^2(\Omega)}^2 + \|u_1 - u_2\|_{L^2(\Omega)}^2 + \varepsilon_4(t) \|u_1 + u_2\|_{L^4(\Omega)}^2 \|u_1 - u_2\|_{L^4(\Omega)}^2 \\ &\quad + \frac{c}{\varepsilon_4(t)} \|w_1 - w_2\|_{L^2(\Omega)}^2 \end{aligned}$$

and we select $\varepsilon_4(t) = \frac{\varepsilon_4}{1 + \|u_1\|_{L^4(\Omega)}^2 + \|u_2\|_{L^4(\Omega)}^2}$. Collecting together the latter inequality with (6.58), we finally conclude that

$$\begin{aligned} \frac{d}{dt} \left(\|u_1 - u_2\|_{L^2(\Omega)}^2 + \|w_1 - w_2\|_{L^2(\Omega)}^2 \right) + k_1 \|u_1 - u_2\|_{H^1(\Omega)}^2 \\ \leq A(t) \left(\|u_1 - u_2\|_{L^2(\Omega)}^2 + \|w_1 - w_2\|_{L^2(\Omega)}^2 \right) \end{aligned} \quad (6.59)$$

with $A(t) = c(1 + \|u_1(\cdot, t)\|_{L^4(\Omega)}^2 + \|u_2(\cdot, t)\|_{L^4(\Omega)}^2)$. By Gronwall's inequality, it holds that

$$\begin{aligned} \|u_1(\cdot, t) - u_2(\cdot, t)\|_{L^2(\Omega)}^2 + \|w_1(\cdot, t) - w_2(\cdot, t)\|_{L^2(\Omega)}^2 \\ \leq e^{\tilde{A}} \left(\|u_1(\cdot, 0) - u_2(\cdot, 0)\|_{L^2(\Omega)}^2 + \|w_1(\cdot, 0) - w_2(\cdot, 0)\|_{L^2(\Omega)}^2 \right), \end{aligned}$$

being \tilde{A} bounded independently of u_1, u_2 because

$$\tilde{A} = \int_0^T A(t) dt \leq c(T + \|u_1\|_{L^2(0,T;H^1(\Omega))}^2 + \|u_2\|_{L^2(0,T;H^1(\Omega))}^2)$$

and because of the *a priori* estimates for the $L^2(0, T; H^1(\Omega))$ norm previously proved. Since $u_1(\cdot, 0) = u_2(\cdot, 0) = u_0$ and $w_1(\cdot, 0) = w_2(\cdot, 0) = w_0$ we have that

$$\|u_1 - u_2\|_{L^\infty(0,T;L^2(\Omega))}, \|w_1 - w_2\|_{L^\infty(0,T;L^2(\Omega))} = 0.$$

Again from (6.59), integrating from 0 to T ,

$$k_1 \|u_1 - u_2\|_{L^2(0,T;H^1(\Omega))}^2 \leq \int_0^T A(t) \left(\|u_1 - u_2\|_{L^2(\Omega)}^2 + \|w_1 - w_2\|_{L^2(\Omega)}^2 \right) dt = 0.$$

Analogously, one immediately notices that $\|\partial_t u_1 - \partial_t u_2\|_{L^2(0,T;H^*) + L^{4/3}(Q_T)} = 0$ and also that $\|\partial_t w_1 - \partial_t w_2\|_{L^1(0,T;L^2(\Omega))} = 0$, hence the weak solution is unique.

6.4 Proof of Theorem 6.3

Since χ_ω is an indicator function, surely $\chi_\omega \in L^2(\Omega)$ and by density arguments

$$\exists\{\phi_k\} \subset C^2(\Omega) : \quad \phi_k \rightarrow \chi_\omega \text{ in } L^2(\Omega) \text{ and a.e., } \quad 0 \leq \phi_k(x) \leq 1 \quad \forall x \in \Omega. \quad (6.60)$$

Define (u_k, w_k) the solution of problem (6.2) when χ_ω is replaced with ϕ_k . We observe that, for any fixed k , an application of Theorem 6.1 ensures the existence and uniqueness of a classical solution of the problem: indeed, the conductivity tensor is again a smooth function of x , and one should replace the function f with $(1 - \phi_k)f$, and the assumptions on ϕ_k ensure that if f, g satisfy the Nagumo condition on S , the same holds for $(1 - \phi_k)f$ and g . Observe that $(u_k, w_k) \in \langle \hat{u}, \tilde{u} \rangle$ provides a uniform bound both from above and from below.

We now prove that the limit $\phi_k \xrightarrow{L^2} \chi_\omega$ implies the convergence of (u_k, w_k) to a weak solution (u, w) of (6.2). We start by proving some *a priori* estimate. Consider the weak form of the problem solved by (u_k, w_k) and take the classical solutions u_k, w_k as test functions:

$$\begin{aligned} & \frac{1}{2} \frac{d}{dt} \left(\|u_k(\cdot, t)\|_{L^2(\Omega)}^2 + \|w_k(\cdot, t)\|_{L^2(\Omega)}^2 \right) + \int_{\Omega} K(\phi_k) \nabla u_k(\cdot, t) \cdot \nabla u_k(\cdot, t) \\ &= - \int_{\Omega} (1 - \phi_k) f(u_k(\cdot, t), w_k(\cdot, t)) u_k(\cdot, t) - \int_{\Omega} g(u_k(\cdot, t), w_k(\cdot, t)) w_k(\cdot, t). \end{aligned}$$

Recall now that k_1 is the minimum between the eigenvalues of K_1 and K_0 , whereas k_{max} is the maximum among them (see Assumption 4). Moreover, since ϕ_k, u_k, w_k are bounded independently of k (indeed, $\phi_k \in [0, 1]$ and $(u_k, w_k) \in S$) and f, g are continuous, we can introduce $M_f = \max_{(x,t) \in Q_T} |(1 - \phi_k)f(u_k, w_k)|$ and $M_g = \max_{(x,t) \in Q_T} |g(u_k, w_k)|$ which are independent of k . Hence, by Hölder and Young inequalities,

$$\begin{aligned} & \frac{1}{2} \frac{d}{dt} \left(\|u_k(\cdot, t)\|_{L^2(\Omega)}^2 + \|w_k(\cdot, t)\|_{L^2(\Omega)}^2 \right) + k_1 \|u_k(\cdot, t)\|_{H^1(\Omega)}^2 \\ & \leq \left(k_1 + \frac{1}{2} \max\{M_f, M_g\} \right) \left(\|u_k(\cdot, t)\|_{L^2(\Omega)}^2 + \|w_k(\cdot, t)\|_{L^2(\Omega)}^2 \right) + \frac{1}{2} |\Omega| (M_f + M_g). \end{aligned}$$

Integrating from 0 to t and using Gronwall's inequality, we get

$$\begin{aligned} & \left(\|u_k(\cdot, t)\|_{L^2(\Omega)}^2 + \|w_k(\cdot, t)\|_{L^2(\Omega)}^2 \right) \\ & \leq \left(\|u_0\|_{L^2(\Omega)}^2 + \|w_0\|_{L^2(\Omega)}^2 + \frac{1}{2} |\Omega| (M_f + M_g) t \right) e^{(k_{min} + \frac{1}{2} \max\{M_f, M_g\})t}, \end{aligned}$$

whence

$$\begin{aligned} & \|u_k\|_{L^\infty(0,T;L^2(\Omega))}^2, \|u_k\|_{L^\infty(0,T;L^2(\Omega))}^2 \\ & \leq \left(\|u_0\|_{L^2(\Omega)}^2 + \|w_0\|_{L^2(\Omega)}^2 + \frac{1}{2} |\Omega| (M_f + M_g) T \right) e^{(k_{min} + \frac{1}{2} \max\{M_f, M_g\})T} := c_1^2. \end{aligned}$$

It also follows that

$$\|u_k\|_{L^2(0,T,H^1(\Omega))}^2 \leq \frac{1}{k_1} \left(k_1 + \frac{1}{2} \max\{M_f, M_g\} \right) c_1^2 T + \frac{1}{2k_1} |\Omega| (M_f + M_g) T =: c_2^2.$$

Regarding the derivatives, in these hypothesis we can prove that $\partial_t u_k \in L^2(0, T, H^*)$; indeed, for each $\varphi \in H^1(\Omega)$,

$$\begin{aligned} |\langle \partial_t u_k(\cdot, t), \varphi \rangle_*| &\leq k_{max} \|\nabla u_k(\cdot, t)\|_{L^2(\Omega)} \|\nabla \varphi\|_{L^2(\Omega)} + M_f |\Omega|^{\frac{1}{2}} \|\varphi\|_{L^2(\Omega)} \\ &\leq max\{k_{max}, M_f |\Omega|^{\frac{1}{2}}\} \|u_k(\cdot, t)\|_{H^1(\Omega)} \|\varphi\|_{H^1(\Omega)} \end{aligned}$$

and computing the L^2 norm in time

$$\|u_k\|_{L^2(0, T, H^*)} \leq max\{k_{max}, M_f |\Omega|^{\frac{1}{2}}\}^2 c_2^2 =: c_3^2.$$

Analogously, one proves that $\|\partial_t w_k\|_{L^2(Q_T)} \leq c_4$.

As a consequence of the uniform bounds (the constants c_1, c_2, c_3, c_4 do not depend on k), we can ensure that $\exists u \in L^2(0, T; H^1(\Omega)) \cap L^\infty(0, T; L^2(\Omega))$, $\exists w \in L^\infty(0, T; L^2(\Omega))$, $\exists u^* \in L^2(0, T; H^*)$, $\exists w^* \in L^2(Q_T)$ such that

$$u_k \xrightarrow{L^2(0, T, H^1)} u, \quad \partial_t u_k \xrightarrow{L^2(0, T, H^*)} u^*, \quad w_k \xrightarrow{L^2(Q_T)} w, \quad \partial_t w_k \xrightarrow{L^2(Q_T)} w^*.$$

We immediately remark that this implies in particular that $u_k \xrightarrow{L^2(Q_T)} u$ (see [122, Theorem 8.1]), hence $u_k \rightarrow u$ a.e. in Q_T . A pointwise convergence result could be stated also for w_k by considering the additional regularity of g : nevertheless, taking into the account the expression of f and g we do not need it in the sequel. Consider now the expression of the problem solved by (u_k, w_k) : $\forall \varphi \in H^1(\Omega)$, $\psi \in L^2(\Omega)$.

$$\begin{aligned} \langle \partial_t u_k, \varphi \rangle_* + \int_{\Omega} K(\phi_k) \nabla u_k \cdot \nabla \varphi + \int_{\Omega} (1 - \phi_k) A u_k (u_k - a)(u_k - 1) \varphi + \int_{\Omega} (1 - \phi_k) u_k w_k \varphi \\ + \int_{\Omega} \partial_t w_k \psi + \int_{\Omega} A \epsilon (u_k^2 - (1 + a) u_k) \psi + \int_{\Omega} \epsilon w_k \psi = 0. \end{aligned} \quad (6.61)$$

We proceed term by term:

- by the weak convergence of $\partial_t u_k$,

$$\lim_{k \rightarrow +\infty} \langle \partial_t u_k, \varphi \rangle_* = \langle \partial_t u, \varphi \rangle_*$$

in the sense of the distributions. Moreover, for each $\Phi \in \mathcal{D}(0, T)$,

$$\langle \lim_{k \rightarrow +\infty} \langle \partial_t u_k, \varphi \rangle_*, \Phi \rangle = - \langle \lim_{k \rightarrow +\infty} \langle u_k, \Phi' \rangle, \varphi \rangle_* = - \langle \langle u, \Phi' \rangle, \varphi \rangle_* = \langle \langle \partial_t u, \varphi \rangle_*, \Phi \rangle, \quad (6.62)$$

whence $\partial_t u = u^* \in L^2(0, T; H^*) \subset L^2(0, T; H^*) + L^{4/3}(Q_T^*)$.

- For any $\varphi \in H^1(\Omega)$, $\Phi \in \mathcal{D}(0, T)$, consider the difference

$$\begin{aligned} \langle \int_{\Omega} K(\phi_k) \nabla u_k \cdot \nabla \varphi, \Phi \rangle - \langle \int_{\Omega} K(\chi_\omega) \nabla u \cdot \nabla \varphi, \Phi \rangle \\ = \langle \int_{\Omega} K(\phi_k) \nabla (u_k - u) \cdot \nabla \varphi, \Phi \rangle + \langle \int_{\Omega} (K(\phi_k) - K(\chi_\omega)) \nabla u \cdot \nabla \varphi, \Phi \rangle. \end{aligned}$$

The first term in the latter expression converges to 0 due to weak convergence of u and since $K(\phi_k)$ is bounded in $L^\infty(\Omega)$; whereas the second term tends to 0 according to the Lebesgue's theorem, because of the pointwise (a.e.) convergence of ϕ_k to χ_ω and since the integrand is uniformly bounded by $K_0 \nabla u \cdot \nabla \varphi \Phi$, which is an integrable function. Thus,

$$\langle \int_{\Omega} K(\phi_k) \nabla u_k \cdot \nabla \varphi, \Phi \rangle \rightarrow \langle \int_{\Omega} K(\chi_\omega) \nabla u \cdot \nabla \varphi, \Phi \rangle. \quad (6.63)$$

- Using the theorem of dominated convergence, we can assess

$$\left\langle \int_{\Omega} (1 - \phi_k) A u_k (u_k - a) (u_k - 1) \varphi, \Phi \right\rangle \rightarrow \left\langle \int_{\Omega} (1 - \chi_{\omega}) A u (u - a) (u - 1) \varphi, \Phi \right\rangle, \quad (6.64)$$

indeed the (a.e.) pointwise convergence is guaranteed and the quantity

$$\|(1 - \phi_k) A u_k (u_k - a) (u_k - 1) \varphi\|_{L^1(Q_T)} \leq \|A u_k (u_k - a) (u_k - 1) \varphi\|_{L^1(Q_T)}$$

is bounded independently of k since $u_k \in [\underline{u}, \bar{u}]$.

- Consider the term $\int_{\Omega} (1 - \phi_k) u_k w_k \varphi$:

$$\begin{aligned} & \left\langle \int_{\Omega} (1 - \phi_k) u_k w_k \varphi, \Phi \right\rangle - \left\langle \int_{\Omega} (1 - \chi_{\omega}) u w \varphi, \Phi \right\rangle \\ &= \left\langle \int_{\Omega} (1 - \phi_k) u_k (w_k - w) \varphi, \Phi \right\rangle + \left\langle \int_{\Omega} ((1 - \phi_k) u_k - (1 - \chi_{\omega}) u) w \varphi, \Phi \right\rangle. \end{aligned}$$

The first addend in the summation vanishes due to weak $L^2(Q_T)$ convergence of w_k , because $\|(1 - \phi_k) u_k\|_{L^\infty(\Omega)}$ is bounded independently of k and $\varphi \in L^2(Q_T)$. The latter term instead vanishes due to Lebesgue's theorem, since ϕ_k and u_k have pointwise limit almost everywhere, and

$$\begin{aligned} & \|((1 - \phi_k) u_k - (1 - \chi_{\omega}) u) w \varphi\|_{L^1(Q_T)} \leq \\ & \|((1 - \phi_k) u_k - (1 - \chi_{\omega}) u) \Phi\|_{L^\infty(Q_T)} \|\varphi\|_{L^2(Q_T)} \|w\|_{L^2(Q_T)}. \end{aligned}$$

We finally conclude

$$\left\langle \int_{\Omega} (1 - \phi_k) u_k w_k \varphi, \Phi \right\rangle \rightarrow \left\langle \int_{\Omega} (1 - \chi_{\omega}) u w \varphi, \Phi \right\rangle. \quad (6.65)$$

- By the weak convergence of $\partial_t w_k$ in $L^2(Q_T)$,

$$\lim_{k \rightarrow +\infty} \int_{\Omega} \partial_t w_k \psi = \int_{\Omega} \partial_t w \psi$$

in the sense of the distributions. Moreover, for each $\Phi \in \mathcal{D}(0, T)$,

$$\left\langle \lim_{k \rightarrow +\infty} \int_{\Omega} \partial_t w_k \psi, \Phi \right\rangle = - \int_{\Omega} \lim_{k \rightarrow +\infty} \langle w_k, \Phi' \rangle \psi = - \int_{\Omega} \langle w, \Phi' \rangle \psi = \left\langle \int_{\Omega} \partial_t w \psi, \Phi \right\rangle, \quad (6.66)$$

thus $\partial_t w = w^* \in L^2(Q_T) \subset L^1(0, T; L^2(\Omega))$.

- The convergence

$$\left\langle \int_{\Omega} A \epsilon (u_k^2 - (1 + a) u_k) \psi, \Phi \right\rangle \rightarrow \left\langle \int_{\Omega} A \epsilon (u^2 - (1 + a) u) \psi, \Phi \right\rangle \quad (6.67)$$

can be deduced by Lebesgue's theorem.

- Finally,

$$\left\langle \lim_{k \rightarrow +\infty} \int_{\Omega} \epsilon w_k \psi, \Phi \right\rangle = \int_{\Omega} \lim_{k \rightarrow +\infty} \epsilon \langle w_k, \Phi \rangle \psi = \left\langle \int_{\Omega} \epsilon w \psi, \Phi \right\rangle \quad (6.68)$$

is an immediate consequence of the weak convergence of w_k in $L^2(Q_T)$.

Combining (6.62), (6.63), (6.64), (6.65), (6.66), (6.67), and (6.68), we can ensure that the limit (u, w) is a weak solution of (6.2). Moreover, by expressing w in closed formula we can conclude that $w_k \rightarrow w$ pointwise (a.e.) in Q_T , hence also $(u(x, t), w(x, t)) \in S$ a.e. in Q_T .

Eventually, the additional (Hölder) regularity on u can be recovered via Theorem 10.1 of [115, Chapter 3]. Indeed, consider the first equation in (6.2):

$$\partial_t u - \operatorname{div}(K(\chi_\omega)\nabla u) = -(1 - \chi_\omega)f(u, w);$$

the hypothesis of the theorem hold since $K(\chi_\omega) \in L^\infty(\Omega)$, $f(u, w) \in L^\infty(Q_T)$, and $u \in L^\infty(Q_T)$. We can extend the results up to the boundary due to the hypothesis on $\partial\Omega$ and u_0 contained in Assumption 4, and conclude $u \in C^{\alpha, \alpha/2}(\overline{Q_T})$. Regarding w , again by exploiting the representation in (6.52) we can recover the expected regularity, namely $w \in C^{\alpha, 1+\alpha/2}(\overline{Q_T})$.

Chapter 7

A posteriori error analysis for the monodomain model

This final chapter is devoted to the numerical analysis of the monodomain model. This is a preliminary study for the development of efficient techniques for the inverse problem which motivates the present thesis. In fact, the reconstruction algorithms proposed in Chapter 2 and 5 respectively for the detection of small and large inclusions in simplified models strictly rely on the solution of the associated direct problem (once or several times). The main issue of the numerical analysis of the monodomain problem is not only to formulate an algorithm for the approximation of the solution of the problem, but also to provide suitable convergence estimates for the error between the discrete and the exact solution as the discretization parameters tend to 0. In this context, the development of *a posteriori* error estimates (i.e., estimates based on indicators which can be computed by the knowledge of the discrete solution) is a key result for the introduction of an adaptive numerical scheme, allowing for a significant speedup of the computation.

Regarding the numerical analysis of models for the electrical activity of the heart, we remark that the bidomain model has been the subject of numerous studies from a numerical standpoint. Several works in the recent years have tackled the numerical approximation of this model, by employing, e.g., the Finite Element Method (FEM) for the spatial discretization, as well as an implicit scheme for the temporal discretization, endowed with a suitable Newton algorithm for the treating of the nonlinearities (see [61, Chapter 7] and references therein). In [127], a careful *a priori* analysis of the Galerkin semidiscrete space approximation of this system is performed, investigating convergence properties and stability estimates for the semidiscrete solution. This result, coupled with the argument regarding the time-discretization analysis provided in [62], allows for an exhaustive *a priori* error analysis for the bidomain model. In [59] the authors introduce a space-time adaptive algorithm for the solution of the bidomain model by resorting to a stepsize control for the temporal adaptivity, whereas spatial adaptivity is performed by virtue of *a posteriori* local error estimators. However, a complete *a posteriori* error analysis is missing.

The purpose of this chapter is to propose an *a posteriori* error analysis for the monodomain model. In particular, we consider a Newton-Galerkin approximation of the monodomain system, possibly in presence of an ischemic region. Inspired by the seminal work [137] and by the recent

papers [73, 16] we derive *a posteriori* error bounds by providing a suitable splitting of the total residual into three operators, accounting for different sources of error entailed by the discretization process. Specifically, we introduce a linearization residual, a time discretization residual, and a space discretization residual, with the additional difficulty with respect, e.g., to [16] represented by the coupled structure of the system of differential equations.

The chapter is organized as follows: in Section 7.1 we introduce the Newton-Galerkin full discretization of the monodomain model. In Section 7.2 we introduce the residual operators associated with the discrete solution and prove the equivalence between the error and the residual (in suitable norms). In Section 7.3 we define three *a posteriori* estimators and employ them to prove an upper bound for the approximation error. We also provide a lower estimate for the error in terms of the same indicators, assessing their efficiency. Finally, Section 7.4 reports some numerical experiments assessing the validity of the derived estimates and investigating convergence rates both of the error and of the estimators as the discretization parameters are reduced.

Notation: we use the symbol \lesssim to denote that an inequality holds up to a positive multiplicative constant.

7.1 A Newton-Galerkin scheme for the approximation of the monodomain model

Consider the coupled problem

$$\left\{ \begin{array}{ll} \partial_t u - \operatorname{div}(k(\chi)\nabla u) + (1 - \chi)f(u, w) = 0 & \text{in } \Omega \times (0, T), \\ k(\chi)\partial_\nu u = 0 & \text{on } \partial\Omega \times (0, T), \\ u|_{t=0} = u_0 & \text{in } \Omega, \\ \partial_t w + g(u, w) = 0 & \text{in } \Omega \times (0, T), \\ w|_{t=0} = w_0 & \text{in } \Omega, \end{array} \right. \quad (7.1)$$

being u the transmembrane electrical potential in the cardiac tissue, k the conductivity coefficient, altered by the presence of an ischemic area $\omega \subset \Omega$. Let $\chi = \chi_\omega$, $k(\chi) = k_0 - (k_0 - k_1)\chi$, $k_0 > k_1 > 0$. The nonlinear term $f(u, w)$ (which is switched off in the ischemic area) models the current induced by the motion of ions across the membrane, and is addressed as ionic current. According to a well established phenomenological approach, f is a function of the potential u and of a recovery variable w , whose dynamics is governed by a coupled nonlinear ordinary differential equation involving a nonlinear term g . We focus in particular on the Aliev-Panfilov model of the cardiac tissue, according to *linearized* version reported, e.g., in [41]; namely, the nonlinear terms f and g are as follows:

$$f(u, w) = Au(u - a)(u - 1) + uw, \quad g(u, w) = \epsilon(Au(u - 1 - a) + w), \quad (7.2)$$

with $A, \epsilon_0, \mu_1, \mu_2 > 0$, $0 < a < 1$. Such a problem is mathematically well-posed: in [41] the existence of a weak solution globally in time is proved by a Faedo-Galerkin technique in the case no ischemic area is present. For the same result in the case of the ischemic heart, we refer to a preliminary result contained in Chapter 6:

Proposition 7.1. *Let the initial data $u_0, w_0 \in C^\alpha(\bar{\Omega})$ satisfy the bound $0 \leq u_0 \leq 1$ and $0 \leq w_0 \leq \frac{A(1+a)^2}{4}$, and consider the compatibility conditions $u_0 \in C^1(\Omega)$, $\partial_\nu u_0 = 0$, being $\partial\Omega \in C^{2+\alpha}$. Then, there exists a unique weak solution (u, w) of (7.1), $u \in L^2(0, T; H^1(\Omega)) \cap L^\infty(0, T; L^2(\Omega))$, $\partial_t u \in L^2(0, T; H^*)$, $w \in L^\infty(0, T; L^2(\Omega))$, $\partial_t w \in L^2((0, T) \times \Omega)$, where $H^* = (H^1(\Omega))^*$. Moreover, $u \in C^{\alpha, \alpha/2}(\Omega \times (0, T))$, $w \in C^{\alpha, 1+\alpha/2}(\Omega \times (0, T))$ and it holds*

$$0 \leq u(x, t) \leq 1, \quad 0 \leq w(x, t) \leq \frac{A(1+a)^2}{4} \quad \forall (x, t) \in \Omega \times (0, T)$$

We will extensively take advantage of the fact that the functions f, g in (7.2) are continuously differentiable on the rectangle $[0, 1] \times [0, \frac{A(1+a)^2}{4}]$.

The weak formulation of (7.1) reads

$$\begin{cases} \int_{\Omega} \partial_t u \varphi + \int_{\Omega} k \nabla u \cdot \nabla \varphi + \int_{\Omega} (1 - \chi) f(u, w) \varphi = 0 & \forall \varphi \in H^1(\Omega), \\ \int_{\Omega} \partial_t w \psi + \int_{\Omega} g(u, w) \psi = 0 & \forall \psi \in L^2(\Omega). \end{cases} \quad (7.3)$$

For each time interval $(t_a, t_b) \subset (0, T)$, we introduce the following functional spaces:

$$\begin{aligned} X(t_a, t_b) &= \{u \text{ s.t. } u \in L^2(t_a, t_b; H^1(\Omega)) \cap L^\infty(t_a, t_b; L^2(\Omega)), \partial_t u \in L^2(t_a, t_b; H^*)\} \\ Y(t_a, t_b) &= \{w \text{ s.t. } w \in L^\infty(t_a, t_b; L^2(\Omega)), \partial_t w \in L^2((t_a, t_b) \times \Omega)\}, \end{aligned}$$

which are Banach spaces endowed with the norms:

$$\begin{aligned} \|u\|_{X(t_a, t_b)} &= \left(\|u\|_{L^2(t_a, t_b; H^1(\Omega))}^2 + \|u\|_{L^\infty(t_a, t_b; L^2(\Omega))}^2 + \|\partial_t u\|_{L^2(t_a, t_b; H^*)}^2 \right)^{\frac{1}{2}} \\ \|w\|_{Y(t_a, t_b)} &= \left(\|w\|_{L^\infty(t_a, t_b; L^2(\Omega))}^2 + \|\partial_t w\|_{L^2((t_a, t_b) \times L^2(\Omega))}^2 \right)^{\frac{1}{2}}. \end{aligned}$$

We denote only with X and Y the spaces $X(0, T)$ and $Y(0, T)$, respectively.

We now consider a semidiscretization of the problem in time by means of an implicit Euler scheme (see [61]): consider a partition of the time interval

$$\{t_n\}_{n=0}^N \subset [0, T]; \quad t_0 = 0, \quad t_N = T; \quad t_n - t_{n-1} = \tau_n > 0,$$

and define the semidiscrete solution as a couple $(\{u^n\}, \{w^n\})$, $\{u^n\}_{n=0}^N \subset H^1(\Omega)$, $\{w^n\}_{n=0}^N \subset L^2(\Omega)$ such that

$$\begin{cases} u^0 = u_0; \quad w^0 = w_0; & (7.4) \\ \int_{\Omega} \frac{u^n - u^{n-1}}{\tau^n} \varphi + \int_{\Omega} k(\chi) \nabla u^n \cdot \nabla \varphi + \int_{\Omega} (1 - \chi) f(u^n, w^n) \varphi = 0 & \forall \varphi \in H^1(\Omega), \quad (7.5) \\ \int_{\Omega} \frac{w^n - w^{n-1}}{\tau^n} \psi + \int_{\Omega} g(u^n, w^n) \psi = 0 & \forall \psi \in L^2(\Omega). \quad (7.6) \end{cases}$$

Consider the operators $\mathcal{F}^1 : H^1(\Omega) \times L^2(\Omega) \rightarrow (H^1(\Omega))^*$, $\mathcal{F}^2 : H^1(\Omega) \times L^2(\Omega) \rightarrow L^2(\Omega)$, which are defined interval-wise as follows: if $t \in (t_{n-1}, t_n]$

$$\begin{aligned} \langle \mathcal{F}^1(u, w), \varphi \rangle &= \int_{\Omega} \frac{u - u^{n-1}}{\tau^n} \varphi + \int_{\Omega} k(\chi) \nabla u \cdot \nabla \varphi + \int_{\Omega} (1 - \chi) f(u, w) \varphi \\ \langle \mathcal{F}^2(u, w), \psi \rangle &= \int_{\Omega} \frac{w - w^{n-1}}{\tau^n} \psi + \int_{\Omega} g(u, w) \psi; \end{aligned}$$

both \mathcal{F}^1 and \mathcal{F}^2 are (Fréchet) differentiable with respect to the $H^1(\Omega)$ norm in the variable u and $L^2(\Omega)$ norm in the variable w . This allows to define a Newton scheme for the solution of the nonlinear system (7.5)-(7.6):

- 1: Set $u_0^n = u^{n-1}$, $w_0^n = w^{n-1}$, $k = 1$;
- 2: **while** *exit criterion is not satisfied* **do**
- 3: compute δu , δw by solving

$$\begin{bmatrix} \mathcal{F}_u^1(u_{k-1}^n, w_{k-1}^n) & \mathcal{F}_w^1(u_{k-1}^n, w_{k-1}^n) \\ \mathcal{F}_u^2(u_{k-1}^n, w_{k-1}^n) & \mathcal{F}_w^2(u_{k-1}^n, w_{k-1}^n) \end{bmatrix} \begin{bmatrix} \delta u \\ \delta w \end{bmatrix} = \begin{bmatrix} -\mathcal{F}^1(u_{k-1}^n, w_{k-1}^n) \\ -\mathcal{F}^2(u_{k-1}^n, w_{k-1}^n) \end{bmatrix} \text{ in } H^* \times L^2 \quad (7.7)$$

- 4: update: $u_k^n = u_{k-1}^n + \delta u$, $w_k^n = w_{k-1}^n + \delta w$, $k = k + 1$;
- 5: **end while**
- 6: **return** $u^n = u_k^n$, $w^n = w_k^n$

Computing the expression of the derivatives of \mathcal{F}^1 and \mathcal{F}^2 , and substituting $\delta u = u_k^n - u_{k-1}^n$, $\delta w = w_k^n - w_{k-1}^n$, the system (7.7) can be rewritten as

$$\begin{aligned} & \int_{\Omega} \frac{1}{\tau^n} u_k^n \varphi + \int_{\Omega} k(\chi) \nabla u_k^n \cdot \nabla \varphi + \int_{\Omega} (1 - \chi) [f_u(u_{k-1}^n, w_{k-1}^n) u_k^n + f_w(u_{k-1}^n, w_{k-1}^n) w_k^n] \varphi \\ & = \int_{\Omega} (1 - \chi) [f_u(u_{k-1}^n, w_{k-1}^n) u_{k-1}^n + f_w(u_{k-1}^n, w_{k-1}^n) w_{k-1}^n - f(u_{k-1}^n, w_{k-1}^n)] \varphi + \int_{\Omega} \frac{u^{n-1}}{\tau^n} \varphi \end{aligned} \quad (7.8)$$

$$\begin{aligned} & \int_{\Omega} \frac{1}{\tau^n} w_k^n \psi + \int_{\Omega} [g_u(u_{k-1}^n, w_{k-1}^n) u_k^n + g_w(u_{k-1}^n, w_{k-1}^n) w_k^n] \psi \\ & = \int_{\Omega} [g_u(u_{k-1}^n, w_{k-1}^n) u_{k-1}^n + g_w(u_{k-1}^n, w_{k-1}^n) w_{k-1}^n - g(u_{k-1}^n, w_{k-1}^n)] \psi + \int_{\Omega} \frac{w^{n-1}}{\tau^n} \psi \end{aligned} \quad (7.9)$$

For each instant t_n , we introduce a regular triangular tessellation \mathcal{T}_h^n satisfying the following assumptions, as in [137]:

- i) $\forall n > 0$, $\exists \tilde{\mathcal{T}}_h^n$ s.t. $\tilde{\mathcal{T}}_h^n$ is a refinement of both \mathcal{T}_h^n and \mathcal{T}_h^{n-1} ;
- ii) $\exists \rho_*, \rho^* > 0$ independent of n and h s.t., defined

$$\rho(K', K) = \left\{ \frac{\text{diam}(K')}{\text{diam}(K)}, K' \in \mathcal{T}_h^n, K \in \tilde{\mathcal{T}}_h^n : K \subset K' \right\},$$

it holds $\rho_* \leq \rho(K', K) \leq \rho^* \forall K \in \mathcal{T}_h^n, \forall n = 1, \dots, N$;

- iii) the mesh is conforming to ω , i.e., defined $\omega_h^n = \bigcup_{K \in \mathcal{T}_h^n} K : K \subset \omega$, $\omega_h^n \equiv \omega$.

Taking advantage of $\tilde{\mathcal{T}}_h^n$, we introduce the Finite Element discrete space $V_h^n \subset H^1(\Omega)$

$$V_h^n = \{v_h \in C(\bar{\Omega}), v_h|_K \in \mathbb{P}_1(K) \forall K \in \tilde{\mathcal{T}}_h^n\}$$

and the L^2 orthogonal projection $\Pi_H^n : L^2(\Omega) \rightarrow V_h^n$.

The fully discrete solution of (7.1) consists in the pair $(\{u_{h,k}^n\}, \{w_{h,k}^n\})$, with $n = 0, \dots, N$ and $k = 0, \dots, K_n$, being K_n the maximum number of iterations performed in each timestep: such number may vary with n . In particular, $\{u_{h,K_n}^n\}$ and $\{w_{h,K_n}^n\}$ are such that:

- $u_h^0 = \Pi_H^0 u_0$, $w_h^0 = \Pi_H^0 w_0$, the projections of the initial data on \mathcal{T}_h^0 ;
- for each $n = 1, \dots, N$, $u_{h,0}^n = \Pi_H^n u_{h,K_{n-1}}^{n-1}$, the last iteration associated to the previous timestep;
- for each $n = 1, \dots, N$, for each $k = 1, \dots, K_n$, $u_{h,k}^n$ and $w_{h,k}^n$ solve (7.8), (7.9) for all $\varphi_h, \psi_h \in V_h$.

7.2 Residual operators

For a fixed fully discrete solution $(\{u_{h,k}^n\}, \{w_{h,k}^n\})$ as above, collecting all the final indices K_n in a multi-index $\mathbf{k} = [K_n]_{n=1}^N$, the associated linear interpolated solution $(u_{h,\tau}^{(\mathbf{k})}, w_{h,\tau}^{(\mathbf{k})})$ is a couple of continuous functions on $(0, T)$, defined timestep-wise as follows: for each $t \in (t_{n-1}, t_n]$, $n = 1, \dots, N$,

$$u_{h,\tau}^{(\mathbf{k})} = \frac{t - t_{n-1}}{\tau_n} u_{h,K_n}^n + \frac{t_n - t}{\tau_n} u_{h,K_{n-1}}^{n-1}, \quad w_{h,\tau}^{(\mathbf{k})} = \frac{t - t_{n-1}}{\tau_n} w_{h,K_n}^n + \frac{t_n - t}{\tau_n} w_{h,K_{n-1}}^{n-1}. \quad (7.10)$$

We now define for almost each instant t the *residual* operator $R(t)$ in the product space $(H^1(\Omega) \times L^2(\Omega))^* = H^* \times L^2(\Omega)$, being H^* the dual space of $H^1(\Omega)$:

$$\begin{aligned} \langle R(t), (\varphi, \psi) \rangle &= \langle R_1(t), \varphi \rangle + \langle R_2(t), \psi \rangle \quad \forall \varphi \in H^1(\Omega), \psi \in L^2(\Omega) \\ \langle R_1(t), \varphi \rangle &= - \int_{\Omega} \partial_t u_{h,\tau}^{(\mathbf{k})} \varphi - \int_{\Omega} k(\chi) \nabla u_{h,\tau}^{(\mathbf{k})} \cdot \nabla \varphi - \int_{\Omega} (1 - \chi) f(u_{h,\tau}^{(\mathbf{k})}, w_{h,\tau}^{(\mathbf{k})}) \varphi \\ \langle R_2(t), \psi \rangle &= - \int_{\Omega} \partial_t w_{h,\tau}^{(\mathbf{k})} \psi - \int_{\Omega} g(u_{h,\tau}^{(\mathbf{k})}, w_{h,\tau}^{(\mathbf{k})}) \psi. \end{aligned} \quad (7.11)$$

It is possible to prove a result of equivalence between the X, Y norms of the error and the dual norms of the residual operators. More precisely, it holds:

Theorem 7.1. *The operators $R_1(t)$ and $R_2(t)$ are s.t. the functions $\|R_1(t)\|_{H^*}$ and $\|R_2(t)\|_{L^2(\Omega)}$ are square integrable on each interval $(t_a, t_b) \subset (0, T)$, and moreover*

$$\left\{ \|R_1\|_{L^2(t_a, t_b, H^*)}^2 + \|R_2\|_{L^2((t_a, t_b) \times \Omega)}^2 \right\}^{\frac{1}{2}} \leq c^* \left\{ \|u - u_{h,\tau}^{(\mathbf{k})}\|_{X(t_a, t_b)}^2 + \|w - w_{h,\tau}^{(\mathbf{k})}\|_{Y(t_a, t_b)}^2 \right\}^{\frac{1}{2}} \quad (7.12a)$$

$$\begin{aligned} c_* \left\{ \|u - u_{h,\tau}^{(\mathbf{k})}\|_{X(0,t)}^2 + \|w - w_{h,\tau}^{(\mathbf{k})}\|_{Y(0,t)}^2 \right\}^{\frac{1}{2}} &\leq \left\{ \|u_0 - \Pi_H^0 u_0\|_{L^2(\Omega)}^2 + \|w_0 - \Pi_H^0 w_0\|_{L^2(\Omega)}^2 \right. \\ &\quad \left. + \|R_1\|_{L^2(0,t, H^*)}^2 + \|R_2\|_{L^2((0,t) \times \Omega)}^2 \right\}^{\frac{1}{2}}, \end{aligned} \quad (7.12b)$$

where c_* and c^* depend on Ω, k_0, k_1, f, g and T .

Proof. By summing and subtracting the expression of $\langle R_1(t), \varphi \rangle$ and $\langle R_2(t), \psi \rangle$ to equation (7.3) we obtain, $\forall \varphi \in H^1(\Omega), \forall \psi \in L^2(\Omega)$, a.e. $t \in (0, T)$

$$\begin{aligned} \int_{\Omega} \partial_t (u - u_{h,\tau}^{(\mathbf{k})}) \varphi + \int_{\Omega} k(\chi) \nabla (u - u_{h,\tau}^{(\mathbf{k})}) \cdot \nabla \varphi + \int_{\Omega} (1 - \chi) (f(u, w) - f(u_{h,\tau}^{(\mathbf{k})}, w_{h,\tau}^{(\mathbf{k})})) \varphi \\ + \int_{\Omega} \partial_t (w - w_{h,\tau}^{(\mathbf{k})}) \psi + \int_{\Omega} (g(u, w) - g(u_{h,\tau}^{(\mathbf{k})}, w_{h,\tau}^{(\mathbf{k})})) \psi = \langle R_1(t), \varphi \rangle + \langle R_2(t), \psi \rangle. \end{aligned} \quad (7.13)$$

Fixing $\psi = 0$ and employing the Cauchy-Schwarz inequality and the mean value theorem for Banach spaces *

$$\begin{aligned} |\langle R_1(t), \varphi \rangle| &\leq \left\| \partial_t(u - u_{h,\tau}^{(\mathbf{k})}) \right\|_{H^*} \|\varphi\|_{H^1(\Omega)} + k_0 \left\| \nabla(u - u_{h,\tau}^{(\mathbf{k})}) \right\|_{L^2(\Omega)} \|\nabla\varphi\|_{L^2(\Omega)} \\ &\quad + \left\| f_u(\xi, \eta)(u - u_{h,\tau}^{(\mathbf{k})}) + f_w(\xi, \eta)(w - w_{h,\tau}^{(\mathbf{k})}) \right\|_{L^2(\Omega)} \|\varphi\|_{L^2(\Omega)} \\ &\leq \left(\left\| \partial_t(u - u_{h,\tau}^{(\mathbf{k})}) \right\|_{H^*} + k_0 \left\| u - u_{h,\tau}^{(\mathbf{k})} \right\|_{H^1(\Omega)} + c_{f_u} \left\| u - u_{h,\tau}^{(\mathbf{k})} \right\|_{L^2(\Omega)} \right. \\ &\quad \left. + c_{f_w} \left\| w - w_{h,\tau}^{(\mathbf{k})} \right\|_{L^2(\Omega)} \right) \|\varphi\|_{H^1(\Omega)}. \end{aligned}$$

Computing the L^2 norm on (t_a, t_b) we obtain

$$\begin{aligned} \|R_1\|_{L^2(t_a, t_b; H^*)} &\leq \left(\left\| \partial_t(u - u_{h,\tau}^{(\mathbf{k})}) \right\|_{L^2(t_a, t_b; H^*)} + k_0 \left\| u - u_{h,\tau}^{(\mathbf{k})} \right\|_{L^2(t_a, t_b; H^1)} \right. \\ &\quad \left. + c_{f_u} \left\| u - u_{h,\tau}^{(\mathbf{k})} \right\|_{L^2((t_a, t_b) \times \Omega)} + c_{f_w} \left\| w - w_{h,\tau}^{(\mathbf{k})} \right\|_{L^2((t_a, t_b) \times \Omega)} \right). \end{aligned} \quad (7.14)$$

Analogously, when taking $\varphi = 0$, we recover:

$$\begin{aligned} \|R_2\|_{L^2((t_a, t_b) \times \Omega)} &\leq \left(\left\| \partial_t(w - w_{h,\tau}^{(\mathbf{k})}) \right\|_{L^2((t_a, t_b) \times \Omega)} + c_{g_u} \left\| u - u_{h,\tau}^{(\mathbf{k})} \right\|_{L^2((t_a, t_b) \times \Omega)} \right. \\ &\quad \left. + c_{g_w} \left\| w - w_{h,\tau}^{(\mathbf{k})} \right\|_{L^2((t_a, t_b) \times \Omega)} \right), \end{aligned} \quad (7.15)$$

and summing (7.14) and (7.15) we prove (7.12a).

Vice versa, consider (7.13) and take $\varphi = u - u_{h,\tau}^{(\mathbf{k})}$, $\psi = w - w_{h,\tau}^{(\mathbf{k})}$; by mean value theorem † it holds that

$$\begin{aligned} &\frac{1}{2} \frac{d}{dt} \left(\left\| u - u_{h,\tau}^{(\mathbf{k})} \right\|_{L^2(\Omega)}^2 + \left\| w - w_{h,\tau}^{(\mathbf{k})} \right\|_{L^2(\Omega)}^2 \right) + \int_{\Omega} k(\chi) \nabla(u - u_{h,\tau}^{(\mathbf{k})}) \cdot \nabla(u - u_{h,\tau}^{(\mathbf{k})}) \\ &\quad + \int_{\Omega} (1 - \chi) (f_u(\xi_1, \eta_1)(u - u_{h,\tau}^{(\mathbf{k})}) + f_w(\xi_1, \eta_1)(w - w_{h,\tau}^{(\mathbf{k})}))(u - u_{h,\tau}^{(\mathbf{k})}) \\ &\quad + \int_{\Omega} (g_u(\xi_2, \eta_2)(u - u_{h,\tau}^{(\mathbf{k})}) + g_w(\xi_2, \eta_2)(w - w_{h,\tau}^{(\mathbf{k})}))(w - w_{h,\tau}^{(\mathbf{k})}) \\ &= \langle R_1, u - u_{h,\tau}^{(\mathbf{k})} \rangle + \langle R_2, w - w_{h,\tau}^{(\mathbf{k})} \rangle. \end{aligned}$$

Consider now the quadratic form $\mathcal{Q} : H^1(\Omega) \times L^2(\Omega) \rightarrow \mathbb{R}$,

$$\mathcal{Q}(m, n) = \int_{\Omega} -(1 - \chi) f_u(\xi_1, \eta_1) m^2 - ((1 - \chi) f_w(\xi_1, \eta_1) + g_u(\xi_2, \eta_2)) mn - g_w(\xi_2, \eta_2) n^2,$$

*Applying Theorem 4.A in [140] on the Banach space $H^1 \times L^2$ we have $\left\| f(u, w) - f(u_{h,\tau}^{(\mathbf{k})}, w_{h,\tau}^{(\mathbf{k})}) \right\|_{L^2} \leq \sup_{0 \leq \tau \leq 1} \left\| f_u(u + \tau(u_{h,\tau}^{(\mathbf{k})} - u), w + \tau(w_{h,\tau}^{(\mathbf{k})} - w))(u_{h,\tau}^{(\mathbf{k})} - u) + f_w(u + \tau(u_{h,\tau}^{(\mathbf{k})} - u), w + \tau(w_{h,\tau}^{(\mathbf{k})} - w))(w_{h,\tau}^{(\mathbf{k})} - w) \right\|_{L^2}$, whereas by the continuity of the derivatives of f and via the boundedness of the solutions of (7.3) we assess that $\|f_u(\xi, \eta)\|_{L^\infty} \leq c_{f_u}$, $\|f_w(\xi, \eta)\|_{L^\infty} \leq c_{f_w}$. Analogous procedure holds on g .

† in this case we consider the Lagrange mean value theorem on the real valued function $h : \tau \in \mathbb{R} \rightarrow h(\tau) = \int_{\Omega} (1 - \chi) f(u + \tau(u_{h,\tau}^{(\mathbf{k})} - u), w + \tau(w_{h,\tau}^{(\mathbf{k})} - w))(u_{h,\tau}^{(\mathbf{k})} - u)$: there exists $\tau^* \in [0, 1]$ s.t. $h(1) - h(0) = h'(\tau^*)$.

which allows to rewrite the previous equation as

$$\begin{aligned} & \frac{1}{2} \frac{d}{dt} \left(\|u - u_{h,\tau}^{(\mathbf{k})}\|_{L^2(\Omega)}^2 + \|w - w_{h,\tau}^{(\mathbf{k})}\|_{L^2(\Omega)}^2 \right) + \int_{\Omega} k(\chi) \nabla(u - u_{h,\tau}^{(\mathbf{k})}) \cdot \nabla(u - u_{h,\tau}^{(\mathbf{k})}) \\ & = \mathcal{Q}(u - u_{h,\tau}^{(\mathbf{k})}, w - w_{h,\tau}^{(\mathbf{k})}) + \langle R_1, u - u_{h,\tau}^{(\mathbf{k})} \rangle + \langle R_2, w - w_{h,\tau}^{(\mathbf{k})} \rangle. \end{aligned}$$

It holds that $|\mathcal{Q}(m, n)| \leq \lambda_{max}(\|m\|_{H^1(\Omega)} + \|n\|_{L^2(\Omega)})$, being λ_{max} a continuous function of f_u, f_w, g_u, g_w , hence bounded from above on $\Omega \times (0, T)$ by a positive constant Λ . Via Cauchy-Schwartz and Young inequalities,

$$\begin{aligned} & \frac{1}{2} \frac{d}{dt} \left(\|u - u_{h,\tau}^{(\mathbf{k})}\|_{L^2(\Omega)}^2 + \|w - w_{h,\tau}^{(\mathbf{k})}\|_{L^2(\Omega)}^2 \right) + k_1 \|u - u_{h,\tau}^{(\mathbf{k})}\|_{H^1(\Omega)}^2 \leq k_1 \|u - u_{h,\tau}^{(\mathbf{k})}\|_{L^2(\Omega)}^2 \\ & + \Lambda \left(\|u - u_{h,\tau}^{(\mathbf{k})}\|_{L^2(\Omega)}^2 + \|w - w_{h,\tau}^{(\mathbf{k})}\|_{L^2(\Omega)}^2 \right) + \frac{1}{2k_1} \left(\|R_1\|_{H^*}^2 + \|R_2\|_{L^2(\Omega)}^2 \right) \\ & + \frac{k_1}{2} \left(\|u - u_{h,\tau}^{(\mathbf{k})}\|_{H^1(\Omega)}^2 + \|w - w_{h,\tau}^{(\mathbf{k})}\|_{L^2(\Omega)}^2 \right), \end{aligned}$$

hence

$$\begin{aligned} & \frac{1}{2} \frac{d}{dt} \left(\|u - u_{h,\tau}^{(\mathbf{k})}\|_{L^2(\Omega)}^2 + \|w - w_{h,\tau}^{(\mathbf{k})}\|_{L^2(\Omega)}^2 \right) + \frac{k_1}{2} \|u - u_{h,\tau}^{(\mathbf{k})}\|_{H^1(\Omega)}^2 \\ & \leq (\Lambda + k_1) \left(\|u - u_{h,\tau}^{(\mathbf{k})}\|_{L^2(\Omega)}^2 + \|w - w_{h,\tau}^{(\mathbf{k})}\|_{L^2(\Omega)}^2 \right) + \frac{1}{2k_1} \left(\|R_1\|_{H^*}^2 + \|R_2\|_{L^2(\Omega)}^2 \right) \end{aligned}$$

Take now a fixed $t \in (0, T)$ and integrate from 0 to t , obtaining

$$\begin{aligned} & \left(\| (u - u_{h,\tau}^{(\mathbf{k})})(t) \|_{L^2(\Omega)}^2 + \| (w - w_{h,\tau}^{(\mathbf{k})})(t) \|_{L^2(\Omega)}^2 \right) + k_1 \|u - u_{h,\tau}^{(\mathbf{k})}\|_{L^2(0,t;H^1)}^2 \leq \\ & \int_0^t 2(\Lambda + k_1) \left(\| (u - u_{h,\tau}^{(\mathbf{k})})(s) \|_{L^2(\Omega)}^2 + \| (w - w_{h,\tau}^{(\mathbf{k})})(s) \|_{L^2(\Omega)}^2 \right) ds \\ & + \int_0^t \frac{1}{k_1} \left(\|R_1(s)\|_{H^*}^2 + \|R_2(s)\|_{L^2(\Omega)}^2 \right) ds + \left(\|u_0 - u_{h,\tau}^{(\mathbf{k})}(0)\|_{L^2(\Omega)}^2 + \|w_0 - w_{h,\tau}^{(\mathbf{k})}(0)\|_{L^2(\Omega)}^2 \right). \end{aligned} \tag{7.16}$$

Via Gronwall's inequality, we obtain

$$\begin{aligned} & \left(\|u(t) - u_{h,\tau}^{(\mathbf{k})}(t)\|_{L^2(\Omega)}^2 + \|w(t) - w_{h,\tau}^{(\mathbf{k})}(t)\|_{L^2(\Omega)}^2 \right) \leq e^{2(\Lambda+k_1)t} \left(\|u_0 - \Pi_H^0 u_0\|_{L^2(\Omega)}^2 + \|w_0 - \Pi_H^0 w_0\|_{L^2(\Omega)}^2 \right) \\ & + \frac{1}{k_1} \left(\|R_1\|_{L^2(0,t;H^*)}^2 + \|R_2\|_{L^2((0,t)\times\Omega)}^2 \right), \end{aligned}$$

whence the bound on $\|u - u_{h,\tau}^{(\mathbf{k})}\|_{L^\infty(0,t;L^2(\Omega))}, \|w - w_{h,\tau}^{(\mathbf{k})}\|_{L^\infty(0,t;L^2(\Omega))}$. It also holds by (7.16) that

$$\begin{aligned} & k_1 \|u - u_{h,\tau}^{(\mathbf{k})}\|_{L^2(0,t;H^1)}^2 \leq 2(\Lambda + k_1)t \left(\|u - u_{h,\tau}^{(\mathbf{k})}\|_{L^\infty(0,t;L^2(\Omega))}^2 + \|w - w_{h,\tau}^{(\mathbf{k})}\|_{L^\infty(0,t;L^2(\Omega))}^2 \right) \\ & + \frac{1}{k_1} \left(\|R_1\|_{L^2(0,t;H^*)}^2 + \|R_2\|_{L^2((0,t)\times\Omega)}^2 \right) + \left(\|u_0 - u_{h,\tau}^{(\mathbf{k})}(0)\|_{L^2(\Omega)}^2 + \|w_0 - w_{h,\tau}^{(\mathbf{k})}(0)\|_{L^2(\Omega)}^2 \right). \end{aligned}$$

Finally, taking $\psi = 0$ in (7.13), by Cauchy-Schwarz inequality we get

$$\| \partial_t(u - u_{h,\tau}^{(\mathbf{k})})(t) \|_{H^*} \leq k_0 \| (u - u_{h,\tau}^{(\mathbf{k})})(t) \|_{H^1(\Omega)} + c_{f_u} \| (u - u_{h,\tau}^{(\mathbf{k})})(t) \|_{L^2(\Omega)} + c_{f_w} \| (w - w_{h,\tau}^{(\mathbf{k})})(t) \|_{L^2(\Omega)}$$

thus

$$\begin{aligned} \left\| \partial_t (u - u_{h,\tau}^{(\mathbf{k})}) \right\|_{L^2((0,t) \times \Omega)} &\leq k_0 \left\| u - u_{h,\tau}^{(\mathbf{k})} \right\|_{L^2(0,t;H^1(\Omega))} + c_{f_u} \sqrt{t} \left\| u - u_{h,\tau}^{(\mathbf{k})} \right\|_{L^\infty(0,t;L^2(\Omega))} \\ &\quad + c_{f_w} \sqrt{t} \left\| w - w_{h,\tau}^{(\mathbf{k})} \right\|_{L^\infty(0,t;L^2(\Omega))}. \end{aligned}$$

A similar strategy allows to conclude that an analogous bound holds for $\partial_t (w - w_{h,\tau}^{(\mathbf{k})})$, hence every part of the norms $\left\| u - u_{h,\tau}^{(\mathbf{k})} \right\|_{X(0,t)}$, $\left\| w - w_{h,\tau}^{(\mathbf{k})} \right\|_{Y(0,t)}$ is bounded as in the thesis. \square

It is now possible to perform a decomposition of the residual operators: according to the strategy proposed in [16], we distinguish the contribution of space discretization, time discretization and linearization as follows :

$$\begin{aligned} \langle R_1^h(t), \varphi \rangle &= - \int_{\Omega} \frac{u_{h,K_n}^n - u_{h,K_{n-1}}^{n-1}}{\tau_n} \varphi - \int_{\Omega} k(\chi) \nabla u_{h,K_n}^n \cdot \nabla \varphi \\ &\quad - \int_{\Omega} (1 - \chi) [f(u_{h,K_{n-1}}^n, w_{h,K_{n-1}}^n) + f_u(u_{h,K_{n-1}}^n, w_{h,K_{n-1}}^n)(u_{h,K_n}^n - u_{h,K_{n-1}}^n) \\ &\quad + f_w(u_{h,K_{n-1}}^n, w_{h,K_{n-1}}^n)(w_{h,K_n}^n - w_{h,K_{n-1}}^n)] \varphi; \end{aligned} \quad (7.17a)$$

$$\begin{aligned} \langle R_1^\tau(t), \varphi \rangle &= - \int_{\Omega} k(\chi) \nabla (u_{h,\tau}^{(\mathbf{k})} - u_{h,K_n}^n) \cdot \nabla \varphi - \int_{\Omega} (1 - \chi) [f(u_{h,\tau}^{(\mathbf{k})}, w_{h,\tau}^{(\mathbf{k})}) \\ &\quad - f(u_{h,K_n}^n, w_{h,K_n}^n)] \varphi; \end{aligned} \quad (7.17b)$$

$$\begin{aligned} \langle R_1^k(t), \varphi \rangle &= - \int_{\Omega} (1 - \chi) [f(u_{h,K_n}^n, w_{h,K_n}^n) - f_u(u_{h,K_{n-1}}^n, w_{h,K_{n-1}}^n)(u_{h,K_n}^n - u_{h,K_{n-1}}^n) \\ &\quad - f_w(u_{h,K_{n-1}}^n, w_{h,K_{n-1}}^n)(w_{h,K_n}^n - w_{h,K_{n-1}}^n) - f(u_{h,K_{n-1}}^n, w_{h,K_{n-1}}^n)] \varphi \end{aligned} \quad (7.17c)$$

$$\begin{aligned} \langle R_2^h(t), \psi \rangle &= - \int_{\Omega} \frac{w_{h,K_n}^n - w_{h,K_{n-1}}^{n-1}}{\tau_n} \psi - \int_{\Omega} [g(u_{h,K_{n-1}}^n, w_{h,K_{n-1}}^n) \\ &\quad + g_u(u_{h,K_{n-1}}^n, w_{h,K_{n-1}}^n)(u_{h,K_n}^n - u_{h,K_{n-1}}^n) \\ &\quad + g_w(u_{h,K_{n-1}}^n, w_{h,K_{n-1}}^n)(w_{h,K_n}^n - w_{h,K_{n-1}}^n)] \psi; \end{aligned} \quad (7.18a)$$

$$\langle R_2^\tau(t), \psi \rangle = - \int_{\Omega} [g(u_{h,\tau}^{(\mathbf{k})}, w_{h,\tau}^{(\mathbf{k})}) - g(u_{h,K_n}^n, w_{h,K_n}^n)] \psi; \quad (7.18b)$$

$$\begin{aligned} \langle R_2^k(t), \psi \rangle &= - \int_{\Omega} [g(u_{h,K_n}^n, w_{h,K_n}^n) - g_u(u_{h,K_{n-1}}^n, w_{h,K_{n-1}}^n)(u_{h,K_n}^n - u_{h,K_{n-1}}^n) \\ &\quad - g_w(u_{h,K_{n-1}}^n, w_{h,K_{n-1}}^n)(w_{h,K_n}^n - w_{h,K_{n-1}}^n) - g(u_{h,K_{n-1}}^n, w_{h,K_{n-1}}^n)] \psi \end{aligned} \quad (7.18c)$$

It is immediate to verify that $R_1^h(t) + R_1^\tau(t) + R_1^k(t) = R_1(t)$ in H^* and $R_2^h(t) + R_2^\tau(t) + R_2^k(t) = R_2(t)$ in $L^2(\Omega)$; moreover, according to the expression of the discrete problem (7.8), (7.9), it holds the orthogonality:

$$\begin{aligned} \langle R_1^h(t), \varphi_h \rangle &= 0 & \forall \varphi_h \in V_h \\ \langle R_2^h(t), \psi_h \rangle &= 0 & \forall \psi_h \in H_h. \end{aligned} \quad (7.19)$$

7.3 A posteriori estimators

We now provide *a posteriori* estimators for the residual operators. In order to do so, we adopt the following notation: for each element $K \in \tilde{\mathcal{T}}_h^n$, the common refinement of \mathcal{T}_h^n and \mathcal{T}_h^{n-1} , recall h_K its diameter, $\chi_K = \chi|_K$ (i.e., according to the assumptions on χ , $\chi_K = 1$ if $K \subset \omega$ and 0 otherwise), $k_K = k(\chi_K)$. Moreover, each face of the tessellation $E \in \tilde{\mathcal{E}}_h^n$ has diameter h_E , and, apart from the edges on the external boundary, belong to two distinct elements $K_{E,1}$ and $K_{E,2}$: we recall

$$[k_E \nu_E \cdot \nabla u_h]_E = (k_{K_{E,1}} \nu_{E,1} \cdot \nabla u_h|_{K_{E,1}} - k_{K_{E,2}} \nu_{E,2} \cdot \nabla u_h|_{K_{E,2}})|_E,$$

where $\nu_{E,1}$ and $\nu_{E,2}$ are outer the normals of E with respect to $K_{E,1}$ and $K_{E,2}$, hence $\nu_{E,1} = -\nu_{E,2}$. Instead, each face E of the external boundary belongs to a single element K of the tessellation, and we define

$$[k_E \nu_E \cdot \nabla u_h]_E = (k_{K_E} \nu_E \cdot \nabla u_h|_{K_E})|_E,$$

We now introduce the *a posteriori* quantities which will be involved in estimates from above and from below for the residual error.

$$\begin{aligned} \eta_k^n &= \left(\sum_{K \in \tilde{\mathcal{T}}_h^n} h_K^2 \|R_{K,1}\|_{L^2(K)}^2 + \sum_{E \in \tilde{\mathcal{E}}_h^n} h_E \|R_E\|_{L^2(E)}^2 + \sum_{K \in \tilde{\mathcal{T}}_h^n} \|R_{K,2}\|_{L^2(K)}^2 \right)^{\frac{1}{2}} \\ R_{K,1} &= \left(-\frac{u_{h,K_n}^n - u_{h,K_{n-1}}^{n-1}}{\tau_n} + k_K \Delta u_{h,K_n}^n - (1 - \chi_K)(f(u_{h,K_{n-1}}^n, w_{h,K_{n-1}}^n) \right. \\ &\quad \left. - f_u(u_{h,K_{n-1}}^n, w_{h,K_{n-1}}^n)(u_{h,K_n}^n - u_{h,K_{n-1}}^n) - f_w(u_{h,K_{n-1}}^n, w_{h,K_{n-1}}^n)(w_{h,K_n}^n - w_{h,K_{n-1}}^n)) \right)|_K \\ R_E &= [k_E \nu_E \cdot \nabla u_h^n]_E \\ R_{K,2} &= \left(-\frac{w_{h,K_n}^n - w_{h,K_{n-1}}^{n-1}}{\tau_n} - (g(u_{h,K_{n-1}}^n, w_{h,K_{n-1}}^n) - g_u(u_{h,K_{n-1}}^n, w_{h,K_{n-1}}^n)(u_{h,K_n}^n - u_{h,K_{n-1}}^n) \right. \\ &\quad \left. - g_w(u_{h,K_{n-1}}^n, w_{h,K_{n-1}}^n)(w_{h,K_n}^n - w_{h,K_{n-1}}^n)) \right)|_K. \\ \vartheta_k^n &= \left(\frac{1}{3} \left\| \nabla(u_{h,K_n}^n - u_{h,K_{n-1}}^{n-1}) \right\|_{L^2(\Omega)}^2 + \frac{1}{\tau_n} \|P_1(t)\|_{L^2((t_{n-1}, t_n) \times \Omega)}^2 + \frac{1}{\tau_n} \|P_2(t)\|_{L^2((t_{n-1}, t_n) \times \Omega)}^2 \right)^{\frac{1}{2}} \\ P_1(t) &= -(1 - \chi)(f(u_{h,\tau}^{(\mathbf{k})}, w_{h,\tau}^{(\mathbf{k})}) - f(u_{h,K_n}^n, w_{h,K_n}^n)) \\ P_2(t) &= -(g(u_{h,\tau}^{(\mathbf{k})}, w_{h,\tau}^{(\mathbf{k})}) - g(u_{h,K_n}^n, w_{h,K_n}^n)). \\ \gamma_k^n &= \left(\|Q_1\|_{L^2(\Omega)}^2 + \|Q_2\|_{L^2(\Omega)}^2 \right)^{\frac{1}{2}} \\ Q_1 &= -(1 - \chi) \left(f(u_{h,K_n}^n, w_{h,K_n}^n) - f_u(u_{h,K_{n-1}}^n, w_{h,K_{n-1}}^n)(u_{h,K_n}^n - u_{h,K_{n-1}}^n) \right. \\ &\quad \left. - f_w(u_{h,K_{n-1}}^n, w_{h,K_{n-1}}^n)(w_{h,K_n}^n - w_{h,K_{n-1}}^n) - f(u_{h,K_{n-1}}^n, w_{h,K_{n-1}}^n) \right). \\ Q_2 &= - \left(g(u_{h,K_n}^n, w_{h,K_n}^n) - g_u(u_{h,K_{n-1}}^n, w_{h,K_{n-1}}^n)(u_{h,K_n}^n - u_{h,K_{n-1}}^n) \right. \\ &\quad \left. - g_w(u_{h,K_{n-1}}^n, w_{h,K_{n-1}}^n)(w_{h,K_n}^n - w_{h,K_{n-1}}^n) - g(u_{h,K_{n-1}}^n, w_{h,K_{n-1}}^n) \right). \end{aligned}$$

The fundamental result we prove in this section is the following bound from above of the error involving the introduced *a posteriori* estimators:

Theorem 7.2. *For each discrete solution $(\{u_{h,k}^n\}, \{w_{h,k}^n\})$ with $n = 1, \dots, N$, $k = 1, \dots, K_n$, collecting all K_n in the multi-index $\mathbf{k} = [K_n]_{n=1}^N$ and defining $u_{h,\tau}^{(\mathbf{k})}, w_{h,\tau}^{(\mathbf{k})}$ as in (7.10), it holds that for each $n = 1, \dots, N$:*

$$\left\{ \|u - u_{h,\tau}^{\mathbf{k}}\|_{X(0,t_n)}^2 + \|w - w_{h,\tau}^{(\mathbf{k})}\|_{Y(0,t_n)}^2 \right\}^{\frac{1}{2}} \lesssim \left\{ \|u_0 - \Pi_V^0 u_0\|_{L^2(\Omega)}^2 + \|w_0 - \Pi_H^0 w_0\|_{L^2(\Omega)}^2 + \sum_{m=1}^n \tau_n ((\eta_k^m)^2 + (\vartheta_{k,U}^m)^2 + (\gamma_{k,U}^m)^2) \right\}^{\frac{1}{2}} \quad (7.20)$$

In order to prove Theorem 7.2, we need a preliminary results involving the spatial residual operators alone. First, we remark that $R_1^k(t)$ and $R_2^k(t)$ are constant in time within each interval (t_{n-1}, t_n) . Hence, as remarked in [137] and [16], upper and lower estimates of their norms in each instant $t \in (t_{n-1}, t_n)$ involving the *a posteriori* estimator η_k^n can be proved by similar arguments as the ones for elliptic problems. This allows to conclude that

Lemma 7.1. *There exist two positive constants c_\dagger, c^\dagger independent of n s.t., for almost every $t \in (t_{n-1}, t_n)$ and for each $n = 1, \dots, N$, it holds:*

$$\frac{1}{c_\dagger} \eta_k^n \leq \left(\|R_1^h(t)\|_{H^*}^2 + \|R_2^h(t)\|_{L^2(\Omega)}^2 \right)^{\frac{1}{2}} \leq c^\dagger \eta_k^n. \quad (7.21)$$

Proof. Throughout the computation, we consider $t \in (t_{n-1}, t_n)$ and neglect the dependence of R_1^h, R_2^h on t . First we prove the upper bound. Integrating by parts the expression of R_1^h and exploiting assumption *iii*) on the tessellation, which ensures that each k_K is a constant scalar on each K , we obtain that for each $\varphi \in H^1(\Omega)$

$$\langle R_1^h, \varphi \rangle = \sum_{K \in \tilde{\mathcal{T}}_h^n} \int_K R_{K,1} \varphi + \sum_{E \in \tilde{\mathcal{E}}_h^n} \int_E R_E \varphi.$$

Introduce now the Clément interpolation operator $I_h : H^1(\Omega) \rightarrow V_h^n$: by the orthogonality result in (7.19), and by the properties of I_h (see [58],[138]),

$$\begin{aligned} |\langle R_1^h, \varphi \rangle| &= |\langle R_1^h, I_h \varphi \rangle + \langle R_1^h, \varphi - I_h \varphi \rangle| \leq \sum_{K \in \tilde{\mathcal{T}}_h^n} \left| \int_K R_{K,1} (\varphi - I_h \varphi) \right| + \sum_{E \in \tilde{\mathcal{E}}_h^n} \left| \int_E R_E (\varphi - I_h \varphi) \right| \\ &\leq c_1 \sum_{K \in \tilde{\mathcal{T}}_h^n} h_K \|R_{K,1}\|_{L^2(K)} \|\nabla \varphi\|_{L^2(\tilde{\omega}_K)} + c_2 \sum_{E \in \tilde{\mathcal{E}}_h^n} h_E^{\frac{1}{2}} \|R_E\|_{L^2(E)} \|\nabla \varphi\|_{L^2(\tilde{\omega}_E)}, \end{aligned}$$

where $\tilde{\omega}_K$ ($\tilde{\omega}_E$) is the union of all the elements of $\tilde{\mathcal{T}}_h^n$ containing at least a vertex of K (E). This entails that

$$\|R_1^h\|_{H^*} \lesssim \sum_{K \in \tilde{\mathcal{T}}_h^n} h_K \|R_{K,1}\|_{L^2(K)} + \sum_{E \in \tilde{\mathcal{E}}_h^n} h_E^{\frac{1}{2}} \|R_E\|_{L^2(E)}.$$

By an application of Cauchy-Schwartz inequality the upper bound on R_2^h immediately follows:

$$\|R_2^h\|_{L^2(\Omega)} \leq \sum_{K \in \tilde{\mathcal{T}}_h^n} \|R_{K,2}\|_{L^2(\Omega)}.$$

In order to prove the lower bound, we construct

$$W_n = \alpha \sum_{K \in \tilde{\mathcal{T}}_h^n} h_K^2 \phi_K R_{K,1} - \beta \sum_{E \in \tilde{\mathcal{E}}_h^n} h_E \phi_E R_E,$$

with $\alpha, \beta > 0$, ϕ_K, ϕ_E the barycentric bubble functions respectively on K and $\omega_E = K_{E,1} \cup K_{E,2}$. Analogously to [137, Lemma 5.1], we can show that

$$\langle R_1^h, W_n \rangle \geq \left(\sum_{K \in \tilde{\mathcal{T}}_h^n} h_K^2 \|R_K\|_{L^2(K)}^2 + \sum_{E \in \tilde{\mathcal{E}}_h^n} h_E \|R_E\|_{L^2(E)}^2 \right)$$

and

$$\|W_n\|_{H^1(\Omega)} \leq c_{\dagger} \left(\sum_{K \in \tilde{\mathcal{T}}_h^n} h_K^2 \|R_K\|_{L^2(K)}^2 + c_2 \sum_{E \in \tilde{\mathcal{E}}_h^n} h_E \|R_E\|_{L^2(E)}^2 \right)^{\frac{1}{2}}.$$

Regarding R_2^h , the following equality holds

$$\|R_2^h\|_{L^2(\Omega)}^2 = \sum_{K \in \tilde{\mathcal{T}}_h^n} \langle R_2^h, R_{K,2} \rangle = \sum_{K \in \tilde{\mathcal{T}}_h^n} \|R_{K,2}\|_{L^2(K)}^2,$$

and this concludes the proof of the lower bound. \square

It is now possible to prove the upper estimate (7.20).

Proof of Theorem 7.2. We impose $k_0 = 1$ and $\omega = \emptyset$ for the sake of simplicity. In view of (7.12a), we only aim at proving that, for each $n = 1, \dots, N$, it holds

$$\|R_1\|_{L^2(t_{n-1}, t_n, H^*)}^2 + \|R_2\|_{L^2((t_{n-1}, t_n) \times \Omega)}^2 \leq \tau_n ((\eta_k^m)^2 + (\vartheta_k^m)^2 + (\gamma_k^m)^2) \quad (7.22)$$

According to Lemma 7.1,

$$\|R_1^h(t)\|_{H^*}^2 + \|R_2^h(t)\|_{L^2(\Omega)}^2 \lesssim (\eta_k^n)^2 \quad \forall t \in (t_{n-1}, t_n),$$

and since by definition both R_1^h and R_2^h are constant in each interval (t_{n-1}, t_n) , we conclude that

$$\|R_1^h\|_{L^2(t_{n-1}, t_n, H^*)}^2 + \|R_2^h\|_{L^2((t_{n-1}, t_n) \times \Omega)}^2 \lesssim \tau_n (\eta_k^n)^2. \quad (7.23)$$

Moreover, it is immediate to verify via Cauchy-Schwarz inequality that

$$\|R_1^k(t)\|_{H^*}^2 + \|R_2^k(t)\|_{L^2(\Omega)}^2 \lesssim (\gamma_k^n)^2 \quad \forall t \in (t_{n-1}, t_n),$$

and by integration

$$\|R_1^k\|_{L^2(t_{n-1}, t_n, H^*)}^2 + \|R_2^k\|_{L^2((t_{n-1}, t_n) \times \Omega)}^2 \lesssim \tau_n (\gamma_k^n)^2. \quad (7.24)$$

Eventually, again by Cauchy-Schwarz inequality, for each $t \in (t_{n-1}, t_n)$

$$\begin{aligned} \|R_1^r(t)\|_{H^*} + \|R_2^r(t)\|_{L^2(\Omega)} &\leq \left\| \nabla(u_{h,\tau}^{(\mathbf{k})} - u_{h,K_n}^n) \right\|_{L^2(\Omega)} + \left\| f(u_{h,\tau}^{(\mathbf{k})}, w_{h,\tau}^{(\mathbf{k})}) - f(u_{h,K_n}^n, w_{h,K_n}^n) \right\|_{L^2(\Omega)} \\ &\quad + \left\| g(u_{h,\tau}^{(\mathbf{k})}, w_{h,\tau}^{(\mathbf{k})}) - g(u_{h,K_n}^n, w_{h,K_n}^n) \right\|_{L^2(\Omega)} \\ &\leq \frac{t_n - t}{\tau_n} \left\| \nabla(u_{h,K_n}^n - u_{h,K_{n-1}}^{n-1}) \right\|_{L^2(\Omega)} + \left\| f(u_{h,\tau}^{(\mathbf{k})}, w_{h,\tau}^{(\mathbf{k})}) - f(u_{h,K_n}^n, w_{h,K_n}^n) \right\|_{L^2(\Omega)} \\ &\quad + \left\| g(u_{h,\tau}^{(\mathbf{k})}, w_{h,\tau}^{(\mathbf{k})}) - g(u_{h,K_n}^n, w_{h,K_n}^n) \right\|_{L^2(\Omega)} \end{aligned}$$

Since $\int_{t_{n-1}}^{t_n} \left(\frac{t_n-t}{\tau_n}\right)^2 = \frac{\tau_n}{3}$, we get

$$\begin{aligned} & \|R_1^\tau\|_{L^2(t_{n-1}, t_n, H^*)}^2 + \|R_2^\tau\|_{L^2((t_{n-1}, t_n) \times \Omega)}^2 \lesssim \frac{\tau_n}{3} \left\| \nabla(u_{h, K_n}^n - u_{h, K_{n-1}}^{n-1}) \right\|_{L^2(\Omega)}^2 \\ & + \left\| f(u_{h, \tau}^{(\mathbf{k})}, w_{h, \tau}^{(\mathbf{k})}) - f(u_{h, K_n}^n, w_{h, K_n}^n) \right\|_{L^2((t_{n-1}, t_n) \times \Omega)}^2 \\ & + \left\| g(u_{h, \tau}^{(\mathbf{k})}, w_{h, \tau}^{(\mathbf{k})}) - g(u_{h, K_n}^n, w_{h, K_n}^n) \right\|_{L^2((t_{n-1}, t_n) \times \Omega)}^2 \lesssim \tau_n (\theta_k^n)^2 \end{aligned} \quad (7.25)$$

By means of the triangular inequality, (7.23), (7.24) and (7.25) allow to conclude (7.22), and hence (7.20). \square

7.3.1 Efficiency of the estimators

The upper estimate provided in (7.20) holds for any choice of \mathbf{k} , i.e., the total number of Newton iterations K_n computed in each interval (t_{n-1}, t_n) can be selected arbitrarily. We now prove a result of efficiency (namely, an estimate from below for the error in terms of the introduced *a posteriori* estimators), which can be stated when a specific condition is satisfied by the indices K_n . In particular, for each $n \geq 1$, we assume there exists K_n such that

$$\gamma_k^n \leq \sigma \eta_k^n, \quad (7.26)$$

being $\sigma \leq \frac{1}{c_\dagger}$, where c_\dagger is the constant appearing in Lemma 7.1. Such an hypothesis can be compared to the one introduced in [73, equation (3.12)].

Moreover, we need to introduce the following assumption on the nonlinear terms f and g :

$$\begin{aligned} & \exists \lambda > 0 \quad \text{s.t.} \quad \forall u_1, u_2, w_1, w_2 \in \mathbb{R} \\ & (f(u_1, w_1) - f(u_2, w_2))(u_1 - u_2) + (g(u_1, w_1) - g(u_2, w_2))(w_1 - w_2) \\ & \geq \lambda ((u_1 - u_2)^2 + (w_1 - w_2)^2). \end{aligned} \quad (7.27)$$

This assumption is verified under small modifications of the original problem by a large class of models including Aliev-Panfilov, see Remark 7.1.

Theorem 7.3. *Let f, g satisfy (7.27) and let $(\{u_{h,k}^n\}, \{w_{h,k}^n\})$, $n = 0, \dots, N$, $k = 0, \dots, K_n$ be the fully discrete solution of (7.1) obtained by the Newton scheme (7.8), (7.9), satisfying assumption (7.26) on the choice of K_n . Then,*

$$\sqrt{\tau_n} ((\eta_k^n)^2 + (\vartheta_k^n)^2 + (\gamma_k^n)^2)^{\frac{1}{2}} \lesssim \left\{ \left\| u - u_{h, \tau}^{(\mathbf{k})} \right\|_{X(t_{n-1}, t_n)}^2 + \left\| w - w_{h, \tau}^{(\mathbf{k})} \right\|_{Y(t_{n-1}, t_n)}^2 \right\}^{\frac{1}{2}}, \quad (7.28)$$

being $u_{h, \tau}^{(\mathbf{k})}, w_{h, \tau}^{(\mathbf{k})}$ the interpolants defined in (7.10).

Proof. First of all, we exploit the assumption (7.27) on f, g to obtain a useful inequality. Consider the temporal residual operators R_1^τ, R_2^τ with test functions $\varphi_1 = u_{h, \tau}^{(\mathbf{k})} - u_{h, K_n}^n$, $\psi_1 = w_{h, \tau}^{(\mathbf{k})} - w_{h, K_n}^n$:

$$\begin{aligned} \langle R_1^\tau, \varphi_1 \rangle + \langle R_2^\tau, \psi_1 \rangle & \geq \left\| \nabla(u_{h, \tau}^{(\mathbf{k})} - u_{h, K_n}^n) \right\|_{L^2(\Omega)}^2 + \lambda \left(\left\| u_{h, \tau}^{(\mathbf{k})} - u_{h, K_n}^n \right\|_{L^2(\Omega)}^2 + \left\| w_{h, \tau}^{(\mathbf{k})} - w_{h, K_n}^n \right\|_{L^2(\Omega)}^2 \right) \\ & \geq \lambda \left(\frac{t - t_{n-1}}{\tau_n} \right)^2 \left(\left\| u_{h, K_n}^n - u_{h, K_{n-1}}^{n-1} \right\|_{H^1(\Omega)}^2 + \left\| w_{h, K_n}^n - w_{h, K_{n-1}}^{n-1} \right\|_{L^2(\Omega)}^2 \right) \end{aligned}$$

Since

$$\langle R_1^\tau, \varphi_1 \rangle + \langle R_2^\tau, \psi_1 \rangle = \langle R_1, \varphi_1 \rangle + \langle R_2, \psi_1 \rangle - \langle R_1^h, \varphi_1 \rangle - \langle R_2^h, \psi_1 \rangle - \langle R_1^k, \varphi_1 \rangle - \langle R_2^k, \psi_1 \rangle,$$

integrating in time and making use of (7.21), (7.12a) and of the Jensen inequality $A + B \leq \sqrt{2}(A^2 + B^2)^{\frac{1}{2}}$ we get

$$\lambda \frac{\tau_n}{3} \left(\left\| u_{h,K_n}^n - u_{h,K_{n-1}}^{n-1} \right\|_{H^1(\Omega)}^2 + \left\| w_{h,K_n}^n - w_{h,K_{n-1}}^{n-1} \right\|_{L^2(\Omega)}^2 \right)^{\frac{1}{2}} \leq 2\sqrt{\tau_n} c^* \|err\|_{XY} + 2\tau_n c^\dagger \eta_k^n + 2\tau_n \gamma_k^n, \quad (7.29)$$

where we denote $\|err\|_{XY} = \left(\left\| u - u_{h,\tau}^{(\mathbf{k})} \right\|_{X(t_{n-1}, t_n)}^2 + \left\| w - w_{h,\tau}^{(\mathbf{k})} \right\|_{Y(t_{n-1}, t_n)}^2 \right)^{\frac{1}{2}}$ for the sake of simplicity.

We focus now on the spatial estimator η_k^n . According to the proof of Lemma 7.1, there exists a couple of test functions φ_2, ψ_2 such that

$$\langle R_1^h, \varphi_2 \rangle + \langle R_2^h, \psi_2 \rangle \geq (\eta_k^n)^2, \quad \left(\|\varphi_2\|_{H^1(\Omega)}^2 + \|\psi_2\|_{L^2(\Omega)}^2 \right)^{\frac{1}{2}} \leq c_\dagger \eta_k^n$$

whence

$$\frac{1}{c_\dagger} \eta_k^n \left(\|\varphi_2\|_{H^1(\Omega)}^2 + \|\psi_2\|_{L^2(\Omega)}^2 \right)^{\frac{1}{2}} \leq \langle R_1^h, \varphi_2 \rangle + \langle R_2^h, \psi_2 \rangle.$$

By the decomposition of the residual, $R_1^h = R_1 - R_1^\tau - R_1^k$ and $R_2^h = R_2 - R_2^\tau - R_2^k$. Moreover,

$$\begin{aligned} |\langle R_1^\tau, \varphi_2 \rangle + \langle R_2^\tau, \psi_2 \rangle| &\leq \int_{\Omega} \left| \nabla(u_{h,\tau}^{(\mathbf{k})} - u_{h,K_n}^n) \cdot \nabla \varphi_2 \right| + \int_{\Omega} \left| \left[f(u_{h,\tau}^{(\mathbf{k})}, w_{h,\tau}^{(\mathbf{k})}) - f(u_{h,K_n}^n, w_{h,K_n}^n) \right] \varphi_2 \right| \\ &\quad + \int_{\Omega} \left| \left[g(u_{h,\tau}^{(\mathbf{k})}, w_{h,\tau}^{(\mathbf{k})}) - g(u_{h,K_n}^n, w_{h,K_n}^n) \right] \psi_2 \right| \\ &\leq \left\| \nabla(u_{h,\tau}^{(\mathbf{k})} - u_{h,K_n}^n) \right\|_{L^2(\Omega)} \|\nabla \varphi_2\|_{L^2(\Omega)} \\ &\quad + K_f \left(\left\| u_{h,\tau}^{(\mathbf{k})} - u_{h,K_n}^n \right\|_{L^2(\Omega)} + \left\| w_{h,\tau}^{(\mathbf{k})} - w_{h,K_n}^n \right\|_{L^2(\Omega)} \right) \|\varphi_2\|_{L^2(\Omega)} \\ &\quad + K_g \left(\left\| u_{h,\tau}^{(\mathbf{k})} - u_{h,K_n}^n \right\|_{L^2(\Omega)} + \left\| w_{h,\tau}^{(\mathbf{k})} - w_{h,K_n}^n \right\|_{L^2(\Omega)} \right) \|\psi_2\|_{L^2(\Omega)} \\ &\leq K_{fg} \left(\left\| u_{h,\tau}^{(\mathbf{k})} - u_{h,K_n}^n \right\|_{H^1(\Omega)} + \left\| w_{h,\tau}^{(\mathbf{k})} - w_{h,K_n}^n \right\|_{L^2(\Omega)} \right) \left(\|\varphi_2\|_{H^1(\Omega)} + \|\psi_2\|_{L^2(\Omega)} \right), \end{aligned}$$

where K_f and K_g are the Lipschitz constants of f and g (which are obviously related to the constants $c_{f_u}, c_{f_w}, c_{g_u}, c_{g_w}$ previously introduced) and $K_{fg} = \max\{1, K_f, K_g\}$. Exploiting (7.12a), the Cauchy-Schwarz and the Jensen inequalities and the definition of γ_k^n ,

$$\frac{1}{c_\dagger} \eta_k^n \leq 2 \left(\|R_1\|_{H^*}^2 + \|R_2\|_{L^2(\Omega)}^2 \right)^{\frac{1}{2}} + 2\gamma_k^n + 2K_{fg} \left(\left\| u_{h,\tau}^{(\mathbf{k})} - u_{h,K_n}^n \right\|_{H^1(\Omega)}^2 + \left\| w_{h,\tau}^{(\mathbf{k})} - w_{h,K_n}^n \right\|_{L^2(\Omega)}^2 \right)^{\frac{1}{2}},$$

and since $u_{h,\tau}^{(\mathbf{k})} - u_{h,K_n}^n = \frac{t_n - t}{\tau_n} (u_{h,K_n}^n - u_{h,K_{n-1}}^{n-1})$,

$$\begin{aligned} \frac{1}{c_\dagger} \eta_k^n &\leq 2 \left(\|R_1\|_{H^*}^2 + \|R_2\|_{L^2(\Omega)}^2 \right)^{\frac{1}{2}} + 2\gamma_k^n \\ &\quad + 2 \frac{t_n - t}{\tau_n} K_{fg} \left(\left\| u_{h,K_n}^n - u_{h,K_{n-1}}^{n-1} \right\|_{H^1(\Omega)}^2 + \left\| w_{h,K_n}^n - w_{h,K_{n-1}}^{n-1} \right\|_{L^2(\Omega)}^2 \right)^{\frac{1}{2}}. \end{aligned} \quad (7.30)$$

We take advantage of the strategy used in the proof of the lower bound in [137], in particular, choosing a positive α , we multiply the inequality (7.30) by $(\alpha + 1) \left(\frac{t-t_{n-1}}{\tau_n} \right)^\alpha$ and integrate from t_{n-1} to t_n . We observe that

$$\begin{aligned} \int_{t_{n-1}}^{t_n} (\alpha + 1) \left(\frac{t-t_{n-1}}{\tau_n} \right)^\alpha &= \tau_n; \\ \int_{t_{n-1}}^{t_n} \left(\frac{t-t_{n-1}}{\tau_n} \right)^\alpha (\alpha + 1) \left(\frac{t_n-t}{\tau_n} \right) &= \tau_n \frac{1}{\alpha + 2}; \\ \int_{t_{n-1}}^{t_n} (\alpha + 1) \left(\frac{t-t_{n-1}}{\tau_n} \right)^\alpha \left(\|R_1\|_{H^*}^2 + \|R_2\|_{L^2(\Omega)}^2 \right)^{\frac{1}{2}} &\leq \\ \sqrt{\tau_n} \frac{\alpha + 1}{\sqrt{2\alpha + 1}} \left(\|R_1\|_{L^2(t_{n-1}, t_n; H^*)}^2 + \|R_2\|_{L^2((t_{n-1}, t_n) \times \Omega)}^2 \right)^{\frac{1}{2}}. \end{aligned}$$

We obtain (applying (7.12a) and (7.29)):

$$\begin{aligned} \frac{1}{c_\dagger} \tau_n \eta_k^n &\leq \sqrt{\tau_n} \frac{\alpha + 1}{\sqrt{2\alpha + 1}} c^* \|err\|_{XY} + \tau_n \gamma_k^n \\ &\quad + \tau_n \frac{2}{\alpha + 2} K_{fg} \left(\|u_{h, K_n}^n - u_{h, K_{n-1}}^{n-1}\|_{L^2(\Omega)} + \|w_{h, K_n}^n - w_{h, K_{n-1}}^{n-1}\|_{L^2(\Omega)} \right)^{\frac{1}{2}} \\ &\leq \sqrt{\tau_n} \frac{\alpha + 1}{\sqrt{2\alpha + 1}} c^* \|err\|_{XY} + \tau_n \gamma_k^n \\ &\quad + \frac{1}{\alpha + 2} \frac{12K_{fg}}{\lambda} (\sqrt{\tau_n} c^* \|err\|_{XY} + \tau_n c_\dagger^\dagger \eta_k^n + \tau_n \gamma_k^n) \end{aligned}$$

Taking advantage of the assumption (7.26) and dividing by $\sqrt{\tau_n}$,

$$\frac{1}{c_\dagger} \sqrt{\tau_n} \eta_k^n \leq c^* \left(\frac{\alpha + 1}{\sqrt{2\alpha + 1}} + \frac{12K_{fg}}{\lambda(\alpha + 2)} \right) \|err\|_{XY} + \sqrt{\tau_n} \left(\frac{12K_{fg}(\sigma + c^\dagger)}{\lambda(\alpha + 2)} + \sigma \right) \eta_k^n. \quad (7.31)$$

Now η_k^n appears on both sides of the estimate, but we can require that

$$\frac{12K_{fg}(\sigma + c^\dagger)}{\lambda(\alpha + 2)} + \sigma < \frac{1}{c_\dagger},$$

by selecting (according to the assumption on σ)

$$\alpha > \frac{12K_{fg}(c^\dagger + \sigma)c_\dagger}{\lambda(1 - c_\dagger\sigma)} - 2.$$

Thus, we deduce

$$\sqrt{\tau_n} \eta_k^n \lesssim \|err\|_{XY}; \quad (7.32)$$

from now on, we omit the explicit expression of the constants in front of each term in the inequality. As an immediate consequence, again by (7.26), we conclude that also

$$\sqrt{\tau_n} \gamma_k^n \leq \sqrt{\tau_n} \sigma \eta_k^n \lesssim \|err\|_{XY}. \quad (7.33)$$

We now aim at estimating the last *a posteriori* estimator, θ_k^n . By definition,

$$\begin{aligned}
(\vartheta_k^n)^2 &= \frac{1}{3} \left\| \nabla(u_{h,K_n}^n - u_{h,K_{n-1}}^{n-1}) \right\|_{L^2(\Omega)}^2 + \frac{1}{\tau_n} \left\| f(u_{h,\tau}^{(\mathbf{k})}, w_{h,\tau}^{(\mathbf{k})}) - f(u_{h,K_n}^n, w_{h,K_n}^n) \right\|_{L^2((t_{n-1}, t_n) \times \Omega)}^2 \\
&\quad + \frac{1}{\tau_n} \left\| g(u_{h,\tau}^{(\mathbf{k})}, w_{h,\tau}^{(\mathbf{k})}) - g(u_{h,K_n}^n, w_{h,K_n}^n) \right\|_{L^2((t_{n-1}, t_n) \times \Omega)}^2 \\
&\leq \frac{1}{3} \left\| \nabla(u_{h,K_n}^n - u_{h,K_{n-1}}^{n-1}) \right\|_{L^2(\Omega)}^2 + \frac{K_{fg}^2}{\tau_n} \int_{t_{n-1}}^{t_n} \left(\left\| u_{h,\tau}^{(\mathbf{k})} - u_{h,K_n}^n \right\|_{L^2(\Omega)}^2 + \left\| w_{h,\tau}^{(\mathbf{k})} - w_{h,K_n}^n \right\|_{L^2(\Omega)}^2 \right) \\
&\leq \frac{1}{3} \left\| \nabla(u_{h,K_n}^n - u_{h,K_{n-1}}^{n-1}) \right\|_{L^2(\Omega)}^2 + \frac{K_{fg}^2}{3} \left(\left\| u_{h,K_n}^n - u_{h,K_{n-1}}^{n-1} \right\|_{L^2(\Omega)}^2 + \left\| w_{h,K_n}^n - w_{h,K_{n-1}}^{n-1} \right\|_{L^2(\Omega)}^2 \right) \\
&\leq \frac{K_{fg}^2}{3} \left(\left\| u_{h,K_n}^n - u_{h,K_{n-1}}^{n-1} \right\|_{H^1(\Omega)}^2 + \left\| w_{h,K_n}^n - w_{h,K_{n-1}}^{n-1} \right\|_{L^2(\Omega)}^2 \right)
\end{aligned}$$

Therefore, in view of (7.29)

$$\begin{aligned}
\vartheta_k^n &\leq \frac{K_{fg}^2}{3} \left(\left\| u_{h,K_n}^n - u_{h,K_{n-1}}^{n-1} \right\|_{H^1(\Omega)}^2 + \left\| w_{h,K_n}^n - w_{h,K_{n-1}}^{n-1} \right\|_{L^2(\Omega)}^2 \right)^{\frac{1}{2}} \\
&\leq \frac{K_{fg}^2}{\lambda \tau_n} (2\sqrt{\tau_n} c^* \|err\|_{XY} + 2\tau_n c^\dagger \eta_k^n + \tau_n \gamma_k^n),
\end{aligned}$$

and eventually (using (7.32) and (7.33))

$$\sqrt{\tau_n} \vartheta_k^n \leq \frac{K_{fg}^2}{\lambda} (2c^* \|err\|_{XY} + 2\sqrt{\tau_n} c^\dagger \eta_k^n + \sqrt{\tau_n} \gamma_k^n) \lesssim \|err\|_{XY} \quad (7.34)$$

Eventually, collecting the results (7.32), (7.33), (7.34) we conclude that

$$\sqrt{\tau_n} ((\eta_k^n)^2 + (\theta_k^n)^2 + (\gamma_k^n)^2)^{\frac{1}{2}} \leq \sqrt{\tau_n} (\eta_k^n + \theta_k^n + \gamma_k^n) \lesssim \|err\|_{XY}. \quad (7.35)$$

□

Remark 7.1. Assumption (7.27) is in general not satisfied by f and g as in (7.2). In particular, inequality (7.27) holds with a possibly negative constant, $-\tilde{K}$. This can be deduced by mean value theorem, exploiting the fact that f, g in (7.2) are continuously differentiable and take values on a bounded subset of \mathbb{R}^2 due to the uniform *a priori* bounds on the solutions prescribed in Proposition 7.1. We can thus perform an alteration of the original problem (7.1): for a positive λ , consider a change of variable in the original problem: $\tilde{u} = e^{-(\tilde{K}+\lambda)t}u$, $\tilde{w} = e^{-(\tilde{K}+\lambda)t}w$. It holds $\partial_t \tilde{u} = -(\tilde{K} + \lambda)\tilde{u} + e^{-(\tilde{K}+\lambda)t}\partial_t u$, hence (\tilde{u}, \tilde{w}) is the solution of

$$\begin{cases} \partial_t \tilde{u} - \operatorname{div}(k(\chi)\nabla \tilde{u}) + (1 - \chi)\tilde{f}(\tilde{u}, \tilde{w}) = 0 & \text{in } \Omega \times (0, T) \\ \partial_t \tilde{w} + \tilde{g}(\tilde{u}, \tilde{w}) = 0 & \text{in } \Omega \times (0, T), \end{cases}$$

where $\tilde{f} = e^{-(\tilde{K}+\lambda)t}f(e^{(\tilde{K}+\lambda)t}\tilde{u}, e^{(\tilde{K}+\lambda)t}\tilde{w}) + (\tilde{K} + \lambda)\tilde{u}$ and \tilde{g} analogously defined satisfy (7.27).

Remark 7.2. In the particular case where the source of error coming from the linearization process is disregarded, the simplified counterpart of Theorem 7.1 holds with the only estimators η^n , θ^n

defined as

$$\begin{aligned}
\eta^n &= \left(\sum_{K \in \tilde{\mathcal{T}}_h^n} h_K^2 \left\| \frac{u_h^n - u_h^{n-1}}{\tau_n} + k_K \Delta u_h^n + (1 - \chi_K) f(u_h^n, w_h^n) \right\|_{L^2(K)}^2 + \sum_{E \in \tilde{\mathcal{E}}_h^n} h_K \|\nabla u_h^n \cdot n_E\|_{L^2(E)}^2 \right. \\
&\quad \left. + \sum_{K \in \tilde{\mathcal{T}}_h^n} \left\| \frac{w_h^n - w_h^{n-1}}{\tau_n} + g(u_h^n, w_h^n) \right\|_{L^2(K)}^2 \right)^{\frac{1}{2}} \\
\vartheta^n &= \left(\frac{1}{3} \|\nabla(u_h^n - u_h^{n-1})\|_{L^2(\Omega)}^2 + \frac{1}{\tau_n} \|(1 - \chi_K)(f(u_{h,\tau}) - f(u_h^n))\|_{L^2((t_{n-1}, t_n) \times \Omega)}^2 \right. \\
&\quad \left. + \frac{1}{\tau_n} \|(g(u_{h,\tau}) - g(u_h^n))\|_{L^2((t_{n-1}, t_n) \times \Omega)}^2 \right)^{\frac{1}{2}},
\end{aligned} \tag{7.36}$$

being $u_{h,\tau} = \frac{t_n - t}{\tau_n} u_h^{n-1} + \frac{t - t_{n-1}}{\tau_n} u_h^n$ and $w_{h,\tau} = \frac{t_n - t}{\tau_n} w_h^{n-1} + \frac{t - t_{n-1}}{\tau_n} w_h^n$. An efficiency result analogous to Theorem 7.3 holds with the same estimators, without any further assumption on the discretization.

7.4 Numerical experiments

We now assess the validity of the derived *a posteriori* estimates of Theorem 7.2 via numerical experiments. We consider the following two-dimensional setup: the domain Ω is the square $(0, 1)^2$, whereas the time interval in consideration is $(0, 16)$. All the experiments are performed in a healthy tissue, whence $\chi = 0$. We consider the initial data

$$u_0 = e^{-\frac{(x-1)^2 + y^2}{0.25}}, \quad w_0 = 0,$$

whereas the value of the constants of the problem are reported in Table 1. We report in Figure

k_1	A	ϵ_0	μ_1	μ_2	a
1	8	0.04	0.2	0.3	0.15

Table 7.1: Values of the main parameters of the model

7.1 several snapshots of the evolution of the electrical potential u throughout time. The results are obtained via the Newton-Galerkin scheme in (7.8)-(7.9), making use of the same computational mesh \mathcal{T}_h for each instant, with maximum diameter $h = 0.0125$ and a fixed timestep $\tau = 0.025$. As an exit criterion for the Newton iterations we assess if the distance between two following iterations (measured in H^1 and L^2 norm respectively for u and w) is below a suitable tolerance, which we set as $tol = 10^{-14}$. In accordance with experimental observations (see, e.g., [61]), the nonlinear dynamics shows a first quick propagation of the stimulus in the tissue and, after a plateau phase, a slow decrease of the electrical potential.

7.4.1 Spatial and temporal analysis

We now verify the validity of the estimates stated in Theorem 7.1. Due to the lack of an analytical expression for the solution of (7.1), we need to build a high-fidelity numerical solution (\tilde{u}, \tilde{w}) . In

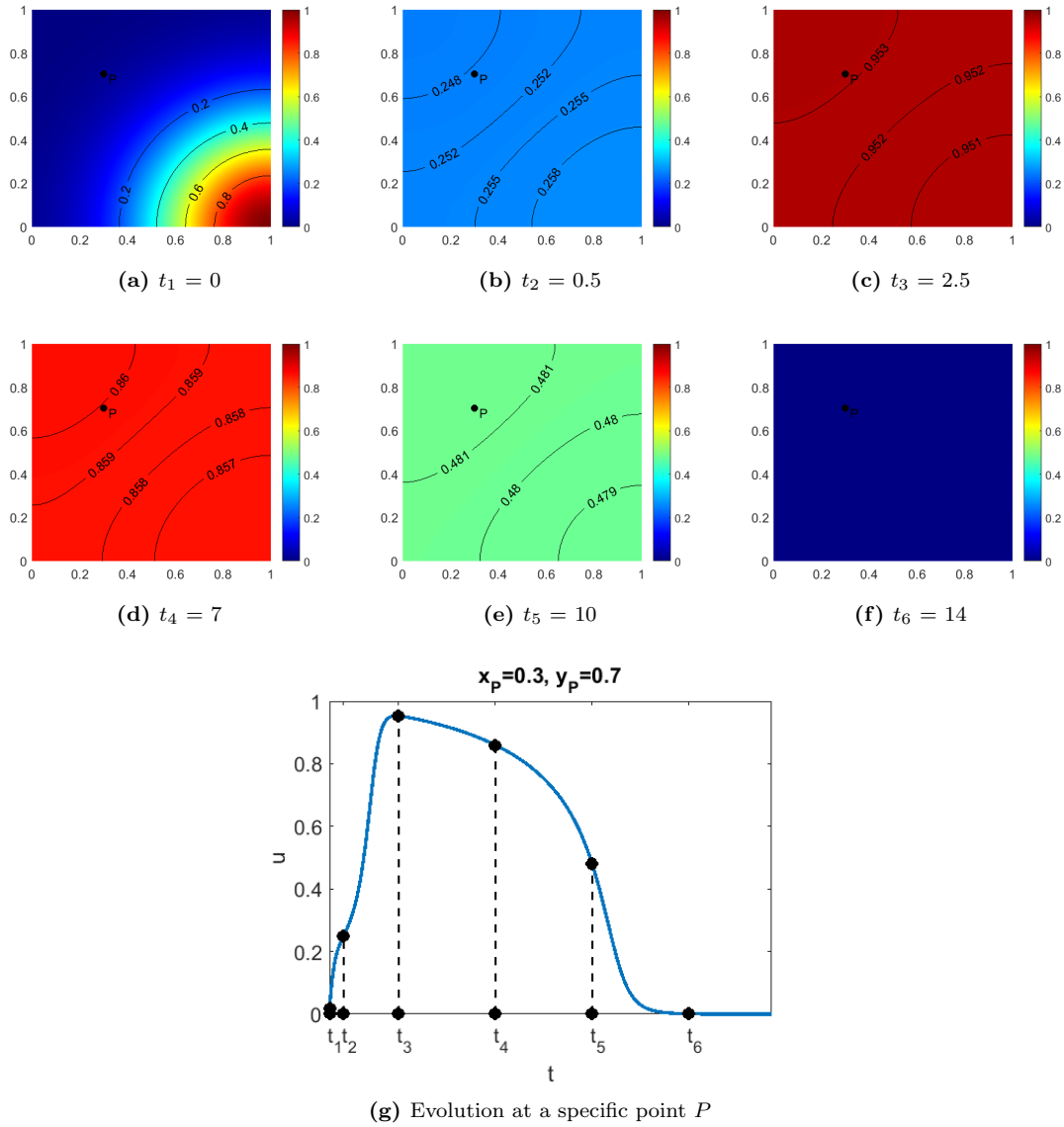


Figure 7.1: Snapshots of the evolution of the electrical potential. In Figures (a)-(f) the contour plots are shown in some selected instants t_1, \dots, t_6 . Figure (g) reports the value of the electrical potential in a specific point P ; the instants t_1, \dots, t_6 are remarked.

particular, we employ a reference fine mesh with $h_{ref} = 4 \cdot 10^{-3}$ and a time step $\tau_{ref} = 2 \cdot 10^{-3}$ to solve the Newton scheme (7.8)-(7.9), where $tol = 10^{-15}$ is employed to make negligible the linearization error (see Remark 7.2). Employing (\tilde{u}, \tilde{w}) it is possible to compute the error associated to different discrete solutions, obtained with different values of h and τ , and to assess the validity of the a posteriori error estimates introduced in Theorem 7.1 employing the estimators defined in (7.36).

In Figure 7.2 we report the numerical verification of the upper bound (7.20) for two different

choices of the discretization parameters h and τ . Each line is piecewise constant on every interval (t_{n-1}, t_n) . The red line represents the X, Y norm of the error (computed with respect to the high-fidelity solution) on the interval $(0, t_n)$, whereas the blue line shows the sum of the estimator contributions in each interval until t_n . In this case the upper bound holds with constant 1.

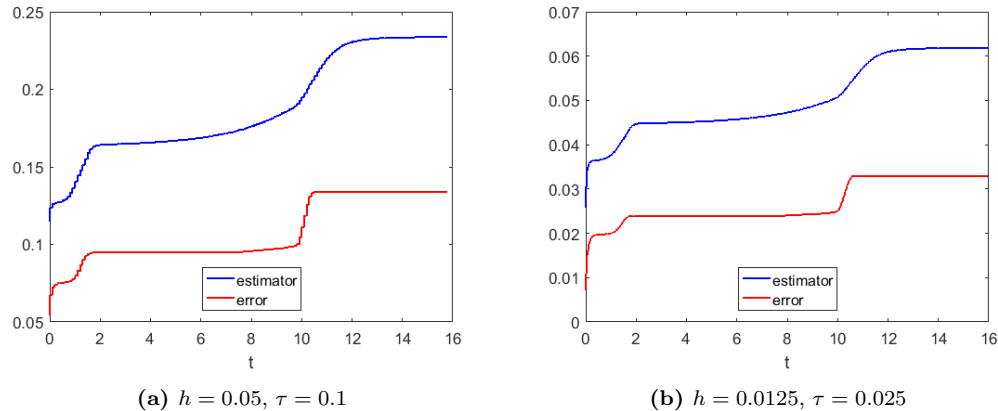
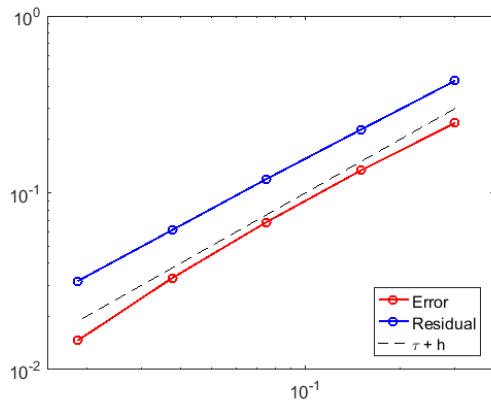


Figure 7.2: Assessment of the upper bound

Moreover, in Figure 7.3 we investigate the convergence rates for both the estimator and the error norm with respect to the mesh size h and the timestep τ . The results are obtained by linearly reducing both h and τ at the same time. The convergence history reported in Figure 7.3 shows that the error and the *a posteriori* estimator decay with the same (linear) rate.

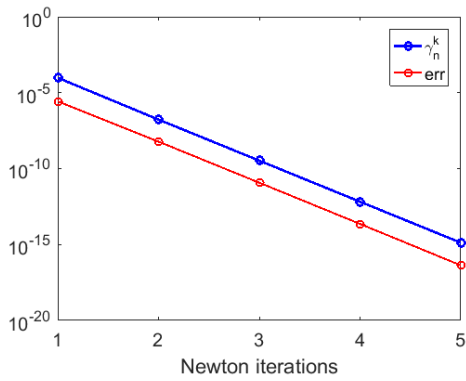
7.4.2 Linearization analysis

We now numerically assess the validity of the estimates concerning the linearization error. In order to reduce as much as possible the numerical error induced by spatial and temporal approximations, we perform the numerical experiments with the same discretization parameters ($h_{ref} = 4 \cdot 10^{-3}$, $\tau_{ref} = 2 \cdot 10^{-3}$) employed to build the high-fidelity numerical solution. Selecting an instant t_n , we compute several iterations of the Newton scheme (7.8)-(7.9) until the convergence criterion is satisfied with $tol = 10^{-15}$. The iterative scheme produces a sequence $\{u_{h,K_n}^n, w_{h,K_n}^n\}_{k=0,\dots,K}$. Then, for each k we compute γ_k^n and compare it with the error. In Figure 7.4 we report the described comparison at $t_n = 2.5$ and $t_n = 10$. We observe that for each $k = 1, \dots, K$ the estimator is above the error, and they decrease with the same rate.

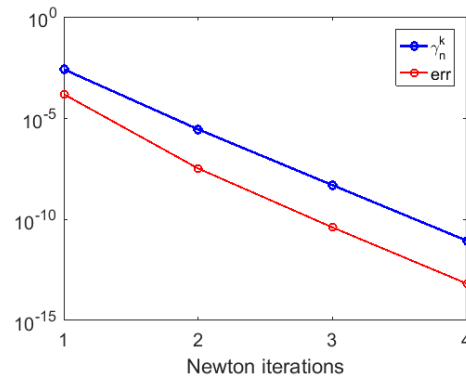


h	τ	tol
0.1	0.2	10^{-14}
0.05	0.1	10^{-14}
0.025	0.05	10^{-14}
0.0125	0.025	10^{-14}
0.00625	0.0125	10^{-14}

Figure 7.3: Convergence analysis in h and τ



(a) $t_n = 2.5$; accepted at iteration 5



(b) $t_n = 10$; accepted at iteration 4

Figure 7.4: Assessment of the *a posteriori* indicator γ_k^n for the linearization error

Conclusions

In this thesis, we have tackled the inverse problem of detecting discontinuous coefficients in semilinear elliptic and parabolic problems. The purpose of reconstructing inhomogeneities in the electrical activity of the heart (modeled via a system of coupled nonlinear equations) by means of a single boundary measurement has motivated our study. In particular, due to the lack of measurements at disposal, we had to deal with ill-posed inverse problems, for which suitable regularization hypotheses have been introduced. Moreover, the nonlinearity of the direct problem has implied significant restrictions on the application of existing techniques. As a consequence, it has been necessary to extend and design novel methods for the problem of interest, both for analytical and reconstruction purposes. In particular, we have achieved the following results:

- **Localization of small inclusions in semilinear boundary value problems:** under the regularization hypothesis that the inclusion to be identified is of small size, we have been able to prove rigorous results regarding the analysis of the inverse problem. Specifically, both in a simplified elliptic and parabolic case (see Chapter 2 and 3 respectively), we have derived an asymptotic expansion of the boundary potential with respect to the size of the inclusion, also entailing a local stability estimate for the inverse problem in the elliptic case. We have employed such results also for reconstruction purposes, deriving a variational algorithm based on the topological optimization of a suitable cost functional.
- **Detection of large inclusions in semilinear boundary value problems:** without any *a priori* assumption on the inclusion to be identified, we have been able to devise a reconstruction algorithm, based on a phase-field approach, allowing for satisfactory reconstructions. In Chapter 5 we have investigated the convergence of the proposed algorithm, and we have reported a detailed comparison with some state-of-the-art alternative approaches. We point out that, due to its generality and feasibility, this technique is likely to be extended to a wider class of identification problems.
- **Introduction of preliminary results for the analysis of the monodomain case:** in order to extend the outlined approach to the complexity of the monodomain model for the full heartbeat, some preliminary studies have been performed. The well-posedness results obtained in Chapter 6 pave the way for further analytical results regarding the inverse problem: in particular, we expect to be able to deduce an asymptotic expansion of the boundary voltage in presence of small ischemias. Moreover, the *a posteriori* error analysis performed in Chapter 7 allows to efficiently extend the reconstruction algorithm (especially in the assumption of large inclusions) to the case in which the monodomain model is considered.

Bibliography

- [1] R. A. Adams and J. J. F. Fournier. *Sobolev Spaces*. Second Edition. Pure and Applied Mathematics. Elsevier, 2003.
- [2] L. Afraites, M. Dambrine, and D. Kateb. Conformal mappings and shape derivatives for the transmission problem with a single measurement. *Numer. Func. Anal. Opt.* 28 (2007), 519–551.
- [3] G. Alessandrini. Stable determination of conductivity by boundary measurements. *Applicable Analysis* 27.1-3 (1988), 153–172.
- [4] G. Alessandrini and M. Di Cristo. Stable determination of inclusion by boundary measurements. *SIAM J. Math. Anal.* 37 (2005), 200–217.
- [5] G. Alessandrini, L. Rondi, E. Rosset, and S. Vessella. The stability for the Cauchy problem for elliptic equations. *Inverse Problems* 25.12 (2009), 123004.
- [6] G. Alessandrini and S. Vessella. Lipschitz stability for the inverse conductivity problem. *Advances in Applied Mathematics* 35.2 (2005), 207–241.
- [7] R.R. Aliev and A.V. Panfilov. A simple two-variable model of cardiac excitation. *Chaos, Solitons & Fractals* 7.3 (1996), 293–301.
- [8] A. Álvarez, F. Alonso-Atienza, J.L. Rojo-Álvarez, A. Garcia-Alberola, and M. Moscoso. Shape reconstruction of cardiac ischemia from non-contact intracardiac recordings: a model study. *Math. Computer Modeling* 55 (2012), 1770–1781.
- [9] L. Ambrosio, N. Fusco, and D. Pallara. *Functions of Bounded Variation and Free Discontinuity Problems*. Oxford Science Publications. Clarendon Press, 2000.
- [10] H. Ammari, E. Beretta, E. Francini, H. Kang, and M. Lim. Optimization algorithm for reconstructing interface changes of a conductivity inclusion from modal measurements. *Math. Comp.* 79(271) (2010), 1757–1777.
- [11] H. Ammari, J. Garnier, V. Jugnon, and H. Kang. Stability and resolution analysis for a topological derivative based imaging functional. *SIAM Journal on Control and Optimization* 50.1 (2012), 48–76.
- [12] H. Ammari, E. Iakovleva, H. Kang, and K. Kim. Direct algorithms for thermal imaging of small inclusions. *Multiscale Modeling & Simulation* 4.4 (2005), 1116–1136.
- [13] H. Ammari and H. Kang. *Reconstruction of small inhomogeneities from boundary measurements*. Lectures Notes in Mathematics Series, Volume 1846. Springer, 2004.

- [14] H. Ammari and Jin K. Seo. An accurate formula for the reconstruction of conductivity inhomogeneities. *Adv. in Appl. Math.* 30(4) (2003), 679–705.
- [15] H. Ammari, P. Garapon, F. Jouve, H. Kang, M. Lim, and Y. Sanghyeon. A new optimal control approach for the reconstruction of extended inclusions. *J. Control Optim.* 51 (2013), 1372–1394.
- [16] M. Amrein and T.P. Wihler. An adaptive space-time Newton–Galerkin approach for semilinear singularly perturbed parabolic evolution equations. *IMA J NUMER ANAL* 37.4 (2016), 2004–2019.
- [17] S. Amstutz. Sensitivity analysis with respect to a local perturbation of the material property. *Asymptotic Analysis* 49(1,2) (2006), 87–108.
- [18] S. Amstutz, I. Horchani, and M. Masmoudi. Crack detection by the topological gradient method. *Contr. Cyber.* 34(1) (2005), 81–101.
- [19] K. Aras, B. Burton, D. Swenson, and R. MacLeod. Spatial organization of acute myocardial ischemia. *Journal of electrocardiology* 49.3 (2016), 323–336.
- [20] K. Astala and L. Päivärinta. Calderón’s inverse conductivity problem in the plane. *Annals of Mathematics* (2006), 265–299.
- [21] D. Auroux. From Restoration by Topological Gradient to Medical Image Segmentation via an Asymptotic Expansion. *Math. Comput. Model.* 49.11-12 (2009), 2191–2205.
- [22] M. Bachmayr and M. Burger. Iterative total variation schemes for nonlinear inverse problems. *Inverse Problems* 25.10 (2009), 105004.
- [23] S. Baldo. Minimal interface criterion for phase transitions in mixtures of Cahn-Hilliard fluids. *Ann. IHP Anal. Non Linéaire*. Vol. 7. 2. 1990, pp. 67–90.
- [24] B. Barcelo, E.B. Fabes, and J. K. Seo. The inverse conductivity problem with one measurement, uniqueness for convex polyhedra. *Proc. Amer. Math. Soc.* 122 (1994), 183–189.
- [25] J.A. Barceló, T. Barceló, and A. Ruiz. Stability of the inverse conductivity problem in the plane for less regular conductivities. *Journal of Differential Equations* 173.2 (2001), 231–270.
- [26] S. Bartels. *Numerical methods for nonlinear partial differential equations*. Vol. 47. Springer, 2015.
- [27] M. Bendahmane and K. H. Karlsen. Analysis of a class of degenerate reaction-diffusion systems and the bidomain model of cardiac tissue. *Netw. Heterog. Media* 1 (2006), 185–218.
- [28] E. Beretta, C. Cavaterra, M.C. Cerutti, A. Manzoni, and L. Ratti. An inverse problem for a semilinear parabolic equation arising from cardiac electrophysiology. *Inverse Problems* 33(10) (2017).
- [29] E. Beretta, C. Cavaterra, and L. Ratti. Asymptotic expansion of boundary voltage perturbation in presence of small ischemic regions in the monodomain model of cardiac electrophysiology. *in preparation* (2018).
- [30] E. Beretta, M. C. Cerutti, A. Manzoni, and D. Pierotti. An asymptotic formula for boundary potential perturbations in a semilinear elliptic equation related to cardiac electrophysiology. *Math. Mod. Meth. Appl. S.* (2014).

- [31] E. Beretta, E. Francini, and S. Vessella. Differentiability of the Dirichlet to Neumann Map Under Movements of Polygonal Inclusions with an Application to Shape Optimization. *SIAM Journal on Mathematical Analysis* 49.2 (2017), 756–776.
- [32] E. Beretta, M. Grasmair, M. Muszkieta, and O. Scherzer. A variational algorithm for the detection of line segments. *Inverse Probl. Imag.* 8(2) (2014).
- [33] E. Beretta, A. Manzoni, and L. Ratti. A reconstruction algorithm based on topological gradient for an inverse problem related to a semilinear elliptic boundary value problem. *Inverse Problems* 33.3 (2017).
- [34] E. Beretta, S. Micheletti, S. Perotto, and M. Santacesaria. Reconstruction of a piecewise constant conductivity on a polygonal partition via shape optimization in EIT. *Journal of Computational Physics* 353 (2018), 264–280.
- [35] E. Beretta, L. Ratti, and M. Verani. Detection of conductivity inclusions in a semilinear elliptic problem arising from cardiac electrophysiology. *to appear in Commun. Math. Sci.* (2018).
- [36] Elena Beretta and Cecilia Cavaterra. Identifying a space dependent coefficient in a reaction-diffusion equation. *Inverse Problems and Imaging* 5.2 (2011), 285–296.
- [37] M. Bergounioux and K. Kunisch. Augmented Lagrangian Techniques for Elliptic State Constrained Optimal Control Problems. *SIAM Journal on Control and Optimization* 35.5 (1997), 1524–1543.
- [38] L. Blank, H. Garcke, C. Hecht, and C. Rupprecht. Sharp interface limit for a phase field model in structural optimization. *SIAM J. Control Optim.* 54.3 (2016), 1558–1584.
- [39] M. Boulakia, M. A. Fernández, J.F. Gerbeau, and N. Zenzemi. A coupled system of PDEs and ODEs arising in electrocardiograms modeling. *Applied Math. Res. Exp.* 2008 (2008).
- [40] M. Boulakia, E. Schenone, and J-F. Gerbeau. Reduced-order modeling for cardiac electrophysiology. Application to parameter identification. *Int. J. Numer. Meth. Biomed. Engng.* 28.6–7 (2012), 727–744.
- [41] Y. Bourgault, Y. Coudiere, and C. Pierre. Existence and uniqueness of the solution for the bidomain model used in cardiac electrophysiology. *Nonlinear Anal Real World Appl* 10.1 (2009), 458–482.
- [42] M. Brühl and M. Hanke. Numerical implementation of two noniterative methods for locating inclusions by impedance tomography. *Inverse Problems* 16.4 (2000), 1029.
- [43] M. Brühl, M. Hanke, and M. S. Vogelius. A direct impedance tomography algorithm for locating small inhomogeneities. *Numer. Math* 93(4) (2003), 635–654.
- [44] M. Burger. Levenberg–Marquardt level set methods for inverse obstacle problems. *Inverse problems* 20.1 (2003), 259.
- [45] J. Céa, S. Garreau, P. Guillame, and M. Masmoudi. The shape and topological optimizations connection. *Comput. Methods Appl. Mech. Engrg.* 188 (2000), 713–726.
- [46] AP Calderón. On an inverse boundary value problem, Seminar on Numerical Analysis and its Applications to Continuum Physics, 65–73. *Soc. Brasil. Mat., Rio de Janeiro* (1980).

- [47] Y. Capdeboscq and M. Vogelius. A general representation formula for boundary voltage perturbations caused by internal conductivity inhomogeneities of low volume fraction. *Math. Modelling and Num. Analysis* 37 (2003), 159–173.
- [48] P. Caro and K.M. Rogers. Global uniqueness for the Calderón problem with Lipschitz conductivities. *Forum of Mathematics, Pi*. Vol. 4. Cambridge University Press. 2016.
- [49] A. Carpio and M. L. Rapún. “Topological derivatives for shape reconstruction”. *Inverse problems and imaging*. Springer, 2008, pp. 85–133.
- [50] A. Carpio and M.L. Rapún. “Inverse Problems and Imaging: Lectures given at the C.I.M.E. Summer School held in Martina Franca, Italy September 15–21, 2002”. Ed. by L.L. Bonilla. Springer Berlin Heidelberg, 2008. Chap. Topological Derivatives for Shape Reconstruction, pp. 85–133.
- [51] D. J. Cedio-Fengya, S. Moskow, and M. S. Vogelius. Identification of conductivity imperfections of small diameter by boundary measurements. Continuous dependence and computational reconstruction. *Inverse Problems* 14 (2008), 553–595.
- [52] S. Chaabane, M. Masmoudi, and H. Meftahi. Topological and shape gradient strategy for solving geometrical inverse problems. *J. Math. Anal. Appl.* 400 (2013), 724–742.
- [53] T. F. Chan and X. Tai. Level set and total variation regularization for elliptic inverse problems with discontinuous coefficients. *J. Comput. Phys.* 193(1) (2004), 40–66.
- [54] C. E. Chávez, N. Zemzemi, Y. Coudière, F. Alonso-Atienza, and D. Alvarez. Inverse problem of electrocardiography: Estimating the location of cardiac ischemia in a 3d realistic geometry. *International Conference on Functional Imaging and Modeling of the Heart*. Springer. 2015, pp. 393–401.
- [55] Z. Chen and J. Zou. An augmented Lagrangian method for identifying discontinuous parameters in elliptic systems. *SIAM Journal on Control and Optimization* 37.3 (1999), 892–910.
- [56] M. Cheney, D. Isaacson, J.C. Newell, S. Simske, and J. Goble. NOSER: An algorithm for solving the inverse conductivity problem. *International Journal of Imaging Systems and Technology* 2.2 (1990), 66–75.
- [57] P. G. Ciarlet, M. H. Schultz, and R.S. Varga. Numerical methods of high-order accuracy for nonlinear boundary value problems. *Numerische Mathematik* 9.5 (1967), 394–430.
- [58] P. Clément. Approximation by finite element functions using local regularization. *Revue française d’automatique, informatique, recherche opérationnelle. Analyse numérique* 9.R2 (1975), 77–84.
- [59] P. Colli Franzone, P. Deuffhard, B. Erdmann, J. Lang, and L.F. Pavarino. Adaptivity in space and time for reaction-diffusion systems in electrocardiology. *SIAM J Sci Comput* 28.3 (2006), 942–962.
- [60] P. Colli Franzone, L. F. Pavarino, and S. Scacchi. Dynamical effects of myocardial ischemia in anisotropic cardiac models in three dimensions. *Math. Mod. Meth. Applied Sciences* 17.12 (2007), 1965–2008.

- [61] P. Colli Franzone, L.F. Pavarino, and S. Scacchi. *Mathematical Cardiac Electrophysiology*. Vol. 13. MS&A. Springer, 2014.
- [62] P. Colli Franzone and G. Savaré. “Degenerate evolution systems modeling the cardiac electric field at micro-and macroscopic level”. *Evolution equations, semigroups and functional analysis*. Springer, 2002, pp. 49–78.
- [63] D. Colton and A. Kirsch. A simple method for solving inverse scattering problems in the resonance region. *Inverse problems* 12.4 (1996), 383.
- [64] Y. Coudière and C. Pierre. Stability and convergence of a finite volume method for two systems of reaction-diffusion equations in electro-cardiology. *Nonlinear analysis: real world applications* 7.4 (2006), 916–935.
- [65] E. De Giorgi. New problems on minimizing movements. *Ennio de Giorgi: Selected Papers* (1993), 699–713.
- [66] K. Deckelnick, C. M Elliott, and V. Styles. Double obstacle phase field approach to an inverse problem for a discontinuous diffusion coefficient. *Inverse Problems* 32 (2016).
- [67] M. C Delfour and J.-P. Zolésio. *Shapes and geometries: metrics, analysis, differential calculus, and optimization*. SIAM, 2011.
- [68] A.J. Devaney. Super-resolution Processing of Multi-static Data Using Time Reversal and MUSIC (2000).
- [69] G. Dogan, P. Morin, R. H. Nochetto, and M. Verani. Discrete gradient flows for shape optimization and applications. *Computer methods in applied mechanics and engineering* 196.37 (2007), 3898–3914.
- [70] A. Drogoul. Numerical Analysis of the Topological Gradient Method for Fourth Order Models and Applications to the Detection of Fine Structures in Imaging. *SIAM J. Imaging Sci.* 7(4) (2014), 2700–2731.
- [71] V. Druskin. On uniqueness of the determination of the three-dimensional underground structures from surface measurements with variously positioned steady-state or monochromatic field sources. *Sov. Phys.–Solid Earth* 21 (1985), 210–4.
- [72] H.W. Engl, M. Hanke, and A. Neubauer. *Regularization of Inverse Problems*. Mathematics and Its Applications. Springer Netherlands, 1996. ISBN: 9780792341574.
- [73] A. Ern and M. Vohralík. Adaptive inexact Newton methods with a posteriori stopping criteria for nonlinear diffusion PDEs. *SIAM J Sci Comput* 35.4 (2013), A1761–A1791.
- [74] L. C. Evans. *Partial differential equations* (2010).
- [75] L.C. Evans and R.F. Gariepy. *Measure theory and fine properties of functions*. CRC press, 2015.
- [76] M. A. Fernández and N. Zenzemi. Decoupled time-marching schemes in computational cardiac electrophysiology and ECG numerical simulation. *Math. Biosci.s* 226.1 (2010), 58–75.
- [77] R. FitzHugh. Impulses and physiological states in theoretical models of nerve membrane. *Biophysical journal* 1.6 (1961), 445–466.

- [78] A. Friedman and M. Vogelius. Identification of small inhomogeneities of extreme conductivity by boundary measurements: a theorem on continuous dependence. *Arch. Rat. Mech. Anal.* 105 (1989), 299–326.
- [79] H. Garcke. The Γ -limit of the Ginzburg-Landau energy in an elastic medium. *AMSA* 18.2 (2008), 345–379.
- [80] J.F. Gerbeau, D. Lombardi, and E. Schenone. Reduced order model in cardiac electrophysiology with approximated Lax pairs. *Adv. Comput. Math.* 41.5 (2015), 1103–1130.
- [81] Y. Giga and N. Kajiwara. On a resolvent estimate for bidomain operators and its applications. *Journal of Mathematical Analysis and Applications* 459.1 (2018), 528–555.
- [82] D. Gilbarg and N. S. Trudinger. *Elliptic Partial Differential Equations of Second Order*. Springer, 2001.
- [83] E. Giusti. *Minimal surfaces and functions of bounded variation*. Springer, 1984.
- [84] P. Grisvard. *Elliptic problems in nonsmooth domains*. Vol. 69. SIAM, 2011.
- [85] Y. He and D.E. Keyes. Large-scale parameter extraction in electrocardiology models through Born approximation. *Inverse Problems* 29.1 (2012), 015001.
- [86] D. Henry. *Geometric theory of semilinear parabolic equations*. Vol. 840. Springer, 2006.
- [87] F. Hettlich and W. Rundell. The determination of a discontinuity in a conductivity from a single boundary measurement. *Inverse Problems* 14 (1998), 311–318.
- [88] M. Hintermüller and A. Laurain. Electrical impedance tomography: from topology to shape. *Control & Cybernetics* 37.4 (2008).
- [89] M. Ikehata and S. Siltanen. Numerical method for finding the convex hull of an inclusion in conductivity from boundary measurements. *Inverse Problems* 16.4 (2000), 1043.
- [90] V. Isakov. *Inverse Problems for Partial Differential Equations*. Second Edition. Springer, 2006.
- [91] V. Isakov. On uniqueness in inverse problems for semilinear parabolic equations. *Arch. Rational Mech. Anal.* 124.1 (1993), 1–12.
- [92] V. Isakov. On uniqueness of recovery of a discontinuous conductivity coefficient. *Comm. Pure Appl. Math.* 41(7) (1988), 865–877.
- [93] V. Isakov and J. Powell. On the inverse conductivity problem with one measurement. *Inverse Problems* 6 (1990), 311–318.
- [94] J. Kaipio and E. Somersalo. *Statistical and Computational Inverse Problems*. Springer-Verlag, 2004.
- [95] A. Kirsch. *An introduction to the mathematical theory of inverse problems*. Vol. 120. Springer Science & Business Media, 2011.
- [96] R. Kohn and M. Vogelius. Determining conductivity by boundary measurements. *Communications on Pure and Applied Mathematics* 37.3 (1984), 289–298.

- [97] V. Kolehmainen, S. R. Arridge, W. R. B. Lionheart, M. Vauhkonen, and J. P. Kaipio. Recovery of region boundaries of piecewise constant coefficients of an elliptic PDE from boundary data. *Inverse Problems* 15.5 (1999), 1375.
- [98] K. Kunisch and M. Wagner. Optimal control of the bidomain system (IV): corrected proofs of the stability and regularity theorems. *arXiv preprint arXiv:1409.6904* (2014).
- [99] O. A. Ladyzhenskaia, V. A. Solonnikov, and N. N. Ural'ceva. *Linear and quasi-linear equations of parabolic type*. Vol. 23. AMS Transl. Monographs, 1968.
- [100] S. Larnier, J. Fehrenbach, and M. Masmoudi. The topological gradient method: From optimal design to image processing. *Milan Journal of Mathematics* 80(2) (2012), 411–441.
- [101] Y. Li and L. Nirenberg. Estimates for elliptic systems from composite material. *Comm. Pure Appl. Math.* 56(7) (2003), 892–925.
- [102] E. H. Lieb and M. Loss. *Analysis-second edition, Graduate Studies in Mathematics*. Vol. 14. 2001.
- [103] J. L. Lions. Quelques méthodes de résolution des problèmes aux limites non linéaires (1969).
- [104] A. Lunardi. *Analytic semigroups and optimal regularity in parabolic problems*. Springer Science & Business Media, 2012.
- [105] M. Lysaker and B. F. Nielsen. Towards a level set framework for infarction modeling: an inverse problem. *Int. J. Numer. Anal. Model.* 3 (2006), 377–394.
- [106] N. Mandache. Exponential instability in an inverse problem for the Schrödinger equation. *Inverse Problems* 17.5 (2001), 1435.
- [107] N. G. Meyers. An L^p -estimate for the gradient of solutions of second order elliptic divergence equations. *Ann. Sc. Norm. Super. Pisa Cl. Sci.* 17(3) (1963), 189–206.
- [108] C.C. Mitchell and D.G. Schaeffer. A two-current model for the dynamics of cardiac membrane. *Bulletin of mathematical biology* 65.5 (2003), 767–793.
- [109] A.I. Nachman. Global uniqueness for a two-dimensional inverse boundary value problem. *Annals of Mathematics* (1996), 71–96.
- [110] J. Nagumo, S. Arimoto, and S. Yoshizawa. An active pulse transmission line simulating nerve axon. *Proceedings of the IRE* 50.10 (1962), 2061–2070.
- [111] G. Nakamura and S. Sasayama. Inverse boundary value problem for the heat equation with discontinuous coefficients. *J. Inverse Ill-Posed Probl.* 21.2 (2013), 217–232.
- [112] B. F. Nielsen, M. Lysaker, and A. Tveito. On the use of the resting potential and level set methods for identifying ischemic heart disease: An inverse problem. *J. Comput. Phys.* 220 (2007), 772–790.
- [113] L. Nirenberg. On elliptic partial differential equations. *Ann. Scuola Norm. Sup. Pisa* 13 (1959), 115–162.
- [114] J. Nocedal and S. J. Wright. *Numerical Optimization*. 2nd. Springer, 2006.
- [115] V.A. Solonnikov O.A. Ladyzhenskaja and N.N. Ural'ceva. *Linear and Quasi-linear Equations of Parabolic Type*. AMS Transl. Monographs, 1968.

- [116] C.V. Pao. *Nonlinear parabolic and elliptic equations*. Springer Science & Business Media, 2012.
- [117] W.K. Park. Topological derivative strategy for one-step iteration imaging of arbitrary shaped thin, curve-like electromagnetic inclusions. *J Comput. Phys.* 231.4 (2012), 1426–1439.
- [118] A. Quarteroni, T. Lassila, S. Rossi, and R. Ruiz-Baier. Integrated Heart—Coupling multiscale and multiphysics models for the simulation of the cardiac function. *Comput. Methods Appl. Mech. Engrg.* 314 (2017), 345–407.
- [119] A. Quarteroni, A. Manzoni, and C. Vergara. The cardiovascular system: Mathematical modelling, numerical algorithms and clinical applications. *Acta Numerica* 26 (2017), 365–590.
- [120] L. Ratti and M. Verani. *A posteriori* error estimates for the monodomain model in cardiac electrophysiology. *arXiv preprint arXiv:1901.07468* (2019).
- [121] P.A. Raviart and J.M. Thomas. *Introduction à l'analyse numérique des équations aux dérivées partielles*. Vol. 2. Dunod Paris, 1998.
- [122] J.C. Robinson. *Infinite-dimensional dynamical systems: an introduction to dissipative parabolic PDEs and the theory of global attractors*. Vol. 28. Cambridge University Press, 2001.
- [123] J.M. Rogers and A.D. McCulloch. A collocation-Galerkin finite element model of cardiac action potential propagation. *IEEE Transactions on Biomedical Engineering* 41.8 (1994), 743–757.
- [124] L. Rondi and F. Santosa. Enhanced electrical impedance tomography via the Mumford–Shah functional. *ESAIM: Control, Optimisation and Calculus of Variations* 6 (2001), 517–538.
- [125] S. Rossi, T. Lassila, R. Ruiz-Baier, A. Sequeira, and A. Quarteroni. Thermodynamically consistent orthotropic activation model capturing ventricular systolic wall thickening in cardiac electromechanics. *Eur. J. Mech. A-Solid*. 48 (2014), 129–142.
- [126] T. S. Ruud, B. F. Nielsen, M. Lysaker, and J. Sundnes. A computationally efficient method for determining the size and location of myocardial ischemia. *IEEE Trans. Biomed. Engine.* 56.2 (2009), 263–272.
- [127] S. Sanfelici. Convergence of the Galerkin approximation of a degenerate evolution problem in electrocardiology. *Numer. Methods Partial Differential Equations* 18.2 (2002), 218–240.
- [128] F. Santosa. A level-set approach for inverse problems involving obstacles. *ESAIM Control Optim. Calc. Var.* 1 (1996), 17–33.
- [129] R.M. Shaw and Y. Rudy. Electrophysiologic effects of acute myocardial ischemia: a theoretical study of altered cell excitability and action potential duration. *Cardiovascular research* 35.2 (1997), 256–272.
- [130] S. Siltanen, J. Mueller, and D. Isaacson. An implementation of the reconstruction algorithm of A Nachman for the 2D inverse conductivity problem. *Inverse Problems* 16.3 (2000), 681.
- [131] Joel Smoller. *Shock waves and reaction—diffusion equations*. Vol. 258. Springer Science & Business Media, 2012.

- [132] J. Sundnes, G. T. Lines, X. Cai, B. F. Nielsen, K.A. Mardal, and A. Tveito. *Computing the electrical activity in the heart*. Monographs in Computational Science and Engineering Series, Volume 1. Springer, 2006.
- [133] Uhlmann G. Sylvester J. A Global Uniqueness Theorem for an Inverse Boundary Value Problem. *Ann. Math.* 125(1) (1987), 153–169.
- [134] A. Tamburrino and G. Rubinacci. A new non-iterative inversion method for electrical resistance tomography. *Inverse Problems* 18.6 (2002), 1809.
- [135] L. Tung. *A bidomain model for describing ischemic myocardial D-C potentials*. Ph.D. Thesis. MIT, Cambridge, MA, 1978.
- [136] M. Veneroni. Reaction–diffusion systems for the microscopic cellular model of the cardiac electric field. *Mathematical methods in the applied sciences* 29.14 (2006), 1631–1661.
- [137] R. Verfürth. A posteriori error estimates for finite element discretizations of the heat equation. *Calcolo* 40.3 (2003), 195–212.
- [138] R. Verfürth. *A review of a posteriori error estimation and adaptive mesh-refinement techniques*. John Wiley & Sons Inc, 1996.
- [139] A. D. Waller. A demonstration on man of electromotive changes accompanying the heart’s beat. *J. Physiol* 8 (1887), 229–234.
- [140] E. Zeidler. *Nonlinear functional analysis and its applications*. Volume I: Fixed point theorems. Springer-Verlag, 1985.
- [141] A. Zygmund. *Trigonometric series*. Vol. 1. Cambridge University Press, 2002.

